TU/e EINDHOVEN UNIVERSITY OF TECHNOLOGY

Ionic systems in materials research : new materials and processes based on ionic polymerizations and/or ionic liquids

Citation for published version (APA):
Guerrero-Sanchez, C. A. (2007). *Ionic systems in materials research : new materials and processes based on ionic polymerizations and/or ionic liquids*. [Phd Thesis 1 (Research TU/e / Graduation TU/e), Chemical Engineering and Chemistry]. Technische Universiteit Eindhoven. https://doi.org/10.6100/IR628894

DOI:
10.6100/IR628894

Document status and date:
Published: 01/01/2007

Document Version:
Publisher's PDF, also known as Version of Record (includes final page, issue and volume numbers)

Please check the document version of this publication:

• A submitted manuscript is the version of the article upon submission and before peer-review. There can be important differences between the submitted version and the official published version of record. People interested in the research are advised to contact the author for the final version of the publication, or visit the DOI to the publisher's website.
• The final author version and the galley proof are versions of the publication after peer review.
• The final published version features the final layout of the paper including the volume, issue and page numbers.

Link to publication

General rights
Copyright and moral rights for the publications made accessible in the public portal are retained by the authors and/or other copyright owners and it is a condition of accessing publications that users recognise and abide by the legal requirements associated with these rights.

• Users may download and print one copy of any publication from the public portal for the purpose of private study or research.
• You may not further distribute the material or use it for any profit-making activity or commercial gain
• You may freely distribute the URL identifying the publication in the public portal.

If the publication is distributed under the terms of Article 25fa of the Dutch Copyright Act, indicated by the "Taverne" license above, please follow below link for the End User Agreement:

www.tue.nl/taverne

Take down policy
If you believe that this document breaches copyright please contact us at:

openaccess@tue.nl

providing details and we will investigate your claim.

Download date: 04. Oct. 2023

Ionic systems in materials research:

New materials and processes based on ionic polymerizations and/or ionic liquids

PROEFSCHRIFT

ter verkrijging van de graad van doctor aan de Technische Universiteit Eindhoven, op gezag van de Rector Magnificus, prof.dr.ir. C.J. van Duijn, voor een commissie aangewezen door het College voor Promoties in het openbaar te verdedigen op maandag 24 september 2007 om 16.00 uur

door

Carlos Antioco Guerrero Sanchez

geboren te Mexico stad, Mexico

Dit proefschrift is goedgekeurd door de promotor:

prof.dr. U.S. Schubert

Copromotor:
dr.ir. R. Hoogenboom

Ionic systems in materials research:

New materials and processes based on ionic polymerizations and/or ionic liquids

About the cover

The cover is designed by the author. It represents the use of ionic liquids as carriers of magnetorhoelogical fluids. In the presence of a magnetic field these fluids behave as solids owing to a stronger interaction between their suspended magnetic particles. In the absence of the magnetic field, they become liquids again in a fully reversible process (see chapter 6). The back cover shows: A scanning electron micrograph of a polymeric bead synthesized by suspension polymerization using water soluble ionic liquds as reation media (top, see chapter 4), an image of anionic polymerization experiments performed in a parallel synthesizer (middle, see chapters 2 and 3), and a conceptual representation of ionic liquids as "environmentally-friendly" materials (bottom, adapted from http://www.chemdat.info/ionic_liquids/ionic_liquids.html (accessed August 2007)).

Kerncommissie:	prof. dr. U. S. Schubert (Eindhoven University of Technology)
	dr. R. Hoogenboom (Eindhoven University of Technology)
	prof. dr. J.-F. Gohy (Université Catholique de Louvain)
	prof. dr. N. Hadjichristidis (University of Athens)
	prof. dr. C. E. Koning (Eindhoven University of Technology)
Overige commissieleden:	prof. dr. R. D. Rogers (University of Alabama)
	dr. Harald Haeger (Degussa GmbH)

This research has been financially supported by the Dutch Polymer Institute (DPI, project #401)

Printed by PrintPartners Ipskamp, Enschede, The Netherlands

Ionic systems in materials research: New materials and processes base don ionic polymerizations
by Carlos A. Guerrero Sanchez.
Eindhoven: Technische Universiteit Eindhoven, 2007.

A catalogue record is available from the Eindhoven University of Technology Library
ISBN: 978-90-386-1086-3

A la memoria de Rosaura y Fila,

gracias por haberme dado la oportunidad de existir.

Table of contents

CHAPTER 1

Materials science: A search for the new and the useful

Abstract

Brief introductions to material science as well as polymer science are presented, which are the basis for the scope of this work. Hence, this work focuses on the use of established or emerging ionic systems (e.g., ionic polymerizations and/or ionic liquids) in combination with other new approaches in polymer synthesis (e.g., combinatorial and high-throughput approaches and microwave irradiation) to develop diverse materials and/or alternative methods for their fabrication.

1.1 Introduction to materials science

1.1.1 A general overview

Nowadays, it is not an exaggeration to say that the prosperity of an economy will depend, at large extend, on the development and use of new materials which will satisfy the actual and future needs of its society. From this point of view, what determines the progress of a civilization is its mastery over materials. The key indicators of progress (military prowess, the ability to produce goods, advances in transportation, agriculture, development of more efficient and cleaner technologies, etc.) all reflect the degree to which humans have been able to work with materials and put them to productive use. Humans have progressed from the Stone Age, the Bronze Age, and the Iron Age to the Silicon Age and current times might be seen as the Age of Materials Science[1] besides the Internet Age. Scientists and engineers have achieved mastery over not only silicon, but also over glass, ceramics, copper, concrete, alloys or combinations of aluminum and exotic metals like titanium, magnetic materials, semiconductors, polymers, medical implant materials, biological materials and newly designed materials that are configured at specific molecular and atomic levels. Materials science is one of the oldest forms of engineering and applied science, has driven, and been driven by, the development of revolutionary technologies. For instance, important elements of modern materials science are a product of the space race: The understanding and engineering of the metallic alloys and other materials that went into the construction of space vehicles was one of the enablers of space exploration.

In this day and age, materials science has become a remarkably interdisciplinary field which couples fundamental research of properties of matter with engineering applications of end-products. Knowing and producing are never separated. The interplay of cognitive purposes and technological interests is seen in the definition of materials. Unlike matter, the notion of materials refers to a substance which is useful or of value for human purpose. Materials are usually defined as substances having properties which make them useful in machines, structures, devices, and products.[1] Because of this dual aspect, materials science has contributed to a deep transformation of the overall organization of research and teaching. Hence, materials science explores the basic structure and properties of matter, down to the molecular, atomic, and even subatomic levels. One major objective of materials science and engineering is to create materials by design (*e.g.*, structures tailored for specific purposes, whose properties are adapted to a set of specific tasks). The achievement of this goal was accelerated when instruments provided access to the micro, nano, molecular and atomic structures of materials. Instead of adopting linear sequences of research and development, materials scientists and engineers have to embrace conceptually structures, properties, functions, processes and end-uses in combined, highly interrelated, and complex approaches. Thus, materials science includes elements of applied physics, chemistry and biology, as well as chemical, mechanical, civil and electrical engineering. Furthermore, with significant attention on nanoscience and nanotechnology in the recent years, materials science has been propelled to the forefront of research. Both, experimental and theoretical research in materials science have three primary objectives: to synthesize novel materials with desirable properties, to advance fundamental understanding of the behavior and properties of materials, and to develop new, creative, more efficient, and environmentally-friendly approaches to materials processing.

Among the many branches of study in materials science are the development of superconducting materials, biomaterials, metal alloys, ceramics, surface engineering, composite materials, and polymers just for citing some examples.

Superconductors can be highlighted among one of many important developments that are currently being investigated in materials science. A superconducting material transmits electricity with virtually no energy loss. In a world where every electrical cord steals some of the current passing through it, the development of a room temperature superconductor could save considerable amount of energy and allow

the development of superconducting computers that could run 100 times faster than today's fastest supercomputers.[2] Similar to superconducting materials, work on semiconductor lasers made the photonics revolution of the last three decades possible.[3] Photonics uses light for signaling and conducting information along a pathway (electronics uses electrons for the same purpose). Photonics is a field that has already produced compact disk players, laser printers, bar code readers, and medical applications, as well as new systems for displaying information.

In another example, new metal alloys are being created and investigated every year by researchers, which must learn about the chemistry of the alloy, the microstructure basic to the alloy, and its macroscopic behavior.[4] Some of the alloys can be used to fabricate thin films that may be applied in the electrical industry.[5] Others may be used in newly designed vehicles. These new alloys are obviously not only stronger and lighter than their predecessors, but also more resistant to stress and fatigue, which may allow to produce more fuel-efficient and longer-lasting vehicles. Still in the field of inorganic materials, an additional example is the transformation of toughness in ceramics. Strong ceramics are capable of operating and surviving in extremely demanding environments. However, as ceramics cool after firing, their tiny constituent particles expand slightly and cause occasional micro-cracks.[6] To reduce the risk of cracking, the particles that make up the ceramics must be in the order of one micron. Using zirconium dioxide-based ceramics, scientists were able to prevent cracking by using appropriate processing to control the expansion of the particles during cooling.[7] To the delight of the automotive industry, these tough ceramics, when integrated into catalytic converters, also increased fuel efficiency.

Composites are another very important kind of materials in which two or more individual materials are combined to fulfill very specific applications. Hence, composite materials are often used in recreational applications such as tennis rackets, golf clubs, and sailboat masts. These materials also bring comfort to thousands of people through medical therapies such as prosthetic arms and legs that are much lighter than wood or metal versions.[8] At higher performance levels, the success of satellites and aircrafts depends on composites. In aircrafts, weight affects every performance factor, and composites offer high load bearing at minimal weight without deterioration at high or low temperatures.[9] Designing composites is one method of fabricating novel materials with special properties. Surface engineering is another. Thermal and plasma spray processing,[10] nano-lithography,[11] surface chemistry,[12] and inkjet printing[13] are in a group of techniques that can propel a range of materials including metals, ceramics, polymers, and composites onto substrates to form new outer layers. Some of these methods have proven to be cost-effective methods for engineering surfaces that are resistant to corrosion, wear, high or low temperatures, or other stresses. Current applications include the aerospace, marine and automobile industries, power generation, paper processing and printing, and infrastructure building.

Regarding the applications in life sciences and biotechnology, chemists work next to physicians and biological specialists to develop, for instance, biocompatible composites for patching wounds, casings for cell transplants, scaffolds that guide and encourage cells to form tissue, bioreactors for large-scale production of therapeutic cells, and experimental and theoretical models that predict behavior of these materials *in vivo*.[14] In addition, other investigators are looking for more environmentally benign and safer substitutes for chemically synthesized materials currently in use. For example, dragline silk from the orb-weaving spider *Nephila clavipes* is one of the most promising biomolecular materials, thanks to the silk's great strength and flexibility-greater even than the lightweight fiber used to reinforce bulletproof helmets. Also attractive is the environmentally friendly process used to make the silk, which the spider spins from a water-based solution.[15] Intrigued by this spider, researchers have had a vision that high-performance, renewable, silk-like biomaterials eventually can be made using tools of biotechnology. The resultant compounds might be used in products ranging from reinforced tennis rackets to tires.

1.1.2 Synthetic polymeric materials

A specifically important branch of materials science are the compounds known as synthetic polymers, gigantic molecules made up of single units, or monomers, that are linked together in chains of varying lengths.[16] Basically, the modern age of polymers has begun during World War II, when researchers were working on durable forms of synthetic rubber that could withstand elevated temperatures and pressures, and to replace the scare of the natural sources. Since then, it has been a relatively smooth transition from rubber to an ever-widening range of synthetic polymers, examples of which are found today in products ranging from clothing, packaging, and personal care products to automobile and aircraft components. Polymers have arisen as a new and important class of materials, which offer both challenges and opportunities in research as well as in the development of new technologies. Nowadays, the field of polymers has become a very diverse and complex branch of research, and therefore it has also become a multidisciplinary area. Thus, very specific research areas have been developed in the field of polymers, such as synthesis, mechanical, physical and chemical characterizations, processing, as well as engineering. For instance, polymer synthesis itself has become a very broad research field, which covers different polymerization reaction mechanisms (*e.g.*, step-growth,[17] controlled/free radical,[18] cationic,[19] anionic,[20] metathesis,[21] Ziegler-Natta-Kaminsky[22] polymerizations) and polymerization processes (*e.g.*, bulk, solution, suspension,[23] emulsion,[24] catalytic,[25] interfacial,[26] bulk-suspension polymerizations).

Due to the continuous diversification of research and applications of polymeric materials, nowadays the markets demand for new materials with very specific properties. Part of this demand can be supplied, for instance, by synthetic developments of new monomers. However, these approaches are often limited and expensive. An interesting example of these approaches is the development of conducting polymers (considered as synthetic metals). Researchers have demonstrated that conjugated polymers can be "doped" or intentionally changed to the metallic state.[27] The process of doping involves introducing into a substance an additive or impurity that produces a specific and deliberate change in the substance itself. This development has remarkably stimulated research worldwide on metallic organic polymers; applications include rechargeable batteries, electromagnetic interference shielding, and corrosion inhibition.[27]

Whenever the development of new monomers is not possible to create new polymers, new materials can be also created by combining existing monomers, which has created the field related to the synthesis of copolymers. In a copolymerization reaction two or more monomers of different characteristics are incorporated into a polymeric chain. The materials obtained by these methods combine properties of the respective homopolymers. Thus, a suitable selection of monomers and their composition can allow for the synthesis of new polymeric materials with very specific properties.[28] The molecular architecture of these materials also plays an important role for their properties. For instance, amphiphilic block copolymers can self-assemble in several nanostructures, which can be used from drug delivery systems for medical therapies to nanotechnology for electronic applications.[29]

Another approach for creating new polymeric materials makes use of the ways in which polymers interact when blended with other polymers and/or with other materials. Polymer blends are a powerful way of enhancing toughness or otherwise tailoring the performance of a given material.[30] This approach has allowed for the development of high-performance polymeric alloys that could be used to replace metal components in automobiles. These lightweight and easy-to-fabricate alloys could help create vehicles that have greater fuel efficiency and produce fewer emissions.

One of the main goals in synthetic polymer chemistry has been and is the preparation of well-defined molecular architectures due to the fact that this determines to a large extent the final properties of the materials. Synthetic polymerization approaches proceeding in the absence of chain transfer and chain termination reactions are suitable and well-known for obtaining well-defined polymers with a high degree of homogeneity (narrow molecular weight distributions). Thus, the discovery of the ionic polymerizations,

which proceed in the absence of chain transfer and termination reactions, around five decades ago gave birth to the field of “living” polymerizations and to some of the most used synthetic techniques for the preparation of well-defined polymeric moieties: anionic[31] and cationic[32] polymerizations.

The development of environmentally benign methods of polymer synthesis has also been an important issue during all these decades. The first important development in this regard was the fabrication of polymers in heterogeneous systems based on water (*e.g.*, emulsion[24] and suspension[23] polymerizations) during World War II. Almost four decades after, the use of liquid carbon dioxide was also proposed to replace highly toxic volatile organic solvents widely used throughout the industry.[33] More recently, the appearance of a new class of “environmentally-friendly” substances, ionic liquids (*e.g.*, molten salts below 100 °C), has triggered research towards the development of more efficient and cleaner technologies.[34] Due to their negligible vapor pressure and flammability, ionic liquids have arisen as very promising substances to replace toxic and unsafe volatile organic solvents in many chemical processes,[35] including polymer synthesis.[36]

Thus, discoveries of new materials always lead to new questions and their answers create opportunities to still find additional new materials. Hence, materials research is a very powerful catalyst for innovation and at the same time a very complex and highly interrelated field of science pushing the edge of the technologies of a whole array of societal systems. As new materials become available and processable, they will make possible improvements in the quality of life.

1.2 Scope of this work

1.2.1 Ionic systems in materials research

Despite the impressive developments that materials science has achieved in the last six decades, there are still much more challenges to be solved, and chemical, physical and biological phenomena to be understood in the field. This has, *e.g.*, the goal of creating environmentally-friendly, more efficient and cheaper materials, and processes for their production. Thus, material science will always offer endless opportunities for research and development. Being the field of polymer research as vast as materials science, nowadays materials (or polymer) scientist must be specialized in specific branches of science and, at the same time, must have a general vision of the entire field, which will allow them to innovate and find new applications of their developments and/or influence on other braches of science. Hence, in these days, materials scientists must also be able to recognize, incorporate and communicate emerging developments and/or technologies, which may have in the future an important impact in their own research areas and/or in other branches of science and technology.

Systems based on ionic interactions are usually related to reversible self-assembly processes and/or transitory chemical states since they are weaker than covalent bonds. Nowadays, they are believed to be key factors for the understanding and for the development of processes in several branches of chemistry and materials research. During the last decades, scientists have created different approaches for the preparation of new materials and/or substances with outstanding properties based on ionic and other non-covalent interactions. In this dissertation work, different chemical systems, based on ionic interactions, have been employed for the preparation of new materials and for the development of more efficient synthetic methods in materials research. All developments and findings achieved during this work have been and will be document in the scientific literature. Thus, it is hoped that the results of this thesis will provide a better understanding of the studied chemical processes and the products derived from them will have a positive impact on the society and its constant search for new and better materials as well as more efficient methods for their preparation. In fact, all the developments achieved are illustrated with potential and/or established applications.

1.2.2 Development of materials and processes based on ionic polymerizations and/or ionic liquids

This work focuses on the incorporation of emerging synthetic approaches into polymer and materials sciences in order to develop diverse materials and/or alternative methods for their fabrication. One of these emerging synthetic approaches to be considered in this work is the incorporation of high-throughput methods[37,38] into one of the most demanding ionic polymerization methods, anionic polymerization.[39] Other important emerging technologies to be included in this research work are the use of ionic liquids[34] and/or microwave irradiation[40,41] for the development of cleaner polymerization processes.[36] In addition, ionic liquids are combined with polymeric and other substances to create novel systems and composite materials.[42] Due to the potentially "green" characteristics of ionic liquids, it is thought that these emerging, non-volatile and non-flammable solvents will be an important basis for the development of new sustainable processes and materials in the coming years.[43]

Thus, the scope of this work can be summarized as the use of established and/or emerging ionic systems (*e.g.*, ionic polymerizations and/or ionic liquids) in combination with other new approaches of polymer synthesis (*e.g.*, combinatorial and high-throughput approaches and microwave irradiation) for developing different materials and/or alternative processes for their fabrication. On the one hand "classical" and new approaches based on ionic interactions for the preparation of polymeric moieties and new materials are employed, and on the other hand some of the results derived from these single approaches are combined in order to investigate advanced composite systems. These new systems may find applications in several fields of science and technology: From drug delivery and medical therapies to engineering devices and catalytic reaction systems. Thus, this dissertation thesis is divided in three sections.

In the first section of this thesis (chapters 2 and 3), the enhancement of a well-established polymer synthetic approach, anionic polymerization, is achieved by incorporating this technique into a high-throughput work flow. This experimental approach has allowed and accelerated the synthesis of "new" block copolymer libraries and end-functionalized polymers containing supramolecular moieties.[44] Besides the systematic and accelerated synthesis of these polymers, it has been shown that this technique can be a very useful tool for performing detailed kinetic investigations of these ionic polymerizations in a short time. Thus, the high-throughput approach was established for one of the most demanding processes in polymer synthesis. This new tool may help to speed up research in this field towards a better understanding of structure-property relationships in polymer science.

In the second part of the thesis (chapter 4), ionic liquids[34] are investigated as a new reaction media to carry out polymerizations by different reaction mechanisms. Due to their outstanding chemical and physical stabilities, ionic liquids are proposed as novel ionic systems that can offer multiple advantages in polymer synthesis.[36] Thus, it is demonstrated that ionic liquids can be efficiently utilized to perform homogeneous and heterogeneous polymerization reactions. In the homogeneous case, another ionic polymerization mechanism, cationic ring opening polymerization, is chosen as an example to perform the "living" polymerization of well-defined polymers. It was found that the substitution of conventional volatile organic solvents by ionic liquids as reaction media can lead to faster polymerization rates in some of the investigated systems. Furthermore, the proposed synthetic method is not just limited to one reaction mechanism and can be readily extended to other types of polymerizations such as free radical or controlled free radical. Because not all monomers and/or polymers will show a good solubility in specific ionic liquids, it is also demonstrated that heterogeneous polymerizations can be carried out in ionic liquids. For these cases, apart from ionic liquids acting as a reaction medium, it was found that ionic liquids also function as novel surfactants to stabilize these heterogeneous systems. Hence, heterogeneous polymerizations performed in ionic liquids have allowed for the synthesis of polymer beads with controlled particle sizes from the nanometer to the millimeter range. Besides the mentioned

advantages of using ionic liquids as reaction media in polymers synthesis, it is also shown that "green" processes can be developed using these approaches due to the known "environmentally-friendly" characteristics of ionic liquids (*e.g.*, negligible vapor pressure and negligible flammability).[43] Thus, the substitution of volatile organic solvents by ionic liquids in polymer synthesis is achieved, for both homogeneous and heterogeneous cases, and the "green" character in the synthetic methods proposed is kept by using other environmentally-friendly substance, water, for the isolation of the products synthesized and the ionic liquid recovery for additional polymerizations cycles. In this way the development of more efficient and cleaner polymerization processes has been achieved by avoiding the use of organic volatile compounds.

In the last part of the thesis (chapters 5 and 6), some of the materials synthesized in the first section as well as other materials are combined with the findings and/or concepts developed in the second part to obtain advanced materials systems. More specifically, block copolymers synthesized in the first section (and by other synthetic methods) are utilized for the preparation of block copolymer micelles using ionic liquids as thermodynamically good and bad solvents for amphiphilic polymers.[45] The use of ionic liquids for the preparation of block copolymer micellar systems has revealed some advantages in this regard since multiple-phase systems can be prepared and the micelles can be reversible transferred between the different phases.[46] Moreover, it is also shown that the transportation of encapsulated guest molecules in the micelles can be also achieved between the different phases. These studies may find applications in catalytic reaction systems[47] and/or in drug delivery processes.[48] Finally, taking advantage of the surface active properties shown by ionic liquids, the preparation of composite materials is illustrated with two examples. The utilization of ionic liquids has allowed the efficient and homogeneous incorporation of inorganic materials (*e.g.*, magnetite) into a polymeric matrix, which cannot be easily achieved by other methods. Thus, polymer composites showing magnetic and conductivity properties were prepared by an inexpensive method. In addition, this latter concept is also extended to the preparation of novel magnetic composite materials in a liquid state. Hence, a new class of magnetorheological fluids[49] have been developed by dispersing magnetic particles in ionic liquids. Apart from the known magnetorheological effect shown by the materials, the use of ionic liquids as carriers of these dispersions has allowed the preparation of magnetorheological fluids with enhanced properties (*e.g.*, low sedimentation rate of the dispersed particles, negligible vapour pressure and flammability, use in a wider temperature range, electric conductivity, miscibility/immiscibility with diverse substances, etc.) in comparison to other preparation approaches.[50] Potential and/or established applications for magnetorheological fluids based on ionic liquids are vast (from engineering devices to medical therapies) and are briefly addressed in the work.[51]

1.3 References

[1] Wikipedia, the free encyclopedia, *Materials science*, http://en.wikipedia.org/wiki/Materials_science (accessed: July 2, **2007**).
[2] J. G. Bednorz, K. A. Mueller, *Rev. Mod. Phys.* **1988**, *60*, 585.
[3] M. Meschke, W. Guichard, J. P. Pekola, *Nature* **2006**, *444*, 187.
[4] A. Alam, T. Saha-Dasgupta, A. Mookerjee, A. Chakrabarti, G. P. Das, *Phys. Rev. B* **2007**, *75*, 134203.
[5] M. M. Ozer, Y. Jia, Z. Y. Zhang, J. R. Thompson, H. H. Weitering, *Science* **2007**, *316*, 1594.
[6] H. Kahn, R. Ballarini, J. J. Bellante, A. H. Heuer, *Science* **2002**, *298*, 1215.
[7] G. A. Gogotsi, *Powder Metall. Met. Ceram.* **2006**, *45*, 328.
[8] S. Cavalu, V. Simona, C. Albona, C. Hozan, *J. Optoelectron. Adv. Mater.* **2007**, *9*, 690.
[9] C. Soutis, *Prog. Aerosp. Sci.* **2005**, *41*, 143.
[10] A. J. Allen, G. G. Long, H. Boukari, J. Ilavskya, A. Kulkarni, S. Sampath, H. Herman, A. N. Goland, *Surf. Coat. Technol.* **2001**, *146*, 544.
[11] D. Wouters, U. S. Schubert, *Angew. Chem. Int. Edit.* **2004**, *43*, 2480.
[12] D. Wouters, U. S. Schubert, *J. Mat. Chem.* **2005**, *15*, 2353.

[13] J. Perelaer, B. J. de Gans, U. S. Schubert, *Adv. Mater.* **2006**, *18*, 2101.
[14] D. E. Ingber, C. van Mow, D. Butler, L. Niklason, J. Huard, J. Mao, I. Yannas, D. Kaplan, G. Vunjak-Novakovic, *Tissue Eng.* **2006**, *12*, 3265.
[15] A. Seidel, O. Liivak, S. Calve, J. Adaska, G. D. Ji, Z. T. Yang, D. Grubb, D. B. Zax, L. W. Jelinski, *Macromolecules* **2000**, *33*, 775.
[16] G. Odian, *Principles of polymerization*, 4th ed., Wiley-Interscince: Hoboken, **2004**.
[17] H. R. Kricheldorf, *Polycondensation 2002: Progress in step-growth polymerization and structure-property relationships of polycondensates, 4th Int. Symp. on polycondensates,* Wiley-VCH Verlag, **2003**.
[18] K. Matyjaszewski, *Advances in controlled/living radical polymerization*, *ACS Symp. Ser., 854*, American Chemical Society: Washington, **2003**.
[19] K. Matyjaszewski, *Cationic polymerizations: Mechanisms, synthesis and applications*, Marcel Dekker: Basel, **1996**.
[20] H. L. Hsieh, R. P. Quirk, *Anionic polymerization: Principles and practical applications*, Dekker: New York, **1996**.
[21] M. R. Buchmeiser, *Metathesis polymerization*, Springer: Berlin, **2005**.
[22] T. Keii, *Heterogeneous kinetics: Theory of Ziegler-Natta-Kaminsky polymerization*, Springer: New York, **2004**.
[23] H. Arastoopour, *Advanced technologies for fluid-particle systems*, American Institute of Chemical Engineers: New York, **1999**.
[24] A. M. van Herk, *Chemistry and technology of emulsion polymerization*, Blackwell Publishing: Oxford, **2005**.
[25] V. Dragutan, R. Streck, *Catalytic polymerization of cycloolefins: Ionic, Ziegler-Natta, and ring-opening metathesis polymerization*, Elsevier: Amsterdam, **2000**.
[26] P. W. Morgan, *Condensation polymers by interfacial and solution methods*, Interscience Publishers: New York, **1965**.
[27] R. Kiebooms, A. Aleshin, K. Hutchinson, F. Wudl, A. Heeger, *Synth. Met.* **1999**, *101*, 436.
[28] K. Matyjaszewski, Y. Gnanou, L. Leibler, *Macromolecular engineering: Precise synthesis, materials properties and applications*, Wiley: Weinheim, **2007**.
[29] N. Hadjichristidis, S. Pispas, G. Floudas, *Block copolymers synthetic strategies, physical properties, and applications*, Wiley-Interscince: Hoboken, **2003**.
[30] D. R. Paul, S. Newman, *Polymer blends*, Academic Press: New York, **1978**.
[31] M. Szwarc, *Nature* **1956**, *78*, 1168.
[32] D. A. Tomalia, D. P. Sheetz, *J. Polym. Sci.* **1966**, *4*, 2253.
[33] M. F. Kemmere, T. Meyer, *Supercritical carbon dioxide in polymer reaction engineering*, Wiley-VHC: Weinheim, **2005**.
[34] M. Deetlefs, K. R. Seddon, *Chim. Oggi* **2006**, *24(2)*, 16.
[35] P. Wasserchеid, T. Welton, *Ionic Liquids in Synthesis*, Wiley-VCH Verlag: Weinheim, **2003**.
[36] P. Kubisa, *Prog. Polym. Sci.* **2004**, *29*, 3.
[37] K. C. Nicolau, R. Hanko, W. Hartwig, *Handbook of Combinatorial Chemistry*, Wiley-VCH: Weinheim **2002**.
[38] M. A. R. Meier, R. Hoogenboom, U. S. Schubert, *Macromol. Rapid Commun.* **2004**, *25*, 21.
[39] N. Hadjichristidis, H. Iatrou, S. Pispas, M. Pitsikalis, *J. Polym. Sci. Part A: Polym. Chem.* **2000**, *38*, 3211.
[40] C. O. Kappe, *Angew. Chem. Int. Ed.* **2004**, *43*, 6250.
[41] R. Hoogenboom, R. M. Paulus, A. Pilotti, U. S. Schubert, *Macromol. Rapid Commun.* **2006**, *27*, 1556.
[42] N. Winterton, *J. Mater. Chem.* **2006**, *16*, 4281.
[43] R. D. Rogers, K. R. Seddon, *Ionic Liquids: Industrial Applications for Green Chemistry*, *ACS Symp. Ser., 818*, Oxford University Press: Oxford, **2002**.
[44] J. M. Lehn, *Supramolecular Chemistry: Concepts and Perspectives*, VCH: Weinheim, **1995**.
[45] Y. He, Z. Li, P. Simone, T. P. Lodge, *J. Am. Chem. Soc.* **2006**, *128*, 2745.
[46] Y. He, T. P. Lodge, *J. Am. Chem. Soc.* **2006**, *128*, 12666.
[47] M. Kramer, J. F. Stumbe, H. Turk, S. Krause, A. Komp, L. Delineau, S. Prokhorova, H. Kautz, R. Haag, *Angew. Chem. Int. Ed.* **2002**, *41*, 4252.
[48] C. Allen, J. Han, Y. Yu, D. Maysinger, A. Eisenberg, *J. Control. Release* **2000**, *63*, 275.
[49] J. Rabinow, *Proc. AIEE Trans.* **1948**, *67*, 1308.
[50] J. D. Carlson, *US Patent 6 475 404*, **2002**.
[51] S. Odenbach, in *Magnetoviscous effects in ferrofluids*, *Lecture notes in Physics: Monograph 71*, Springer-Verlag: Berlin, **2002**.

CHAPTER 2

Automated parallel anionic polymerization: Enhancement of an important synthetic technique in polymer science

Abstract

Anionic polymerizations were successfully carried out in a commercially available automated parallel synthesizer. The main problems related to the implementation of this synthetic procedure in the automated synthesizer were addressed as well as some examples of the potential applications of this experimental technique. The results obtained have shown that the automated parallel approach allows performing detailed kinetic investigations of anionic polymerization reactions in a remarkable short period of time. The obtained results were reproducible and in concordance with literature knowledge. In addition, the feasibility of synthesizing block copolymer libraries via sequential anionic polymerization within the automated synthesizer was demonstrated, including the synthesis of block copolymers at low reaction temperatures (−78 °C). Thus, one of the most demanding synthetic approaches in polymer chemistry has been successfully introduced into a combinatorial and high-throughput workflow. This new automated approach for anionic polymerizations may allow accelerating the systematic synthesis of new materials and research in the field.

Parts of this chapter have been published: (1) C. Guerrero-Sanchez, U. S. Schubert, *Polym. Mat. Sci. Eng.* **2004**, *90*, 647. (2) C. Guerrero-Sanchez, C. Abeln, U. S. Schubert, *J. Polym. Sci. Part A: Polym. Chem.* **2005**, *43*, 4151. (3) C. Guerrero-Sanchez, U. S. Schubert, *Chim. Oggi* **2005**, *23(6)*, 24. (4) C. Guerrero-Sanchez, R. M. Paulus, M. W. M. Fijten, M. J. de la Mar, R. Hoogenboom, U. S. Schubert, *Appl. Surf. Sci.* **2006**, *252*, 2555.

2.1 State of the art of experimental techniques in anionic polymerization

In synthetic polymer chemistry one of the main goals is the preparation of well-defined molecular architectures due to the fact that this determines to a large extent the final properties of the materials. Synthetic polymerization approaches proceeding in the absence of chain transfer and chain termination reactions are suitable and well-known for obtaining well-defined polymers with a high degree of homogeneity. The discovery of the polymerization of styrene induced by an electron transfer reaction from sodium naphthalenide in the absence of chain transfer and termination reactions five decades ago gave birth to the field of "living" polymerizations and to one of the most widely used synthetic techniques for the preparation of well-defined polymeric moieties: anionic polymerization.[1]

During the fifty years after the discovery of "living" anionic polymerizations other synthetic approaches aiming at the preparation of polymers with controlled architectures have been developed based on the same principle of absence or strong suppression of chain transfer and termination reactions (*e.g.,* controlled radical polymerizations (CRP)[2] and cationic ring-opening polymerizations (CROP)[3]). These synthetic approaches have shown some advantages and limitations in comparison to the anionic polymerization mechanism. Among the CRP synthetic techniques three main mechanisms can be identified: atom transfer radical polymerization (ATRP),[4] nitroxide mediated radical polymerization (NMRP)[5] and reversible addition-fragmentation chain transfer (RAFT).[6] Even though CRP techniques show a good tolerance against impurities in the reaction systems, some main drawbacks still have to be solved: difficult purification of the synthesized polymers (ATRP), long reaction times and high reaction temperatures (NMRP) as well as the obtaining colored polymers (RAFT).[7] For these reasons, "classical" "living" anionic polymerization techniquesare still widely used in research as well as in industry.[8] Unlike "living" anionic polymerizations, termination reactions can (always) occur in CRP techniques.

However, the main drawback related to anionic polymerization (and other ionic polymerizations such as CROP) is the extremely high reactivity of the anionic species towards impurities present in the involved chemical reagents and the reaction environment (oxygen, moisture, and carbon dioxide).[9] This feature has obligated synthetic polymer chemists to develop specific experimental setups and techniques to avoid spontaneous termination reactions of the reactive species.[10] Even though anionic polymerization can be a time-consuming technique and requires customized setups, synthetic polymer chemists have been willing to overcome these disadvantages due to its high potential of synthesizing complex and well-defined polymeric structures with low polydispersity indices and with a full control over the molecular structure. For these reasons, anionic polymerization has provided both, model materials to perform novel studies in polymer physics[12] as well as commodity polymers on industrial scale[8b] since its appearance 50 years ago.[1]

Laboratories performing anionic polymerizations around the world have mainly used of two experimental techniques: high-vacuum and inert atmosphere (schlenk technique).

The development of high-vacuum techniques started few years after the discovery of anionic polymerization due to the fact that it was noticed that obtaining narrow molecular weight distributions in the anionic polymerization of styrenic monomers is dependent on the rigorousness of the used experimental techniques.[13] Therefore, in the early 1960's the description of setups for performing anionic polymerizations of styrene and isoprene under high vacuum environment started to be published.[14] For the middle of 1970's a full compendium of setups (including polymerization reactors, treatment of glassware, removal of air from liquids, distillation of liquids in vacuum systems, preparation of sodium mirrors, determination of the activity of the initiators, etc.) was described in detail in the literature.[10a] Thereafter, high-vacuum techniques have been further modified and improved to allow the synthesis of well-defined polymeric architectures with a high degree of complexity (*e.g.*, block copolymers, star polymers, comb-shaped polymers, block-graft copolymers, branched architectures, cyclic polymers, and functional polymers)[11] (see for example Figure 2-1). Detailed reviews summarizing these latter

improvements have been recently published in the literature.[10b,d] Thus, anionic polymerizations utilizing high-vacuum techniques have been and are still extensively used for the preparation of novel and well-defined macromolecules. However, the required demanding glass blowing techniques and the limited scale of polymers that can be synthesized are still their main drawbacks (see for example Figure 2-1b).[10b]

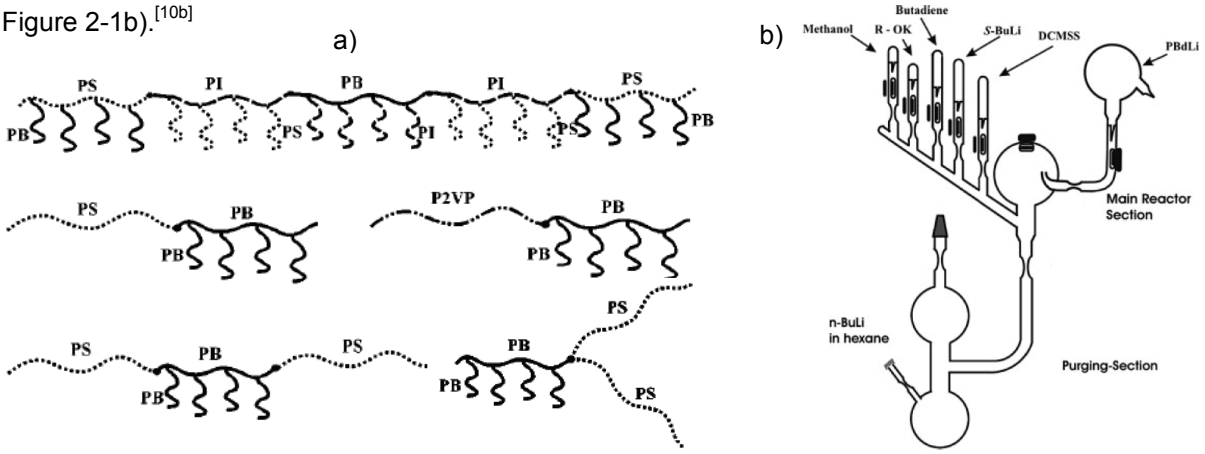

Figure 2-1: *(a) Schematic representation of block-graft and miktoarm star copolymers (adapted from reference[11d]) (b) Schematic representation of an anionic polymerization setup based on high-vacuum techniques for the synthesis of linear/star double combs and double-molecular brushes (adapted from reference[11e]).*

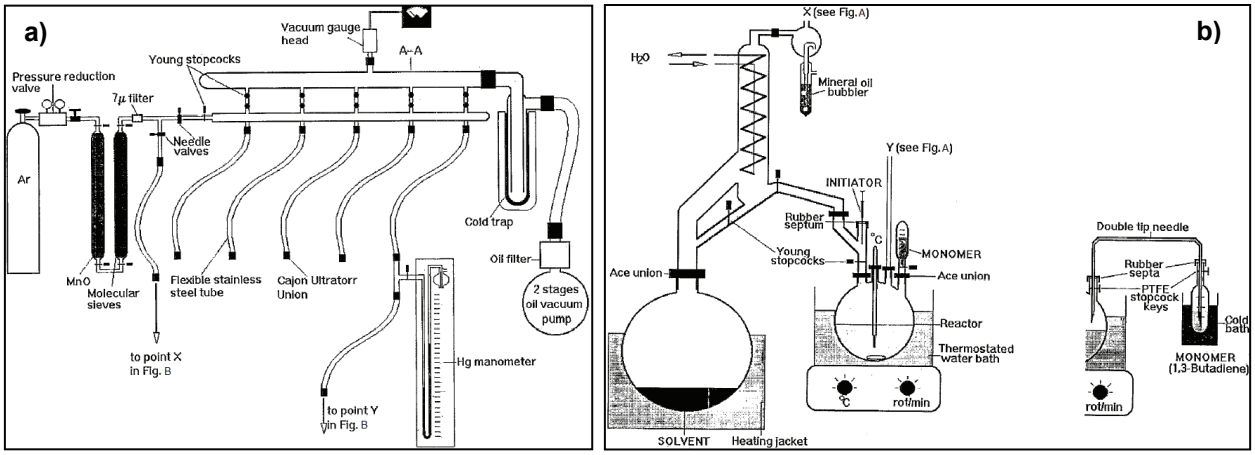

Figure 2-2: *Schematic representation of an anionic polymerization setup based on inert atmosphere techniques. (a) shows an arrangement to supply an inert gas (argon) to distillation and reaction setups displayed in (b) (adapted from reference[10c]).*

Due to the fact that it can take several days to synthesize one sample of polymer by anionic polymerization using high-vacuum techniques, a “faster” experimental technique, inert atmosphere,[15] was developed almost parallel to high-vacuum techniques. With time several detailed descriptions about the use of inert atmosphere techniques in anionic polymerization have been published.[10c, 16] The principle of these techniques is the application of a slight overpressure of an inert gas (normally nitrogen, argon or helium) into polymerization reactors and/or distillation setups after thorough flaming of the apparatus and/or glassware (see Figure 2-2). Among the main advantages of using the inert atmosphere experimental approach are: the time required for the preparation of a polymer moiety is reduced considerably, larger amounts can be synthesized in one experiment, and sampling during the polymerization reactions for kinetics investigations is feasible. Even though the characteristics of the polymers synthesized using the inert atmosphere techniques are comparable to those obtained by high-vacuum techniques, a main restriction for the inert atmosphere technique is that the synthesis of polymers of high molecular weight and/or very complex architectures (such as those depicted in

Figure 2-1a) becomes very difficult due to the presence of impurity traces that can terminate the growing polymeric chains during the polymerization reactions.

Despite of the advantages that anionic polymerization can offer in terms of synthetic capabilities, the use of their experimental techniques is not trivial and requires intensive purification procedures of the reagents as well as oxygen- and moisture-free reaction conditions to obtain reliable results.[10] These limitations have restricted the development of experimental setups to a "one at time" synthetic approach, which is a slow research process. In addition, anionic polymerization experiments may be difficult to reproduce in certain cases (*e.g.*, in inert atmosphere techniques), mainly due to an ineffective and inhomogeneous removal of impurity traces for different experiments performed in a specific set up. This is obviously an important aspect to take into account in research (for example, in kinetic investigations) to obtain reliable results and conclusions. For these reasons, the development of a faster and reliable experimental approach (in terms of reproducibility) to perform anionic polymerization reactions would be very useful. Such an experimental approach would allow accelerating research in the field of anionic polymerization and establishing more accurate structure-property relationships of polymeric materials by synthesizing systematically and faster different polymers.

2.2 A high-throughput approach as a new experimental technique and method to speed-up research in anionic polymerization

So far anionic polymerization reactions were mainly performed using the two aforementioned experimental techniques, which have been relatively time-consuming and difficult to implement. Thus, these techniques are considered as "classical" lab-scale synthetic approaches. However, with the advent of automation, the tendency of performing automated, parallel and high-throughput experimentation in order to accelerate the development of new products or research approaches has grown considerably in recent years. These experimental approaches have been already successfully implemented in many fields of chemistry such as the pharmaceutical industry.[17] In this regard, polymer research has not been an exception.[18] New findings and polymeric materials have been achieved applying (automated) parallel experimentation approaches in a short time.[19-22] Combinatorial and high-throughput techniques have found applications ranging from kinetic studies of polymerization mechanisms,[19] via coating technology[20] and library preparation[21] to the development and evaluation of novel polymerization catalysts.[22] The use of combinatorial and high-throughput experimental techniques has obvious advantages over the "classical" lab-scale synthetic approaches: (1) Savings of time and resources; (2) speeding-up the research; (3) all the experiments are performed under the same reaction conditions (*e.g.,* same reactors, same inert atmosphere, same experimental error, etc.) and therefore the obtained results are easily comparable and reproducible. Significant advances in performing automated parallel synthesis for almost all sort of polymerization methods have been reported recently.[18-22] However, oxygen and moisture sensitive polymerization (*e.g.,* anionic, cationic or polymerizations of olefins) are difficult to implement in an automated and parallel fashion due to the fact that different levels of impurities in different reaction chambers might cause problems of experimental reproducibility. Recently, the automated parallel synthesis of poly(olefins) and polymers via cationic polymerization have been reviewed.[18c,d] Nevertheless, the incorporation of anionic polymerization into a high-throughput experimental workflow has not been discussed in the open literature until now. This might be related to the fact that such an implementation is not a straight forward task due to the discussed characteristics of anionic polymerization (*e.g.*, remarkable sensitivity towards oxygen and moisture).[10] Hence, the development of such experimental approach would be of great interest and help for the synthetic polymer chemists. This would provide, for instance, well-defined polymer libraries for systematic investigations in polymer science. Therefore, the main discussion of this chapter focuses on the implementation of anionic

polymerization processes in a commercially available automated parallel synthesizer using the inert atmosphere approach. Special emphasis is placed on the problems that had to be solved to obtain reproducible and reliable results in the setup. Thereafter, application examples of this experimental technique are discussed such as the possibility to perform detailed kinetic studies in a short time and the construction of block copolymer libraries. These examples are the preamble for the detailed discussion about more specific and complex synthetic tasks such as the synthesis of a new library of block copolymers and functionalized polymers, which are presented in chapter 3.

2.3 Automated parallel anionic polymerizations: Incorporation of the synthetic technique into a high-throughput experimental workflow

The experimental method derived from the implementation of anionic polymerization in a commercially available automated parallel synthesizer can be classified under the category of the inert atmosphere techniques due to the use of a glove box with a slight overpressure of an inert gas (argon) (see experimental part for a complete description of the synthesizer). Figure 2-3 displays images of the automated synthesizer used during the experiments of this chapter.

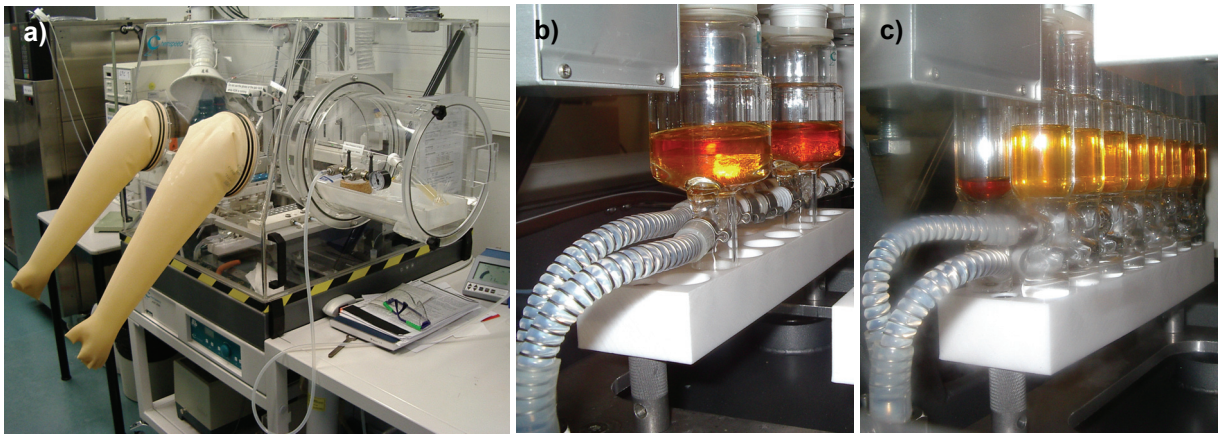

Figure 2-3: *(a) Overview of a Chemspeed ASW2000 synthesizer used during the automated parallel anionic polymerization of styrene. The glove box provides an inert atmosphere in the interior of the apparatus. The polymerizations can be performed in two different reaction volumes ((b) 75 mL or (c) 13 mL) (see experimental part for a complete description of the synthesizer).*

The main challenge that had to be solved before achieving a successful performance of the experimental method proposed was related to the reproducibility of anionic polymerization reactions carried out in the parallel synthesizer. Even though the use of a glove box provides an acceptable inert atmosphere in the interior of the apparatus, it was found that different levels of impurities in the reactors of the synthesizer provoke a lack of reproducibility in the experiments or simply the polymerizations were not initiated properly. Hence, a homogeneous and effective removal of all impurities in the different reaction vessels of the synthesizer was mandatory before performing parallel anionic polymerization experiments. In order to overcome this problem, a simple method was developed to reach the required inert conditions for reproducible experiments. This inertization method is performed in an automatic fashion using the liquid handling system of the synthesizer and consists of the following steps for a 13 mL reactor: (1) The glove box of the apparatus is exposed to a continuous argon flow overnight, while the reactors of the synthesizer were heated to 140 °C and exposed to 6 cycles of subsequently filling with argon (5 min) and applying vacuum (25 min) in order to eliminate as much oxygen and moisture as possible from the glass walls of the vessels. (2) 0.5 mL of *sec*-butyllithium (*s*-BuLi) (from a vial cooled to

5 °C) and 5 mL of cyclohexane were added into the reactors, followed by the mixing of the solutions with the vortex system (1000 rpm) for 1.5 h at room temperature and for 0.5 h at 50 °C. (3) Subsequently, 5 mL of this latter solution is removed from the reactors and placed into the waste. (4) Thereafter, 2.5 mL of fresh cyclohexane is added into the reactors and the system is kept at 1000 rpm and 50 °C for 0.5 h. (5) The remaining solution is then removed from the reactors by adjusting the aspiration height of the needle of the automated liquid-handling system down to the bottom of the fixed reactors in the synthesizer. (6) Finally, one cycle of filling with argon (5 min) and applying vacuum (25 min) into the reactors at 140 °C is performed. Figure 2-4 shows a schematic representation of the inertization method described.

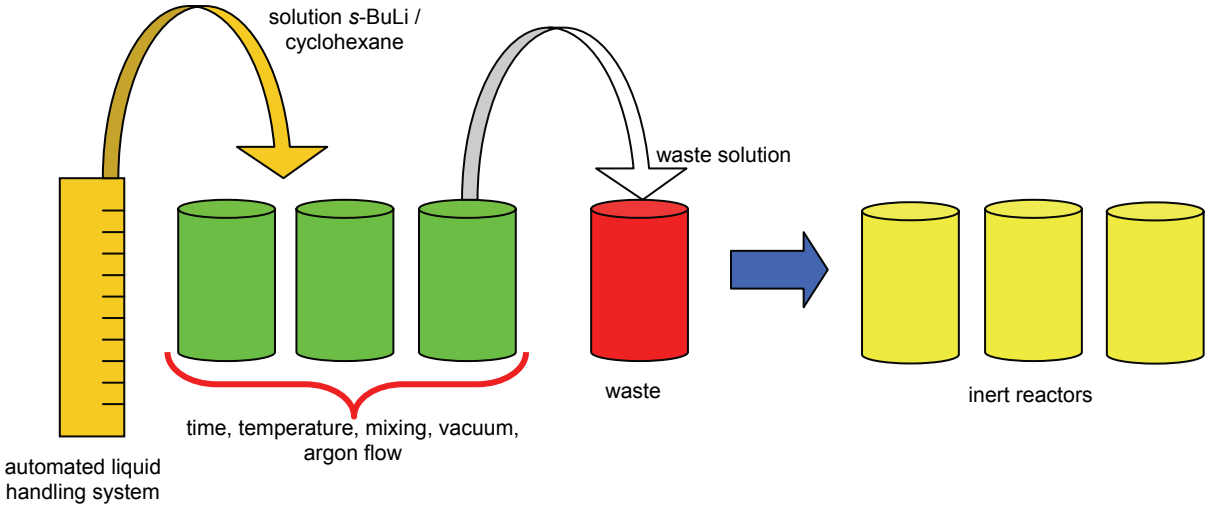

Figure 2-4: *Schematic representation of the method utilized for the homogeneous removal of impurities in the reaction vessels of the automated parallel synthesizer of Figure 2-3. This method must be carried out before performing anionic polymerization experiments in the equipment.*

In order to investigate the effectiveness of the proposed inertization method and the reproducibility of the parallel synthesizer, several reactors were used to study the anionic polymerization of styrene in cyclohexane initiated by *s*-BuLi. All reactors were filled with the same amount of reagents and exposed to the same reaction conditions. For this purpose, two different reaction conditions were investigated: (1) 285 µL of monomer (0.51 M) for 20 µL of initiator and (2) 570 µL of monomer (1.02 M) for 40 µL of initiator. The addition of the reagents into the reaction vessels was performed with the automated liquid-handling system of the synthesizer in the following manner: (1) Styrene monomer was first added into each reactor followed by a chase of cyclohexane (solvent) at the desired reaction temperature and under vigorous mixing (vortex system of the apparatus was set to 450 rpm). (2) Thereafter, the polymerization were initiated upon adding *s*-BuLi into the previously filled reactors with monomer-solvent followed by an extra chase of cyclohexane (solvent) to ensure the complete addition of the required amount of initiator and to adjust the reaction volumes (or reagent concentrations) to the desired values. At the end, the obtained polymers were analyzed by gel permeation chromatography (GPC) in order to determine the molecular weights and to evaluate the reproducibility of the experiments. Figure 2-5 shows the GPC traces of these experiments performed in three different reactors of the synthesizer and using two different reaction conditions; the average of the obtained molecular weight values of the polymers for each experimental set is also shown. According to Figure 2-5, it can be seen that the error of the two different experimental sets was 3%, which is well within the experimental error of the GPC measurements. This clearly shows that parallel and reproducible anionic polymerization experiments can be carried out in the investigated synthesizer. In order to establish the deviation of the experimentally obtained molecular weights from the theoretical or expected value, the real concentration of the utilized initiator had to be determined using the method of double titration.[23] Sampling for the determination of

this concentration was performed with the automated handling liquid system of the apparatus. Before and after the experimentation, two samples of 350 µL were taken from the utilized initiator container and placed in two glass vials of 1.5 mL capped with rubber septa under argon atmosphere. Immediately after sampling, titrations were performed outside the glove box revealing that the concentration of initiator was 1.126 M. According to the obtained concentration of initiator and the reaction conditions used in the experiments of Figure 2-5, the expected molecular weights for a monomodal distribution can be calculated from the monomer to initiator ratio. For both cases the expected molecular weight is 11500 Da, which is in good agreement with the obtained results in Figure 2-5. However, according to Figure 2-5 one can see that the automatic liquid handling system is slightly less accurate for dispensing small amounts of reagents (20 µL) but, in this case, the experimental results are still in concordance with the expected values (with less than 5% of deviation).

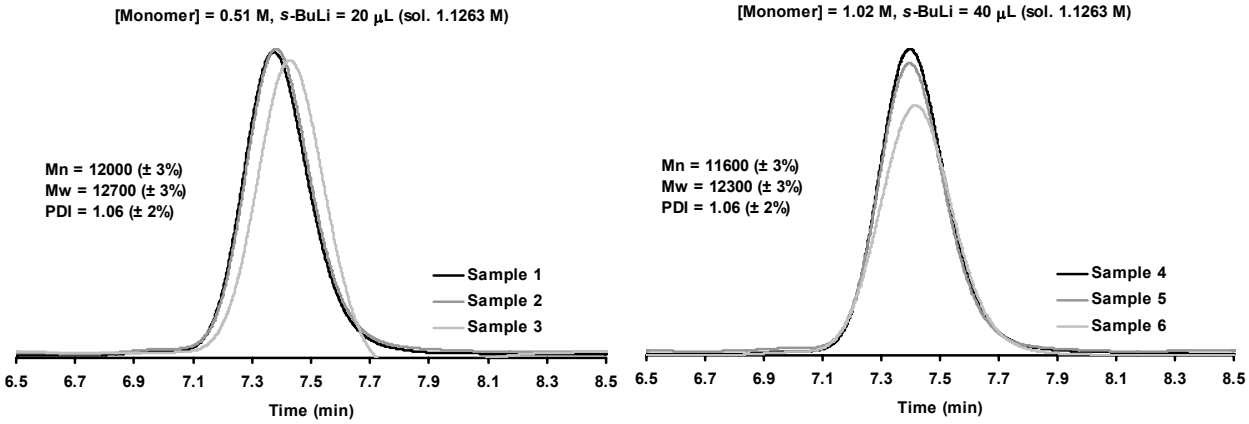

Figure 2-5: *GPC traces of anionic polymerization experiments of styrene in cyclohexane initiated by sec-butyllithium (s-BuLi) performed in different reactors of the automated parallel synthesizer of Figure 2-3. The results show the reproducibility of the experiments.*

2.4 Applications of automated parallel anionic polymerizations

In this section, application examples of the developed automated parallel experimental technique for anionic polymerization reactions are addressed. Thus, the feasibilities to perform detailed kinetic studies in a short time, as well as the preparation of block copolymers at different reaction conditions and libraries are demonstrated.

2.4.1 Kinetic Investigations

One useful application of the implemented high-throughput experimental technique is the possibility to perform detailed and rapid kinetic investigations of the anionic polymerization mechanism. This task is described in this section taking as an example the anionic polymerization of styrene in cyclohexane initiated by *s*-BuLi. The apparent rate constant could be determined for this reaction at different concentrations of monomer and initiator in the temperature range from 10 to 60 °C. In addition, the evolution of the molecular weight and polydispersity index during the polymerization could also be followed by GPC. The obtained results were in concordance with kinetic investigations reported in the literature.[24]

For the kinetic investigations, isothermal experiments were carried out in the automated parallel synthesizer of Figure 2-3 under various reaction conditions. This allowed to perform a detailed study in a short time and practically unattended. A typical experimental procedure (after the application of the

aforementioned inertization method) was as follows. First, the reactors were set at the desired temperature and the vortex system of the equipment was set to 450 rpm then predetermined amounts of solvent (cyclohexane) and monomer (styrene) were added into the reaction vessel using the automated liquid handling system of the apparatus. Subsequently, the polymerization was initiated upon adding *s*-BuLi (from a vial cooled to 5 °C). This addition time was considered as time zero for the kinetic measurements. Thereafter, samples (50 µL) were taken at predetermined times (using the automated liquid handling system) from the reactors and dispensed into 1.5 mL glass vials containing 25 µL of methanol in order to stop the polymerizations (previous to the experimentation, degassed methanol was first added into the glass vials under argon atmosphere and then they were capped with rubber septa). These samples were used to determine both, monomer conversion and the molecular weight of the polymers obtained at the established times. In this work, the monomer conversions were determined by gas chromatography (GC) (see experimental part); however, other analytic techniques can also be used for this purpose (Raman spectroscopy,[24b] GPC[25] and ultraviolet-visible (UV-Vis) spectroscopy[26]).

Figure 2-6 summarizes the results for the polymerizations performed at different reaction conditions in the automated synthesizer. For these experiments the temperature has been systematically varied for different concentrations of monomer and initiator. Linear dependencies of the time as a function of –ln(1–X) (where X is the monomer conversion) and of the conversion as a function of the molecular weight can be observed in Figure 2-6 for all the investigated reaction conditions. This indicates the "living" character of the performed anionic polymerizations.[9] In Figure 2-6 it can also be observed that the polydispersity index (PDI) values of the polymers at the end of the reaction were around 1.10 or below, except for the case of a higher monomer concentration and a lower level of initiator (higher molecular weights expected). For this latter case, the obtained PDI values were between 1.15 and 1.25.

In order to determine the activation energy of the apparent rate constant for the studied reactions, the polymerizations were considered to have a pseudo-first order kinetic behavior and obey the following kinetic expression:

$$-\frac{d[M]}{dt} = k_p[M][P*]$$

where $[M]$ and $[P*]$ represents the concentrations of monomer and of the "living" propagating species, respectively, t is the time, and k_p the propagation rate constant. Because the concentration of "living" propagating species remain constant and is equal to the concentration of initiator in polymerization reactions showing "living" characteristics,[9] k_p and $[P*]$ can be comprised in an apparent rate constant k_{app}. Thus, the integration of the previous kinetic equation for isothermal conditions yields:

$$\ln\frac{[M]}{[M]_O} = -k_{app}t$$

$$\ln(1-X) = -k_{app}t$$

where $[M]_O$ is the initial concentration of monomer, and X the monomer conversion. With this approach, the values of k_{app} can be easily obtained from the slopes of plots of $-\ln(1-X)$ vs. t shown in Figure 2-6 for the different reactions conditions investigated.

In addition, the values of Ln(k_{app}) can be plotted against the inverse of the temperature (1/T) in order to obtain the corresponding Arrhenius plots. Thereafter, the activation energy of the apparent rate constant of the polymerization reactions investigated can be determined from the slopes of the linear relationships of Ln(k_{app}) against the inverse of the temperature (1/T) of the respective plots and according to the Arrhenius' equation:

$$k_{app} = Ae^{\left(-\frac{Ea}{RT}\right)}.$$

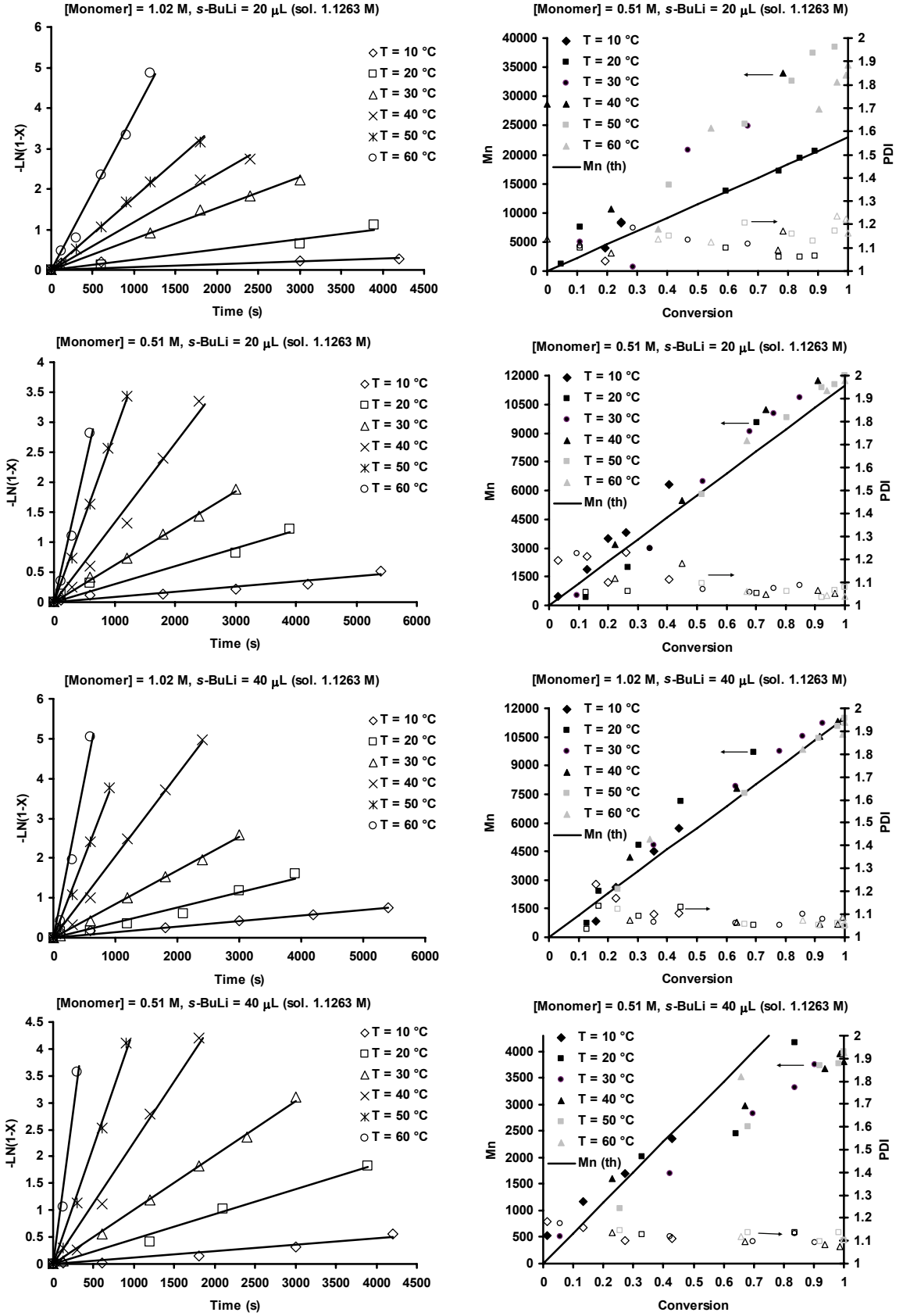

Figure 2-6: *Experimental results for the kinetic investigations obtained for anionic polymerization experiments of styrene in cyclohexane initiated by sec-butyllithium (s-BuLi) performed under different reaction conditions in the synthesizer of Figure 2-3.*

Figure 2-7 shows the Arrhenius plots obtained for each of the investigated reaction conditions, as well as the values of the corresponding activation energies. As expected due to the fact that it is the same polymerization system, the values of the activation energy obtained were very similar for the four different cases investigated. Other values of activation energy, reported in the literature, for the propagation reaction of the anionic polymerization of styrene in different solvents are shown in Table 2-1, as well as the value obtained in this investigation. According to the data given in Table 2-1, the activation energy found in this work is in good agreement with those reported in the literature where hydrocarbon solvents were used. However, values of activation energy as low as 1 kJ mol^{-1} for the same polymerization reaction have been reported[27] when it is performed in polar solvents (*e.g.*, tetrahydrofuran (THF)).

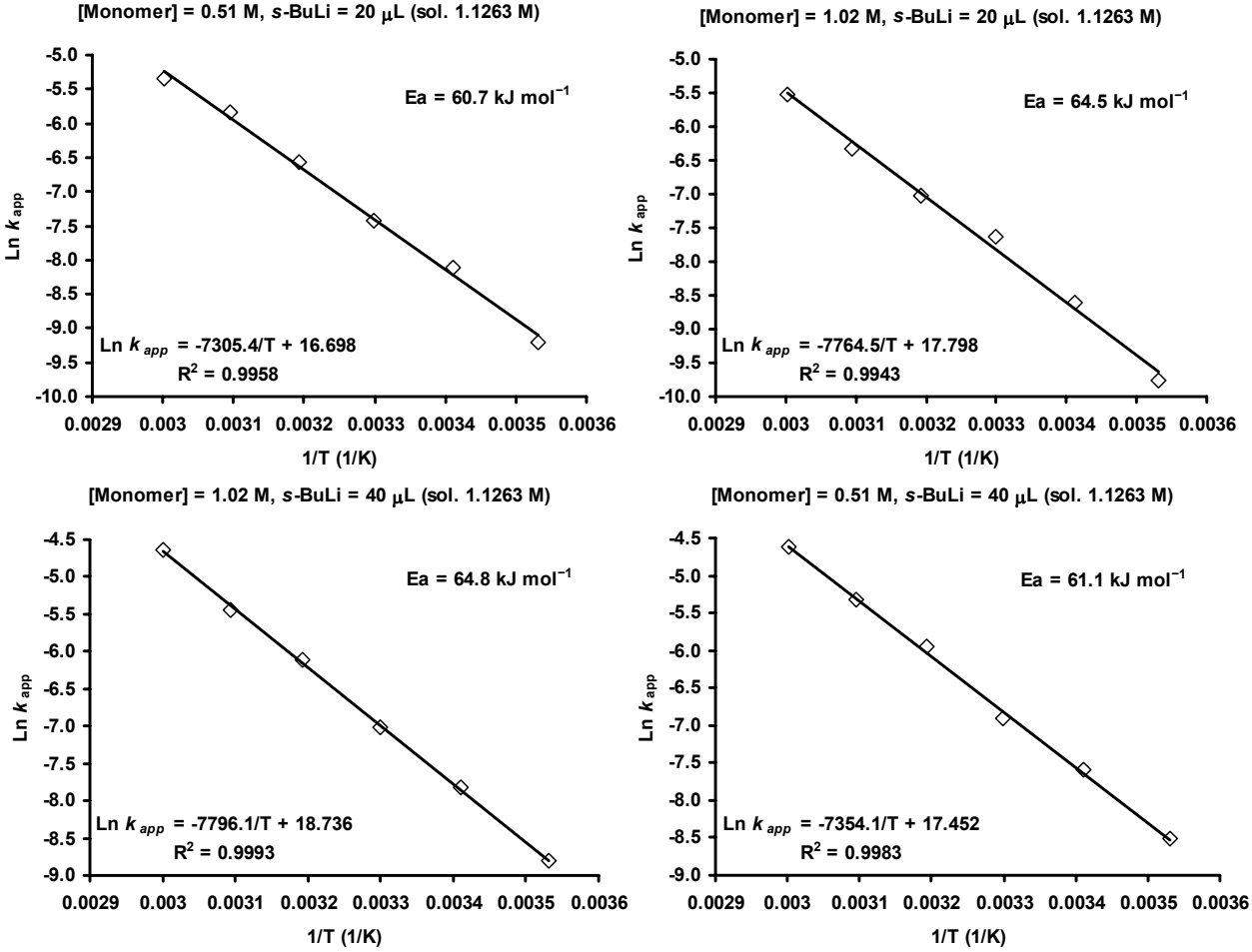

Figure 2-7: *Arrhenius plots for the determination of the activation energy (Ea) of the propagation reaction of the anionic polymerization of styrene in cyclohexane initiated by sec-butyllithium (s-BuLi). The plots are obtained from the experimental data of the kinetic investigations of Figure 2-6.*

Table 2-1: *Values of the activation energy reported for the propagation reaction of the anionic polymerization of styrene in different solvents.*

Solvent	Activation energy kJ mol^{-1}	Reference
Ethylbenzene	75	24b
Benzene	59.9	24g
Toluene	64.8	24h
Toluene	59.9	24i
Cyclohexane	62.7 ± 2.2	This work

One interesting application of the developed experimental technique is the possibility of following, in detail, the evolution of the molecular weight distributions in time of the polymers formed during the anionic

polymerization. Figure 2-8 displays an example of such experimental determinations with the automated parallel synthesizer utilized.

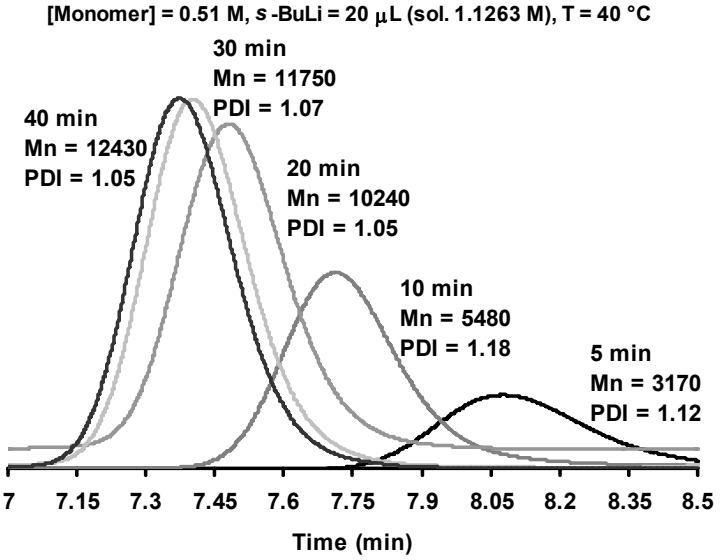

Figure 2-8: *Evolution of the molecular weight distribution in time of polystyrene synthesized by anionic polymerization in the synthesizer of Figure 2-3.*

The screening of all the variables (*e.g.*, solvents, counter-ions, reaction temperature, polar modifiers, and reagent concentrations) that influence the reaction mechanism and the final properties of the polymers synthesized by anionic polymerization is a resource- and time-consuming task. Therefore, the automated parallel anionic polymerization procedure demonstrated in this work could be a valuable tool to explore the synthetic parameter space in greater detail and in shorter times. In addition, this experimental method may allow, for instance, accelerating the anionic synthesis of well-defined and model polymeric materials for establishing structure-property relationships in shorter times.

2.4.2 Synthesis of block copolymers

Another application of the proposed experimental procedure is the possibility of synthesizing, in an automated and in a systematic way, block copolymer libraries covering the full-range of block compositions. Thus, in this section the implementation of sequential anionic polymerizations in the utilized synthesizer is discussed. For this purpose, two synthetic approaches were selected: (1) The synthesis of a block copolymer library using moderate reaction temperatures (30 - 55 °C) (case of poly(styrene-*block*-isoprene) (PS-*b*-PI) in cyclohexane) and (2) the synthesis of block copolymers at low reaction temperatures (−78 °C) (case of poly(styrene-*block*-methyl methacrylate) (PS-*b*-PMMA) in a THF/cyclohexane mixture).

The synthetic method for the first approach is summarized in Figure 2-9, where an image of the automated synthesizer is also displayed during the experiment. Besides the inertization procedure discussed before, this synthetic method consisted of the following steps: (1) Predetermined amounts of styrene were polymerized in cyclohexane at 50 °C for 1 h simultaneously in multiple reactors of the synthesizer, using *s*-BuLi as initiator. (2) Subsequently, predetermined amounts of isoprene were slowly added (1 mL min^{-1}) into the different reactors at 20 °C. (3) The resulting mixtures were allowed to react for 6 h. Note that after the synthesis of the first blocks, samples were taken from the reactors in order to determine their molecular weights and to verify whether the formation of the different block copolymers

occurred upon looking at the effectiveness of the polymer chain extension process. To investigate this process, sampling from the reactors and GPC measurements were performed for each compound as described before (see experimental part). (4) Finally, the obtained block copolymers were manually precipitated in methanol and dried in a vacuum oven at 40 °C overnight before further analysis by proton nuclear magnetic resonance (^{1}H-NMR) spectroscopy.

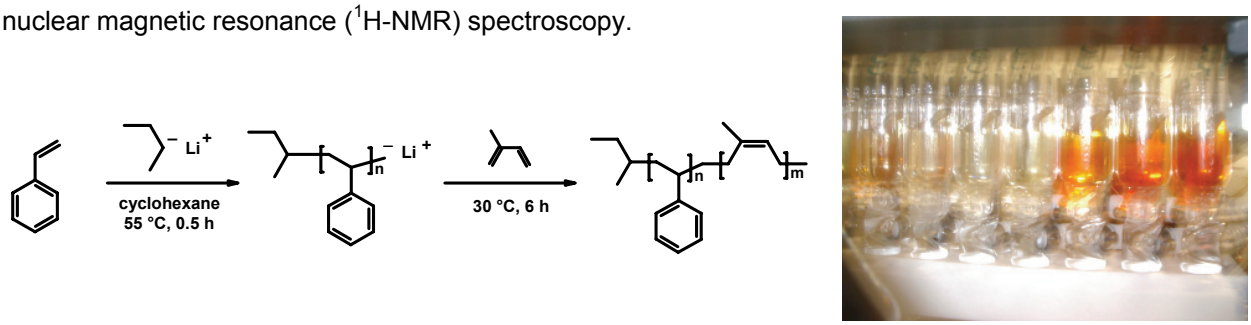

Figure 2-9: *Left: Schematic representation of the synthesis of poly(styrene-block-isoprene) block copolymers via sequential anionic polymerization. Right: Image of the synthesizer during the polymerization experiment.*

Table 2-2 summarizes the specifications of a block copolymer library of PS-*b*-PI synthesized utilizing the described method. Figure 2-10 depicts the obtained GPC traces of polystyrene (PS) homopolymer precursors as well as their corresponding chain extended PS-*b*-PI block copolymers, whereas Figure 2-11 shows selected ^{1}H-NMR spectra of some of the materials synthesized. The ^{1}H-NMR signals related to the functional groups of each block can be observed in the spectra displayed in Figure 2-11 (the aromatic protons of the styrenic block arise between 6.5 and 7.5 ppm, the residual double bonds of the poly(isoprene) (PI) around 5.1 ppm), which have been used for the estimations of mol % of PI obtained in the block copolymers (Table 2-2).

Table 2-2: *Molar masses and PDI values as obtained by GPC measurements (see Figure 2-10 for the corresponding traces) of a seven member block copolymer library of poly(styrene-block-isoprene) (PS-b-PI) prepared via sequential anionic polymerization in the automated parallel synthesizer (characteristics of the precursor and final polymers are shown). The composition of poly(isoprene) (PI) in the block copolymers obtained by ^{1}H-NMR are also summarized.*

Exp.	Mn (kDa) / PDI (GPC) PS (precursor)	Mn (kDa) / PDI (GPC) PS-*b*-PI (block copolymer)	Mol % (^{1}H-NMR) PI
1	1.2 / 1.16	26.7 / 1.20	91
2	1.8 / 1.13	19.9 / 1.09	79
3	2.8 / 1.15	18.6 / 1.09	76
4	6.5 / 1.08	12.2 / 1.13	58
5	6.8 / 1.08	14.0 / 1.11	45
6	7.4 / 1.15	13.1 / 1.12	39
7	10.2 / 1.09	12.2 / 1.11	21

The chain extension process related to the formation of the block copolymers can be clearly seen in the GPC traces of Figure 2-10. However, in the GPC traces of Figure 2-10 it can also be observed that the chain extension process is not 100% effective due to the presence of small peaks in the corresponding traces of the block copolymers arising at the same elution time of the precursor homopolymers. It is obvious that these small peaks are related to the presence of impurity traces in the polymerization system, which terminates with a fraction of the reactive and growing polymeric chains. For instance, this fraction of un-reacted homopolymer can be calculated from the relative intensities in the signals of the respective peaks of the GPC measurements where the peaks are well-apart from each other (*e.g.*, Exps. 1 to 4 in Figure 2-10). Thus, it was found that the fraction of un-reacted homopolymer during the sequential anionic polymerization reactions of Figure 2-10 was 0.051, 0.050, 0.038, and 0.098 for Exps. 1, 2, 3, and 4, respectively. The fraction of un-reacted homopolymer can be removed from the final products, for instance by fractionation using preparative GPC systems. In addition, this fraction of

un-reacted homopolymer can be reduced or avoided by eliminating the presence of impurity traces more effectively, either by improving the purification methods of the reagents (especially for the second monomer addition) or by improving the quality of the inert atmosphere in the synthetic setups (*e.g.*, the features of the glove box in the case of the parallel synthesizer utilized in this work). The PDI values of the block copolymers obtained from Exps. 1 to 4 (Table 2-2) correspond to the main peak of the respective GPC traces without taking into account the peak related to the fraction of un-reacted homopolymer precursors.

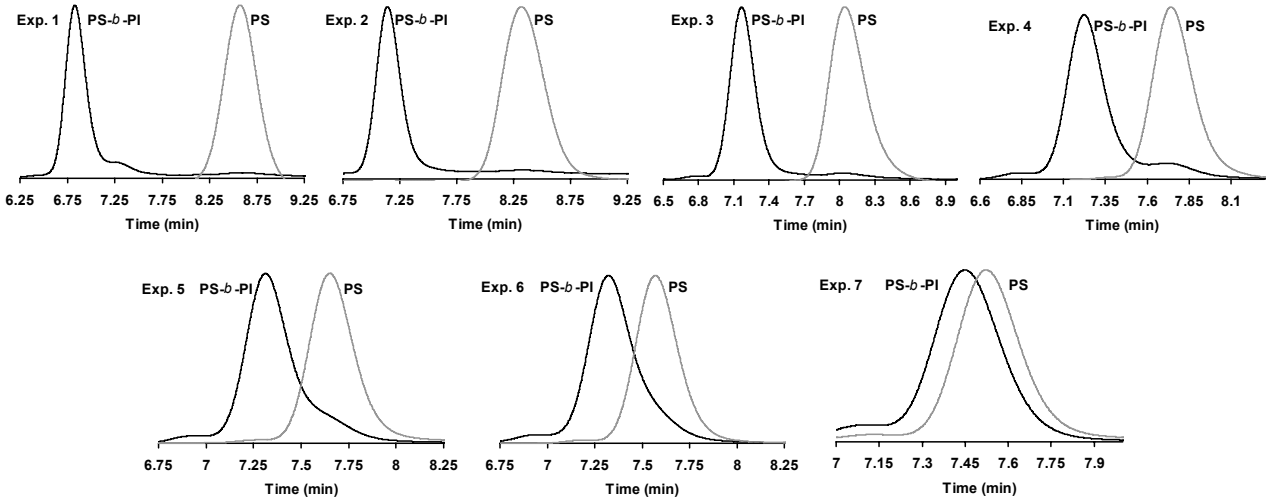

Figure 2-10: *GPC traces of a block copolymer library of poly(styrene-block-isoprene) (Table 2-2) synthesized via sequential anionic polymerization in the synthesizer (traces for the precursor (PS) and final polymers (PS-b-PI) are shown in each case).*

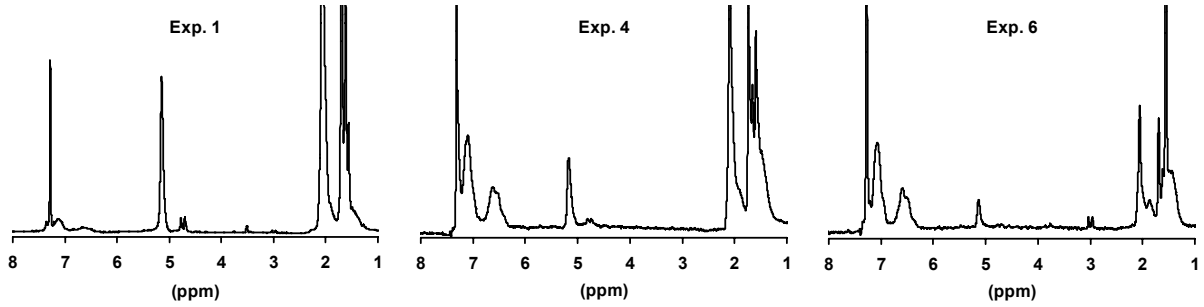

Figure 2-11: *^{1}H-NMR spectra of selected polymers of a block copolymer library of poly(styrene-block-isoprene) (Table 2-2) synthesized via sequential anionic polymerization in the synthesizer.*

The second example related to the preparation of block copolymers uses an experimental method taken from literature,[28] which was modified from its original version in order to investigate the synthesis of PS-*b*-PMMA block copolymers within the automated parallel synthesizer. Figure 2-12 summarizes this sequential anionic polymerization procedure and shows images of different stages of the polymerization in the parallel synthesizer. In this case the characterization of the obtained materials was performed in a similar way as described before for the synthesis of (PS-*b*-PI). Note that in the reaction scheme displayed in Figure 2-12, an intermediate reaction step consisting of an end-capping reaction of poly(styryl) anions with 1,1-diphenylethylene (DPE) is necessary in order to reduce the reactivity of the poly(styryl) anions and to promote a proper incorporation of the first methyl methacrylate (MMA) monomeric unit into the reactive PS chains (avoidance of spontaneous termination of the reactive polymer chains by the undesired reaction between the polymeric anions and the carbonyl groups of MMA instead of the vinyl groups).[28]

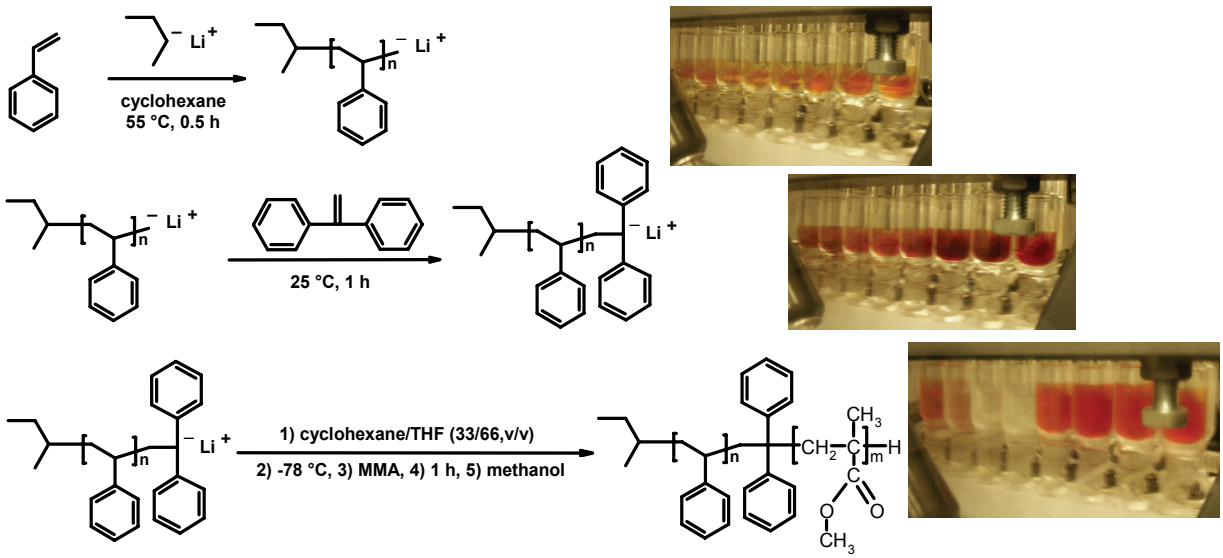

Figure 2-12: *Left: Schematic representation of the synthesis of poly(styrene-block-methyl methacrylate) block copolymers via sequential anionic polymerization. Right: Images of the synthesizer during the polymerization experiment.*

The GPC traces displayed in Figure 2-13 reveal a successful chain extension process during the synthesis of PS-*b*-PMMA block copolymers via sequential anionic polymerization (Figure 2-12). These results demonstrate the feasibility of performing the anionic synthesis of polymers at low reaction temperatures (−78 °C in this case) in the utilized synthesizer. In addition, Figure 2-13 also displays the ^{1}H-NMR spectrum of the block copolymer corresponding to the referred GPC traces, where the signals related to the functional groups of each block (aromatic protons of styrenic block arising between 6.5 and 7.5 ppm and the O-CH_3 group in the acrylic block around 3.7 ppm) can be observed.

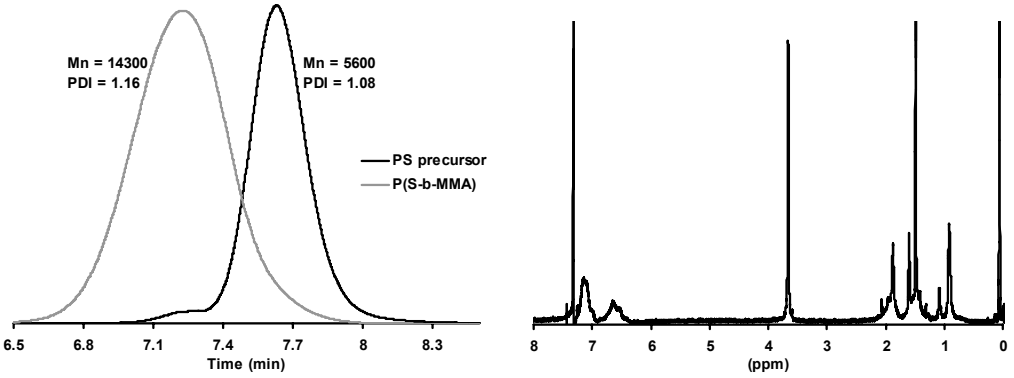

Figure 2-13: *GPC traces (left) and ^{1}H-NMR spectrum (right) of a block copolymer of poly(styrene-block-methyl methacrylate) synthesized via sequential anionic polymerization at −78 °C. The GPC traces of the precursor and final block copolymer reveal a successful chain extension process, which demonstrates the feasibility of performing anionic polymerizations also at such low temperatures in the synthesizer.*

However, it was found that the synthetic procedure utilized for the synthesis of PS-*b*-PMMA block copolymers (Figure 2-12) in the synthesizer is even more sensitive to the presence of impurity traces in the setup than in the case of PS-*b*-PI block copolymers described above. This effect has caused deficient chain extension processes for some of these polymerization reactions performed in the parallel synthesizer. Even though Figure 2-12 displays a complete array of polymerization reactions, only few materials obtained in this experiment showed a successful chain extension process as depicted in Figure 2-13 for one selected case. Other block copolymers obtained during the experiment of

Figure 2-12, which did not show a 100% effective chain extension process, could be successfully purified by fractionation using a preparative GPC system. These observations show that anionic polymerization experiments performed in the parallel synthesizer might become instable and lack reproducibility under the reaction conditions of the scheme displayed in Figure 2-12. The reasons of this instability might be related to the presence of higher concentration of impurities either in the reagents utilized (*e.g.*, the removal of impurity traces is a more difficult process in the cases of THF and MMA compared to cyclohexane as solvent or styrene and isoprene as monomers)[10] or in the inert atmosphere of the apparatus (*e.g.*, it was observed during the experiment that due to the low temperature reaction conditions traces of moisture present in the inert atmosphere started to condensate nearby or inside the polymerization reactors). Obviously, larger amount of impurities in the experimental setup will lead to unstable anionic polymerization reactions. These findings open the possibility to improve, in future research, the inert atmosphere system of the commercially-available synthesizer (*e.g.*, placing the synthesizer in a more suitable glove box, for example in a MBraun™ system) and the purification procedures of the reagents utilized, which are still an important bottleneck in anionic polymerization experiments.

2.5 Conclusions

In this chapter, a new experimental approach for carrying out anionic polymerizations was addressed. This approach is based on the use of a commercially available automated parallel synthesizer as tool to increase the throughput of time-consuming and demanding synthetic techniques. For this purpose, a convenient method to achieve the inert conditions required for obtaining reproducible experiments was developed and performed in an automatic fashion. Examples of the capabilities of this high-throughput technique were also shown. In this regard, a detailed kinetic study of the polymerization of styrene in cyclohexane initiated by *s*-BuLi could be performed in a short time and the obtained results were in agreement with the literature knowledge. In addition, the feasibility of synthesizing block copolymer libraries via sequential anionic polymerization within the automated synthesizer was demonstrated, including the synthesis of block copolymers at low reaction temperatures (−78 °C). However, for this latter case a lack of reproducibility during the synthesis of PS-*b*-PMMA block copolymers could be observed. This observation might be related to the low reaction temperature utilized in the polymerization, which may cause the condensation of moisture traces (still present in the glove box of the synthesizer) close or inside the reaction vessels, and therefore the unexpected termination of the polymerizations. This effect could be minimized by placing the automated synthesizer in a better quality inert atmosphere (*e.g.*, MBraun™ glove box).

In the next chapter, the developed experimental approach is utilized for the synthesis of new polymeric materials. More specifically, the preparation of a block copolymer library of poly(styrene-*alt*-diphenylethylene-*block*-isoprene) with varying block compositions and molecular weights, and their micellization behavior is described. In addition, the automated parallel anionic polymerization procedure is used for the development and optimization of a new synthetic approach that allows the preparation of terpyridine-functionalized polymers.

2.6 Experimental part

All anionic polymerizations were performed in a Chemspeed ASW2000 synthesizer, comprising up to 20 parallel glass reactors of 75 mL or 80 parallel glass reactors of 13 mL equipped with heating/cooling jacket. The systems has a glove box for inert atmosphere, a vortex mixing system (0 to 1400 rpm), heating/cooling system (−90 to 150 °C) and

a fully automated liquid handling system (Figure 2-3). Optional features of the synthesizer are the possibilities to connect on-line gas chromatography (GC) and GPC systems.[19b]

All solvents and monomers were distilled after the corresponding purification procedure[10] and stored under argon. Cyclohexane (Biosolve) was distilled from poly(styryllithium) oligomers. Tetrahydrofuran (THF) (Biosolve) was refluxed and distilled from a deep purple sodium-benzophenone complex solution. 1,1-Diphenylethylene (DPE) (Aldrich) was dried over *sec*-butyllithium (*s*-BuLi) and distilled from (diphenylmethyl)lithium under reduced pressure. Styrene (Acros Organics), isoprene (Aldrich) and methyl methacrylate (MMA) (Aldrich) were refluxed over calcium hydride (Aldrich) for 24 h, distilled under reduced pressure (styrene and MMA) and stored at –25 °C. Before the experiments MMA was dried with a 1.9 M (triethyl)aluminum solution in toluene (Aldrich) until a persistent yellowish green color was observed and subsequently redistilled under reduced pressure. *s*-BuLi (1.4 M) in cyclohexane (Aldrich) was used as received. Methanol (Biosolve) was degassed with argon for 15 minutes just prior to use.

A typical experimental procedure for the anionic synthesis of polymers in the commercially available automated parallel synthesizer (after the application of the inertization method developed in this work) was as follows. First, the reactors were set at the desired temperature and the vortex system of the equipment was set to 450 rpm, thereafter predetermined amounts of solvent and monomer were added into the reaction vessel using the automated liquid handling system of the apparatus. Subsequently, the polymerization was initiated upon adding *s*-BuLi (from a vial cooled to 5 °C). For kinetic measurements, samples (50 µL) were taken at predetermined times (using the automated liquid handling system) from the reactors and dispensed into 1.5 mL glass vials containing 25 µL of methanol in order to stop the polymerizations (previous to the experimentation, degassed methanol was first added into the glass vials under argon atmosphere and then they were capped with a rubber septa). These samples were used to determine both, monomer conversion and the molecular weight of the polymers obtained at the times predetermined. For the synthesis of block copolymers, sequential anionic polymerizations were performed as follows and according to reaction schemes displayed in Figures 2-9 and 2-12: predetermined amount of the first monomer was added into the reactors of the synthesizer containing a predetermined amount of cyclohexane at 55 °C and 450 rpm of vortexing under argon atmosphere. Addition of *s*-BuLi initiated the polymerization reactions of the first block. These mixtures were reacted for 0.5 h. Thereafter, samples were withdrawn from the reactor for GPC characterization of the corresponding precursor blocks (homopolymers). For the case of the synthesis of PS-*b*-PMMA block copolymers, a 1.1 molar excess (in respect to *s*-BuLi) of DPE was introduced into the reaction media at the desired temperature in order to carry out the intermediate end-capping step shown in the reaction scheme in Figure 2-13; this step turned the reaction mixtures red. Subsequently, the addition of a predetermined volume of the second monomer into the reactors at the desired reaction temperatures started the sequential synthesis of the second block. After a pre-determined period of time the reactions were terminated upon adding methanol. The concentration of monomers used in the anionic polymerization reactions was 10 wt % with respect to the amount of solvent (5 mL). For the synthesis of block copolymers, the amounts of monomers used were varied according to the desired compositions of each block in the copolymer. The amount of initiator used in each reactor was also varied according to the molecular weights of the polymers synthesized. The purification of the polymers was performed with two cycles of dissolution/precipitation (chloroform/methanol). The block copolymers obtained with these procedures were dried at 40 °C under vacuum for 24 h and were subsequently characterized by GPC and ^{1}H-NMR in order to obtain the molecular weights and the compositions of each block, respectively.

Monomer conversions were determined on a high-throughput Interscience Trace gas chromatograph (GC) (off-line) with a Trace Column RTX-5 connected to a PAL autosampler using 1.5 mL of THF as eluent and the solvent of the reaction as internal standard (cyclohexane for the case of kinetic measurements).

Gel permeation chromatography (GPC) measurements were performed on a Shimadzu system (off-line) with a SCL-10A system controller, a LC-10AD pump, a RID-6A refractive index detector and a Plgel 5 µm Mixed-D column. The measurements were performed using a solution of 4% triethylamine and 2% isopropanol in chloroform as eluent at a flow rate of 1 mL min^{-1} and a column temperature of 40 °C. Molecular weights were calculated against poly(styrene) standards.

Proton nuclear magnetic resonances (^{1}H-NMR) were recorded on a Varian Gemini 300 spectometer using deuterated chloroform ($CDCl_3$) (Cambridge Isotopes Laboratories) as solvent.

2.7 References

[1] (a) M. Szwarc, *Nature* **1956**, *78*, 1168. (b) M. Szwarc, M. Levy, R. Milkovich, *J. Am. Chem. Soc.* **1956**, *78*, 2656.

[2] K. Matyjaszewski, *"Advances in controlled/living radical polymerization"*, *ACS Symp. Ser.*, *854*, American Chemical Society: Washington D. C, **2003**.

[3] R. R. Schrock, *"Ring Opening Polymerization"*, Hansa Verlag: München, **1993**.

[4] (a) J. S. Wang, K. Matyjaszewski, *J. Am. Chem. Soc.* **1995**, *117,* 5614. (b) M. Kato, M. Kamigaito, M. Sawamoto, T. Higashimura, *Macromolecules* **1995**, *28*, 1721.

[5] (a) E. Rizzardo, *Chem. Aust.* **1987**, *54*, 32. (b) M. K. Georges, R. P. N. Veregin, P. M. Kazmaier, G. K. Hamer, *Macromolecules* **1993**, *26*, 2987. (c) C. J. Hawker, A. W. Bosman, E. Harth, *Chem. Rev.* **2001**, *101*, 3661.

[6] J. Chiefari, J. K. Chong, F. Ercole, J. Krstina, J. Jeffrey, T. P. T. Le, R. T. A. Mayadunne, G. F. Meijs, C. L. Moad, E. Rizzardo, S. H. Thang, *Macromolecules* **1998,** *31*, 5559.

[7] P. C. Wieland, B. Raether, O. Nuyken, *Macromol. Rapid Commun.* **2001**, *22*, 700.

[8] (a) R. Erhardt, A. Böker, H. Zeetl, H. Kaya, W. Pyckhout-Hintzen, G. Krausch, V. Abetz, A. E. H. Müller, *Macromolecules* **2001**, *34*, 1069. (b) J. Scheirs, D. Priddy, *Modern Styrenic Polymers*, Wiley: West Sussex, **2003**.

[9] H. L. Hsieh, R. P. Quirk, *Anionic Polymerization: Principles and Practical Applications*, Dekker: New York, **1996**.

[10] (a) M. Morton, L. J. Fetters, *Rubber Chem. Technol.* **1975**, *48*, 359. (b) N. Hadjichristidis, H. Iatrou, S. Pispas, M. Pitsikalis, *J. Polym. Sci. Part A: Polym. Chem.* **2000**, *38*, 3211. (c) S. Ndoni, C. M. Papadakis, F. S. Bates, K. Almdal, *Rev. Sci. Instrum.* **1995**, *66*, 1090. (d) D. Uhrig, J. W. Mays, *J. Polym. Sci. Part A: Polym. Chem.* **2005**, *43*, 6179.

[11] (a) N. Hadjichristidis, M. Pitsikalis, S. Pispas, H. Iatrou, *Chem. Rev.* **2001**, *101*, 3747. (b) J. Jagur-Grodzinski, *J. Polym. Sci. Part A: Polym. Chem.* **2002**, *40*, 2116. (c) S. Christodoulou, H. Iatrou, D. J. Lohse, N. Hadjichristidis, *J. Polym. Sci. Part A: Polym. Chem.* **2005**, *43*, 4030. (d) G. Koutalas, D. J. Lohse, N. Hadjichristidis, *J. Polym. Sci. Part A: Polym. Chem.* **2005**, *43*, 4040. (e) P. Driva, H. Iatrou, D. J. Lohse, N. Hadjichristidis, *J. Polym. Sci. Part A: Polym. Chem.* **2005**, *43*, 4070.

[12] I. W. Hamley, *The Physics of Block Copolymers*, Oxford University Press: Oxford, **1998.**

[13] (a) H. McCormick, *J. Polym. Sci.* **1959**, *36*, 341. (b) H. McCormick, *J. Polym. Sci.* **1959**, *39*, 87. (c) H. McCormick, *J. Polym. Sci.* **1959**, *41*, 327. (d) F. Wenger, *Makromol. Chem.* **1960**, *36*, 200. (e) F. Wenger, *Makromol. Chem.* **1960**, *37*, 143. (f) F. Wenger, *Makromol. Chem.* **1960**, *37*, 153. (g) F. Wenger, *J. Polym. Sci.* **1962**, *60*, 99. (h) T. A. Orofino, F. Wenger, *J. Chem. Phys.* **1961**, *35*, 532.

[14] (a) D. J. Worsfold, S. Bywater, *Can. J. Chem.* **1960**, *38*, 1891. (b) M. Morton, R. Milkovich, *J. Polym. Sci. Part A: Polym. Chem.* **1963**, *1*, 443. (c) M. Morton, A. A. Rembaum, J. L. Hall, *J. Polym. Sci. Part A: Polym. Chem.* **1963**, *1*, 461. (d) M. Morton, E. E. Bostick, R. G. Clarke, *J. Polym. Sci. Part A: Polym. Chem.* **1963**, *1*, 475.

[15] D. L. Glusker, E. Stilles, B. Yoncoskie, *J. Polym. Sci.* **1961**, *49*, 297.

[16] (a) J. M. Hoover, J. E. McGrath, *Polym. Prepr.* **1986**, *27*, 150. (b) P. Lutz, P. Rempp, *Makromol. Chem.* **1988**, *189*, 1051.

[17] (a) K. C. Nicolau, R. Hanko, W. Hartwig, *Handbook of Combinatorial Chemistry*, Wiley-VCH: Weinheim **2002**. (b) I. Takeuchi, H. Chang, C. Gao, P. G. Schultz, X. D. Xiang, R. P. Sharma, M. J. Downes, T. Venkatesan, *Appl. Phys. Lett.* **1998**, *73*, 894. (c) T. Zech, P. Claus, D. Honicke, *Chimia* **2002**, *56*, 611.

[18] (a) C. Guerrero-Sanchez, R. M. Paulus, M. W. M. Fijten, M. J. de la Mar, R. Hoogenboom, U. S. Schubert, *Appl. Surf. Sci.* **2006**, *252*, 2555. (b) B. Jandeleit, D. J. Schaefer, T. S. Powers, H. W. Turner, W. H. Weinberg, *Angew. Chem. Int. Ed.* **1999**, *38*, 2494. (c) R. Hoogenboom, M. A. R. Meier, U. S. Schubert, *Macromol. Rapid Commun.* **2003**, *24*, 15. (d) M. A. R. Meier, R. Hoogenboom, U. S. Schubert, *Macromol. Rapid Commun.* **2004**, *25*, 21.

[19] (a) V. Sciannamea, C. Guerrero-Sanchez, U. S. Schubert, J. M. Catala, R. Jerome, C. Detrembleur, *Polymer* **2005**, *46*, 9632. (b) R. Hoogenboom, M. W. M. Fijten, U. S. Schubert, *Macromol. Rapid Commun.* **2004**, *25*, 237.

[20] S. Schmatloch, H. Bach, R. A. T. M van Benthem, U. S. Schubert, *Macromol. Rapid Commun.* **2004**, *25*, 95.

[21] O. Lavastre, I. Illitchev, G. Jegou, P. H. Dixneuf, *J. Am. Chem. Soc.* **2002**, *124*, 5278.

[22] H. Y. Cho, D. S. Hong, D. W. Jeong, Y. D. Gong, S. I. Woo, *Macromol. Rapid Commun.* **2004**, *25*, 302.

[23] H. Gilman, A. H. Haubein, *J. Am. Chem. Soc.* **1944**, *66*, 1515.

[24] (a) D. L. Glusker, I. Lysloff, E. Stiles, *J. Polym. Sci.* **1961**, *49*, 315. (b) S. Auguste, H. G. M. Edwards, A. F. Johnson, Z. G. Meszena, *Polymer* **1996**, *37*, 3665. (c) G. Wang, M. Van Beylen, *Polymer* **2003**, *44*, 6205. (d) H. L. Hsieh, *J. Polym. Sci. Part A: Polym. Chem.* **1965**, *3*, 153. (e) H. L. Hsieh, *J. Polym. Sci. Part A: Polym. Chem.* **1965**, *3*, 163. (f) H. L. Hsieh, *J. Polym. Sci. Part A: Polym. Chem.* **1965**, *3*, 173. (g) S. Bywater, *Pure Appl. Chem.* **1962**, *4*, 319. (h) F. J. Welsh, *J. Am. Chem. Soc.* **1959**, *81*, 1345. (i) R. Ohlinger, F. Bandermann, *Makromol. Chem.* **1980**, *181*, 1935.

[25] D. C. Huang, R. C. C. Tsiang, *J. Appl. Polym. Sci.* **1996**, *61*, 333.

[26] J. Hofmans, L. Maeseele, G. Wang, K. Janssens, M. van Beylen, *Polymer* **2003**, *44*, 4109.

[27] (a) C. Geacintov, J. Smid, M. Szwarc, *J. Am. Chem. Soc.* **1962**, *84*, 2508. (b) M. van Beylen, M. Fisher, J. Smid, M. Szwarc, *Macromolecules* **1969**, *2*, 575.

[28] J. M. Yu, P. Dubois, R. Jerome, *Macromolecules* **1997**, *30*, 4984.

CHAPTER 3

Structure-property investigations of novel polymeric materials synthesized by anionic polymerization

Abstract

The utilization of a commercially available automated parallel synthesizer for anionic polymerization reactions has allowed, in a short period of time, the preparation of novel polymeric materials as well as the development of new synthetic methods. In particular, the synthesis of well-defined poly((styrene-alt-1,1-diphenylethylene)-block-isoprene) diblock copolymers via sequential anionic polymerization is discussed. The obtained diblock copolymers were fully characterized and subsequently used for the preparation of block copolymer micelles in a selective solvent. The hydrodynamic radius of the micelles in solution was determined by dynamic light scattering and the size of the core by atomic force microscopy at dry conditions. It was found that the observed characteristics of the studied micelles correlate to theoretical scaling predictions. Moreover, the average size of the unimers could be determined with high precision from the obtained experimental data and theoretical knowledge. In addition, a new synthetic method was developed for the preparation of well-defined terpyridine-functionalized poly(styrene) via anionic polymerization. This was achieved by reacting 4'-chloro-2,2':6',2"-terpyridine (terminating agent) with "living" polymeric carbanions synthesized by anionic polymerization. The conversion of the polystyryllithium species into the corresponding 1,1-diphenylalkyllithium chain ends by reaction with 1,1-diphenylethylene was found to be a necessary step in order to promote an efficient chain-end functionalization and to avoid undesired side reactions (coupling) between the polymeric chains due to the high reactivity of the poly(styryl) anion. The obtained terpyridine-functionalized poly(styrene)s were fully characterized and used for the preparation of metal mono- and bis-complexes (metallo-supramolecular diblock copolymers). The developed synthetic method was also utilized for the preparation of other terpyridine-functionalized polymeric materials such as poly(isoprene) and multi-arm star-shaped polymers.

Parts of this chapter have been published: (1) C. Guerrero-Sanchez, D. Wouters, C. A. Fustin, J. F. Gohy, B. G. G. Lohmeijer, U. S. Schubert, *Macromolecules* **2005**, *38*, 10185. (2) C. Guerrero-Sanchez, B. G. G. Lohmeijer, M. A. R. Meier, U. S. Schubert, *Macromolecules* **2005**, *38*, 10388. (3) C. Guerrero-Sanchez, U. S. Schubert, *Polym. Mat. Sci. Eng.* **2006**, *94*, 226. (4) C. Guerrero-Sanchez, C. Ott, U. S. Schubert, *Polym. Mat. Sci. Eng.* **2007**, *96*, 248.

3.1 Introduction

In the previous chapter, a new experimental approach for performing anionic polymerizations in a parallel synthesizer was developed. This experimental method allowed synthesizing several well-defined polymeric materials as well as carrying out detailed studies related to the anionic polymerization process in a remarkable short period of time. The relevance of utilizing well-defined polymeric architectures for fundamental studies in polymer science was also addressed, due to fact that the molecular characteristics determine to a large extent the final properties of the materials. In this regard, the parallel anionic polymerization method that was previously developed is utilized in this chapter to investigate the synthesis of new polymeric moieties in a systematic way in order to establish structure-property relationships of these materials. More specifically, the first part of this chapter describes the preparation of a block copolymer library of poly(styrene-*alt*-1,1-diphenylethylene-*block*-isoprene) (P(S-*alt*-DPE)-*b*-PI) with varying block compositions and degrees of polymerization in order to study their micellar behavior in selective solvents. In the second part of this chapter, a new synthetic route for the preparation of terpyridine-functionalized polymers based on the anionic polymerization mechanism is developed and optimized within the automated parallel synthesizer. Finally, concluding remarks of the obtained results as well as the future perspectives for the developed synthetic approaches are addressed.

3.2 Structure-property investigations of diblock copolymer micelles: Core and corona radii with varying composition and degree of polymerization

In this section the synthesis and micellization behavior of P(S-*alt*-DPE)-*b*-PI diblock copolymers are discussed. This system is similar to commodity elastomers of the AB- and ABA-type block copolymers where A is formed by poly(styrene) (PS), and B by a poly(diene). The diblock copolymers were synthesized via sequential anionic polymerization utilizing the experimental method developed in the previous chapter (*e.g.*, the use of a commercially available parallel synthesizer for carrying out anionic polymerizations), which allows a systematic variation of the block composition and the degree of polymerization of the polymeric materials. The obtained diblock copolymers were characterized by means of gel permeation chromatography (GPC), nuclear magnetic resonance (^{1}H-NMR) spectroscopy and differential scanning calorimetry (DSC). Thereafter, micelles were prepared from the obtained P(S-*alt*-DPE)-*b*-PI diblock copolymers in a selective solvent for the poly(isoprene) (PI) blocks. The micellar and the core radii of the self-assembled aggregates were experimentally determined by dynamic light scattering (DLS) and by atomic force microscopy (AFM), respectively. Finally, the obtained results are compared to theoretical scaling predictions for block copolymer micelles.

3.2.1 Introduction to block copolymer micelles and polymers containing 1,1-diphenylethylene

Block copolymers are well known for their ability to spontaneously assemble into nano-ordered structures. On surfaces and in bulk, block copolymers with immiscible blocks may phase segregate yielding spherical, cylindrical, and lamellar or gyroidal phase separated structures depending on the block copolymer composition, degree of polymerization and architecture. When block copolymers with incompatible blocks are dissolved in a thermodynamically good solvent for one block which is a bad solvent for the other block the copolymer chains associate reversibly to form micelles or vesicles. Recently, block copolymer micelles received increasing attention because of their possible applications as carriers in drug delivery applications[1] and for the preparation of stabilized nanoparticles.[2] Depending on the block copolymer chain architecture (*e.g.*, linear, cyclic, comb, star)[3] and on the block copolymer composition, not only spherical micelles but also cylinders, rods, vesicles and bilayers can be formed.[4,5]

The preparation of micelles by direct dissolution of a block copolymer in a selective solvent is generally not very suitable due to poor solubility of bulk block copolymers.[5] Moreover, the characteristic features of the obtained micelles could then be determined by the bulk structure, especially in case of high glass transition temperature (*Tg*) core-forming blocks. To circumvent these drawbacks, the initial dissolution of the bulk block copolymer in a common solvent is often preferred because it allows a complete dissolution of the sample and it erases memory effects from the starting bulk morphology. A selective solvent for the coronal blocks is then slowly added, followed by removal of the common solvent by stripping or dialysis.[5,6]

The size of the micelles may be determined experimentally,[6-8] by light scattering, small angle neutron scattering and small angle x-ray scattering techniques, transmission electron microscopy (TEM), and analytical ultracentrifugation and is known to depend on block copolymer composition, interaction parameter χ_{AB} between the blocks, solvent quality, temperature and, in case of block copolymers with ionizable blocks, by pH. For both charged as well as neutral block copolymer systems models have been developed based on mean field theories,[9] Monte Carlo simulations,[10] free energy calculation[11] as well as scaling theories.[12] Systematic studies showing the correlation between block copolymer composition and the hydrodynamic radius of diblock copolymer micelles have been reported, *e.g.*, for poly(ethylene oxide-*block*-caprolactone) in water[13] and poly(styrene-*block*-alkyl methacrylates) in dodecane solutions.[14] In those studies the hydrodynamic radius of the micelles was determined by DLS and has been correlated to different degrees of polymerization and block compositions. The micellar core radius was either estimated from scaling theories or determined using TEM.[14]

For some decades the micellization behavior of commodity block copolymers has been of great interest for scientists.[8] Remarkable differences have been reported for micelles of poly(styrene-*block*-isoprene) (PS-*b*-PI) block copolymers depending on their macromolecular architecture (*e.g.*, miktoarm stars *vs*. linear diblock copolymers or cyclic *vs*. linear).[15] However, the effect of incorporating different comonomers into one of the blocks on the micellar behavior of these block copolymers has been scarcely investigated. The incorporation of different comonomers into the blocks aims, mainly, at the improvement of their properties. In order to achieve this chemical modification, "new" synthetic methods have appeared by polymerizing "bulky" monomers in the glassy portion (A) of the materials, such as α-methylstyrene and 1,1-diphenylethylene (DPE).[16] DPE can be copolymerized via anionic polymerization with styrene (in an alternating fashion due to the reactivity ratios reported for these specific monomers)[16b] and with diene monomers to lead to an important improvement on the long-term service temperature (in the case of PS the *Tg* can increase from 100 °C up to 170-180 °C, depending on the DPE content).[16] For this reason, the incorporation of "bulky" (DPE) into AB-type block copolymers as well as their micellization behavior are addressed in this section.

3.2.2 Synthesis and characterization of poly(styrene-alt-1,1-diphenylethylene-block-isoprene) diblock copolymers

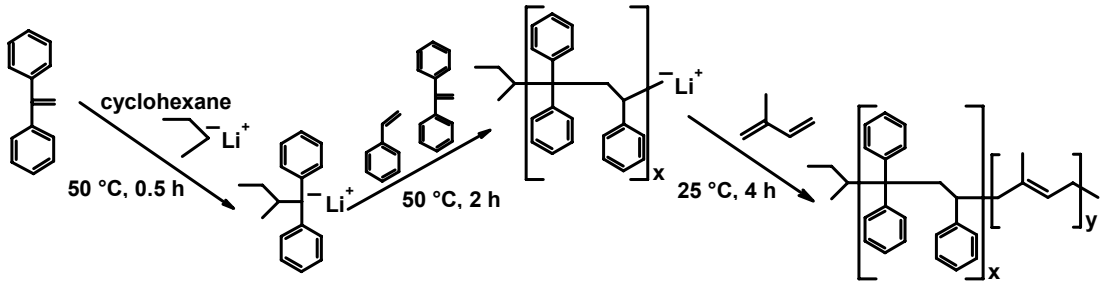

Figure 3-1: *Schematic representation of the synthesis of poly(styrene-alt-1,1-diphenylethylene-block-isoprene) diblock copolymers via sequential anionic polymerization.*

The synthesis of the P(S-*alt*-DPE)-*b*-PI diblock copolymers was performed by sequential anionic polymerization in the synthesizer discussed in chapter 2 (see the experimental part of this chapter for details). The synthetic approach is depicted in Figure 3-1 whereas the characteristics of the investigated diblock copolymers are summarized in Table 3-1.

Table 3-1: *Characteristics of the poly(styrene-alt-1,1-diphenylethylene-block-isoprene) (P(S-alt-DPE)-b-PI) diblock copolymers synthesized via sequential anionic polymerization and their respective precursors poly(styrene-alt-1,1-diphenylethylene) (P(S-alt-DPE)).*

Exp.	Mn (kDa) / PDI (GPC) P(S-*alt*-DPE)	Mn (kDa) / PDI (GPC) P(S-*alt*-DPE-*b*-PI)	Mol % (^{1}H-NMR) PI	Microstructure (^{1}H-NMR) 1,4-unit % PI	Tg_1 (°C) (DSC)	Tg_2 (°C) (DSC
1	7.6 / 1.18	22.0 / 1.10	71	89	-50	175
2	6.1 / 1.20	33.2 / 1.09	83	90	-52	185
3	12.7 / 1.19	27.9 / 1.24	60	90	-47	185
4	8.5 / 1.36	53.3 / 1.11	85	88	-50	179

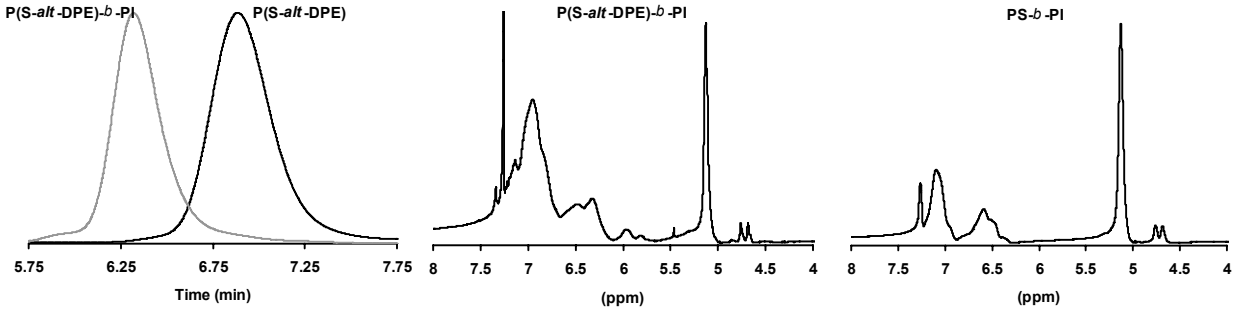

Figure 3-2: *Left: Normalized GPC traces of one of the synthesized poly(styrene-alt-1,1-diphenylethylene-block-isoprene) (P(S-alt-DPE)-b-PI) diblock copolymer and its respective poly(styrene-alt-1,1-diphenylethylene) (P(S-alt-DPE)) precursor (**1**, Table 3-1). The ^{1}H-NMR spectra (in $CDCl_3$ at 25 °C) correspond to one of the investigated P(S-alt-DPE)-b-PI) diblock copolymer (**1**, Table 3-1) (middle) and to a conventional poly(styrene-block-isoprene) (PS-b-PI) diblock copolymer (right) (both materials synthesized and characterized under similar conditions).*

The representative GPC traces depicted in Figure 3-2 (**1**, Table 3-1) reveal a successful chain extension process during the synthesis of the materials. Furthermore, single narrow molecular weight distributions were obtained for both the poly(styrene-*alt*-1,1-diphenylethylene) (P(S-*alt*-DPE)) precursors as well as for the P(S-*alt*-DPE)-*b*-PI diblock copolymers. These characteristics were representative for all the materials listed in Table 3-1. The polydispersity indices (PDI) of the synthesized polymers displayed in Table 3-1 reveal that the molecular weight distributions of the precursor blocks are slightly broader than those of the corresponding P(S-*alt*-DPE)-*b*-PI diblock copolymers. This effect may be related to the presence of impurity traces during the polymerization reactions as addressed in section 2.4.2. Differences between the ^{1}H-NMR spectra of one of the synthesized P(S-*alt*-DPE)-*b*-PI diblock copolymers and one "regular" PS-*b*-PI diblock copolymer (both materials synthesized and characterized under similar conditions) are also shown in Figure 3-2. The main difference between these two spectra arises in the aromatic region. In this region, it can be seen that the incorporation of additional phenyl rings in the styrenic block (copolymerization with DPE) shifts the aromatic signals to lower fields and leads to broader peaks as well as to the appearance of a new signal at 5.93 ppm. The microstructure of the PI block was also determined by ^{1}H-NMR and a content of 1,4-units of around 89% was found for all the investigated samples (Table 3-1). Hence, the average number molecular weight (Mn) value of the PI block can be calculated from the copolymer composition as determined by ^{1}H-NMR and from the molecular weight of the respective diblock copolymers as determined by GPC. An alternative method to obtain the Mn value of the PI block and the copolymer composition is from the difference between the molecular weights of the P(S-*alt*-DPE)-*b*-PI diblock copolymer and the P(S-*alt*-DPE) copolymer as obtained by GPC. The

results obtained by this latter method were found to be in agreement with those found using the ^{1}H-NMR approach. However, note that determination of the molecular weights of block copolymers by GPC might not be always be in agreement with other absolute characterization methods due to the fact that GPC is a relative characterization technique based on the hydrodynamic volume of the polymers in specific solvents, which can influenced by many variables.

Apart from microscopic methods, such as TEM or AFM, DSC is a suitable technique to detect phase segregation in block copolymers with immiscible components where the individual *Tg*'s of the corresponding blocks are sufficiently different from each other and the copolymer composition is far enough from the extreme values. A DSC trace obtained for one of the diblock copolymers investigated (**1**, Table 3-1) is shown in Figure 3-3. This trace is representative for all the materials investigated (Table 3-1). One main transition is clearly observed around –50 °C corresponding to the PI block whereas a small transition could be detected around 175 °C which is related to the P(S-*alt*-DPE) block. It is known that the microstructure of polydienes and polymers in general has a strong influence on the *Tg* of the materials.[17] For all the materials analyzed in this study the diblock copolymers showed a content of 89% of 1,4-units and a *Tg* around –50 °C for the PI block, as summarized in Table 3-1 (Tg_1). The *Tg* corresponding to the P(S-*alt*-DPE) blocks is mainly ruled by the content of DPE as reported elsewhere (*Tg* increases by 1.26 °C / wt% of DPE in the copolymer).[16c] For the diblock copolymers investigated the wt % of DPE within the P(S-*alt*-DPE) block is 63.3 wt % (largest possible content, corresponding to a ratio of 50 mol % of styrene and 50 mol % of DPE) in which case the *Tg* must be around 180 °C. Table 3-1 shows that the experimental *Tg* values of the P(S-*alt*-DPE) block (Tg_2) are in agreement with the knowledge in the literature.[16c]

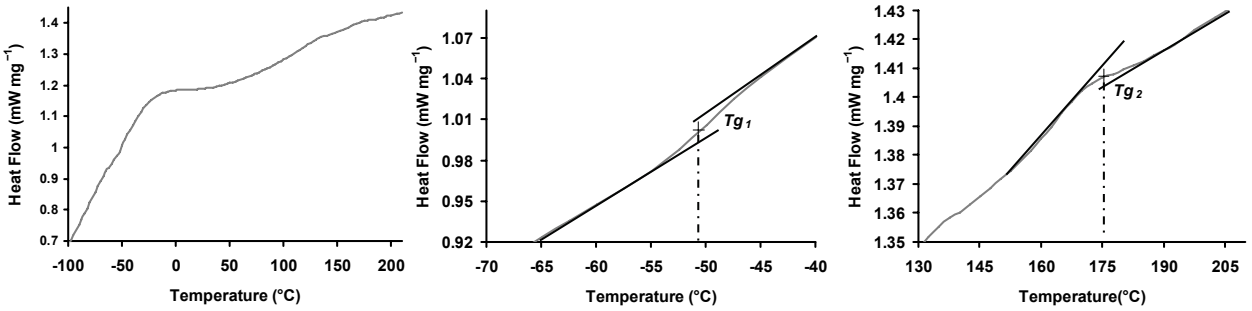

Figure 3-3: *DSC trace of one of the investigated poly(styrene-alt-1,1-diphenylethylene-block-isoprene) (P(S-alt-DPE)-b-PI) diblock copolymer (**1**, Table 3-1) recorded at a heating rate of 20 °C min^{-1}.*

3.2.3 Micellar behavior of poly(styrene-alt-1,1-diphenylethylene-block-isoprene) diblock copolymers

In diblock copolymer micelles, control over the micellar size can be obtained by varying the block copolymer composition and/or the degree of polymerization. Scaling theories for micelles prepared from linear AB block copolymers with an insoluble B block has been examined for two extreme cases.[6,9b,18] Micelles in which the degree of polymerization for the insoluble block (N_B) is considerable smaller than the soluble block (N_A) are called "hairy" micelles while systems in which N_A is smaller than N_B are called "crew-cut" micelles (Figure 3-4).

Assuming uniformly stretched chains for the core, the radius of the core (R_c) and the aggregation number (Z) for "crew-cut"-type micelles can be predicted by:

$$R_C \propto \gamma \cdot N_B^{2/3} \cdot a \qquad Z \propto \gamma \cdot N_B \tag{3-1}$$

where γ is the A/B interfacial tension and *a* the segment length.[6,12] In the case of "hairy" micelles (with $N_A > N_B^{4/5}$) in a good solvent, the radius of the core (R_C), the aggregation number (Z) and the thickness of the corona (L) scale by:

$$Z \propto N_B^{4/5} \qquad R_C \propto N_B^{3/5} \cdot a \qquad L \propto N_A^{3/5} \cdot N_B^{6/25} \cdot a \qquad (3\text{-}2)$$

Thus, the radius of the complete micelle ($R = R_c + L$) is dominated by the degree of polymerization of block A. This demonstrates that for "hairy" micelles the diameter is dominated by the thickness of the corona.

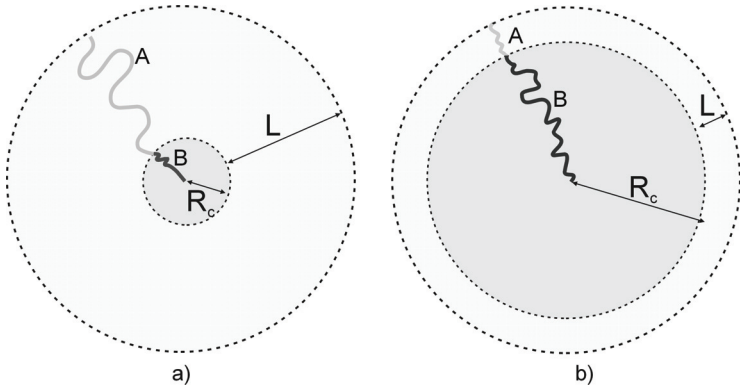

Figure 3-4: *Schematic representation of a "hairy" micelle (a) and a "crew-cut" micelle (b) formed by linear diblock copolymers with a soluble A block and insoluble B block.*

Table 3-2: *Characteristics of the investigated micelles prepared from poly(styrene-alt-1,1-diphenylethylene-block-isoprene) (P(S-alt-DPE)-b-PI) diblock copolymers. The sizes of the micelles were determined by AFM and DLS. Radii of the cores (R_C) of the micelles were estimated form the observed height in AFM images (Figure 3-5). The entire micellar radiuses (R) in n-heptane were obtained by DLS. N_B refers to the degree of polymerization of the P(S-alt-DPE) block (insoluble block) and N_A to the degree of polymerization of the PI block (soluble block).*

Exp.	Mn (kDa) (GPC) P(S-*alt*-DPE-*b*-PI)	N_B (core)	N_B (corona)	R_C (nm) (AFM)	R (nm) (DLS)	L (nm) (R-R_C)
1	22.0	54	228	5.0	29.9	24.9
2	33.2	43	405	4.0	38.3	34.3
3	27.9	89	246	7.7	40.1	32.4
4	53.3	60	665	5.6	52.1	46.5

n-Heptane is known to be a good solvent for the PI block and as a bad solvent for the P(S-*alt*-DPE) block resulting in the formation of micelles in which the core is composed by P(S-*alt*-DPE) blocks and the corona is consisting of extended PI chains. For this study the degree of polymerization of the P(S-*alt*-DPE) blocks (N_B) was determined from GPC data using the average of the molecular weights of styrene and DPE (142.2 g mol^{-1}), whereas the degree of polymerization of the PI block (N_A) was calculated from ^{1}H-NMR and GPC data of the diblock copolymers and the molecular weight of isoprene (68.12 g mol^{-1}). The corresponding values of N_A and N_B of the investigated diblock copolymers (Table 3-1) are shown in Table 3-2.

According to the data in Table 3-2 hairy-type micelles are expected for all the investigated polymers since N_A is larger than $N_B^{4/5}$. The hydrodynamic diameter of the micelles was evaluated by DLS whereas the diameter of the core was obtained from AFM. When compared to the well-known PS-*b*-PI diblock copolymer micelles,[15] P(S-*alt*-DPE) is a relatively harder and stiffer block. This should lead to a decreased critical micelle concentration and may affect the core size of the micelles.[19] Because AFM measurements were performed at room temperature (well below the *Tg* of the P(S-*alt*-DPE) core of the micelles), the core is expected to be thermodynamically frozen[15j] and stable during AFM imaging at dry conditions. Figure 3-5 displays the observed intermittent contact mode height images of the dried

micelles. From the images it can be confirmed that all micelles are spherical and have a narrow size distribution.

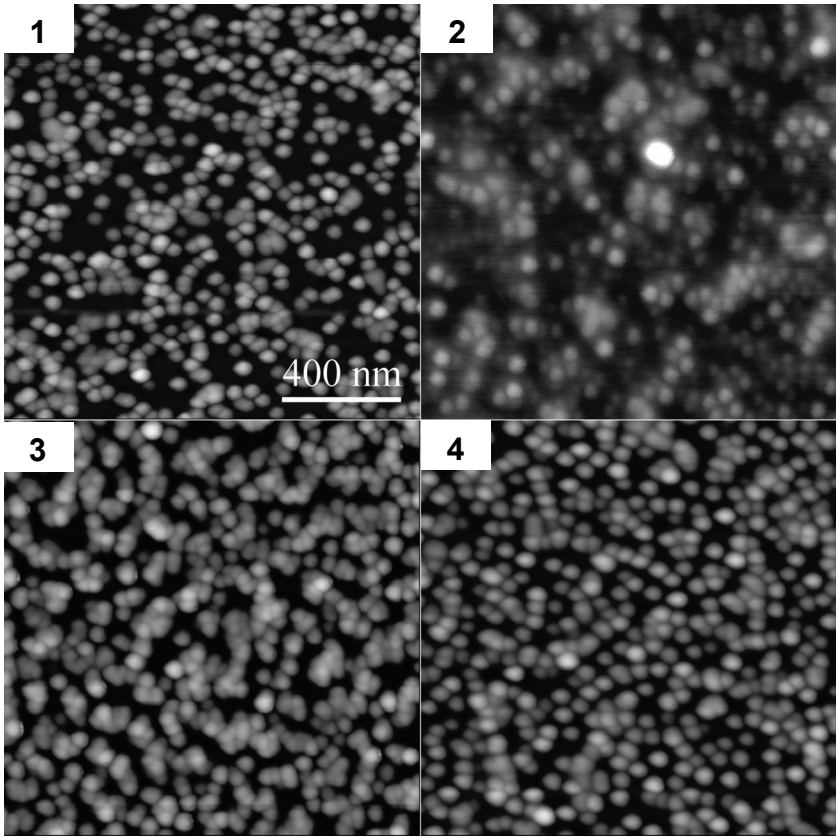

Figure 3-5: *Intermittent contact mode height images of the poly(styrene-alt-1,1-diphenylethylene-block-isoprene) diblock copolymer micelles investigated. The number in the corner of each image indicates different block copolymer compositions according to the investigated samples (Tables 3-1 and 3-2). Lateral dimensions and the z range are 1 x 1 μm^2 and 25 nm, respectively for all images.*

To avoid tip convolution, the diameters of the micelles were estimated by measuring the observed height of the micelles. Because micelles typically have a Gaussian size distribution, accurate determination of their height requires reliable averaging techniques. The average height of the micelles was determined for each polymer composition by two methods (see Figure 3-6 for an example (sample **3**, Table 1)). In the first method, the average micellar heights are determined by evaluating many cross sections (Figure 3-6a). The second method involves the evaluation of histograms for each image. The histogram in Figure 3-6b depicts the relative abundance of heights. For a sample consisting of flat particles on a flat substrate two peaks should appear with the distance between them representing the difference in height between the particles and the background. For the micelles the histogram reveals the presence of two broadened peaks. The peak at low height indicates the level of the mica substrate whereas the other peak indicates the presence of micelles on the surface. A surface with spherical particles shows a tailing peak because the highest point of the sphere is less abundant, and therefore the distance between the peak maxima does not correspond to the sphere height. By evaluating many histograms it was empirically found that the distance between the center of the “mica peak” and the bending point of the “particle peak” corresponds to the average height of the particles determined by the cross section method. It is advantageous to determine the height by this method because it is highly reproducible and in addition it significantly reduces the required analysis time. The sizes of the cores of the investigated micelles (samples of Table 3-1) found by AFM are summarized in Table 3-2. In contrast

to other experimental techniques (such TEM) to determine size of the core of micelles, AFM imaging does not require staining or ultra-high vacuum conditions and reduces the possibility of the core deformation.

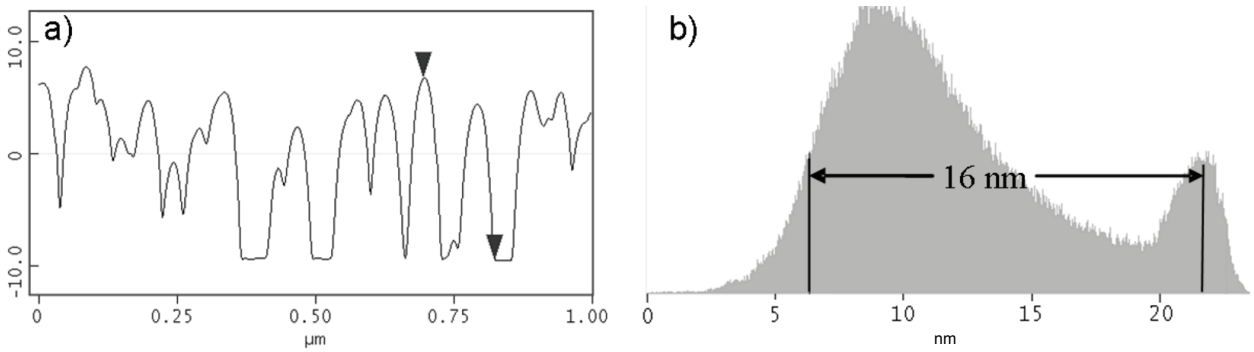

Figure 3-6: *Height of the micelles can be determined in two ways. a) The height can be obtained by averaging the results from cross sections. b) The distance between the surface peak and the bending point of the particle peak corresponds to the average micelle height.*

From the height images in Figure 3-5 it can be already observed that micelles prepared from sample **2** (Tables 3-1 and 3-2) (containing a small fraction of core blocks) are not so well-defined. The micellar heights (8 nm) for this sample are more broadly distributed. DLS measurements also showed that micelles prepared from sample **2** were rather unstable. This observation can be explained by looking at the polymer composition (Table 1). The P(S-*alt*-DPE) block of sample **2** is the shortest one (N_B ~ 43). Obviously, the relatively low degree of polymerization may be the origin of the decreased micellar stability.

DLS was used to study the micellar size in solution using the Cumulants analysis method.[20] Table 3-2 summarizes the hydrodynamic radiuses of the investigated micelles obtained by DLS (R), the radiuses of the cores obtained by AFM (R_C), and the thickness of the corona (L). The thicknesses of the coronas compared to the sizes of the cores confirm that the micelles are all of the 'hairy' type. At first sight the radiuses of the micelles obtained by AFM and DLS do not correlate to the molecular weight, even their relative order is different: by AFM the largest observed micelles are made from diblock copolymer **3**, whereas DLS indicates polymer **4** (Table 3-2). This discrepancy is explained because the radiuses obtained by DLS are the hydrodynamic ones whereas the AFM is used to determine the height of micelles adsorbed on a flat surface. The hydrodynamic diameter is, in case of "hairy" micelles, dominated by the degree of polymerization of the soluble block (PI) (Eq. 3-2). For AFM images on dried micelles, the corona is no longer swollen by the solvent. The flexible coronal chains are expected to be oriented flat on the surface, and therefore the height of the micelles essentially corresponds to the size of the core (Figure 3-7).

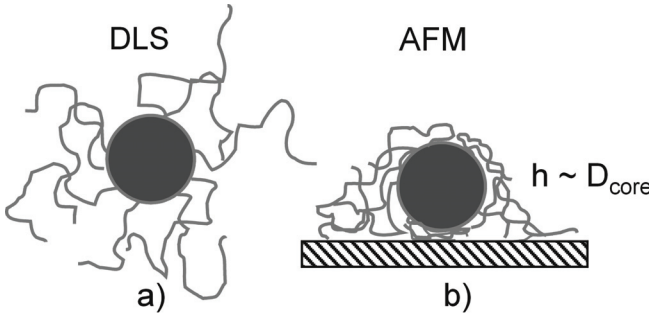

Figure 3-7: *Schematic representation of the architectures of diblock copolymer micelles during their characterization by: (a) Dynamic light scattering (DLS) (hydrodynamic diameter of the entire micelle in solution) and (b) atomic force microscopy (AFM) (diameter of the core of the micelle, height).*

Indeed, it is found that the height of the micelles correlates very well to the degree of polymerization of the core block (P(S-*alt*-DPE)) (Figure 3-8). According to theory[6] the diameter of the corona and the core of the micelle can be estimated from the degree of polymerization of both blocks. In Figure 3-8 the radiuses or the cores (R_C) and the thicknesses of the coronas (L) have been plotted against $N_B^{3/5}$ and $N_A^{3/5} \times N_B^{6/25}$, respectively. Both plots clearly demonstrate a linear correlation indicating the validity of the theoretical model as well as the applicability of using AFM-imaging to micelles in the dried state to determine the diameter of the core.

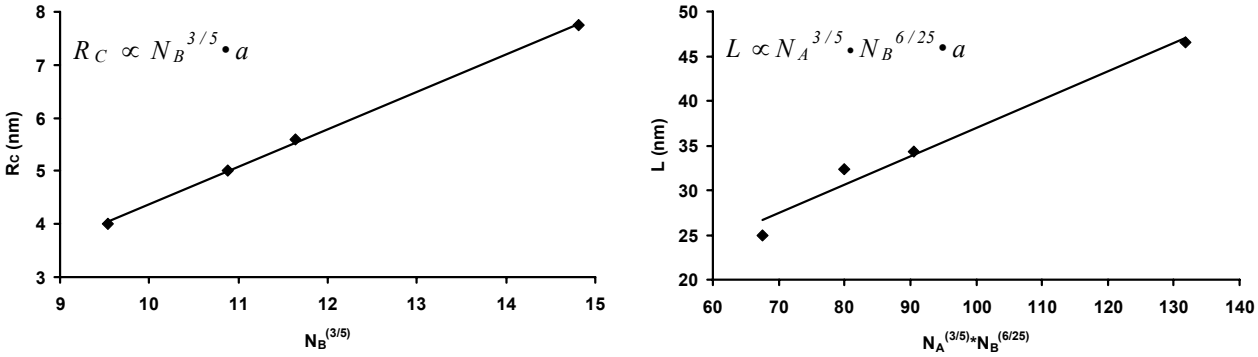

Figure 3-8: *(Left) Radii of the micellar cores (R_c) obtained by AFM have been plotted as a function of the degrees of polymerizations of the insoluble blocks (N_B) (Eq. 3-2). (Right) Thicknesses of the micellar coronas ($L = R–R_C$) obtained from data of DLS and AFM have been plotted as a function of the degrees of polymerizations of the soluble and insoluble blocks (N_A, N_B) (Eq. 3-2). Square dots represent experimental data whereas a linear fits (R = 0.999, left) (R = 0.977, right) are also plotted. See Table 3-2 for details and numerical values.*

In addition, the estimation of the proportionality constants for the equations of R_C and L (Eq. 3-2) can be performed using the data presented in Figure 3-8. These proportionality constants may be the equivalent to the monomer size or segment length a in Eq. 3-2 of the corresponding blocks or sections of the micelles. Table 3-3 summarizes these calculations for the segment length of the core (a_c) and for the segment length of the corona (a_L) of the investigated micelles. From Table 3-3 it can be seen that the obtained values for the different segment lengths of the cores (a_c) have a tendency to be constant with an average value of 0.47 nm and standard deviation of 0.04. The average value of 4.7 Å is a reasonable value for an organic molecule and may correspond to the average molecular size of the involved monomeric units (styrene and DPE). The obtained values for the different segment lengths of the coronas (a_L) revealed an average value of 0.38 nm and standard deviation of 0.02, which is also a reasonable value for the size of a molecule of isoprene. It should be noted that experimental factors related with the DLS measurements and the determination of the degree of polymerization of the PI block can influence the modeling of the thickness of the corona.

Table 3-3: *Obtained values of monomeric unit size or segment length, a, for the corresponding blocks of the investigated micelles (a_C = segment length of the core (poly(styrene-alt-1,1-diphenylethylene) block), a_L = segment length of the corona (poly(isoprene) block). Calculations were performed using Eq. 3-2 and data presented in Figure 3-8.*

	1	2	3	4
a_C (core) (nm)	0.46	0.42	0.52	0.48
a_L (corona) (nm)	0.37	0.38	0.40	0.35

3.3 Synthesis of terpyridine-functionalized polymers by anionic polymerization

In section 3.2, the synthesis of a new block copolymer library via anionic polymerization in an automated parallel synthesizer (chapter 2) was addressed. In addition, the obtained block copolymers

were used for the preparation of self-assembled micelles which were characterized in detail. Apart from the synthesis of well-defined block copolymers, anionic polymerization is a well-known and suitable technique for the preparation of polymers with functional end-groups.[16b,21] Hence, the further discussion of this section focuses on the development and optimization of a new synthetic route for the preparation of terpyridine-functionalized polymers based on the anionic polymerization mechanism. Like in the previous section, all the polymerization reactions of this section were performed within the synthesizer described in chapter 2. The resulting functionalized polymeric materials were characterized by various analytical techniques which validates the proposed synthetic approach. Moreover, some of the obtained functionalized polymers are utilized for the preparation of metallo-supramolecular block copolymers and other metal-coordinated structures.

3.3.1 Introduction to supramolecular and metal-containing polymers, and synthesis of end-group functionalized polymers by anionic polymerization

Non-covalent interactions (*e.g.*, van der Waals, hydrogen bonding, and ionic interactions) are usually related to reversible and self-assembly processes since they are weaker than covalent bonds. Nowadays, they are believed to be key factors for the understanding of natural systems and the development of self-responsive processes in several branches of chemistry.[22] In order to synthesize novel materials, scientists have developed several strategies for the incorporation of chemical moieties bearing non-covalent interactions into polymeric chains.[23] An extensively used non-covalent interaction in synthetic polymers is metal coordination of polymers containing chelating ligands (*e.g.*, phenanthroline, bipyridine and terpyridine) in order to construct novel supramolecular architectures.[24] Metal-containing polymers have been the topic of great attention in recent years due to their wide range of potential applications. These materials have shown interesting properties such as optical activity, electrical conductivity, luminescence and photorefractivity.[25] Metal-containing polymers have also opened a new avenue for the formation of novel supramolecular structures: double helicates, dendrimers, ordered architectures on surfaces and self-assembled block copolymers.[22-24,26] On the one hand, the incorporation of suitable metal-complexing ligands into the polymer chains is a critical step for the formation of well-defined materials, and on the other hand, their properties can be addressed and varied by changing their metal ions. Bipyridine and terpyridine ligands are among the most frequently used compounds to act as metal-complexing ligands in polymer architectures.[24,27] More specifically, terpyridine ligands self-assemble with different transition-metal ions in low oxidation states (Mn, Fe, Ru, Os, Co, Ir, Ni, Pt, Cu, Ag, Zn, Cd and Hg) into octahedral complexes.[28] For this purpose, the outer rings cooperatively rotate along the central C-C bonds connecting the rings to create a stable binding site through the lone pairs of three nitrogen atoms.[29] Bidentate ligands, such as bipyridine or phenantroline, on the other hand give rise to two different conformations (*fac* and *mer* stereoisomers) around an octahedral metal ion,[30] which are not so easy to selectively control.[31] Several synthetic strategies for the incorporation of terpyridine ligands into the polymer chains have been reported: end group modification, copolymerization of terpyridine-modified monomers, functionalized initiators and end-cappers.[26c,d] For the end group modification strategy hydroxy-terminated polymers have been employed as precursors using etherification and urethane-formation reactions. For the implementation of the terpyridine into the polymer via copolymerization, terpyridine-containing monomers have been utilized, *e.g.*, applying free radical polymerization methods.[32] Finally, functionalized initiators have been successfully applied in cationic ring-opening polymerization, atom transfer radical polymerization and nitroxide-mediated radical polymerization.[26c] However, all these procedures show some drawbacks, from rather demanding organic synthetic procedures for the initiators or monomers to several purification steps for the polymers obtained.

Nowadays, perfect control over molecular architecture is one of the most important goals in polymer science because this determines to a large extent the final properties of the materials. In this context controlled and “living” polymerization techniques allow for the synthesis of polymers with tunable chain lengths and low PDI, as well as the possibility to build well-defined block copolymers. Even though some of the modern controlled radical polymerization strategies have been applied for the incorporation of metal-complexing ligands into polymer chains, “living” anionic polymerization techniques have never been used for this purpose. As mentioned before “living” anionic polymerizations offer important advantages over other polymerization techniques: short reaction time, good control over the molecular weight, low polydispersity indices and sequential synthesis of block copolymers and complex polymeric architectures.[3,33] It is also well know that “living” anionic polymerization is a suitable, efficient and straight forward technique to synthesize end-group functionalized polymers.[16b,21] Moreover, it has been reported that the conversion of the polymeric organolithium chain ends to 1,1-diphenylalkyllithium chain ends (by reaction with 1,1-diphenylethylene (DPE)) promotes an efficient chain-end functionalization for several systems.[16b] Among the examples of functionalized polymers via anionic polymerization are the synthesis of 1,2-dicarboxyethyl,[34] nitroxide,[35] dimethylamino,[36] and 2-bromoisobutyryl[37] terminated polymers. In sections 3.3.2 and 3.3.4, the synthesis of terpyridine-functionalized poly(styrene) (Tpy-PS) and poly(isoprene) (Tpy-PI), as well as other polymeric architectures (star polymers), via anionic polymerization is investigated. This approach opens alternative routes for the preparation of terpyridine functionalized polymers. The obtained materials have no ether/urethane linkages (present in other synthetic procedures proposed), which may improve the chemical stability of the materials.

3.3.2 Synthesis of terpyridine-functionalized poly(styrene) by anionic polymerization and its characterization.

The synthesis of Tpy-PS was achieved by reacting the corresponding 1,1-diphenylalkyllithium polymeric chain ends (prepared by anionic polymerization) with 4'-chloro-2,2':6',2''-terpyridine (Cl-Tpy) according to the reaction scheme shown in Figure 3-9. All the anionic polymerization reactions were performed in the synthesizer described in chapter 2 (see the experimental part of this chapter for details). Figure 3-9 also displays an image of the synthesizer during the different stages of the synthesis. For the synthetic approach proposed three main parameters were investigated: (1) the use of DPE as an end-capper of the polystyryl anions previous the functionalization step, (2) the use of tetrahydrofuran (THF) for dissolving Cl-Tpy and (3) the use of toluene for dissolving Cl-Tpy. Other experimental parameters with less relevance for the functionalization process, such as the length of the polymer chains, were also investigated. However, no significant influence of this latter parameter on the process could be observed. Thus, the discussion is mainly focused on the variation of the aforementioned three main parameters. Table 3-4 summarizes the reaction conditions investigated for the synthesis of Tpy-PS via anionic polymerization; molecular weights and PDI values of the obtained polymeric materials and their respective precursors are also shown.

The starting point to achieve a successful synthesis of Tpy-PS via anionic polymerization was the investigation of the direct reaction between the anionically synthesized poly(styryllithium) moieties and Cl-Tpy. For this situation, one could expect a direct electrophilic attack of Cl-Tpy to the living polymeric carbanions in order to yield the corresponding terpyridine-functionalized polymer and the chloride salt (here lithium chloride). However, Figure 3-10a shows that the obtained polymer for this case revealed a bimodal distribution in the GPC traces (gray line (**13**, Table 3-4)). It can be observed that one of the peaks of this distribution appears at the same position as the un-functionalized PS precursor (methanol terminated poly(styryllithium), black line) whereas the other one arises at a lower elution time (with about the double number-average molecular weight of the protonated poly(styryllithium)).

Figure 3-9: *Schematic representation of the synthesis of terpyridine-functionalized poly(styrene) via anionic polymerization as well as the respective visual impression of the reaction steps in a Chemspeed ASW2000 parallel synthesizer.*

Table 3-4: *GPC results for different terpyridine-functionalized poly(styrene)s (Tpy-PS) and their respective poly(styrene) (PS) precursors prepared by anionic polymerization according to the reaction scheme of Figure 3-9. For the functionalization reaction (last reaction step) 4'-chloro-2,2':6',2''-terpyridine has been dissolved in tetrahydrofuran or in toluene. The efficiency of the functionalization reaction as determined by elemental analysis is also summarized.*

Exp.	Mn (kDa) / PDI (GPC) PS (precursor)	End-capping with 1,1-diphenylethylene	Solvent for 4'-chloro-2,2':6',2''-terpyridine	Mn (kDa) / PDI (GPC) Tpy-PS	Functionalization efficiency (%) (elemental analysis)
1	1.5 / 1.16	Yes	Tetrahydrofuran	1.8 / 1.11	66
2	2.2 / 1.16	Yes	Tetrahydrofuran	2.3 / 1.15	65
3	2.7 / 1.12	Yes	Tetrahydrofuran	2.8 / 1.17	63
4	3.5 / 1.12	Yes	Tetrahydrofuran	3.7 / 1.14	67
5	5.1 / 1.11	Yes	Tetrahydrofuran	5.3 / 1.15	59
6	8.5 / 1.09	Yes	Tetrahydrofuran	8.8 / 1.13	60
7	7.5 / 1.06	Yes	Toluene	7.8 / 1.09	91
8	7.5 / 1.06	Yes	Toluene	7.7 / 1.09	95
9	10.6 / 1.07	Yes	Toluene	11.0 / 1.10	97
10	10.6 / 1.07	Yes	Toluene	11.4 / 1.10	97
11	18.7 / 1.11	Yes	Toluene	20.6 / 1.13	96
12	18.7 / 1.11	Yes	Toluene	20.5 / 1.12	99
13	10.6 / 1.07	No	Toluene	17.0 / 1.32	-

The latter finding suggests the presence of undesired coupling reactions between two “living” PS chains promoted perhaps by the presence of Cl-Tpy. In addition, the ^{1}H-NMR characterization of this polymer revealed the absence of the signals related to the terpyridine functional group (from 7.4 to 8.7 ppm) and only signals for the aromatic protons assigned to PS (from 6.2 to 7.4 ppm) could be

found as shown in Figure 3-11a (**13**, Table 3-4). A similar experiment was performed using THF instead of toluene for dissolving Cl-Tpy in order to investigate potential solvent effects. However, GPC and ^{1}H-NMR results revealed qualitatively the same behavior as for the case of toluene (bimodal distribution in the GPC trace and no signals related to the terpyridine moiety in the ^{1}H-NMR spectrum). According to these results it can be concluded that this direct synthetic approach is not an efficient procedure to obtain well-defined Tpy-PS via anionic polymerization.

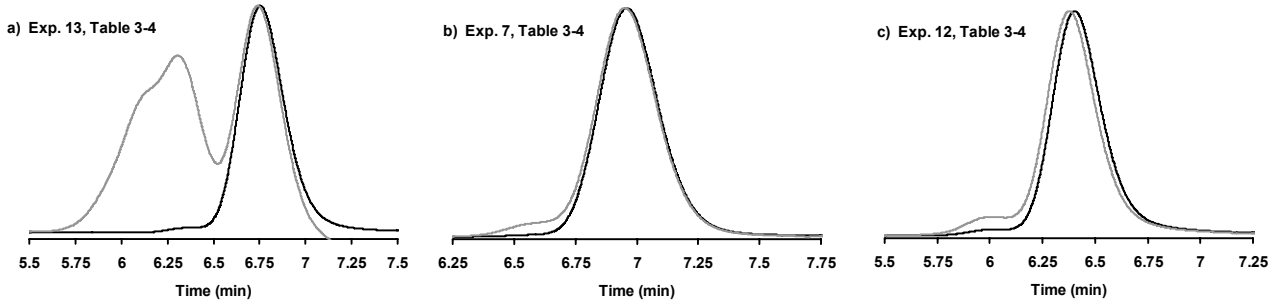

Figure 3-10: *Normalized GPC traces (eluent: triethylamine/2-propanol/chloroform mixture) of selected polymers of Table 3-4. (a) Black line: Protonated poly(styryllithium) precursor; grey line: 4'-Chloro-2,2':6',2''-terpyridine terminated poly(styryllithium) precursor where no end-capping with 1,1-diphenylethylene was used (**13**, Table3-4). (b) and (c) correspond to Exps. **7** and **12** (Table 3-4), respectively; black lines: Protonated poly(styryllithium) precursor; grey lines: 4'-chloro-2,2':6',2''-terpyridine terminated poly(styryllithium) precursor where end-capping with 1,1-diphenylethylene was used.*

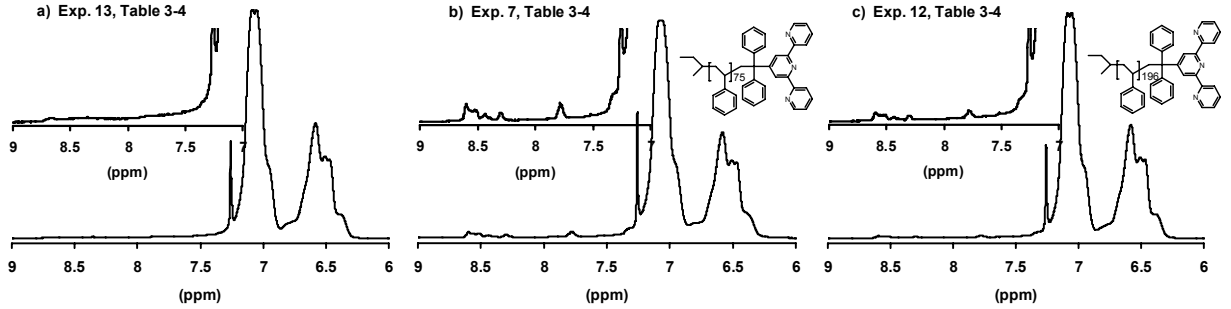

Figure 3-11: *^{1}H-NMR spectra of selected polymers of Table 3-4 in deuterated chloroform ($CDCl_3$) at 25 °C. (a) 4'-Chloro-2,2':6',2''-terpyridine terminated poly(styryllithium) precursor where no end-capping with 1,1-diphenylethylene was used (**13**, Table3-4). (b) and (c) 4'-chloro-2,2':6',2''-terpyridine terminated poly(styryllithium) precursors where end-capping with 1,1-diphenylethylene was used (**7** and **12**, respectively, Table 3-4).*

It is well-known that the conversion of the polymeric organolithium chain ends to the corresponding 1,1-diphenylalkyllithium chain ends (by the reaction with DPE) effectively reduces the reactivity of the respective carbanions.[16b] It is reported that the steric hindrance provided by the addition of DPE to the highly reactive polymeric carbanions and the fact that the resulting chemical species are energetically more stable than their corresponding precursors avoid the broadening of the molecular weight distribution caused by undesired coupling reactions between two or more “living” polymeric chain ends.[16b,34] Hence, the use of DPE to stabilize the highly reactive poly(styryl) anions, in order to promote an efficient functionalization reaction, was proposed as a next step towards the synthesis of well-defined Tpy-PS via anionic polymerization. This proposed approach is summarized schematically in Figure 3-9. GPC results revealed that for the cases where DPE is used for end-capping the highly reactive poly(styryl) anions, the resulting polymers show narrow and mono-modal molecular weight distributions, and that their respective elution times are almost identical to those corresponding to their protonated PS precursors. These findings can be observed in the GPC traces of Figure 3-10b and 3-10c (**7** and **12**, respectively, Table 3-4), which are characteristic examples for the rest of the experiments of Table 3-4 where DPE was used to stabilize the highly reactive poly(styryl) anions before the functionalization reaction with Cl-Tpy.

The effect of the use of DPE to stabilize the highly reactive poly(styryl) anions during the functionalization process can be also observed in the ^{1}H-NMR spectra of the obtained products. Parts b and c of Figure 3-11 show the ^{1}H-NMR spectra of the polymers obtained from **7** and **12** (Table 3-4), respectively. In these ^{1}H-NMR spectra it can be observed that where DPE is used in an intermediate synthetic step during the functionalization procedure, four signals related to the protons of the terpyridine functional group arise from 7.4 to 8.7 ppm besides the signals of the aromatic protons corresponding to the PS (from 6.2 to 7.4 ppm). A tiny shoulder at 7.3 ppm which is related to the fifth signal of the terpyridine functional group can also be observed. However, this signal is less clear due to its overlap with the aromatic signals of PS and the signal of deuterated chloroform solvent ($CDCl_3$) used during the measurements.

Note that the ^{1}H-NMR signals related to the terpyridine moiety become less intense as the molecular weight of the polymer increases for the different PS synthesized. For instance, the signals related to the terpyridine functional group are still visible in the ^{1}H-NMR spectra of Figure 3-11c despite the relatively high molecular weight of sample **12** (20.5 kg mol^{-1}) (Table 3-4). This is not the case where DPE was not used during the functionalization process to prevent undesired coupling reactions between the polymeric chains, even in samples with a relatively lower molecular weight than sample **12** (Table 3-4). This effect is observed in Figure 3-11a for sample **13** (Table 3-4). In addition, the ^{1}H-NMR spectra of the synthesized polymers in Table 3-4 were also used to estimate their molecular weight by integrating and correlating the signals corresponding to the terpyridine functional group with the signals of the aromatic protons of the PS backbones. Calculations of the molecular weights by this method were in good agreement to those obtained by GPC and summarized in Table 3-4.

Matrix-assisted laser desorption / ionisation time of flight mass spectrometry (MALDI-TOF-MS) is a suitable technique to perform end-group analysis of functionalized polymers and to determine absolute molecular weights.[38] In this regard, Figure 3-12 shows the MALDI-TOF-MS spectrum of polymer **3** (Table 3-4). The spectrum clearly reveals the presence of chemical species matching with the mass of several chain lengths of Tpy-PS and the presence of only one molar mass distribution. Moreover, the distance between each peak of the spectrum corresponds to the mass of styrene (104 Da). For instance, the expected mass of a Tpy-PS with 29 styrenic units is 3485 Da, which can be found in the MALDI-TOF-MS spectrum of the polymer **3** (Table 3-4) in Figure 3-12. This finding clearly proves that the synthesis of well-defined Tpy-PS by anionic polymerization is feasible. In addition, the molecular weights of the polymers determined by MALDI-TOF-MS were again in agreement with those found by GPC (Table 3-4) and ^{1}H-NMR spectroscopy.

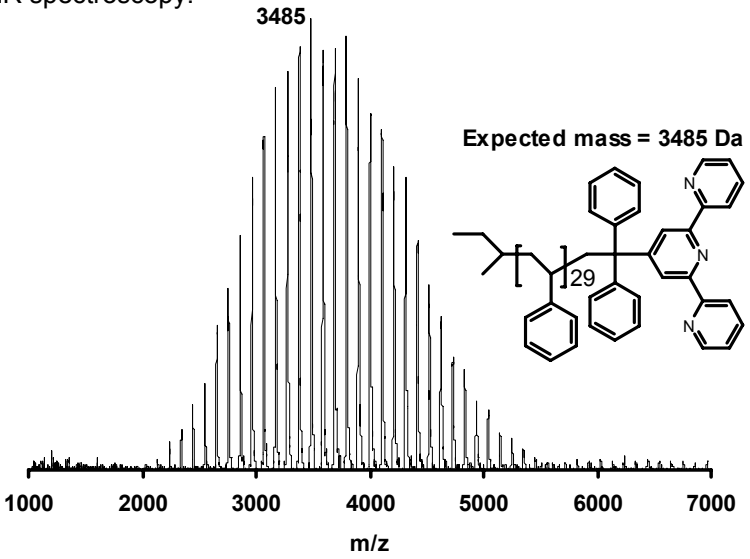

Figure 3-12: *MALDI-TOF-MS spectrum a 4'-chloro-2,2':6',2''-terpyridine terminated poly(styryllithium) precursor end-capped with 1,1-diphenylethylene (**3**, Table 3-4).*

For all the synthesized Tpy-PS (except for polymer **13** (Table 3-4) where the undesirable coupling reactions occurred) the content of nitrogen in the polymers was determined by elemental analysis. Hence, the efficiency of the functionalization reaction could be quantified using these measurements (see experimental part for a detailed explanation). Calculation of the expected content of nitrogen in the polymers (theoretical value) was performed utilizing the molecular weight found by GPC (Mn values of Tpy-PS in Table 3-4). For example, for polymer **3** (Table 3-4) the Mn determined by GPC was 2.8 kg mol^{-1}, the closest molecular weight to this value corresponds to a Tpy-PS (final specie of the reaction scheme in Figure 3-9) with 22 styrenic repeating units (molecular weight of 2.761 kg mol^{-1}) and, hence, the expected nitrogen content is 1.52% for this chemical moiety. Figure 3-13 shows the efficiency (measured by this latter method) of the functionalization process for the cases where THF was used for dissolving Cl-Tpy (**1** to **6**, Table 3-4) and for the cases where toluene was used for dissolving Cl-Tpy (**7** to **12**, Table 3-4). On the one hand, Figure 3-13a reveals that in the cases where THF is used for dissolving Cl-Tpy the measured efficiencies of the functionalization process range from 60% to 70%. It is difficult to conclude at this stage whether the relatively low measured efficiencies in theses cases are due to the relatively high polarity of THF that could modify the functionalization mechanism (chemical effect), or to impurity traces in the solvent that could terminated the "living" polymeric anions before the functionalization reaction (even though the used THF was purified with standard procedures reported in literature (distilled from a deep purple sodium-benzophenone complex solution)). In this regard, further experiments would be required in order to reach a definitive conclusion about the observed effect. On the other hand, in the cases where Cl-Tpy is dissolved in a less polar solvent than THF, such as toluene, the measured efficiencies of the functionalization process increase considerably up to values close to 100% as observed in Figure 3-13b.

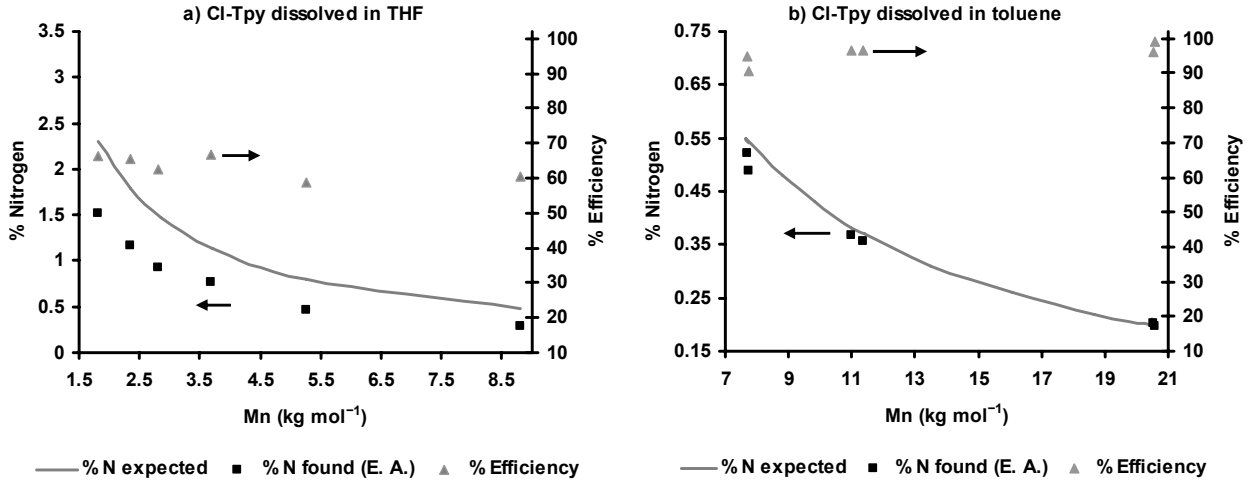

Figure 3-13: *Efficiency of the functionalization reactions investigated (synthesis of terpyridine-functionalized poly(styrene) via anionic polymerization where end-capping with 1,1-diphenylethylene is used (**1** to **12**, Table 3-4)) measured by elemental analysis (E. A.) (content of nitrogen (N) in the polymers and their respective molecular weights (Mn) are utilized to determine the efficiency). (a) 4'-Chloro-2,2':6',2''-terpyridine (Cl-Tpy) was dissolved in tetrahydrofuran (THF) during the functionalization process (**1** to **6**, Table 3-4). (b) 4'-Chloro-2,2':6',2''-terpyridine (Cl-Tpy) was dissolved in toluene during the functionalization process (**7** to **12**, Table 3-4).*

A titration with metal ions to the polymers followed by ultraviolet-visible spectroscopy (UV-Vis) represents an additional analytic technique to characterize and quantify the degree of terpyridine functionalization in polymeric materials.[39] For this purpose, solutions of the Tpy-PS synthesized were titrated with iron(II) chloride ($FeCl_2$) (see experimental part for details about this analytic technique). Hence, an increase of the metal-to-ligand charge-transfer (MLCT) band of the iron(II)-terpyridine complex at 565 nm is expected. Figure 3-14a displays the UV-Vis spectra obtained during the titration process of polymer **7** (Table 3-4), where the absorption increase in the MLCT band at 565 nm can be observed as

the titration is carried out. In this analysis, the titration process can be also monitored by following the increase of the MLCT band at 329 nm. For this case, a plateau is reached after a linear increase upon adding of $FeCl_2$ indicating that the complexation process is complete. These observations are shown in Figure 3-14b for the UV-Vis titration of polymer **7** (Table 3-4), where the absorption of the MLCT band at 329 nm is plotted as a function of the equivalents of iron(II). The equivalence point was observed approximately at a ligand-to-metal ratio of 2:1, indicating a fully quantitative complexation. Based on these UV-Vis titration measurements, it is also possible to estimate the efficiency of the functionalization process in a similar way as discussed above for the elemental analysis approach. In this regard, the estimations of the functionalization efficiencies of the Tpy-PS synthesized based on the obtained results of the UV-Vis titrations were very similar to those values found where the elemental analysis technique was used (Figure 3-13). These findings are an additional proof that the efficiency of the investigated functionalization process was around 60-70% where THF is used for dissolving Cl-Tpy, and close to 100% in the case of toluene.

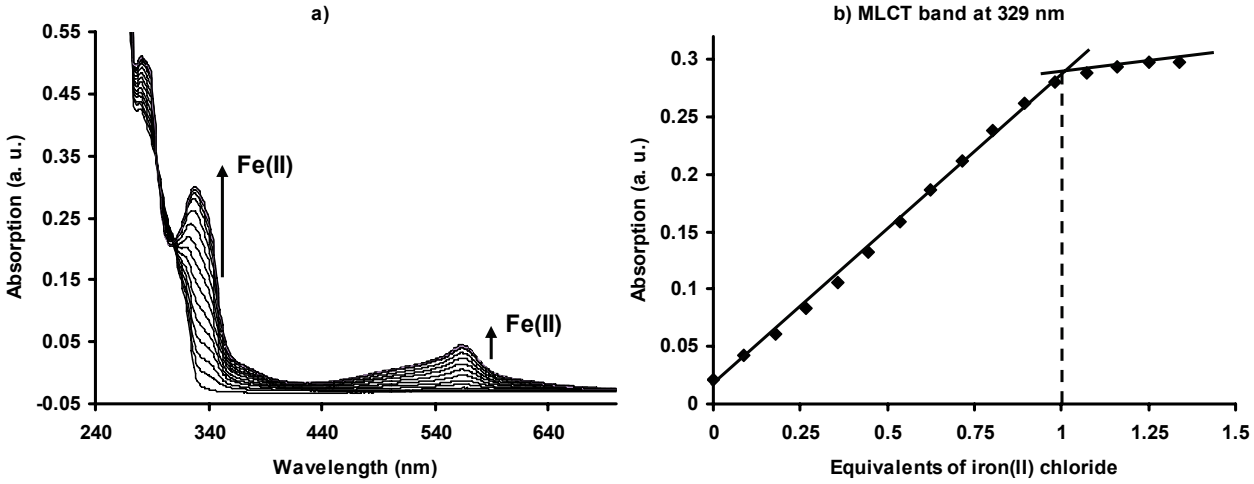

Figure 3-14: *UV-Vis titration with $FeCl_2$ to a solution of terpyridine-functionalized poly(styrene) synthesized via anionic polymerization where end-capping with 1,1-diphenylethylene is used (**7**, Table 3-4). (a) The spectra show the absorption increase of the metal-to-ligand charge-transfer (MLCT) bands at 329 and 565 nm as the titration is carried out. (b) The absorption of the metal-to-ligand charge-transfer (MLCT) band at 329 nm is plotted as a function of the equivalents of iron(II) (the equivalence point was observed approximately at a ligand-to-metal ratio of 2:1, which indicates a fully quantitative complexation).*

The change of color of the reaction mixtures during the synthesis of Tpy-PS via anionic polymerization (see Figure 3-9) is also an interesting observation which is worth discussing. This phenomenon was studied by UV-Vis spectroscopy. Figure 3-15 displays the changes in absorption of the spectra of the reaction mixtures at different stages during the functionalization procedure. In Figure 3-15 the characteristic peak of poly(styryllithium) arising at 338 nm (orange-yellow color solutions in Figure 3-9)[40] can be observed. Furthermore, a new absorption band appears at 617 nm upon adding Cl-Tpy (in solution) into the reaction mixture, which corresponds to the deep blue colored solution (Figure 3-9), whereas the absorption bands related to the precursor species (poly(styryllithium) and poly(styryllithium) with a DPE chain end (red colored solution in Figure 3-9), UV-Vis spectrum not shown in Figure 3-15)) vanish. A UV-Vis spectrum of a recovered Tpy-PS in chloroform (colorless solution) is also shown in Figure 3-15 for comparison. It is thought that the observed deep blue color during the functionalization procedure originates from the electrophilic attack of Cl-Tpy to the “living” polymeric anions. It is worth mentioning that this color also appeared in the reaction mixtures in the cases where DPE was not used for stabilization of the highly reactive poly(styryl) anions (**13**, Table 3-4 (Figures 3-10a and 3-11a)).

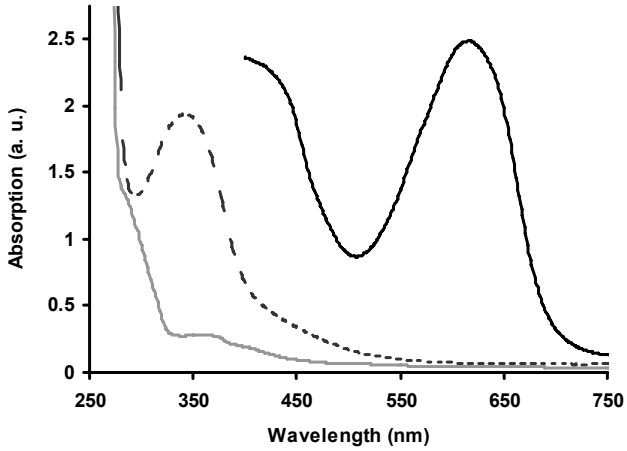

Figure 3-15: *UV-Vis spectra for different chemical species present during the synthesis of terpyridine-functionalized polystyrene via anionic polymerization where end-capping with 1,1-diphenylethylene is used. Dashed line: Poly(styryllithium) precursor. Black line: Poly(styryllithium) precursor converted into the respective 1,1-diphenylalkyllithium reacting with 4'-chloro-2,2':6',2''-terpyridine. These two samples were taken directly from the inert reaction media in cyclohexane. Grey line: An isolated terpyridine-functionalized polystyrene after the reaction completion (in chloroform).*

3.3.3 Synthesis of metallo-supramolecular polymeric complexes based on terpyridine-functionalized poly(styrene)

The discussion presented in this section focuses on the synthesis of metallo-supramolecular polymeric complexes using the previously discussed Tpy-PS. In addition to provide further characterization for the materials synthesized in section 3.3.2, the main goal of the present discussion is to briefly address applications of the terpyridine-functionalized polymers and to demonstrate that the Tpy-PS synthesized via anionic polymerization have comparable properties to similar polymers obtained by other synthetic approaches. Note that the scope of this contribution is mainly to establish an alternative route for the synthesis of terpyridine-functionalized polymers via anionic polymerization, hence a detailed description regarding the characteristics of metallo-supramolecular polymeric complexes (stability, synthesis, purification procedures, characterization, etc.) is not addressed here and can be found elsewhere.[39] The Tpy-PS described in section 3.3.2 could be used as precursor materials for the preparation of novel block copolymer libraries as described in literature.[41] Thus, the ability of the synthesized Tpy-PS to form *mono*- and *bis*-complexes with other terpyridine-functionalized polymeric building blocks is explored in this section. The synthetic procedure utilized for the preparation of the metallo-supramolecular polymeric *mono*- and *bis*-complexes with ruthenium (Ru) ions is summarized in the reaction scheme displayed in Figure 3-16 and is described in detail in the experimental part. The preparation of a metallo-supramolecular block copolymer was achieved by reacting one of the Tpy-PS synthesized in section 3.3.2 (**8**, Table 3-4) with a terpyridine-functionalized poly(ethylene oxide) ruthenium tri-chloride ($RuCl_3$) *mono*-complex (Mn = 3.1 kg mol^{-1}).[42] In Figure 3-17a a GPC trace corresponding to the metallo-supramolecular block copolymer obtained is shown. For the synthetic approach followed, a purification step, by preparative size exclusion chromatography, is normally necessary in order to remove the un-reacted precursors (terpyridine-functionalized polymeric $RuCl_3$ *mono*-complexes and/or terpyridine-functionalized homopolymers).[39] The GPC traces of the precursors materials (terpyridine-terminated poly(ethylene oxide) $RuCl_3$ *mono*-complex (Mn = 3.1 kg mol^{-1}) and Tpy-PS (**8**, Table 3-4)) of the metallo-supramolecular diblock copolymer are also displayed in Figure 3-17a. The differences between the elution times in the GPC traces of the terpyridine-terminated poly(ethylene oxide) $RuCl_3$ *mono*-complex (Mn = 3.1 kg mol^{-1}) and the Tpy-PS (**8**, Table 3-4) precursors

observed in Figure 3-17a can be explained by their respective hydrodynamic volumes in the eluent of the GPC equipment (*N,N*-dimethylformamide).[43] This GPC system, for instance, shows lower retention times for PS standards than for poly(ethylene oxide) standards of the same molecular weight due to the smaller hydrodynamic volume of PS in *N,N*-dimethylformamide when compared to the case of poly(ethylene oxide).[43]

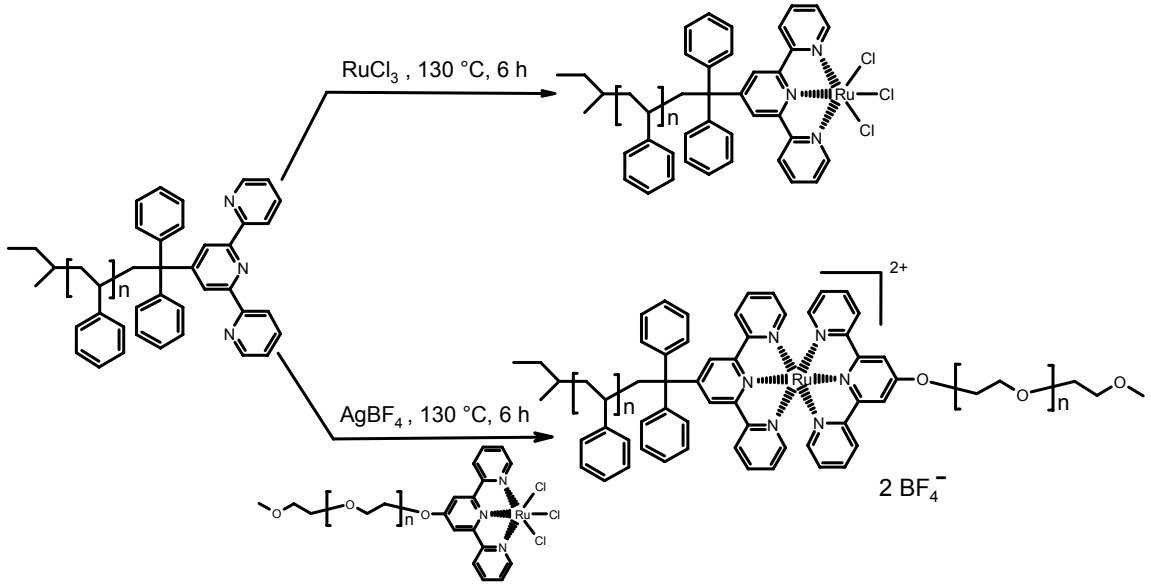

Figure 3-16: *Schematic representation of the synthesis of metallo-supramolecular polymeric complexes. Upper path represents the synthesis of a terpyridine-functionalized poly(styrene) ruthenium tri-chloride mono-complex. The lower path shows the preparation of a metallo-supramolecular block copolymer (bis-complex) using terpyridine-functionalized poly(styrene) (**8**, Table 3-4) and terpyridine-functionalized poly(ethylene oxide) ruthenium tri-chloride ($RuCl_3$) mono-complex (Mn = 3.1 kg mol^{-1})[42] as precursors.*

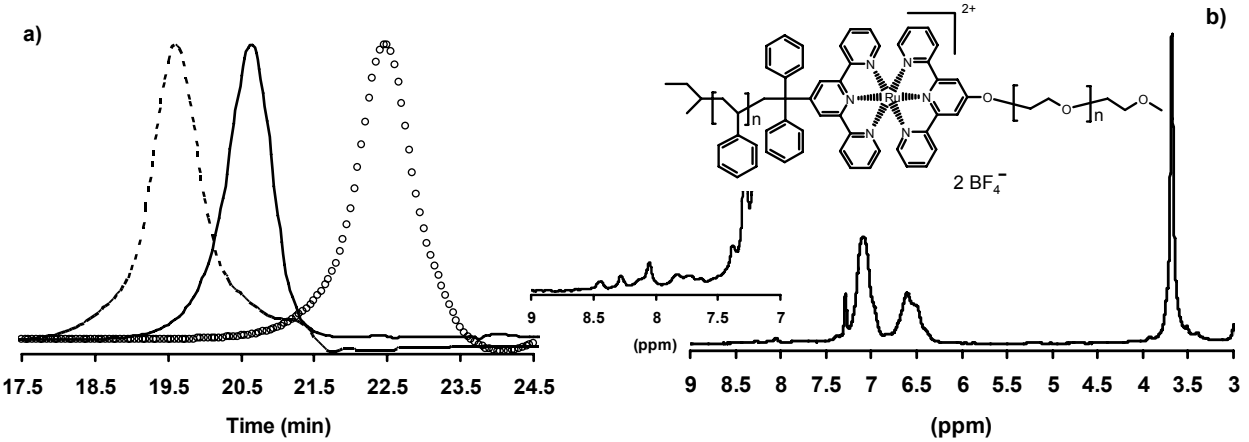

Figure 3-17: *(a) Normalized GPC traces (eluent: 5 mM NH_4PF_6 in N,N-dimethylformamide). Dashed line: Metallo-supramolecular block copolymer ruthenium (II) bis-complex (poly(styrene)-block-poly(ethylene oxide)) after purification by preparative size exclusion chromatography. Open circles: Terpyridine-functionalized poly(styrene) precursor (**8**, Table 3-4). Solid line: Terpyridine-functionalized poly(ethylene oxide) ruthenium tri-chloride mono-complex (Mn = 3.1 kg mol^{-1}).[42] (b) ^{1}H-NMR spectra in deuterated chloroform ($CDCl_3$) at 25 °C of the metallo-supramolecular block copolymer ruthenium (II) bis-complex (poly(styrene)-block-poly(ethylene oxide)) after purification by preparative size exclusion chromatography (precursors: A terpyridine-functionalized poly(styrene) (**8**, Table 3-4) and a terpyridine-functionalized poly(ethylene oxide) ruthenium tri-chloride mono-complex (Mn = 3.1 kg mol^{-1}).[42]*

The block compositions of the metallo-supramolecular block copolymer (poly(styrene)-[Ru]-poly(ethylene oxide)) obtained can be determined from the ^{1}H-NMR spectrum displayed in Figure 3-17b by correlating the signals corresponding to the protons of the backbones of each block (aromatic protons

of the styrenic block between 6.5 and 7.5 ppm and the protons from the $O–CH_2$ group of the poly(ethylene oxide) at 3.7 ppm). For the case displayed in Figure 3-17, the block copolymer composition revealed a content of 46% of poly(ethylene oxide) which is in agreement with the expected value. Note that the ^{1}H-NMR spectrum of Figure 3-17b also shows a shifting of the signals related to the terpyridine group from 7.5 to 8.5 ppm with respect to those observed, for example, in Figure 3-11b for Tpy-PS with uncomplexed terpyridine end-groups. This finding is also an indication of a successful complex formation as reported in the literature.[39]

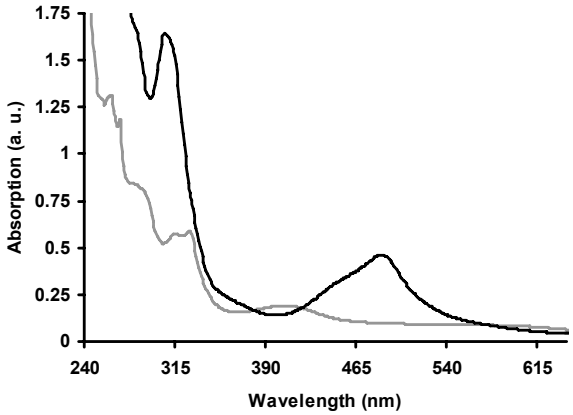

Figure 3-18: *UV-Vis spectra of the metallo-supramolecular polymeric complexes synthesized. Gray line: A terpyridine-functionalized poly(styrene) ruthenium tri-chloride mono-complex (precursor: Sample **7**, Table 3-4). Black line: Metallo-supramolecular block copolymer ruthenium (II) bis-complex (poly(styrene)-block-poly(ethylene oxide)) after purification by preparative size exclusion chromatography (precursors: A terpyridine-functionalized poly(styrene) (**8**, Table 3-4) and a terpyridine-functionalized poly(ethylene oxide) ruthenium tri-chloride mono-complex (Mn = 3.1 kg mol^{-1}).*[42]

Finally, UV-Vis measurements of the obtained polymeric complexes were recorded and are shown in Figure 3-18. The spectrum corresponding to the Tpy-PS $RuCl_3$ *mono*-complex reveals a MLCT band at 400 nm, whereas this band disappears in the spectrum of the self-assembled metallo-supramolecular block copolymer Ru(II) *bis*-complex, and a new band arises at 485 nm.

3.3.4 Synthesis of other terpyridine-functionalized polymeric moieties by anionic polymerization

In section 3.3.2 a new synthetic approach for the preparation of Tpy-PS via anionic polymerization was developed and the obtained polymers were characterized in detail. In addition, the synthesized Tpy-PS were utilized as precursor materials for the preparation of novel metallo-supramolecular polymeric complexes in section 3.3.3. In this section, the functionalization procedure developed, based on anionic polymerization, is investigated for the synthesis of terpyridine-functionalized poly(isoprene)s (Tpy-PI) and poly(methyl methacrylate)s (Tpy-PMMA).

Regarding the preparation of Tpy-PI via anionic polymerization four different reaction conditions were investigated which are summarized in the reaction scheme of Figure 3-19. The first two approaches were carried out using similar reaction conditions as for the functionalization of PS (section 3.3.2, Figure 3-9). This is using cyclohexane as reaction media at 20 °C; the effect of including DPE in order to stabilize the poly(isoprenyl) anions during the functionalization process was also briefly investigated (Figure 3-19). However, it has been reported that some functionalization reactions of polydienes via anionic polymerization can be achieved with higher yields when they are performed in non-polar solvents at low temperature.[35] Therefore, two more reaction conditions for the synthesis of Tpy-PI via anionic polymerization were also investigated. For these cases, the functionalization reactions were performed in

n-heptane as reaction medium at −60 °C, with and without the use of DPE during the functionalization procedure (Figure 3-19). Table 3-5 summarizes the investigated reaction conditions as well as the obtained GPC results of the synthesized Tpy-PI and their respective precursors.

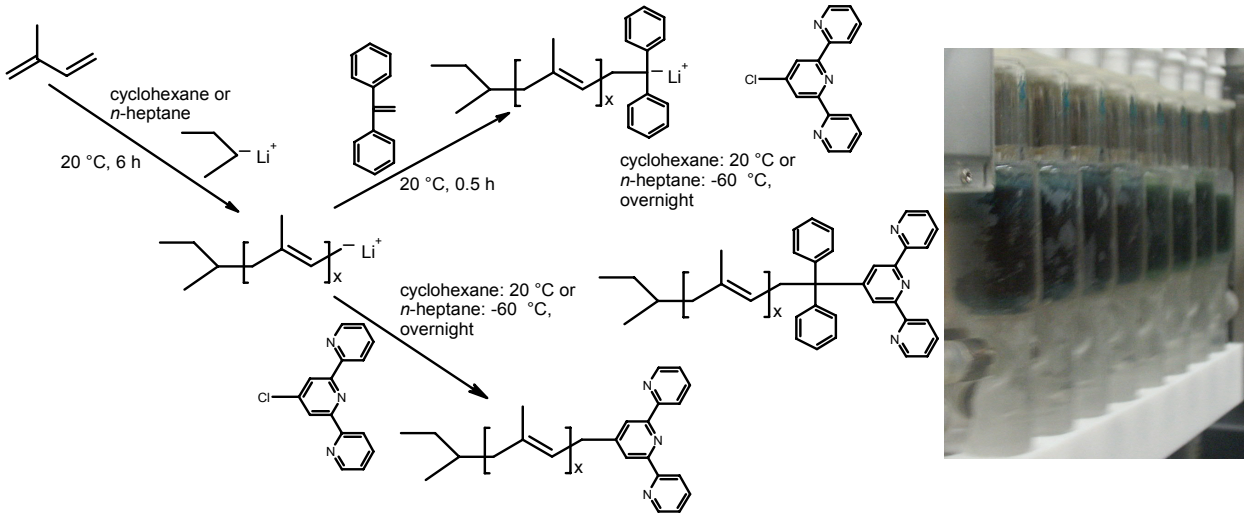

Figure 3-19: *Left: Schematic representation of the investigated methods for the synthesis of terpyridine-functionalized poly(isoprene) via anionic polymerization with and without using 1,1-diphenylethylene for the stabilization of the poly(isoprenyl) anions. Right: An image of a Chemspeed ASW2000 parallel synthesizer during the functionalization process at −60 °C.*

Table 3-5: *GPC results for different terpyridine-functionalized poly(isoprene)s (Tpy-PI) and their respective poly(isoprene) (PI) precursors prepared by anionic polymerization according to the reaction scheme of Figure 3-19. For the functionalization reaction (last reaction step) 4'-chloro-2,2':6',2''-terpyridine has been dissolved in toluene.*

Exp.	Mn (kDa) / PDI PI (precursor)	Reaction medium (solvent)	Temperature of functionalization (°C)	End-capping with 1,1-diphenylethylene	Mn (kDa) / PDI Tpy-PI
1	11.5 / 1.08	Cyclohexane	20	No	12.1 / 1.16
2	6.0 / 1.10	Cyclohexane	20	Yes	6.6 / 1.22
3	9.2 / 1.10	*n*-Heptane	−60	No	11.0 / 1.16
4	9.1 / 1.07	*n*-Heptane	−60	Yes	10.0 / 1.18

All the protonated poly(isoprene)s (PI) (precursor samples, before functionalization) revealed mono-modal and narrow molecular weight distributions (PDI were in the range between 1.07 and 1.10). Moreover, the expected molecular weights (according to the monomer/initiator ratio) of the polymers were in agreement with the found values by GPC.

Regarding the cases where cyclohexane at 20 °C (Figure 3-19) was used to synthesize Tpy-PI via anionic polymerization (**1** and **2**, Table 3-5) (similar conditions as in the case of Tpy-PS, section 3.3.2), ^{1}H-NMR measurements showed that a relatively low degree of functionalization was achieved. Figure 3-20 (**1** and **2**, Table 3-5) reveals the presence of relatively weak signals of the aromatic protons related to the terpyridine group in the ^{1}H-NMR spectra (from 7.5 to 8.8 ppm) in both cases investigated (with and without using DPE as end-capper of the polymeric anions during the functionalization process). In addition, GPC traces of these latter experiments showed that a few un-desired coupling reactions occurred between the “living” polymer chains in both cases since the molecular weight distributions of the Tpy-PI are bimodal (gray lines, Figure 3-21). In Figure 3-21 the main peaks in the distributions of Tpy-PI can be observed at the same position as the un-functionalized PI precursors (methanol-terminated poly(isoprenyllithium), black lines) whereas small peaks arise at lower elution times (with about the double number-average molecular weight of the PI precursors). As observed in Figure 3-21, this latter effect was more pronounced in the case where DPE was used in the functionalization process (**2**, Table 3-5).

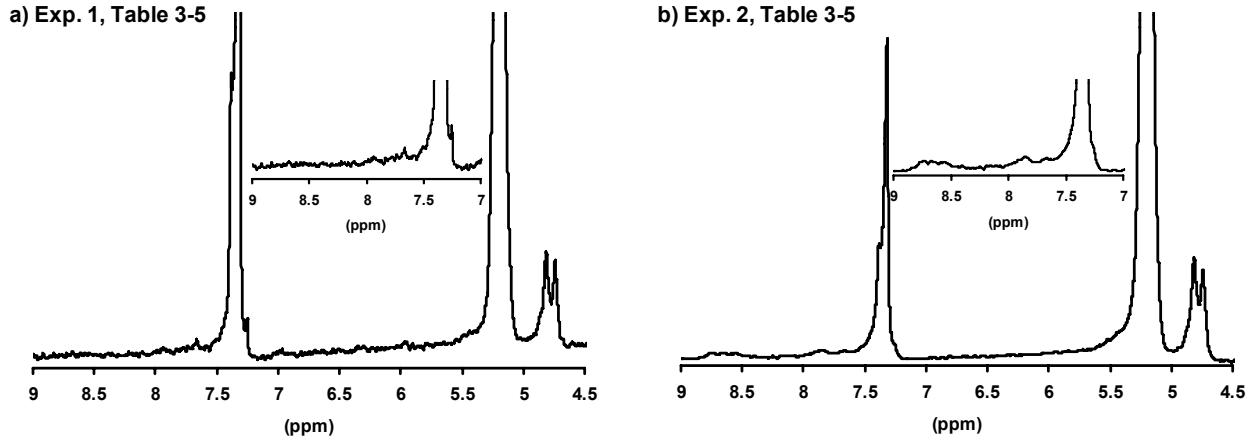

Figure 3-20: *^{1}H-NMR spectra in deuterated chloroform ($CDCl_3$) at 25 °C of terpyridine-functionalized poly(isoprene)s synthesized by anionic polymerization in cyclohexane at 20 °C (**1** and **2,** Table 3-5). (a) No end-capping with 1,1-diphenylethylene was used (**1**, Table3-5). (b) End-capping with 1,1-diphenylethylene was used (**2**, Table 3-5).*

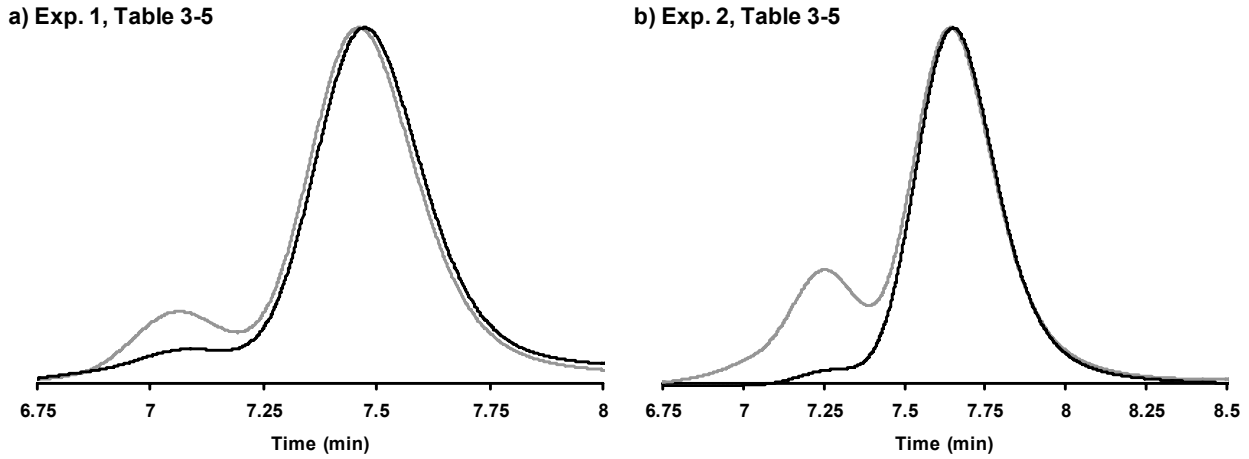

Figure 3-21: *Normalized GPC traces (eluent: triethylamine/2-propanol/chloroform mixture) of terpyridine-functionalized poly(isoprene)s synthesized by anionic polymerization in cyclohexane at 20 °C (**1** and **2,** Table 3-5). (a) Black line: Protonated poly(isoprenyllithium) precursor; grey line: 4'-Chloro-2,2':6',2"-terpyridine terminated poly(isoprenyllithium) precursor without end-capping with 1,1-diphenylethylene (**1**, Table3-5). (b) Black line: Protonated poly(isoprenyllithium) precursor; grey line: 4'-Chloro-2,2':6',2"-terpyridine terminated poly(isoprenyllithium) precursor where end-capping with 1,1-diphenylethylene was used (**2**, Table 3-5).*

Regarding the cases where *n*-heptane at −60 °C (Figure 3-19) was investigated as reaction media for the synthesis of Tpy-PI by anionic polymerization (**3** and **4**, Table 3-5), ^{1}H-NMR measurements showed higher degrees of functionalization for these reaction conditions in comparison to the cases where cyclohexane at 20 °C was used. For both investigated reaction conditions (with and without using DPE during the functionalization process), ^{1}H NMR spectra (Figure 3-22) revealed the presence of clear signals related to the aromatic protons of the terpyridine functional group (region from 7.5 to 8.8 ppm). In addition to the signals of the protons related to the double bonds of PI (between 4.6 and 5.6 ppm), Figure 3-22b also shows the presence of signals related to the aromatic protons of DPE around 7.3 ppm for the case when it was used as an end-capper (**4**, Table 3-5). However, the obtained GPC traces of the Tpy-PI synthesized in these two experiments still revealed that a few undesired coupling reactions occurred between the “living” polymeric anions as observed in Figure 3-23 (gray traces). The undesired coupling reactions in these latter cases are slightly less pronounced than in the cases where cyclohexane at 20 °C was used (**1** and **2**, Table 3-5). Moreover, according to the obtained ^{1}H NMR and GPC results

shown in Figures 3-22 and 3-23, it is thought that the use of DPE as an end-capper of the poly(isoprenyl) anions has no significant influence on the functionalization process of PI where the reactions are carried out in *n*-heptane at –60 °C (**3** and **4**, Table 3-5).

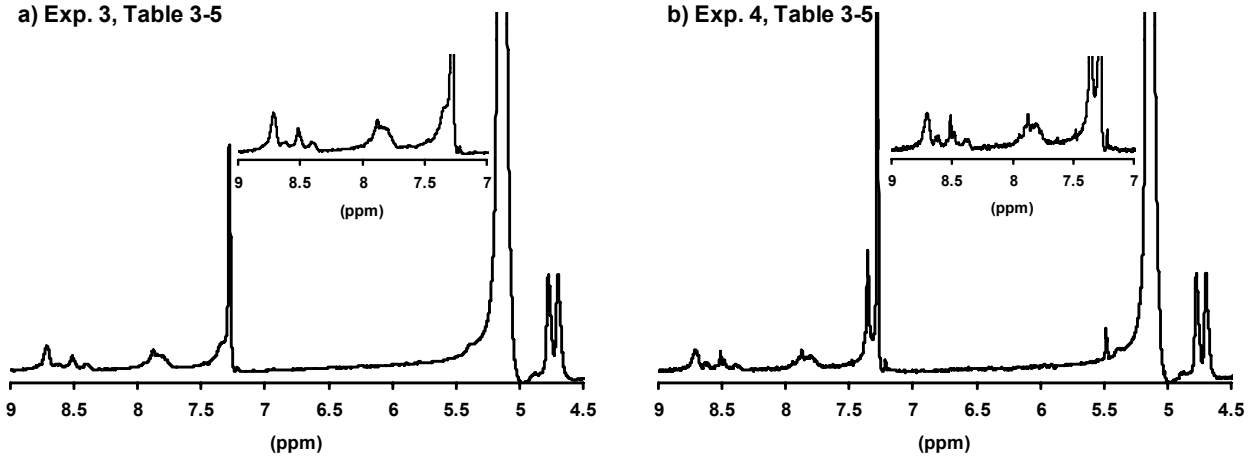

Figure 3-22: *^{1}H-NMR spectra in deuterated chloroform ($CDCl_3$) at 25 °C of terpyridine-functionalized poly(isoprene)s synthesized by anionic polymerization in n-heptane at −60 °C (**3** and **4,** Table 3-5). (a) No end-capping with 1,1-diphenylethylene was used (**3**, Table3-5). (b) End-capping with 1,1-diphenylethylene was used (**4**, Table 3-5).*

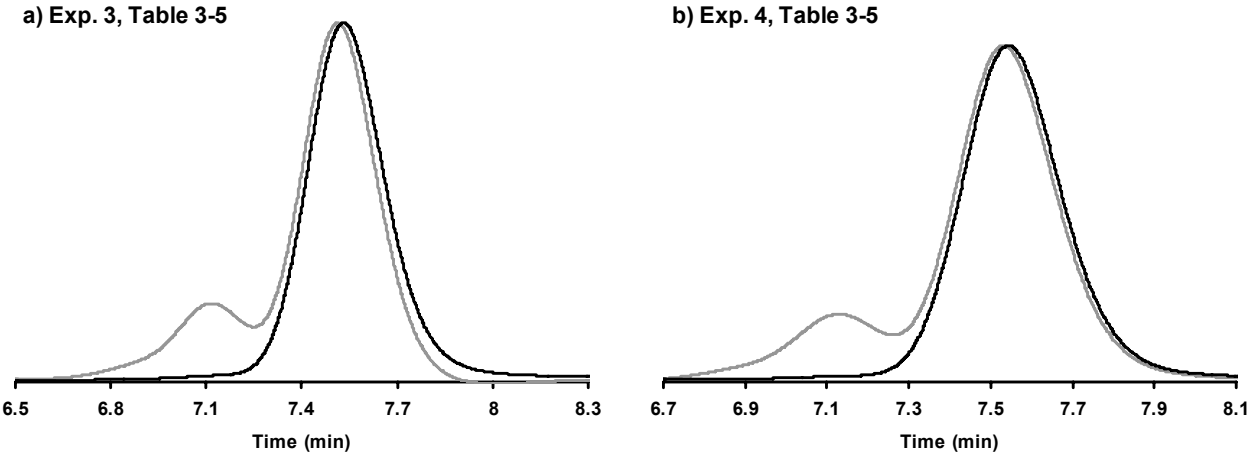

Figure 3-23: *Normalized GPC traces (eluent: triethylamine/2-propanol/chloroform mixture) of terpyridine-functionalized poly(isoprene)s synthesized by anionic polymerization in n-heptane at −60 °C (**3** and **4,** Table 3-5). (a) Black line: Protonated poly(isopryllithium) precursor; grey line: 4'-Chloro-2,2':6',2''-terpyridine terminated poly(isopryllithium) precursor where no end-capping with 1,1-diphenylethylene was used (**3**, Table3-5). (b) Black line: Protonated poly(isopryllithium) precursor; grey line: 4'-Chloro-2,2':6',2''-terpyridine terminated poly(isopryllithium) precursor where end-capping with 1,1-diphenylethylene was used (**4**, Table 3-5).*

In addition to the investigations of the synthesis of Tpy-PI, anionic polymerization is also known to be a suitable technique to synthesize poly(methyl methacrylate) (PMMA) in a controlled manner. However, the functionalization of PMMA with terpyridine moieties via anionic polymerization could not be successfully achieved where THF or toluene were used as a reaction media at −78 °C and at room temperature, respectively. These attempts also failed where DPE was used as an end-capper during the functionalization procedure. Although, the GPC traces remained practically unmodified upon the addition of Cl-Tpy in comparison to the traces of the precursor polymers, ^{1}H-NMR measurements of the polymers synthesized revealed no signals related to the terpyridine group in region of the spectrum between 7.5 to 8.8 ppm. Furthermore, the characteristic deep blue color shown by the reaction mixtures during the preparation of Tpy-PS (Figure 3-9) and Tpy-PI (Figure 3-19) was not observed for the cases of PMMA

investigated. This finding might be related to the difference in reactivity of PMMA anions when compared to the cases of poly(styryl) or poly(isoprenyl) anions.

Apart from the use of Cl-Tpy for the functionalization of polymers with terpyridine moieties via anionic polymerization, 4'(4-bromomethyl phenyl)-2,2':6',2"-terpyridine (Br-Tpy) was also utilized in this context. Additional anionic polymerization experiments were carried out in order to investigate whether the use of Br-Tpy as a terminating agent in the proposed synthetic approach would also yield well-defined functionalized polymers, and perhaps to improve the functionalization process. For theses additional experiments, the functionalization reactions investigated are summarized schematically in Figure 3-24.

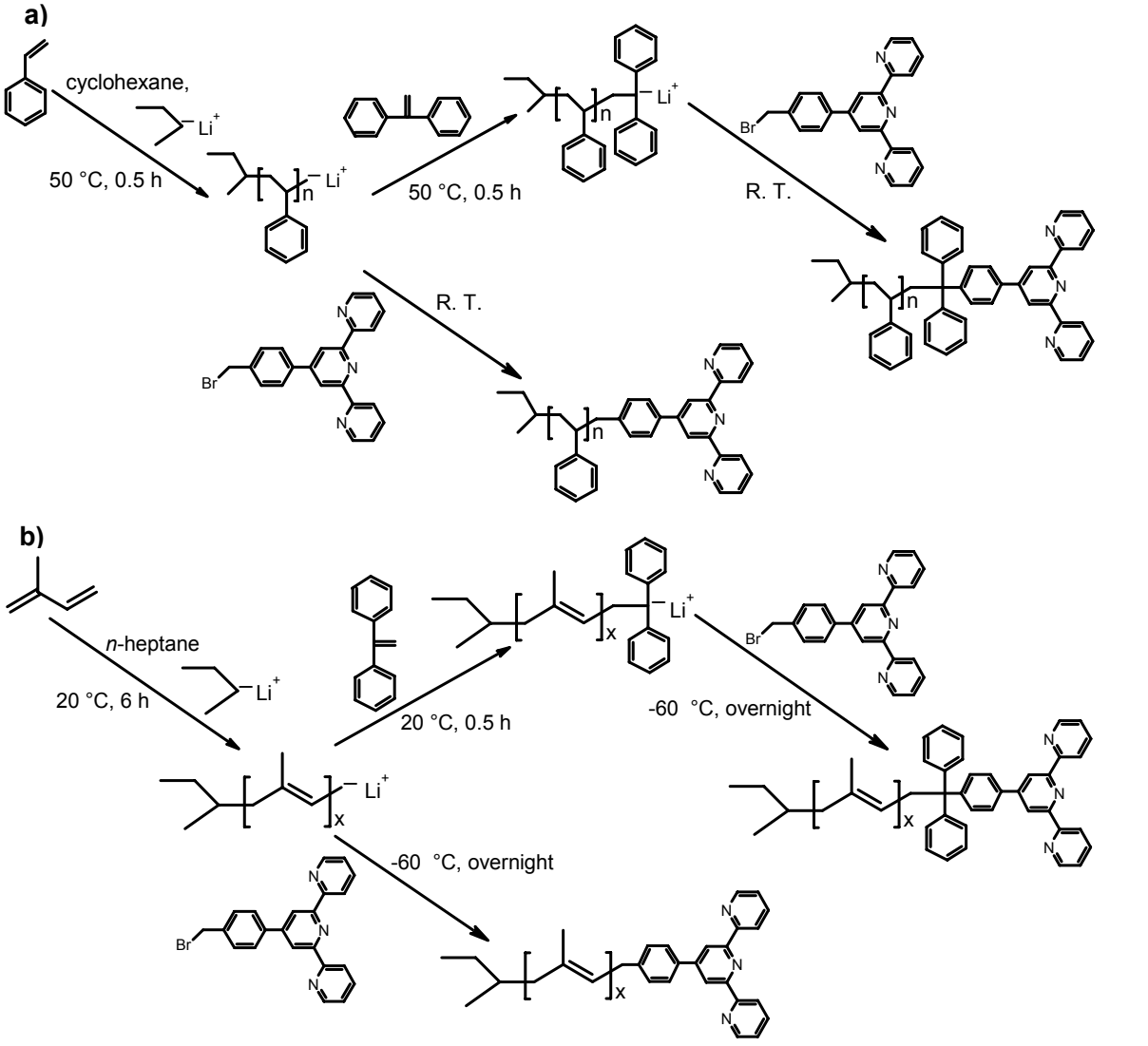

Figure 3-24: *Schematic representation of the investigated methods using 4'(4-bromomethyl phenyl)-2,2':6',2"-terpyridine as a terminating agent for the synthesis of terpyridine-functionalized polymers via anionic polymerization. (a) Terpyridine functionalization of poly(styrene) with and without using 1,1-diphenylethylene for the stabilization of poly(styryl) anions. (b) Terpyridine functionalization of poly(styrene) with and without using 1,1-diphenylethylene for the stabilization of poly(isoprenyl) anions.*

Unfortunately, the results obtained from the experiments where Br-Tpy was used as a terminating agent for the functionalization of polymers via anionic polymerization (Figure 3-24) have revealed that this compound is less efficient for the preparation of well-defined functionalized polymers than its analogous Cl-Tpy. For instance, it was observed from the GPC results that for the functionalization reactions investigated (Figure 3-24) the molecular weight distributions of the synthesized materials become bimodal

and broader than their corresponding protonated precursor polymers for both, PS and PI, cases. In the cases where DPE was used for stabilizing the respective polymeric anions (Figure 3-24) the molecular weight distributions of the polymer obtained become also bimodal and broader than its respective un-functionalized precursor polymers for both, PS and PI, cases. Moreover, clear signals related to the protons of the terpyridine group (region from 7.5 to 8.8 ppm) could not be observed in the ^{1}H-NMR spectra of the polymers synthesized (Figure 3-24) (being this effect more remarkable in the cases of PS than in the cases of PI).

According to the results presented in this section, it is clear that further optimization (in terms of synthesis and characterization) has to be carried out for the functionalization cases investigated in order to achieve the preparation, for instance, of well-defined Tpy-PI by anionic polymerization with comparable properties to those Tpy-PS addressed in section 3.3.2.

3.3.5 Synthesis of terpyridine-functionalized star-shaped polymers by anionic polymerization

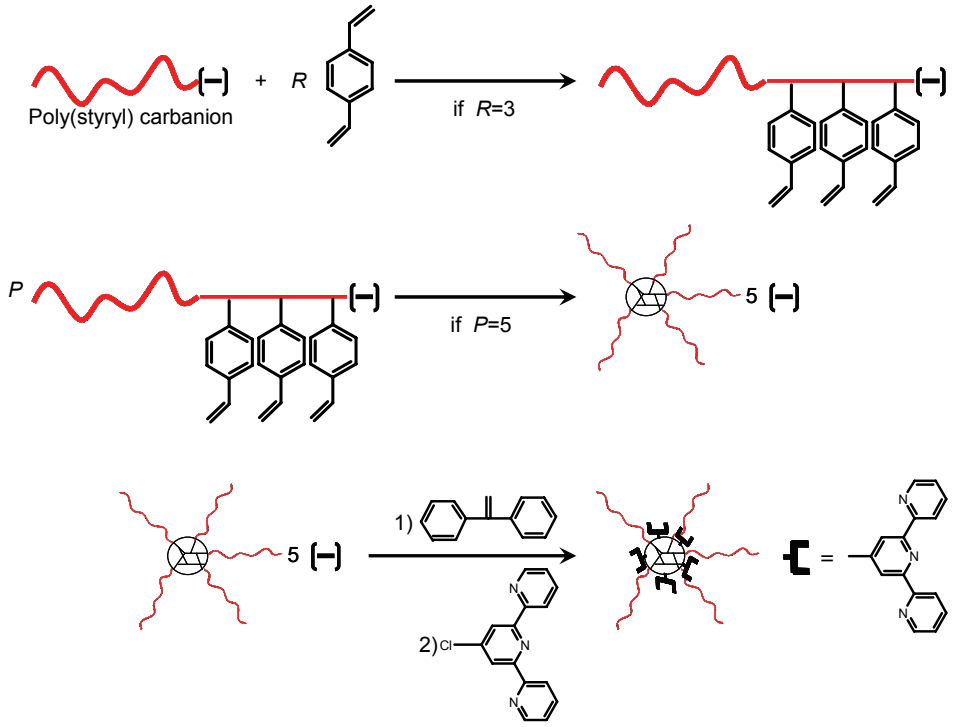

Figure 3-25: *Schematic representation of the investigated method for the synthesis of terpyridine-functionalized multi-arm star polymers via anionic polymerization in cyclohexane at 50 °C using the "arm-first" approach.*[44]

In addition to the synthesis of well-defined linear polymers and block copolymers, anionic polymerization is a suitable technique for the synthesis of other polymeric architectures such as star-shaped polymers.[3] In this regard, the synthesis of terpyridine-functionalized multi-arm star-shaped polymers via anionic polymerization utilizing the "arm-first" approach[44] was briefly investigated according to the reaction scheme shown in Figure 3-25.

In case of the synthesis of terpyridine-functionalized multi-arm star-shaped polymers utilizing the "arm-first" approach, the reaction was not performed in the synthesizer described in chapter 2 due to the fact that a suitable stirring was required, which could not be efficiently supplied by the vortex system of the synthesizer used up to now. The synthetic approach utilized (Figure 3-25) requires suitable and efficient mixing of the reaction solutions to avoid an excess of cross-linking in the polymerization system.[44] Hence, the polymerization was performed in conventional laboratory glassware with magnetic stirring (see experimental part for details). As depicted in the reaction scheme of Figure 3-25, linear

poly(styryl) carbanions precursors must be synthesized in a first step before the synthesis of the multi-arm star polymer. The obtained linear PS chains yielded a Mn = 3.5 kg mol^{-1} and a PDI = 1.12 as revealed by GPC measurements. The expected Mn of this linear polymer (according to the utilized monomer/initiator ratio) was in agreement with the obtained value from GPC. In a subsequent reaction step, the poly(styryl) carbanions obtained are cross-linked upon the addition of *p*-divinylbenze (DVB) into the reaction mixture in order to form the multi-arm polymer with reactive sites (carbanions). These reactive carbanions are utilized in a last reaction step to incorporate terpyridine moieties into the star-shaped polymers (as depicted in Figure 3-25). The terpyridine-functionalized multi-arm star-shaped PS obtained showed a Mn = 42.0 kg mol^{-1} and a PDI = 1.25. Figure 3-26a displays the GPC traces of the precursor PS as well as of the obtained terpyridine-functionalized multi-arm star polymer. It is know from literature[44] that in the investigated synthetic approach the number of branches or arms of the prepared stars, and therefore the number of "living" active sites available for functionalization with terpyrine moieties, is difficult to determine *a priori* since it depends on several reaction parameters, such as the mole ratio of unsaturated monomer added per living site (*e.g.*, R = [DVB] / [*sec*-butyllithium]), the overall concentration, the nature of the solvent, and the efficiency of the utilized mixing system. It is also known that GPC is not the most suitable method for determining the molecular weight distribution of star-shaped molecules since the hydrodynamic volume of star-shaped molecules varies only slightly with the number of branches.[44b] Therefore, the aforementioned Mn and PDI values corresponding to the terpyridine-functionalized multi-arm star PS must not be considered as absolute values. It has also been addressed that the protection exerted by the branches on the cross-linked cores is very efficient and no gelation has been observed, even in cases where the amount of DVB utilized was rather high (up to 40% of the total weight of the star polymer).[44b] For the synthetic approach investigated and depicted in Figure 3-25, it is clear that the terpyridine functional groups are incorporated at the core of the multi-arm star PS. Theoretically (in absence of impurities or unexpected termination reactions), the number of terpyridine units attached to the stars must be determined by the number of branches, which can be estimated by obtaining the absolute molecular weight of the polymer, for example, by viscosimetry.

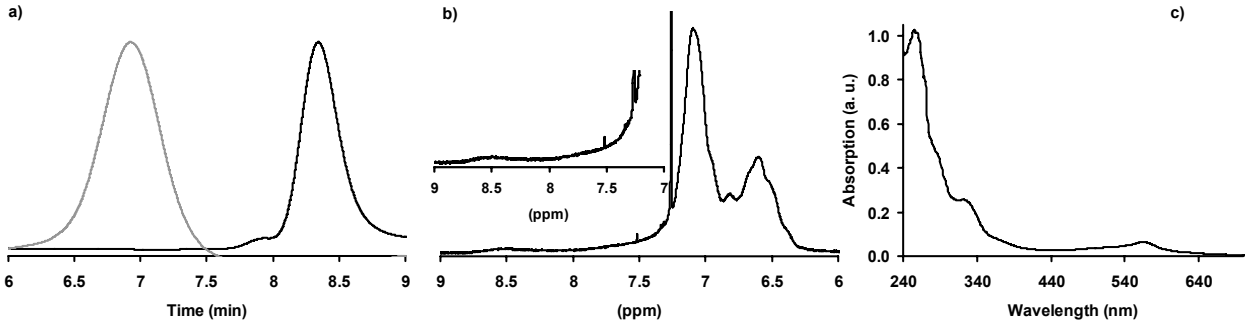

Figure 3-26: *Characterization measurements of the terpyridine-functionalized multi-arm star-shaped poly(styrene) synthesized by anionic polymerization in cyclohexane at 50 °C using 1,1-diphenylethylene to stabilize the poly(styryl) anions and 4'-chloro-2,2':6',2''-terpyridine as a terminating agent (Figure 3-25). (a) Normalized GPC traces (eluent: triethylamine/2-propanol/chloroform mixture); black line: Protonated poly(styryllithium) precursor (Mn = 3.5 kg mol^{-1}, PDI = 1.12); grey line: terpyridine-functionalized multi-arm star poly(styrene) (Mn = 42.0 kg mol^{-1}, PDI = 1.25). (b) ^{1}H-NMR spectra in deuterated chloroform ($CDCl_3$) at 25 °C of the synthesized terpyridine-functionalized multi-arm star-shaped poly(styrene). (c) UV-Vis spectrum of a complex formed by the synthesized terpyridine-functionalized multi-arm star-shaped poly(styrene) and iron(II) metal ions in chloroform (the spectrum shows the presence of metal-to-ligand charge-transfer (MLCT) bands at 329 and 565 nm).*

^{1}H-NMR analysis of the prepared terpyridine-functionalized multi-arm star PS revealed the presence of a broad signal in the region of the spectrum from 7.5 to 8.8 ppm (Figure 3-26b), which is thought to be related to the protons of the terpyridine units. The broadness of this signal may correspond to the facts that several terpyridine units have been attached and are inside a single star-shaped polymeric unit

(see Figure 3-25) For these reasons, it is thought that due to the steric hindrance inside the stars the terpyridine groups do not have sufficient space to move, and therefore the presence of single sharp peaks in the ^{1}H-NMR spectrum must not be expected. It is also known, as addressed in sections 3.3.2 and 3.3.3, that terpyrine moieties self-assemble to form complexes in the presence of different transition metal ions.[28,39] In this regard, a colorless solution of the terpyridine-functionalized multi-arm star PS obtained (after the respective purification procedure) in chloroform turned immediately purple upon adding a predetermined amount of iron(II) ions ($FeCl_2$ solution in methanol). The UV-Vis spectrum of the resulting solution is shown in Figure 3-26c and reveals a MLCT band at 329 and 565 nm related to the presence of iron(II) terpyridine complexes. This demonstrates the feasibility of synthesizing terpyridine-functionalized multi-arm star-shaped polymers by anionic polymerization.

3.4 Conclusions

In this chapter the synthesis and characterization of well-defined diblock copolymers of the type poly(styrene-*alt*-1,1-diphenylethylene-*block*-isoprene) via sequential anionic polymerization in a parallel synthesizer were discussed. The obtained diblock copolymers were utilized for the preparation of self-assembled polymeric micelles using a selective solvent for one of the blocks. The hydrodynamic radius of the micelles could be determined by DLS whereas the size of the micellar core was obtained by AFM measurements at dry conditions. Theory states that the core size, corona thickness and overall micellar diameter depend on the degree of polymerization of both blocks. For so-called “hairy” micelles the overall micellar diameter in solution is mainly dominated by the thickness of the corona. It was found that the observed characteristics of the studied micelles correlate very well to theoretical scaling predictions. Moreover, the average size of the monomeric units could be estimated from the obtained experimental data and the theoretical knowledge.

In addition to the preparation of a “new” diblock copolymer library, the use of the parallel synthesizer allowed the development of an alternative synthetic route for the preparation of well-defined terpyridine-functionalized poly(styrene). Starting from the synthesis of “living” poly(styrene) via anionic polymerization in cyclohexane, an intermediate end-capping step of the highly reactive poly(styryl) anions with 1,1-diphenylethylene was found to be necessary to promote an suitable terpyridine functionalization process of the polymeric chains and to avoid undesired side (coupling) reactions between the polymeric chains due to the high reactivity of the poly(styryl) anions. Moreover, the functionalization process is highly efficient when toluene is used as a solvent for 4'-chloro-2,2':6',2"-terpyridine (terminating agent). The functionalized polymers were fully characterized by means of GPC, ^{1}H-NMR, elemental analysis, MALDI-TOF-MS, and UV-Vis spectroscopy. The materials obtained by this new synthetic approach revealed the typical characteristics of terpyridine-functionalized polymers (*e.g.*, formation of metal complexes and self-assembled diblock copolymers) obtained by other preparation methods. Furthermore, the preparation of terpyridine-functionalized poly(styrene) ruthenium *mono*- and *bis*-complexes (metallo-supramolecular diblock copolymers) was also achieved using the synthesized polymers. This synthetic route offers some advantages in comparison to the existing methods (*e.g.*, direct functionalization, short reaction times, full control over the molecular weight of the polymers, polymers with low polydispersity indices, high efficiency of functionalization) and can be scaled-up due to the fact that anionic polymerization is a well-established industrial process. Finally, the developed synthetic method was used to investigate the possibility of functionalize other polymeric species with terpyridine units, such as poly(isoprene) and multi-arm star-shaped polymers. The terpyridine-functionalization for these latter cases was feasible with the proposed synthetic approach. However, further experimentation in these cases will be necessary in order to optimize the reaction conditions and to improve the functionalization process. Future experimentation using the developed synthetic method may focus on the

direct synthesis of terpyridine-functionalized block copolymers (covalently linked) and of terpyridine-telechelic polymers by using bi-functional anionic initiators as those reported in literature.[17,45]

In the next chapter, the introduction of new ionic systems (ionic liquids) into the polymer field is addressed. Hence, ionic liquids are utilized as novel reaction media for different polymerization processes, which includes other "living" ionic polymerization (cationic ring opening polymerization), and heterogeneous and homogeneous free radical polymerization reactions.

3.5 Experimental part

3.5.1 Experimental part for the synthesis and characterization of diblock copolymer micelles based on poly(styrene-alt-1,1-diphenylethylene-block-isoprene)

Diblock copolymer synthesis. Purification of all used chemical reagents was performed as addressed in chapter 2. Sequential anionic polymerizations for the synthesis of P(S-*alt*-DPE)-*b*-PI were performed in a Chemspeed ASW2000 automated synthesizer (see chapter 2 for a full description of this experimental technique). In a characteristic procedure (Figure 3-1), the anionic synthesis of the diblock copolymers was performed as follows: A predetermined amount of 1,1-diphenylethylene (DPE) was added into the 13 mL reactors of the synthesizer containing 5 mL of cyclohexane. The reactions were set to 50 °C and 450 rpm of vortexing under argon atmosphere. Addition of *sec*-butyllithium into the reactors transformed the DPE into the corresponding 1,1-diphenylalkyllithium resulting in the characteristic red color. After 0.5 h, an equimolar amount of styrene (with respect to DPE) was added into the reaction media. This mixture was allowed to react for 2 h. Thereafter, samples were withdrawn from the reactors for GPC characterization of the respective P(S-*alt*-DPE) precursor blocks. Addition of a predetermined volume of isoprene into the reactors started the sequential synthesis of the second block. After 4 h at 25 °C the reactions were terminated upon adding methanol. The total concentration of three monomers (DPE, styrene, and isoprene) used in the anionic polymerization reactions was 10 wt % with respect to the amount of solvent (5 mL of cyclohexane). Hence, the amount of each monomer used was varied according to the compositions of each block desired in the copolymer, but keeping the styrene/DPE molar ratio constant and equal to 1 for all the cases investigated. The amount of initiator used in each reactor was also varied according to the molecular weights of the polymers synthesized. Purification of the polymers was performed with two cycles of dissolution/precipitation (chloroform/methanol). The obtained block copolymers were dried at 40 °C under vacuum for 24 h and were subsequently characterized by GPC, ^{1}H-NMR spectroscopy and DSC in order to obtain the molecular weights and the compositions of each block, respectively.

Preparation of the diblock copolymer micelles. Preparation of micelles from the synthesized diblock copolymers were performed using methods reported in literature.[6] The diblock copolymers were dissolved in a common solvent (chloroform, good solvent for both blocks) (1 g L^{-1}) at room temperature. Subsequently, a selective precipitant for the styrenic block (*n*-heptane) was gradually added to reach a concentration of 10 wt % of the common solvent (chloroform). The removal of chloroform from the mixtures was achieved by stirring and heating the dispersions at 60 °C in an oil bath for 1 h. The obtained diblock copolymer micellar dispersions were finally diluted with an excess of *n*-heptane (up to 10 fold excess). These dispersions were subsequently characterized by DLS (in *n*-heptane) and AFM (at dry conditions) in order to determine the hydrodynamic diameters and the diameters of the cores of the micelles. It was found that some of the micellar solutions were unstable in time (especially sample **2**, Table 3-1). DLS measurements revealed that when using not freshly prepared micellar solutions bimodal distributions are obtained suggesting the collapse or aggregation of the micelles. Therefore, the herein reported DLS measurements were recorded on freshly prepared micellar solutions and, additionally, the solutions were filtered two times on 200 nm syringe filters immediately after the removal of chloroform in order to avoid the formation of micellar aggregates.

Characterization techniques.

Gel permeation chromatography (GPC) measurements were performed on a Shimadzu system with a SCL-10A system controller, a LC-10AD pump, a RID-6A refractive index detector and a Polymer Laboratories Plgel 5 µm Mixed-D column. A solution of 4% triethylamine and 2% isopropanol in chloroform was used as eluent at a flow rate of 1 mL min^{-1} and a column temperature of 40 °C. Molecular weights were calculated against poly(styrene) standards.

Proton nuclear magnetic resonance (^{1}H-NMR) measurements were recorded at 25 °C on a Varian Gemini 400 spectrometer using deuterated chloroform (Cambridge Isotopes Laboratories). The 1,4-unit contents of the PI blocks were calculated from the relative intensity of the signal at 5.1 ppm (–CH= of 1,4-unit) and the signals at 4.68 and 4.75 ppm (=CH_2 of 3,4-unit and =CH_2 of 1,2-unit). The copolymer compositions were calculated from the relative intensities of the signals for the 1,4-unit, 1,2-unit and 3,4-unit of PI blocks and from the *meta* and *para* hydrogens of the aromatic rings at 6.93 ppm of the P(S-*alt*-DPE) blocks.

Differential scanning calorymetry (DSC) measurements were performed on a Netzsch DSC 204 F1 instrument calibrated with indium. Multiple heating and cooling scans were generated over a temperature range of –150 to 230 °C using scan rates of 10, 20 and 40 °C min^{-1} with nitrogen as the purge gas. The *Tg* values were noted at the inflection points of the heat capacity jump.

Dynamic light scattering (DLS) experiments were performed at 25 °C at 90° on a Malvern CGS-3 apparatus equipped with a 633 nm laser. The used values of the refractive index and viscosity of *n*-heptane were 1.385 and 3.94 Pa s, respectively.

For the atomic force microscopy (AFM) experiments, samples were prepared by spin casting of 100-fold diluted micellar solutions (in order to obtain near monolayer coverage) onto freshly cleaved mica substrates. The samples were prepared and imaged within 30 minutes to reduce the possibility of micelle deformation and/or aggregation. Imaging was performed in intermittent contact mode on a Multimode SPM (Digital Instruments, Santa Barbara, CA) using NSC36-type tips (~1 N m^{-1}, Mikromasch, Spain). The height of the micelles was determined from histograms after zeroth-order leveling of the images.

3.5.2 Experimental part for the synthesis of terpyridine-functionalized polymers by anionic polymerization and their characterization

Reagents and solvents. Purification of all used chemical reagents was performed as addressed in chapter 2. In addition, *n*-heptane (Biosolve) and toluene (Biosolve) were distilled from poly(styryllithium) oligomers and stored under an argon atmosphere at room temperature. *p*-Divinylbenzene (DVB) was purified in a similar way as the styrene monomer (see chapter 2). 4'-Chloro-2,2':6',2"-terpyridine (Cl-Tpy) and 4'(4-bromomethyl phenyl)-2,2':6',2"-terpyridine (Br-Tpy) were purified by repeated sublimation. *N,N*-Dimethylformamide (anhydrous, Biosolve) and *N,N*-dimethylacetamide (anhydrous, Aldrich) were dried over molecular sieves and degassed with argon for 15 min prior to use. All other solvents and reagents were used as received: Chloroform (Biosolve), ruthenium tri-chloride ($RuCl_3$) (anhydrous, Aldrich), iron(II) chloride ($FeCl_2$) (anhydrous, Aldrich) and silver tetrafluoroborate ($AgBF_4$) (Aldrich).

Polymerization and functionalization reactions. Anionic polymerizations were performed in a Chemspeed ASW2000 synthesizer (see chapter 2 for a full description of this experimental technique). Reaction schemes of the investigated terpyridine-functionalization processes in this chapter and images of the Chemspeed ASW2000 automated parallel synthesizer during the different stages of the reactions are shown in Figures 3-9, 3-19 and 3-24. A characteristic functionalization procedure, for example for the synthesis of terpyridine-functionalized poly(styrene)s via anionic polymerization in cyclohexane, was performed as follows: an amount of styrene (10 wt % of monomer with respect to the amount of solvent) was added into the 13 mL reactors of the synthesizer containing 5 mL of cyclohexane (solvent) at 50 °C and 450 rpm of vortexing under argon atmosphere. Upon adding *sec*-butyllithium into the reactors the polymerization started and the reaction mixtures yielded the characteristic orange-yellow color of poly(styryl) anions (the amount of initiator used in each reactor was varied according to the molecular weights of the precursor polymers synthesized). After 0.5 h of reaction time, a 1.2 molar excess (with respect to the amount of *sec*-butyllithium) of 1,1-diphenylethylene (DPE) was introduced into the reaction media turning the solutions red. An intermediate step at this stage consisted in withdrawing aliquots of the reaction mixture for GPC characterization

of the un-functionalized poly(styrene) precursors. After another 0.5 h, predetermined volumes (1.2 molar excess with respect to the amount of *sec*-butyllithium) of a solution of Cl-Tpy in THF or toluene (0.1 mol L^{-1}) were added into the reactors. Immediately the reactions showed a deep blue color. Subsequently, the reaction mixtures were kept under argon atmosphere overnight at room temperature. Methanol was added into the reaction mixtures to finalize the functionalization process (the deep blue color of the mixtures disappeared upon adding methanol). Finally, purification of the polymers was performed with three cycles of dissolution/precipitation steps (chloroform/methanol) in order to remove un-reacted Cl-Tpy molecules. The obtained materials were dried at 40 °C under vacuum for 24 h and were subsequently characterized. For the synthesis of terpyridine-functionalized multi-arm star polymers based on styrene and DVB (Figure 3-25), anionic polymerizations were carried out in a 100 mL round bottom schlenk-type glass flask using inert atmosphere techniques (see chapter 2 for experimental details). All utilized glassware was previously heated above 150 °C, subjected to several cycles of subsequent filling with argon and high-vacuum, and kept under argon prior use. The procedure for this synthetic approach (Figure 3-25) was performed as follows: an amount of styrene was added into the schlenk-type flask containing 25 mL of cyclohexane at 50 °C under vigorous magnetic stirring and an argon atmosphere. The concentration of styrene in the previous mixture was 0.34 mol L^{-1}. The addition of *sec*-butyllithium into the reactor started the polymerization yielding the characteristic orange-yellowish color of a poly(sytryllithium) solution (the amount of initiator used in this case was calculated according to the desired molecular weight of the precursor “arms” of star-shaped polymer). The concentration of *sec*-butyllithium in the reaction mixture was 0.01 mol L^{-1}. After 0.5 h of reaction time a sample was withdrawn from the flask for GPC characterization of this linear polystyrene. Subsequently, an amount of DVB was added into the flask to reach a concentration of DVB of 0.03 mol L^{-1} in the reaction mixture. At this point the solution became pale red. This reaction step proceeded for another 0.5 h at 50 °C. At this stage, a 1.25 molar excess (respect to *sec*-butyllithium) of DPE was introduced into the reaction media turning the solution slightly more red than in the previous step; this reaction step proceeded for another 0.5 h at 50 °C. Thereafter, the functionalization step started with the addition of a solution of Cl-Tpy in toluene (0.1 mol L^{-1}) into the reactor (1.25 molar excess of Cl-Tpy with respect to the amount of *sec*-butyllithium). This last reaction step continued overnight at 50 °C. Immediately after the addition of the Cl-Tpy solution, the reaction mixture revealed a deep blue color as observed for the before addressed functionalizations of the analogous linear terpyridine-functionalized poly(styrene)s. Finally, methanol was added into the flask to ensure the termination of the reaction. Purification of the obtained star polymer was carried out as previously described for the cases of linear functionalized polymers.

Synthesis of metallo-supramolecular polymeric complexes. Complexation reactions using some of the synthesized terpyridine-functionalized poly(styrene)s were performed as follows. Ruthenium tri-chloride *mono*-complexes were obtained by heating a solution of $RuCl_3$ in *N,N*-dimethylacetamide at 130 °C in an oil bath with magnetic stirring followed by the drop wise addition of a solution of terpyridine-functionalized polystyrene in *N,N*-dimethylacetamide in order to obtain a two fold molar excess of $RuCl_3$ with respect to the polymer. The synthesis of a metallo-supramolecular block copolymer ruthenium(II) *bis*-complex (poly(styrene)-*block*-poly(ethylene oxide)) was achieved as follows: A solution of a terpyridine-functionalized poly(ethylene oxide) ruthenium tri-chloride *mono*-complex (Mn = 3.1 kg mol^{-1})[42] in *N,N*-dimethylformamide was heated at 130 °C in an oil bath with magnetic stirring in the presence of three equivalents of $AgBF_4$. Subsequently, a solution of terpyridine-functionalized polystyrene (in *N,N*-dimethylformamide) was added drop wise to obtain a 1.2 fold molar excess of terpyridine-functionalized poly(styrene) with respect to the poly(ethylene oxide) *mono*-complex. For both, *mono* and *bis*-complexation experiments, the total concentration of the polymer was 10 wt % and a reaction time of 6 h was utilized.

Characterization techniques.

GPC and ^{1}H-NMR measurements were performed on the same systems as described in section 3.5.1. For the GPC characterization, aliquots from the reactors of the synthesizer were withdrawn (see chapter 2 for experimental details) before and after the addition of Cl-Tpy solutions into the reaction mixtures containing the polymeric anions. All protonated precursor polymers (before functionalization) showed narrow molecular weight distributions and their calculated molecular weights (according to the monomer/initiator ratio) were in agreement with the experimental values obtained by GPC.

MALDI-TOF-MS analysis was performed on a Voyager-DE™ PRO Biospectrometry™ workstation (Applied Biosystems) in linear operation mode. Spectra were obtained in positive ion mode and ionization was performed with a 337 nm pulsed nitrogen laser. Data were processed using the Data Explorer™ software package (Applied Biosystems).

An additional GPC system (Waters) equipped with photo diode array and refractive index detectors, and a column of poly(styrene/divinylbenzene) cross-linked beads was used for the characterization of the metallo-supramolecular polymeric complexes.[43] A solution of 5 mM of NH_4PF_6 in *N,N*-dimethylformamide was used as eluent at a flow rate of 0.5 mL min^{-1}. The column temperature during the measurements was 50 °C. It is known that (GPC) analysis of bi- and terpyridine metallo-supramolecular polymeric complexes is not a straight forward measurement due to the interactions of the charged compounds with the materials of GPC columns.[43] The determination of the elution time in GPC is, mainly, related to the hydrodynamic volume of the polymeric chain, which is predominately influenced by the measuring conditions (*e.g.*, type of polymer, solvent, temperature). For this reason, polymers of different nature but with similar molecular weights can show different hydrodynamic volumes under specific conditions. This effect was observed for the GPC traces of Figure 3-17a where a terpyridine-functionalized poly(styrene) (**8**, Table 3-4) revealed a longer elution time than a terpyridine-functionalized poly(ethylene oxide) ruthenium tri-chloride *mono*-complex (Mn = 3.1 kg mol^{-1})[42] even though the molar mass of the poly(styrene) is larger. In order to clarify this effect Figure 3-27 shows GPC traces (eluent: 5 mM of NH_4PF_6 in *N,N*-dimethylformamide) of a series of terpyridine-functionalized poly(styrene)s, of a series of terpyridine-functionalized poly(ethylene oxide) ruthenium tri-chloride *mono*-complexes, and of a series of metallo-supramolecular block copolymer ruthenium(II) *bis*-complexes (poly(styrene)-*block*-poly(ethylene oxide)). In Figure 3-27 it can be observed that poly(styrene)s reveal longer elution times (Figure 3-27a) than poly(ethylene oxide)s (Figure 3-27b) in the utilized GPC system, even though the molecular weigths of the poly(styrene)s are considerably larger. For the case of the metallo-supramolecular block copolymer ruthenium(II) *bis*-complexes (poly(styrene)-*block*-poly(ethylene oxide)) the elution time will depend, mainly, on the type and composition of the precursor blocks (Figure 3-27c).

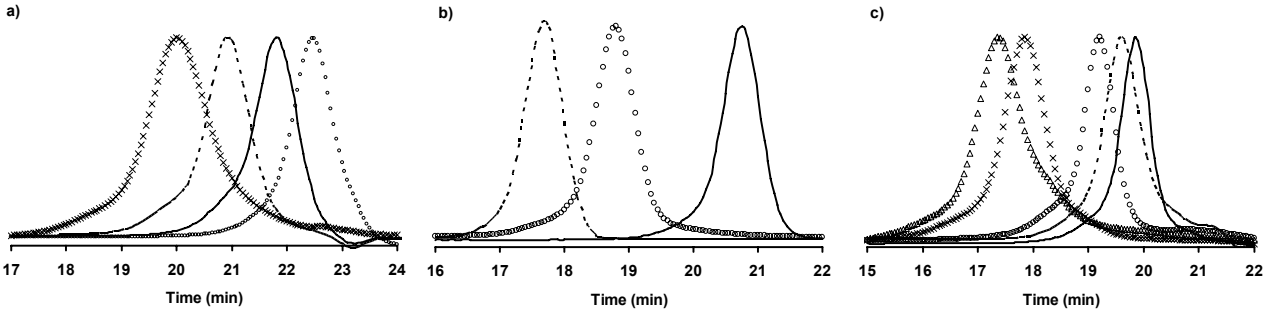

Figure 3-27: *Normalized GPC traces (eluent; 5 mM of NH_4PF_6 in N,N-dimethylformamide). (a) Terpyridine-functionalized poly(styrene)s: Mn = 7.7 kg mol^{-1} (open circles), Mn = 11.0 kg mol^{-1} (solid line), Mn = 20.5 kg mol^{-1} (dashed line) and Mn = 31.4 kg mol^{-1} (crosses). (b) Terpyridine-functionalized poly(ethylene oxide) ruthenium tri-chloride mono-complexes: Mn = 3.1 kg mol^{-1} (solid line), Mn = 9.9 kg mol^{-1} (open circles) and Mn = 16.5 kg mol^{-1} (dashed line). (c) Self-assembled metallo-supramolecular block copolymer ruthenium(II) bis-complexes (poly(styrene)-block-poly(ethylene oxide)): PS = 2.1 kg mol^{-1} + PEO = 3.1 kg mol^{-1} (solid line), PS = 7.7 kg mol^{-1} + PEO = 3.1 kg mol^{-1} (dashed line), PS = 31.4 kg mol^{-1} + PEO = 9.9 kg mol^{-1} (crosses), PS = 31.400 kg mol^{-1} + PEO = 16.5 kg mol^{-1} (open triangles) and self-assembled metallo-supramolecular chain extended polymer ruthenium(II) bis-complex (poly(ethylene oxide)-block-poly(ethylene oxide)): PEO = 3.1 kg mol^{-1} + PEO = 3.1 kg mol^{-1} (open circles).*

UV-Vis spectroscopy was carried out on a Perkin Elmer Lambda 45 UV-VIS spectrometer using quartz cuvettes (1 cm path length). The UV-Vis titrations of the synthesized terpyridine-functionalized poly(styrene)s were performed as follows: The different terpyridine-functionalized poly(styrene)s were dissolved in chloroform to obtain a solution of 175 mg L^{-1}. A solution of $FeCl_2$ in methanol (65 mg L^{-1}) was freshly prepared and used for the titration of 100 mL of previously prepared polymeric solutions in chloroform. Steps of 0.2 mL of the solution of $FeCl_2$ were used during the titration processes, which was monitored by UV-Vis spectroscopy. After each step (additions of the solution of $FeCl_2$) the polymeric solutions were vigorously stirred for 3 minutes in order to reach the equilibrium for the formation of the metal complexes and a UV-Vis measurement was recorded for each step. After each addition of $FeCl_2$ during the

titration, an increment of the metal-to-ligand charge-transfer of the iron(II) complex at 565 nm and 329 nm was observed as expected for this type of complexation processes.[39] Thereafter, a plateau for the signals at 565 nm and 329 nm was reached after a linear increase upon the addition of $FeCl_2$ indicating the completion of the formation of the metallo-supramolecular polymeric complexes (purple solution). The equivalence point of each titration was observed around a ligand-to-metal ratio of 2:1, which indicated quantitative complexation processes. The quantitative determination of the ligand-to-metal ratio of 2:1 and the efficiency of the terpyridine-functionalization reaction obtained by the UV-Vis titration technique were estimated as follows: Figure 3-28a summarizes the UV-Vis titration process for one of the synthesized terpyridine-terminated poly(styrene) (**8**, Table 3-4). Figure 3-28b shows the volume of solution of $FeCl_2$ (2.2 mL, 65 mg L^{-1}) necessary to reach the equivalent point for a full complexation of the polymeric solution (100 mL, 175 mg L^{-1}). Subsequently, from this latter data and the molar mass of $FeCl_2$ (126.75 g mol^{-1}), the molar amount of $FeCl_2$ required for a full complexation of the polymeric solution can be estimated, which was found to be 1.128×10^{-6} mol for the investigated case (**8**, Table 3-4). This value must correspond to the molar amount of polymer for a ligand-to-metal ratio of 2:1 (2.256×10^{-6} mol, two times the experimentally found molar amount of $FeCl_2$). On the other hand, the molar amount of polymer in the titrated solution (100 mL, 175 mg L^{-1}) can be estimated using the obtained molecular weight (by GPC) of the analyzed polymer (**8**, Table 3-4, Mn = 7.7 kg mol^{-1}). In this latter case, the molar amount of polymer corresponds to 2.272×10^{-6} mol. Finally, the efficiency of the functionalization reaction can be estimated by comparison of the molar amounts of polymer obtained in the titration experiment and in the prepared solution of terpyridine-functionalized polymer. For the investigated case (**8**, Table 3-4) the results revealed the presence of 99% terpyridine-functionalized polymeric chains. This was also in agreement with the efficiency found by elemental analysis (95% of functionalized polymer chains) for the same sample (**8**, Table 3-4).

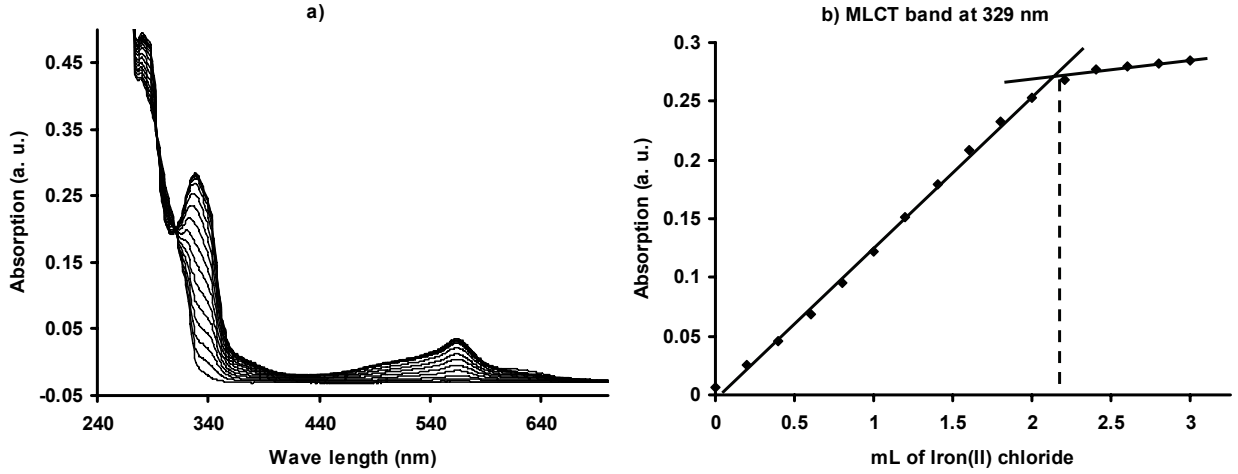

Figure 3-28: *UV-Vis titration with $FeCl_2$ of a terpyridine-functionalized poly(styrene) synthesized via anionic polymerization where end-capping with 1,1-diphenylethylene is used (**8**, Table 3-4). (a) The spectra show the absorption increase of the metal-to-ligand charge-transfer (MLCT) bands at 329 and 565 nm as the titration is carried out. (b) The absorption of the metal-to-ligand charge-transfer (MLCT) band at 329 nm is plotted as a function of the amount of iron(II) (the equivalence point was observed approximately at a ligand-to-metal ratio of 2:1, which indicates a fully quantitative complexation).*

Elemental analyses were recorded on a Euro elemental analyzer from EuroVector. The degree of functionalization of the prepared terpyridine-functionalized poly(styrene)s was determined using the nitrogen content values obtained from elemental analysis (or using the experimental results obtained in the UV-Vis titration measurements) and the molecular weight of the respective polymers as determined by GPC or MALDI-TOF-MS. If the average number molecular weight (Mn) of terpyridine-functionalized polymers is determined by methods such as GPC and/or MALDI-TOF-MS one can estimate the average number of repeating monomeric units of the polymeric chains, and therefore the average theoretical content of nitrogen atoms in the terpyridine-functionalized polymers can be calculated for different repeating monomeric units. Note that for the terpyridine-terminated polymers with a high molecular weight (more repeating monomeric units) the average theoretical content of nitrogen atoms in the polymer becomes smaller (since the polymeric chain becomes larger and there is only one terpyridine functional group attached to each chain). The average theoretical content of nitrogen of terpyridine-functionalized polymers can be easily estimated using commercially available software (*e.g*, Isis Draw™ and Chem Draw™) if the number of

repeating units is previously known. The exact determination of the number of the repeating monomeric units will, mainly, depend on the method of characterization used for the determination of the molecular weigth of the polymer. The GPC system using a solution of 4% triethylamine and 2% isopropanol in chloroform described above is a suitable technique for this purpose in the cases of un-complexed terpyridine-functionalized polymers. However, frequently the obtained Mn values of the polymers do not match exactly with the number of repeating monomeric units. For these cases the closest values of the repeating monomeric units to the experimentally obtained molecular weights were considered. An example of this estimation for polymer **3** (Table 3-4) is as follows: A Mn = 2.8 kg mol^{-1} was obtained by GPC for polymer **3** (Table 3-4), thus the closest theoretical molecular weight to this value corresponds to a terpyridine-functionalized poly(styrene) (final compound in the reaction scheme of Figure 3-9) with 23 styrenic units (molecular weight of 2.865 kg mol^{-1}). Hence, the expected average content of nitrogen in the polymer is 1.47%. Table 3-6 shows detailed calculations for the theoretical average content of nitrogen of the terpyridine-functionalized polymers of Table 3-4, the experimental values obtained of the content of nitrogen found by elemental analysis, and the estimated efficiency values of the functionalization reactions. The data presented in Table 3-6 were utilized for the preparation of Figure 3-13.

Table 3-6: *Detailed calculation for the functionalization efficiency of the terpyridine-functionalized poly(styrene)s synthesized via anionic polymerization (Table 3-4).*

Exp.	Mn (kDa) Tpy-PS (GPC)	Repeating monomeric units of Tpy-PS	Theoretical Mn (kg mol^{-1}) (closest value to measured Mn (GPC))	Theoretical content of nitrogen (%)	Measured content of nitrogen (%) (elemental analysis)	Functionalization efficiency (%)
1	1.8	13	1.823	2.30	1.52	66
2	2.3	18	2.344	1.79	1.17	65
3	2.8	23	2.865	1.47	0.92	63
4	3.7	31	3.698	1.14	0.76	67
5	5.3	46	5.260	0.80	0.47	59
6	8.8	80	8.801	0.48	0.29	60
7	7.8	70	7.760	0.54	0.49	91
8	7.7	69	7.656	0.55	0.52	95
9	11.0	101	10.989	0.38	0.37	97
10	11.4	105	11.405	0.37	0.36	97

3.6 References

[1] (a) S. Q. Liu, Y. W. Tong, Y. Y. Yang, *Biomaterials* **2005**, *26*, 5064. (b) F. Zeng, J. Liku, C. Allen, *Biomacromolecules* **2004**, *5*, 1810. (c) R. Savic, L. Luo, A. Eisenberg, D. Maysinger, *Science* **2003**, *300*, 3465. (d) Y. Kakizawa, K. Kataoka, *Adv. Drug Deliver. Rev.* **2002**, *54*, 191.

[2] (a) X. Li, H. A. King, D. H. Kim, W. Knoll, *Langmuir* **2005**, *21*, 5212. (b) Y. Kang, T. A. Taton, *Angew. Chem. Int. Ed.* **2005**, *44*, 409. (c) J. P. Spatz, S. Moessmer, C. Hartmann, M. Moeller, *Langmuir* **2000**, *16*, 407. (d) B. R. Cuenya, S. H. Baeck, T. F. Jaramillo, E. W. McFarland, *J. Am. Chem. Soc.* **2003**, *125*, 12929. (e) G. Kaestle, H.-G. Boyen, F. Weigl, G. Lengl, T. Herzog, P. Ziemann, S. Riethmueller, O. Mayer, C. Hartmann, J. P. Spatz, M. Moeller, M. Ozawa, F. Banhart, M. G. Garnier, P. Oelhafen, *Adv. Funct. Mater.* **2003**, *13*, 853.

[3] N. Hadjichristidis, M. Pitsikalis, S. Pispas, H. Iatrou, *Chem. Rev.* **2001**, *101*, 3747.

[4] (a) J. S. Pedersen, I. W. Hamley, C. Y. Ryu, T. P. Lodge, *Macromolecules* **2000**, *33*, 542. (b) E. Minatti, R. Borsali, M. Schappacher, A. Deffieux, V. Soldi, T. Narayanan, J. L. Putaux, *Macromol. Rapid Commun.* **2002**, *23*, 978. (c) M. Svensson, P. Alexandridris, P. Linse, *Macromolecules* **1999**, *32*, 637. (d) L. Yang, P. Alexandridis, *Curr. Opin. Colloid Interface Sci*. **2000**, *5*, 132. (e) D. E. Discher, A. Eisenberg, *Science* **2002**, *297*, 967. (f) B. M. Discher, Y. Y. Won, D. S. Ege, J. C. M. Lee, F. S. Bates, D. E. Discher, D. A. Hammer, *Science* **1999**, *284*, 1143.

[5] (a) K. Yu, A. Eisenberg, *Macromolecules* **1998**, *31*, 3509. (b) K. Yu, L. Zhang, A. Eisenberg, *Langmuir* **1996**, *12*, 5980. (c) K. Yu, C. Bartels, A. Eisenberg, *Langmuir* **1999**, *15*, 7157. (d) K. Yu, A. Eisenberg, *Macromolecules* **1998**, *31*, 3509.

[6] G. Riess, *Prog. Polym. Sci.* **2003**, *28*, 1107.

[7] (a) K. Mortensen, *Small angle scattering studies of block copolymer micelles, micellar mesophases and networks. In: Amphiphilic block copolymers: self assembly and applications.* Ed. P. Alexandridis, B. Lindman, Elsevier: Amsterdam, **2000**, 191. (b) P. Munk, *Classical methods for the study of block copolymer micelles.*

In: Solvents and self-organization of polymer. Ed. S. E. Webber, P. Munk, Z. Tuzar, NATO ASI series, serie E: applied sciences, vol. 327, Kluwer Academic Publisher: Dordrecht, **1996**, 367.
[8] I. W. Hamley, *The physics of block copolymers,* Oxford University Press: Oxford, **1998**.
[9] (a) P. Linse, *Modelling of self-assembly of block copolymers in selective solvents. In: Amphiphilic block copolymers: self assembly and applications.* Ed. P. Alexandridis, B. Lindman, Elsevier: Amsterdam, **2000**, 13. (b) N. P. Shusharina, P. Linse, A. R. Khokhlov, *Macromolecules* **2000**, *33*, 3892.
[10] A. Milchev, A. Bhattacharya, K. Binder, *Macromolecules* **2001**, *34*, 1881.
[11] (a) R. Noolandi, K. M. Hong, *Macromolecules* **1983**, *16*, 1433. (b) R. Nagarajan, K. Ganesh, *Macromolecules* **1989**, *22*, 4312.
[12] (a) A. Halperin, S. Alexander, *Macromolecules* **1989**, *22*, 2403. (b) A. Halperin, *Macromolecules* **1987**, *20*, 2943.
[13] P. Vangeyte, B. Leyh, M. Heinrich, J. Grandjean, C. Bourgaux, R. Jerome, *Langmuir* **2004**, *20*, 8442.
[14] M. Pitsikalis, E. Siakali-Kioulafa, N. Hadjichristidis, *J. Polym. Sci. Part A: Polym. Chem.* **2004**, *42*, 4177.
[15] (a) T. Inoue, T. Soen, T. Hashimoto, H. Kawai, *J. Polym. Sci: Part A-2* **1969**, *7*, 1283. (b) M. Girolamo, J. R. Urwin, *Eur. Polym. J.* **1971**, *7*, 225. (c) P. Busch, D. Posselt, D. Smilgies, B. Rheinländer, F. Kremer, C. M. Papadakis, *Macromolecules* **2003**, *36*, 8717. (d) D. J. Wilson, G. Riess, *Eur. Polym. J.* **1988**, *24*, 617. (e) S. Pispas, N. Hadjichristidis, I. Potemkim, A. Khokhlov, *Macromolcules* **2000**, *33*, 1741. (f) K. Sotiriou, A. Nannou, G. Velis, S. Pispas, *Macromolcules* **2002**, *35*, 4106. (g) F. Zhu, T. Ngai, Z. Xie, C. Wu, *Macromolecules* **2003**, *36*, 7405. (h) N. Ouarti, P. Viville, R. Lazzaroni, E. Minatti, M. Schappacher, A. Deffieux, R. Borsali, *Langmuir* **2005**, *21*, 1180. (i) G. Mountrichas, M. Mpiri, S. Pispas, *Macromolecules* **2005**, *38*, 940. (j) J. Spevacek, *Makromol. Chem., Rapid Commun.* **1982**, *3*, 697.
[16] (a) W. J. Trepka, *Polym. Lett.* **1970**, *8*, 499. (b) R. P. Quirk, T. Yoo, Y. Lee, J. Kim, B. Lee, *Adv. Polym. Sci.* **2000**, *153*, 67. (c) J. J. Xu, F. S. Bates, *Macromolecules* **2003**, *36*, 5432. (d) J. Scheirs, D. Priddy, *Modern Styrenic Polymers*, Wiley: West Sussex, **2003**.
[17] J. M. Yu, P. Dubois, P. Teyssie, R. Jerome, *Macromolecules* **1996**, *29*, 6090.
[18] (a) A. P. Gast, *Solvents and selforganization of polymers. In: Solvents and self-organization of polymer.* Ed. S. E. Webber, P. Munk, Z. Tuzar, NATO ASI series, serie E: applied sciences, vol. 327, Kluwer Academic Publisher: Dordrecht, **1996**, 259. (b) S. van der Burgh, A. de Keizer, M. A. Cohen Stuart, *Langmuir* **2004**, *20*, 1073.
[19] H. A. Klok, S. Lecommandoux, *Adv. Mater.* **2001**, *13*, 1217.
[20] W. Brown, *Dynamic Light Scattering*, Oxford University Press: Oxford, **1972**.
[21] J. Jagur-Grodzinski, *J. Polym. Sci. Part A: Polym. Chem.* **2002**, *40*, 2116.
[22] J. M. Lehn, *Supramolecular Chemistry: Concepts and Perspectives*, VCH: Weinheim, **1995**.
[23] J. M. Pollino, L. P. Stubbs, M. Weck, *Polym. Prepr.* **2003**, *44*, 730.
[24] H. Hofmeier, U. S. Schubert, *Chem. Soc. Rev.* **2004**, *33*, 373.
[25] (a) Y. S. Cho, H. K. Lee, J. S. Lee, *Macromol. Chem. Phys.* **2002**, *203*, 2495. (b) A. Juris, V. Balazani, F. Barigelletti, S. Campagna, P. Belser, A. von Zelewsky, *Coord. Chem. Rev.* **1998**, *84*, 85. (c) S. C. Yu, X. Gong, W. K. Chan, *Macromolecules* **1998**, *31*, 5639. (d) A. Aoki, T. Miyashita, *Chem. Lett.* **1996**, 563. (e) M. Kimura, T. Horai, K. Hanabusa, H. Shirai, *Adv. Mater.* **1998**, *10*, 549. (f) X. Gong, P. K. Ng, W. K. Chan, *Adv. Mater.* **1999**, *11*, 459. (g) C. T. Wong, W. K. Chan, *Adv. Mater.* **1999**, *11*, 455. (h) S. S. Zhu, T. M. Swager, *Adv. Mater.* **1996**, *8*, 497.
[26] (a) G. R. Newkome, E. He, C. N. Moorefield, *Chem. Rev.* **1999**, *99*, 1689. (b) T. Salditt, Q. R. An, A. Plech, C. Eschbaumer, U. S. Schubert, *Chem. Commun.* **1998**, 2371. (c) B. G. G. Lohmeijer, U. S. Schubert, *J. Polym. Sci. Part A: Polym. Chem.* **2003**, *41*, 413. (d) K. A. Aamer, G. N. Tew, *Macromolecules* **2004**, *37*, 1990.
[27] G. R. Newkome, A. K. Patri, E. Holder, U. S. Schubert, *Eur. J. Org. Chem.* **2004**, 235.
[28] E. C. Constable, *Adv. Inorg. Chem. Radiochem.* **1986**, *30*, 69.
[29] U. S. Schubert, C. Eschbaumer, P. Andres, H. Hofmeier, C. H. Weidl, E. Herdtweck, E. Dulkeith, A. Morteani, N. E. Hecker, J. Feldmann, *Synth. Met.* **2001**, *121*, 1249.
[30] M. J. Cook, A. P. Lewis, G. S. G. McAuliffe, A. J. Thomson, *Inorg. Chim. Acta* **1982**, *64*, L25.
[31] R. Hage, J. G. Haasnoot, J. Reedijk, J. G. Vos, *Inorg. Chim. Acta* **1986**, *118*, 73.
[32] (a) U. S. Schubert, H. Hofmeier, *Macromol. Rapid Commun.* **2002**, *23*, 561. (b) K. J. Calzia, G. N. Tew, *Macromolecules* **2002**, *35*, 6090.
[33] H. L. Hsieh, R. P. Quirk, *Anionic polymerization: Principles and practical applications*, Dekker: New York, **1996**.
[34] X. F. Zhong, A. Eisenberg, *Macromolecules* **1994**, *27*, 4914.
[35] S. Kobatake, H. J. Harwood, R. P. Quirk, D. B. Priddy, *Macromolecules* **1999**, *32*, 10.
[36] S. Pispas, N. Hadjichristidis, J. W. Mays, *Polymer* **1996**, *37*, 3989.
[37] M. H. Acar, K. Matyjaszewski, *Macromol. Chem. Phys.* **1999**, *200*, 1094.
[38] (a) M. W. F. Nielen, *Mass Spectrom. Rev.* **1999**, *18*, 309. (b) H. Pasch, W. Schrepp, *MALDI-TOF Mass spectrometry of synthetic polymers*, Springer: Berlin, **2003**.
[39] B. G. G. Lohmeijer, *Playing LEGO with macromolecules: connecting polymer chains using terpyridine metal complexes*, Dissertation thesis, Technische Universiteit Eindhoven: Eindhoven, **2004**.
[40] S. Bywater, A. F. Johnson, D. J. Worsfold, *Can. J. Chem.* **1964**, *42*, 1255.
[41] B. G. G. Lohmeijer, D. Wouters, Z. Yin, U. S. Schubert, *Chem. Commun.* **2004**, 2886.

[42] J. F. Gohy, B. G. G. Lohmeijer, S. K. Varshney, U. S. Schubert, *Macromolecules* **2002**, *35*, 7427.
[43] M. A. R. Meier, B. G. G. Lohmeijer, U. S. Schubert, *Macromol. Rapid Commun.* **2003**, *24*, 852.
[44] a) H. Eschwey, W. Burchard, *Polymer* **1975**, *16*, 180. (b) D. Rein, P. Rempp, P. J. Lutz, *Makromol. Chem., Macromol Symp.* **1993**, *67*, 237.
[45] R. P. Quirk, J. J. Ma, *Polym. Int.* **1991**, *24*, 197.

CHAPTER 4

Ionic liquids as novel reaction media for polymer synthesis

Abstract

Ionic liquids are explored as reaction media to perform polymerization reactions by different reaction mechanisms (cationic ring opening and free radical) and methods (homogeneous and heterogeneous). In addition, a combination of microwave irradiation, as an efficient and alternative heating source, with the highly ionic reaction medium supplied by ionic liquids is also investigated. The results revealed that polymerization reactions performed under microwave irradiation in the presence of ionic liquids show higher heating rates than their corresponding bulk and solution (in conventional organic solvents) polymerization processes with conventional heating. Moreover, in some of the investigated polymerization reactions, the use of ionic liquids as reaction media has also revealed increased polymerization rates in comparison to the reactions performed in conventional VOCs and, in some cases, even in bulk conditions. The efficient use of water-soluble ionic liquids as stabilizing agents for the synthesis of polymers by suspension polymerization reactions is also addressed in detail. It was found that due to the surface active properties shown by water-soluble ionic liquids, the average particle size (from the macro- to the nanoscale) and the surface area of synthesized polymer beads can be "tuned" by adjusting the concentration and the aliphatic side-chain length of the ionic liquids in the aqueous phase of the suspension polymerizations. In all the polymerization cases investigated, it is demonstrated that the synthesis of polymers can be performed efficiently and under a "green" approach by utilizing water as a co-solvent to perform the polymer isolation and ionic liquid recycling. Furthermore, it is demonstrated that the recovered ionic liquid can be used to perform additional polymerization reactions yielding materials with comparable properties to those obtained in previous cycles. The polymerization methods proposed here open opportunities for the development of more efficient and cleaner processes in polymer synthesis.

Parts of this chapter have been published: (1) C. Guerrero-Sanchez, U. S. Schubert, *Polym. Prepr.* **2004**, *45*, 321. (2) C. Guerrero-Sanchez, F. Wiesbrock, U. S. Schubert, *ACS Symp. Ser.* **2005**, *913*, 37. (3) C. Guerrero-Sanchez, R. Hoogenboom, U. S. Schubert, *Chem. Commun.* **2006**, 3797. (4) C. Guerrero-Sanchez, T. Erdmenger, P. Šereda, D. Wouters, U. S. Schubert, *Chem. Eur. J.* **2006**, *12*, 9036. (5). C. Guerrero-Sanchez, M. Lobert, R. Hoogenboom, U. S. Schubert, *Macromol. Rapid Commun.* **2007**, *28,* 456.

4.1 Ionic liquids and their use as reaction media in polymer synthesis

In chapter 3, an important ionic mechanism in polymer synthesis (anionic polymerization) was utilized in combination with high-throughput experimental approaches for the preparation of novel polymeric materials including block copolymers and terpyridine-functionalized polymers. In the current and the next chapters the use of other ionic systems, namely ionic liquids (ILs), in polymer and materials research is addressed. Hence, ionic liquids are utilized as novel reaction media to perform different polymerizations and they are applied as novel ingredients for the preparation of advanced polymeric systems and materials composites. The main reason for introducing ILs into materials research is to take advantage of their novel properties in order to develop more efficient processes and new compounds.

Table 4-1: *Properties of the ionic liquids utilized in this work (as obtained from different suppliers and literature, or determined experimentally in this work) (*Property not determined).*

Ionic liquid	Density (g cm^{-3})	Melting point (°C)	Viscosity (mPa s)	Conductivity (mS cm^{-1})	Miscibility with H_2O
1-Ethyl-3-methyimidazolium diethylphosphate (**1**)	1.14	*	*	*	Yes
1-Butyl-3-methyimidazolium hexfluorophosphate (**2**)	1.36	11	200	1.34	No
1-Hexyl-3-methyimidazolium chloride (**3**)	1.04	< −65	7830	0.30	Yes
1-Butyl-3-methyimidazolium trifluoromethanesulfonate (**4**)	1.30	17	110	0.37	Yes
1-Butyl-3-methyimidazolium tetrafluoroborate (**5**)	1.21	−71	120	3.53	Yes
AMMOENG 100™ (**6**)	1.10	< −65	1670	*	Gel
1-Ethyl-3-methyimidazolium ethylsulfate (**7**)	1.24	< −65	110	3.95	Yes
Trihexyltetradecylphosphonium chloride (**8**)	0.89	−70	2450	*	No
1-Ethyl-3-methyimidazolium tosylate (**9**)	*	−15	*	18.9 (1 M in H_2O)	Yes
1-Butyl-3-methyimidazolium chloride (**10**)	*	57	*	46.3 (1 M in H_2O)	Yes
1-Decyl-3-methyimidazolium chloride (**11**)	0.99	4	24220	*	Yes
1-Hexadecyl-3-methyimidazolium chloride (**12**)	*	41	*	*	Yes

ILs, substances composed entirely of ions, which are in a liquid state at temperatures below 100 °C, appeared in recent years as novel compounds, and are already used in different industrial processes[1] (for a recent overview about ILs see refs.[1g,h]). Many properties of ILs (*e.g.*, viscosity, solubility, electric conductivity, melting point, etc.) can be tuned by varying the composition of their ions. Furthermore, ILs are considered to be very stable and "environmentally friendly" compounds due to their negligible vapor pressure (see ref.[1i] for a detailed description of this property of ILs), negligible flammability (see ref.[1j] for a detailed description of this property of ILs), and liquid state in a broad temperature range.[1] Nowadays, around 300 ILs are commercially available (and a considerable number of new ILs can be readily synthesized),[1g] covering a wide range of properties. However, the relatively unknown toxicity[1h] and relatively high cost are still the main drawbacks of ILs. Table 4-1 lists the ILs utilized in the present investigations as well as some of their properties, whereas Figure 4-1 displays schematic representations of their chemical structures. ILs **1** to **9** (Table 4-1, Figure 4-1) have been obtained from commercial suppliers, whereas ILs **10** to **12** have been synthesized under microwave irradiation (see experimental part for details). In addition, Figure 4-2 shows the thermal stability of some of the ILs investigated as determined by thermo-gravimetrical analysis.

The governmental policies for the control of emissions of different substances which are released into the environment will become more restrictive as pollution increases world-wide. Due to this increase in the environmental awareness, it is a matter of great concern for scientists to design more efficient and cleaner technologies in chemical manufacturing. Hence, the development of more efficient and environmentally friendly processes is becoming a common practice in these days. These processes must be designed on the basis of two main characteristics: depletion of emissions related to harmful volatile organic compounds (VOCs) and energy saving to avoid the excessive emissions of carbon dioxide (CO_2) (at least, as long as industry depends on the combustion of fossil fuels as a main source of energy).

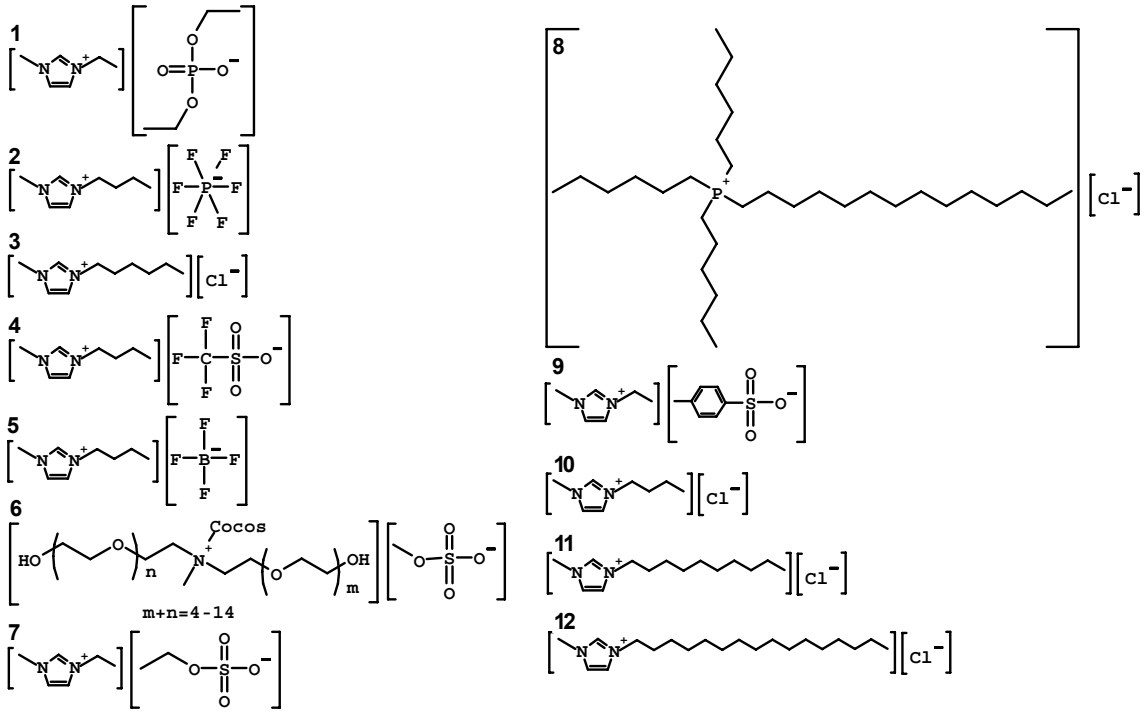

Figure 4-1: *Schematic representation of the chemical structures of the ionic liquids utilized in this work (see Table 4-1). (**1**) 1-Ethyl-3-methyimidazolium diethylphosphate. (**2**) 1-Butyl-3-methyimidazolium hexfluorophosphate. (**3**) 1-Hexyl-3-methyimidazolium chloride. (**4**) 1-Butyl-3-methyimidazolium trifluoromethanesulfonate. (**5**) 1-Butyl-3-methyimidazolium tetrafluoroborate. (**6**) AMMOENG 100™. (**7**) 1-Ethyl-3-methyimidazolium ethylsulfate. (**8**) Trihexyltetradecylphosphonium chloride. (**9**) 1-Ethyl-3-methyimidazolium tosylate. (**10**) 1-Butyl-3-methyimidazolium chloride. (**11**) 1-Decyl-3-methyimidazolium chloride. (**12**) 1-Hexadecyl-3-methyimidazolium chloride.*

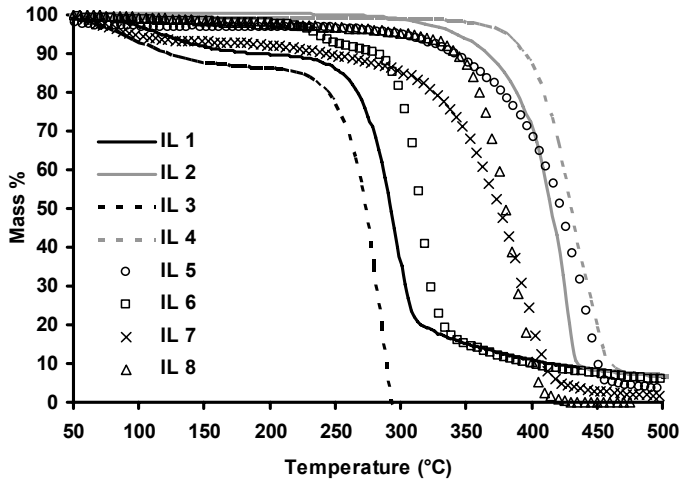

Figure 4-2: *Thermal stability of some of the ionic liquids (ILs) of Table 4-1 as determined by thermo-gravimetric analysis. (**1**) 1-Ethyl-3-methyimidazolium diethylphosphate. (**2**) 1-Butyl-3-methyimidazolium hexfluorophosphate. (**3**) 1-Hexyl-3-methyimidazolium chloride. (**4**) 1-Butyl-3-methyimidazolium trifluoromethanesulfonate. (**5**) 1-Butyl-3-methyimidazolium tetrafluoroborate. (**6**) AMMOENG 100™. (**7**) 1-Ethyl-3-methyimidazolium ethylsulfate. (**8**) Trihexyltetradecylphosphonium chloride.*

Research on chemical and polymer manufacturing has focused on the investigation of different approaches for diminishing the emission of VOCs including: (1) Solvent-free processes and the use of (2) water, (3) supercritical CO_2 and, more recently, (4) ILs as reaction media.[1] The polymer industry uses the two first alternatives with a satisfactory performance.[2] Solvent-free processes may be considered as an “ideal” and cleanest way of chemical manufacture. However, in the polymer industry bulk processes

require an enormous amount of energy and high temperatures in order to overcome the problems related to transportation of the highly viscous polymer melts, which in some cases provokes side-reactions and/or degradation of the products.[3] In addition, the use of water is not a suitable approach in moisture-sensitive systems, such as ionic polymerizations.[4] For these reasons, solution polymerization processes in VOCs are still commonly used due to the intrinsic drawbacks of these first two approaches.[3,4] During the last decade, the use of supercritical CO_2 arose as an alternative replacement of VOCs in polymer synthesis and processing. CO_2 is a readily available, inexpensive, nontoxic, and nonflammable natural product; therefore an environmentally benign reaction media. Heterogeneous polymerizations in liquid and supercritical CO_2 have been studied intensively.[5] However, a main drawback of the use of CO_2 as a reaction medium is the utilization of highly pressurized equipments in order to reach the required critical conditions (73.8 bar at 31.1 °C).[5]

More recently, ILs have been used as reaction media for the preparation of polymers by several synthetic mechanisms.[6] ILs have shown some advantages for this purpose. For instance, some free radical polymerizations (FRP) conducted in ILs have shown an increased polymerization rate and yielded polymers with higher molar masses in comparison to the respective cases in VOCs.[6c] The feasibility to synthesize block copolymers in ILs by a free radical mechanism has been also described.[6d,e] In the cases of copolymerizations carried out in ILs, the comonomers can show significantly different reactivity ratios from those reactions performed in bulk or in VOCs, which allowed the preparation of “new” statistical copolymers.[6f,g] ILs as reaction media to perform other polymerizations (*e.g.*, controlled free radical polymerizations (CRP) and “living” cationic polymerizations) have been also investigated recently.[6h-r] Despite this progress, clear understanding of how to efficiently use ILs and avoid completely the utilization of VOCs in specific polymer systems is still lacking, since many factors must be optimized including polymer isolation, IL recycling, toxicity, cost, etc. In far too many cases, suitable approaches for the isolation of the obtained polymers and the recycling of the used ILs have been not developed and workers resort to VOCs to recover the product, which obviates the advantage of ILs as replacements for VOCs. Only few examples in literature address the problems of polymer isolation and ionic liquid recycling avoiding entirely the use of VOCs. For instance, a polymerization reaction where the monomer is soluble but not the polymer in a water-soluble IL (WSIL) has been reported for the cationic ring opening polymerization (CROP) of 3-ethyl-3-hydroxymethyloxetane, whereby the polymerization starts as a homogeneous process but the polymer then precipitates during the course of the reaction.[6l] Thereafter, it is suggested but not demonstrated that the polymer can be isolated and the WSIL recovered by washing the reaction mixture with water. Other examples have also described heterogeneous polymerization systems in ILs based on free radical mechanisms.[7]

Regarding the development of more efficient processes in terms of energy, in recent years chemists and engineers have investigated microwave irradiation as an efficient and alternative source of energy in several chemical processes, including organic synthesis,[8] polymerizations,[9] and separation processes such as extractions and distillations.[10] Advantages, such as non-contact heating, energy transfer instead of heat transfer, material selective heating, rapid start-up and stopping of the heating, and the fact that the heating process starts from the interior of the material body, make microwave irradiation a more efficient energy source than conventional heating systems (*e.g.*, systems using heat transfer fluids (oils, steam, water, etc.)). In addition, it is well-known that ILs absorb microwave irradiation in a extremely efficient way and therefore reaction mixtures containing ILs can be heated very rapidly under such conditions.[11]

Hence, a combination of ILs as reaction media with microwave irradiation to perform homogeneous polymerization reactions, where water cannot be used for this purpose (*e.g.*, ionic polymerizations such as CROP), is discussed in the second part of this chapter (section 4.2). Apart from the potential depletion of emission of harmful VOCs into the environment, this method may allow for energy savings by using the proposed combination of ILs and microwave irradiation as a heating source. In the third part of the chapter (section 4.3), heterogeneous polymerization systems in ILs based on a free radical mechanism

are described in detail. The advantages of heterogeneous polymerizations in ILs over conventional heterogeneous processes (*e.g.*, emulsion and suspension polymerizations) are also addressed in section 4.3. Both, homogeneous and heterogeneous approaches are investigated on the basis of the development of more efficient and cleaner polymerization processes. In this regard, environmentally friendly methods, which make use of water (another environmentally friendly substance) to solve the problems related to the polymer isolation and the IL recycling, are described. Basically, the proposed separation methods take advantage of the solubility properties of polymers in both, ILs and water, which can facilitate the polymer isolation and the IL recycling where a proper selection of a polymerization process and an IL are made. Thereafter, additional polymerization reaction cycles in the recovered ILs are performed, which demonstrates the potential of the proposed methods. Moreover, the obtained polymers during the additional reaction cycles in recycled ILs show comparable properties to those materials synthesized in new (non-used) ILs. Obviously, the developments of this chapter are based on the avoidance of VOCs at any stage of the polymerization processes (reaction, product isolation and IL recycling steps). Finally for each development, potential drawbacks of the processes proposed that must be solved and/or optimized as well as recommendations for future research are addressed.

4.2 Homogeneous polymerization reactions performed in ionic liquids and under microwave irradiation: An alternative and "green" approach in polymer synthesis

In this section, homogeneous polymerization reactions performed in ILs as reaction media and under microwave irradiation as a heating source are described in detail. As mentioned before, it is thought that a combination of ILs and microwave irradiation may become the basis for the development of "greener" and more efficient polymerization processes in future research, which may allow for the depletion of emission of VOCs as well as for energy savings. Hence, for the purposes of this section, three main homogeneous polymerization systems are investigated based on the mentioned reaction conditions. The first system addresses a case where a hydrophilic polymer is homogeneously synthesized via CROP in a hydrophobic ILs under microwave irradiation. The systems of the second part describe the cases where hydrophobic polymers are homogeneously synthesized in hydrophilic ILs (WSILs) via CROP and FRP, respectively. It was found that the use of ILs and microwave irradiation increases the polymerization rates for most of the investigated cases when compared to the cases where the same reactions are performed in conventional VOCs. In addition, it is demonstrated in each case that the utilized ILs can be efficiently recovered and reused in further polymerization cycles. This is achieved by an extraction of the polymer with water, in the case of hydrophilic polymers in hydrophobic ILs; and by precipitation of the polymer with water, in the case of hydrophobic polymers in hydrophilic ILs.

4.2.1 Synthesis of a hydrophilic polymer via living cationic ring opening polymerization in a hydrophobic ionic liquid under microwave irradiation

In reaction systems where water must be avoided, such as living CROP, ILs are good candidates to replace the VOCs in which these polymerizations are normally performed. The feasibility of performing living cationic[6j,k] and cationic ring opening[6l] polymerizations in ILs has been recently discussed. However, the influence of ILs on these cationic polymerization mechanisms is a research topic relatively unexplored. Therefore, in this section the use of ILs as a reaction medium for the CROP of 2-ethyl-2-oxazoline (EtOx) under microwave irradiation is discussed. In a conventional approach this type of polymerization reaction is performed using acetonitrile as a reaction medium and, in a post-reaction

step, ethyl ether is used to isolate the polymer obtained (see Figure 4-3 for the reaction mechanism).[12] Thus, it is thought that ILs can be good candidates for the replacement of the VOCs used in the conventional synthesis of poly(2-ethyl-2-oxazoline) (PEtOx). Hence, the CROP of EtOx was conducted in different ILs (see experimental section for details) using similar reaction conditions as reported elsewhere (same microwave setup and similar concentrations as for reactions performed in acetonitrile).[12] For this purpose, five different ILs were investigated as reaction media: (**2**) 1-Butyl-3-methylimidazolium hexafluorophosphate, (**4**) 1-butyl-3-methylimidazolium trifluoromethanesulfonate, (**5**) 1-butyl-3-methylimidazolium tetrafluoroborate, (**8**) trihexyltetradecylphosphonium chloride, and (**9**) 1-ethyl-3-methylimidazolium tosylate (see Table 4-1 and Figure 4-1).

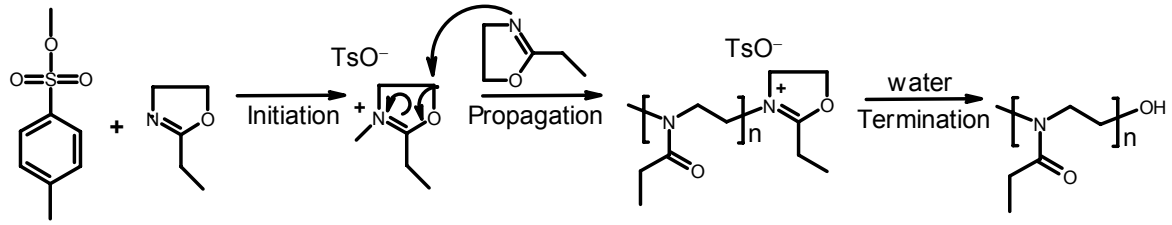

Figure 4-3: *Schematic representation of the synthesis of poly(2-ethyl-2-oxazoline) via living cationic ring opening polymeization.[12]*

It was found that EtOx is soluble in all the investigated ILs. However, only in ILs **2**, **4**, **5** the polymerization was successfully initiated under the reaction conditions investigated. The polymerizations performed in ILs **4** and **5** revealed similar characteristics to those polymerizations carried out in IL **2**. However, for the aforementioned purposes, this work only focused on the investigation of IL **2** as a reaction medium for this specific system, which facilitates the polymer isolation and IL recycling due to the fact that PEtOx is preferable soluble in water than in IL **2**. In addition, IL **2** is an hydrophobic IL, therefore a simple extraction with water is a suitable approach to isolate the polymer and to recover the IL for further polymerization reactions.

Figure 4-4 summarizes the results of the polymerizations performed in IL **2** and in an acetonitrile/IL **2** mixture (50/50 wt %). These results show a pseudo-first order kinetic reaction (see section 2.4.1 or reference[13] for a detailed explanation about the pseudo-first order kinetic analysis for living polymerization reactions) for different reaction temperatures and reveal the living character of the investigated polymerizations due to the found linear dependencies of monomer conversion (X) (represented by –LN(1–X)) against time and the number average molecular weights (Mn) against monomer conversion (X) (see experimental part for an explanation about the determination of X and Mn).[12] In addition, all the obtained polymers exhibited low polydispersity indices (PDI) as it is also observed in Figure 4-4. The final proof for the livingness of the polymerization at the investigated reaction conditions was provided by chain extension experiments performed at 120 °C. The gel permeation chromatographic (GPC) traces of Figure 4-5, before and after the second monomer addition, demonstrate the existence of living chain ends, which allowed for the preparation of chain extended polymers (4.1 kDa (PDI=1.27) from a 1.8 kDa precusor (PDI=1.33) for the case of a polymerization performed in IL **2**, and 5.9 kDa (PDI=1.26) from a 2.7 kDa precusor (PDI=1.31) for the case of a polymerization performed in an acetonitrile/IL **2** mixture (50/50 wt %)).

The results of Figure 4-5 suggest that the synthesis of block copolymers may be feasible by the investigated method. Note that for obtaining a more efficient chain extension process, the second monomer addition must be incorporated properly into the reaction system by a suitable mixing process in order to attach new monomeric units to all the living chain ends in a homogenous way. This is due to the relatively high viscosity generated in the system (intrinsic viscosities of the polymer and IL). However, this effect might be minimized by using other hydrophobic ILs (or co-solvents) of low viscosity since the heat and, in particular, the mass transfers may be improved.

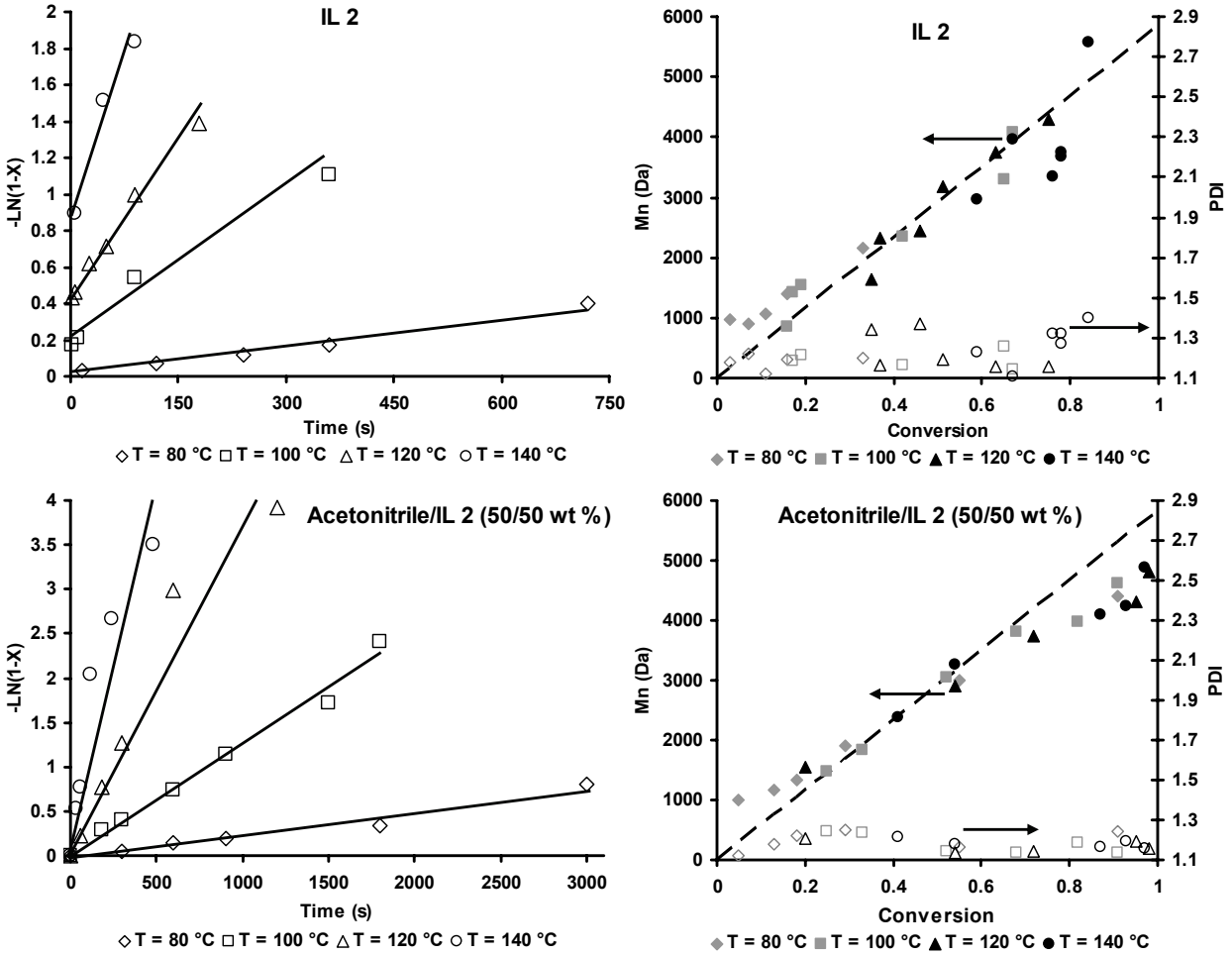

Figure 4-4: *Plots of monomer conversion (X) (represented by –LN(1–X)) against time and number average molecular weights (Mn) against monomer conversion (X) at different temperatures for the living cationic ring opening polymerization of 2-ethyl-2-oxazoline (Figure 4-3) performed under microwave irradiation in the hydrophobic ionic liquid 1-butyl-3-methylimidazolium hexafluorophosphate (IL* ***2****) (Table 4-1, Figure 4-1) as a reaction medium (top), and in an acetonitrile/IL* ***2*** *mixture (50/50 wt %) (bottom).*

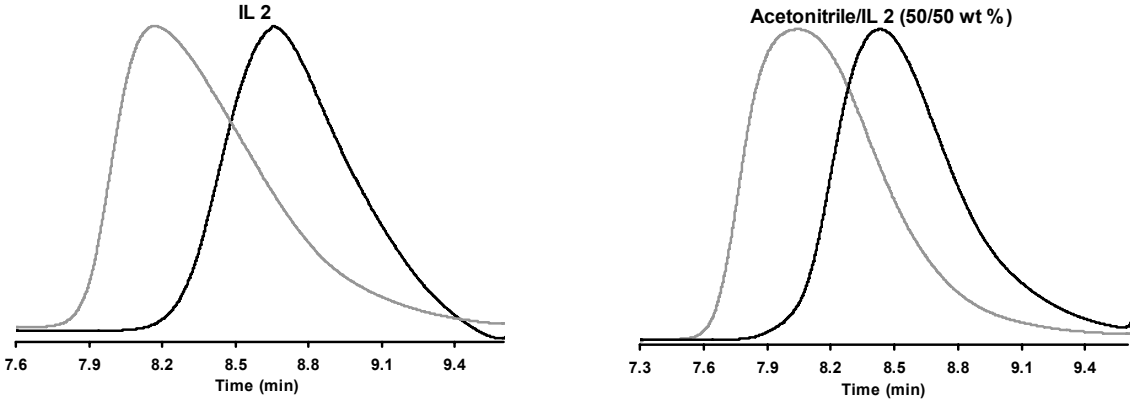

Figure 4-5: *Normalized GPC traces for chain extension experiments at 120 °C of the living cationic ring opening polymerization of 2-ethyl-2-oxazoline (Figure 4-3) performed under microwave irradiation in the hydrophobic ionic liquid 1-butyl-3-methylimidazolium hexafluorophosphate (IL* ***2****) (Table 4-1, Figure 4-1) as a reaction medium (left), and in an acetonitrile/IL* ***2*** *mixture (50/50 wt %) (right). The precursor polymers are shown in black, whereas the chain extended polymers are shown in grey.*

Figure 4-4 also reveals that the reactions performed in IL **2** show faster polymerizations rates than the reactions carried out in the acetonitrile/IL **2** mixture, and in addition, these latter show faster

polymerization rates than those performed in pure acetonitrile.[12] In addition, the apparent constant reaction rate (k_{app}) for the investigated polymerizations at different temperatures can be estimated from the slopes of the linear relationships of –LN(1–X) against time in the plots of Figure 4-4. This can be performed under the assumption that the standard pseudo-first order kinetic analysis for living polymerization reactions is still valid under microwave irradiation (see section 2.4.1 or ref.[13] for a detailed explanation about the pseudo-first order kinetic analysis for living polymerization reactions).

Once that the values of k_{app} at different temperature are available, they can be plotted as LN(k_{app}) against the inverse of the temperature (1/T) in order to obtain the respective Arrhenius plots as displayed in Figure 4-6. Thereafter, the activation energy of the investigated reactions can be calculated from the slopes of the linear relationships of LN(k_{app}) against the inverse of the temperature (1/T) of the respective Arrhenius plots (Figure 4-6).

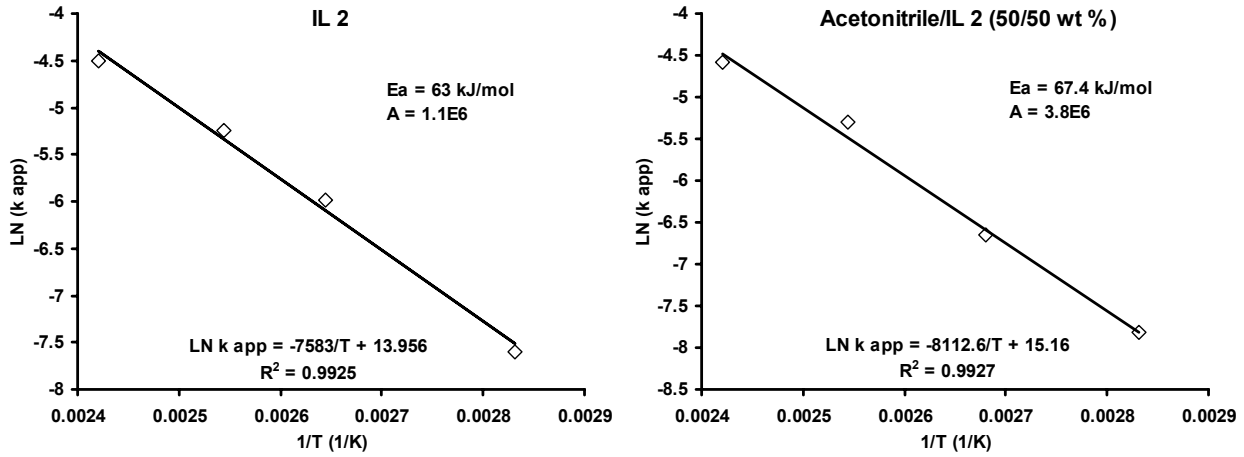

Figure 4-6: *Arrhenius plots for the determination of the activation energy (Ea) of the propagation reaction of the living cationic ring opening polymerization of 2-ethyl-2-oxazoline (Figure 4-3) performed under microwave irradiation in the hydrophobic ionic liquid 1-butyl-3-methylimidazolium hexafluorophosphate (IL **2**) (Table 4-1, Figure 4-1) as a reaction medium (left), and in an acetonitrile/IL **2** mixture (50/50 wt %) (right). The plots are obtained from the experimental data of the kinetic investigations of Figure 4-4.*

Table 4-2: *Estimated and reported values of the activation energy of the propagation reaction of the living cationic ring opening polymerization of 2-ethyl-2-oxazoline (Figure 4-3) performed under microwave irradiation in the hydrophobic ionic liquid 1-butyl-3-methylimidazolium hexafluorophosphate (IL **2**) (Table 4-1, Figure 4-1), in an acetonitrile/IL **2** mixture (50/50% wt), and in acetronitrile.[12]*

Solvent	Activation energy kJ mol^{-1}
IL **2**	63.0
Acetonitrile/IL **2** (50/50% wt)	67.4
Acetonitrile	73.4[12]

Table 4-2 compares the activation energy values obtained from the plots of Figure 4-6 to the value reported for the same polymerization reaction carried out in acetonitrile.[12] According to the data of Table 4-2, the CROP of EtOx performed in IL **2** showed the lowest activation energy value of the three compared cases, which confirms the observed enhancement of the polymerization rate in the case where pure IL **2** is used. These results suggest that, at least for the investigated reaction conditions, the presence of other ionic species (ILs) during the CROP of EtOx may modify the association between the living polymer chain ends and their respective counter-ions. Consequently, this results in a modified kinetic mechanism, which can accelerate the polymerization reaction in the investigated case. Similar effects have been reported for anionic polymerization reactions in the presence of polar additives.[13]

Note that in the kinetic plot corresponding to the polymerizations carried out in IL **2** at temperatures above 100 °C in Figure 4-4, the origin of the Cartesian plane is not intercepted by the curves of monomer conversion (represented by –LN(1–X)) against time. This effect can be explained due to the fact that ILs are known to be heated with exceptional efficiency by microwave irradiation[11] and to the finding of this work related to the faster polymerizations rates shown by the CROP of EtOx when they are carried out in IL **2** and under microwave irradiation. When combining these effects the accurate determination of the onset of the polymerization becomes difficult. For instance, experiments performed during just 1 s (the shortest possible reaction time as programmed in the utilized microwave setup, see experimental part for details) revealed already monomer conversions of 16%, 35%, and 67% for the reaction temperatures of 100 °C, 120 °C, and 140 °C, respectively. This effect is related to the time that the microwave setup takes to reach the desired reaction temperature (time zero) and to stop the polymerization reactions (by cooling the vials). Hence, these polymerizations performed during just 1 s, in fact, are exposed to longer reaction times above 80 °C (at lower temperatures it is reported that the polymerization rate of the investigated system becomes negligible[12]). These times (as obtained from the data of the experimental setup) were 7 s, 11 s and 37 s for the reaction temperatures of 100 °C, 120 °C, and 140 °C, respectively, as observed in Figure 4-7a. In addition to the difficulty of determining the onset of the reaction, it is clear that during this heating time (non-steady state) the polymerization rate is not constant. However, as soon as the desired reaction temperature is stable, the polymerization rate becomes steady. Thereafter, the polymerization rates can be determined as explained above whenever the heating trajectories of the polymerization reactions are reproducible as shown in Figure 4-7b. As a consequence of this inaccuracy in determining the onset and the ending of the polymerizations, in the kinetic plot corresponding to the polymerizations performed in IL **2** at temperatures above 100 °C in Figure 4-4, the origin of the Cartesian plane is not intercepted by the curves of monomer conversion (represented by –LN(1–X)) against time. However, this inaccuracy remains constant where the same experimental setup (microwave reactor) is used for all the kinetic measurements, and might not affect the determination of the values of the polymerization rates (slopes) as soon as the temperature in the reaction mixtures becomes stable.

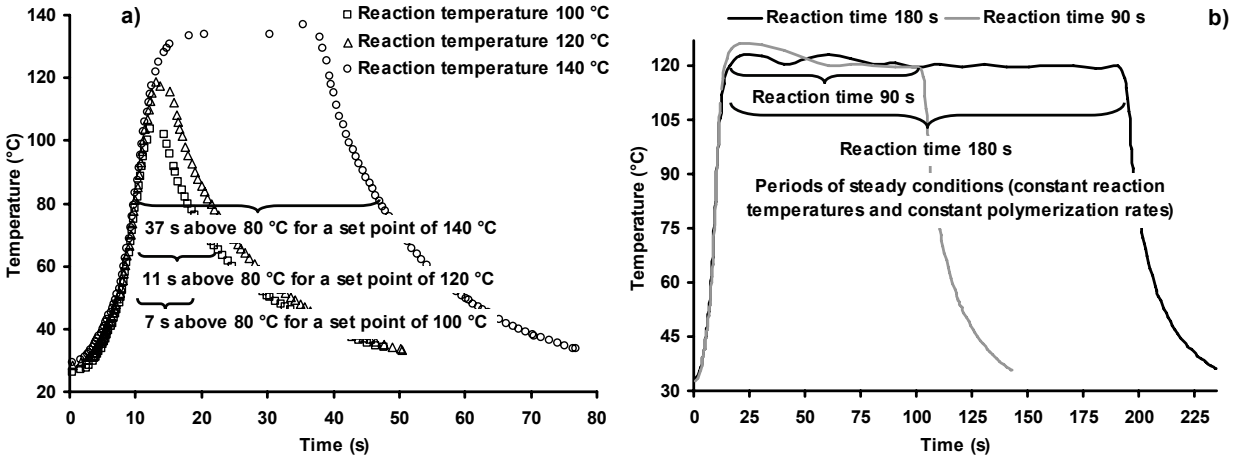

Figure 4-7: *Temperature profiles of the living cationic ring opening polymerization of 2-ethyl-2-oxazoline (Figure 4-3) performed in the hydrophobic ionic liquid 1-butyl-3-methylimidazolium hexafluorophosphate (IL* ***2****) (Table 4-1, Figure 4-1) as a reaction medium and under microwave irradiation. (a) 1 s of reaction time (as programmed in the microwave setup) for different reaction temperatures (set points) showing the transition periods when the polymerizations are above 80 °C. (b) Polymerizations performed at 120 °C for two different reaction times (as programmed in the microwave setup) showing the steady state periods where the polymerization rates can be determined.*

As mentioned above, the advantages of performing reactions in a suitable microwave platform (see experimental part for details) are the more efficient heating of ionic media and a better control in the

reaction temperatures[12] in comparison to the conventional heating systems using heat transfer fluids (*e.g.*, oil-bath). These advantages are related to the fact that the reaction mixtures absorb directly the heating source (microwaves) while in the case of conventional heating systems the heat is transported from the outside to the inside of the reactor. As a direct consequence of this effect, the control of the reaction temperature is more difficult in the conventional heating systems using heat transfer fluids and, therefore, a temperature gradient between the heat transfer fluid and reaction mixture is commonly expected. For instance, Figure 4-8 shows the temperature profile of a CROP of EtOx performed in a conventional oil-bath setup (using the same reaction vials of the microwave platform) with temperature sensors in both the oil and in the reaction mixture. During this experiment, the set point of the oil had to be increased up to 129 °C in order to reach a temperature of 120 °C in the reaction mixture. As observed in Figure 4-8, in the utilized oil-bath setup (at investigated reaction conditions) it takes around 60 s to reach the desired temperature in the reaction mixture whereas in the microwave platform this only takes around 15 s (Figure 4-7b). In addition, the temperature overshoot is more pronounced in the oil-bath setup (up to 131 °C for a desired reaction temperature of 120 °C, as shown in Figure 4-8) than in the microwave platform (up to 125 °C for a desired reaction temperature of 120 °C, as shown in Figure 4-7b). This effect might be related to the heat generated by the polymerization reaction and the efficiency of the temperature control of the experimental setups. Finally, it is observed that there is also an intrinsic uncertainty in the determination of the onset and ending of the polymerizations in the oil-bath setup similar to the case described for the microwave platform.

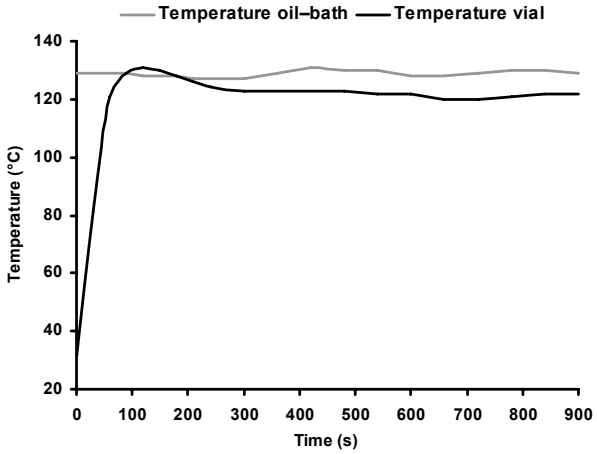

Figure 4-8: *Black: Temperature profile of the living cationic ring opening polymerization of 2-ethyl-2-oxazoline (Figure 4-3) performed in the hydrophobic ionic liquid 1-butyl-3-methylimidazolium hexafluorophosphate (IL* ***2****) (Table 4-1, Figure 4-1) as a reaction medium and in a conventional heating system (oil-bath) at 120 °C. Grey: Temperature profile of the utilized oil-bath.*

Apart from the mentioned effects, many other factors can influence the determination of the onset and the ending of the polymerizations. However, when comparing directly the results for polymerizations performed in both, the oil-bath and in the microwave setups using similar reaction conditions (120 °C and a reaction time of 240 s, applying the criteria described above for each experimental platform), the obtained conversions were very similar (84% for the oil-bath and 83% for the microwave). This observation strongly indicates that the findings of this investigation (accelerated kinetic mechanism for the CROP of EtOx) are due to the presence of the IL species (reaction medium) and might not be related to so-called non-thermal microwave effects.[12]

Further investigations on the CROP of EtOx performed in IL **2** and under microwave irradiation were aimed at efficient recovering of the IL and polymer isolation. As mentioned above, the selection of IL **2** facilitates this task by a simple extraction with water avoiding completely the use of VOCs during the

purification step. For this purpose, the remaining reaction mixtures (after molecular weight and conversion determinations) from the kinetic study were combined and mixed with a 3-fold excess of purified water in order to extract the polymer and the monomer unreacted (which are better soluble in water than in IL **2**) into the aqueous phase. This mixture (15 reaction vials) was magnetically stirred for 0.5 h at room temperature. The resulting heterogeneous mixture was placed into an extraction funnel until a clear phase separation occurred. This procedure is illustrated in Figure 4-9. Subsequently, IL **2** was recovered from the funnel, dried under vacuum at 40 °C, and analyzed by ^{1}H-NMR (which confirmed the absence of polymer and/or monomer). In addition, the ^{1}H-NMR spectra of Figure 4-9 reveal that IL **2** remains practically unmodified after one reaction cycle. Moreover, the IL **2** recovered and dried was used in a second polymerization cycle yielding similar results to those presented in Figure 4-4.

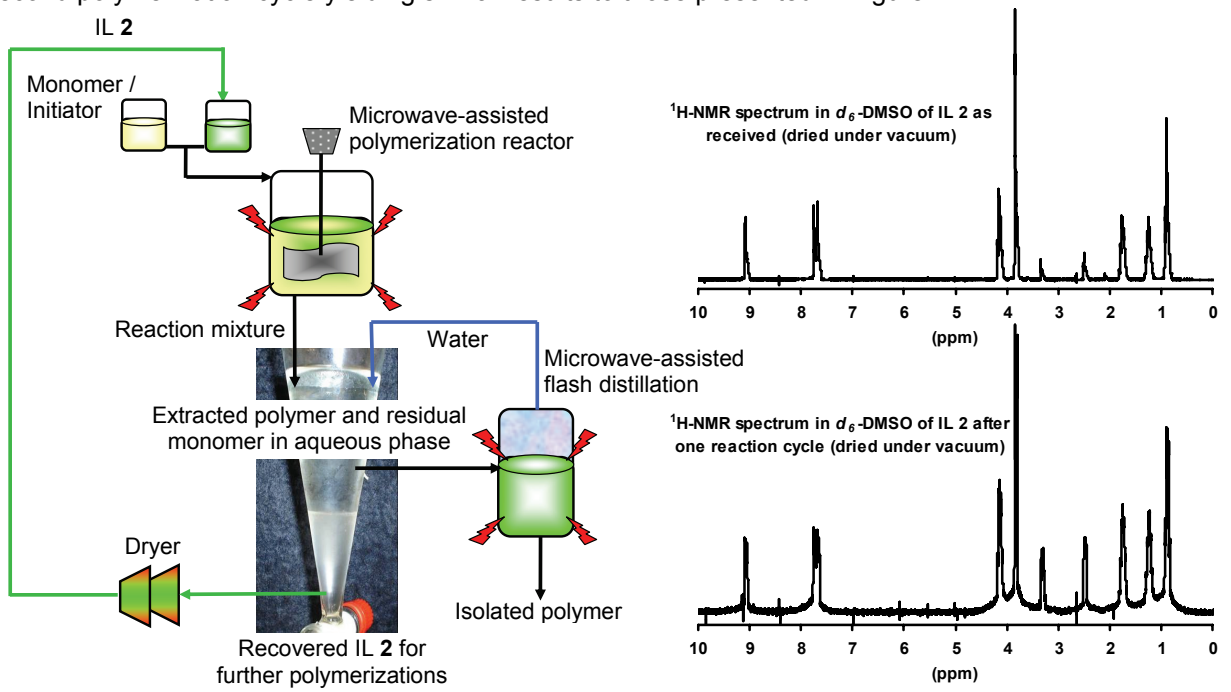

Figure 4-9: *Left: Schematic representation of the efficient recovery of the hydrophobic ionic liquid 1-butyl-3-methylimidazolium hexafluorophosphate (IL **2**) (Table 4-1, Figure 4-1) and polymer isolation by a post-reaction extractive process with water for the living cationic ring opening polymerization of 2-ethyl-2-oxazoline (Figure 4-3). Right: ^{1}H-NMR spectra (in deuterated dimethyl sulfoxide (d_6-DMSO)) as received from the supplier and after one reaction cycle.*

Note that the polymerizations performed in IL **2** above the boiling point of the monomer (EtOx, 128.4 °C) and at long reaction times showed a limited conversion (around 90% for a reaction temperature of 140 °C), which was much less pronounced where the mixture of acetonitrile/IL **2** or lower reaction temperatures were used. This effect can be attributed to the absence of additional volatile substances apart from the monomer in the polymerization system (since ILs have negligible vapor pressure[1i]). Therefore, in the polymerizations carried out at a higher temperature than the boiling point of the monomer, the vapor phase in the reactor will be mainly saturated with monomer that might not polymerize. Where the mixture of acetonitrile/IL **2** was used, higher conversions were obtained since acetonitrile might saturate, due to its lower boiling point, faster the vapor phase than the monomer. This effect may be minimized by applying an over-pressure in the reactor with a different inert substance (*e.g.*, nitrogen and argon).

It is known that ILs containing hexafluorophosphate ($[PF_6]^-$) or tetrafluoroborate ($[BF_4]^-$) anions may hydrolyse under acidic conditions and release hydrogen fluoride.[1g] However, in this work pH measurements of the system during different stages of the process revealed the absence of strong acidic conditions. Although the main IL (IL **2**) investigated in this work is composed of $[PF_6]^-$ anions, that does

not mean that the approach here presented is restricted to the use of this particular IL (*e.g.*, to completely ensure the absence of strong acids in the entire process or its release into the environment, more stable hydrophobic ILs may be used for the same purpose (*e.g.*, 1-hexyl-3-methylimidazolium tris(pentafluoroethyl)trifluorophosphate)). Apart from the cases investigated in this research, nowadays there are many commercially available ILs that may offer additonal advantages for performing different polymerization reactions.

4.2.2 Synthesis of hydrophobic polymers via cationic ring opening and free radical polymerizations in hydrophilic ionic liquids under microwave irradiation

In the previous section it was discussed that the use of a hydrophobic IL as reaction media for performing the synthesis of PEtOx (a hydrophilic polymer) may offer some kinetic advantages (higher reaction rates). It was also demonstrated that the synthesis of block copolymers in ILs by the investigated living cationic ring opening polymerization (CROP) mechanism may be feasible. In addition, it was shown that the recovery of hydrophobic IL and the isolation of the polymers can be efficiently performed by an extraction process with water, which opens opportunities for the development of "green" technologies.

Table 4-3: *Reaction conditions and results for different free radical polymerizations (FRP) of methyl methacrylate (MMA) and cationic ring opening polymerizations (CROP) of 2-(m-difluorophenyl)-2-oxazoline (F_2Ox) and 2-phenyl-2-oxazoline (PhOx) performed under microwave irradiation at different concentrations of two water-soluble ionic liquids (1-butyl-3-methyimidazolium trifluoromethanesulfonate (**4**) and 1-butyl-3-methyimidazolium tetrafluoroborate (**5**) (Table 4-1, Figure 4-1)) as reaction media.*

Exp.	Polymerization / Monomer (wt %)	Ionic liquid / wt %	Reaction temperature (°C)	Reaction time (min)	Yield (%)	Mn (kDa)	PDI
1	FRP / MMA (100)	–	100	20	94	25.1	3.75
2	FRP / MMA (96.5)	IL **4** / 3.5	100	20	90	26.4	3.15
3	FRP / MMA (75)	IL **4** / 25	100	20	67	24.9	3.05
4	FRP / MMA (50)	IL **4** / 50	100	20	56	19.6	2.50
5	FRP / MMA (96.5)	IL **5** / 3.5	100	20	94	23.8	3.47
6	FRP / MMA (75)	IL **5** / 25	100	20	95	23.8	3.09
7	FRP / MMA (50)	IL **5** / 50	100	20	93	20.0	3.16
8	CROP / F_2Ox (100)	–	140	30	94	11.0	1.13
9	CROP / F_2Ox (40)	IL **4** / 60	140	30	53	4.1	1.16
10	CROP / F_2Ox (40)	IL **5** / 60	140	30	61	5.6	1.17
11	CROP / PhOx (100)	–	140	10	96	8.6	1.47
12	CROP / PhOx (60)	IL **4** / 40	140	10	96	3.5	2.05
13	CROP / PhOx (40)	IL **4** / 60	140	10	70	6.9	1.86
14	CROP / PhOx (60)	IL **5** / 40	140	10	77	4.1	2.22
15	CROP / PhOx (40)	IL **5** / 60	140	10	53	2.5	1.67
16	FRP / MMA (25)	IL **5** / 75	100	20	94	22.0	3.19
17	FRP / MMA (25)	IL **5** (reused) / 75	100	20	95	21.1	3.27
18	FRP / MMA (25)	IL **5** (reused) / 75	100	20	94	23.7	3.03

It is clear that the aforementioned approach is not suitable for the homogeneous synthesis of hydrophobic polymers in hydrophobic ILs due to the fact that the recovery of the IL and the isolation of the polymer will not be achieved by an extraction process with water. For such cases, the selection of a proper IL is a key factor to develop efficient polymerization systems. It is thought that the use of hydrophilic ILs in such cases might be convenient since, unlike the system of the previous section, in these cases the ILs can be recovered by an extraction process with water, whereas the precipitated hydrophobic polymers can be isolated by a filtration process. The use of this approach, like in the previous section, avoids the use of VOCs during the polymerization process and allows easy recovery of the IL utilized for further polymerization cycles.

Hence, this section discusses the feasibility of applying this latter concept to the homogeneous synthesis of hydrophobic polymers in water-soluble ILs (WSILs). For this purpose, free radical polymerization (FRP) of methyl methacrylate (MMA) as well as CROP of 2-(*m*-difluorophenyl)-2-oxazoline (F_2Ox) and 2-phenyl-2-oxazoline (PhOx) were performed under microwave irradiation using selected WSILs (1-butyl-3-methyimidazolium trifluoromethanesulfonate (**4**) and 1-butyl-3-methyimidazolium tetrafluoroborate (**5**) (Table 4-1, Figure 4-1)) as reaction media, which are miscible with the monomers used and dissolve the synthesized polymers. The reaction conditions for the different polymerizations performed in this study are summarized in Table 4-3 (Exps. **1**-**15** were performed in a Biotage microwave reactor, and Exps. **16**-**18** in a CEM microwave platform, see experimental part for details).

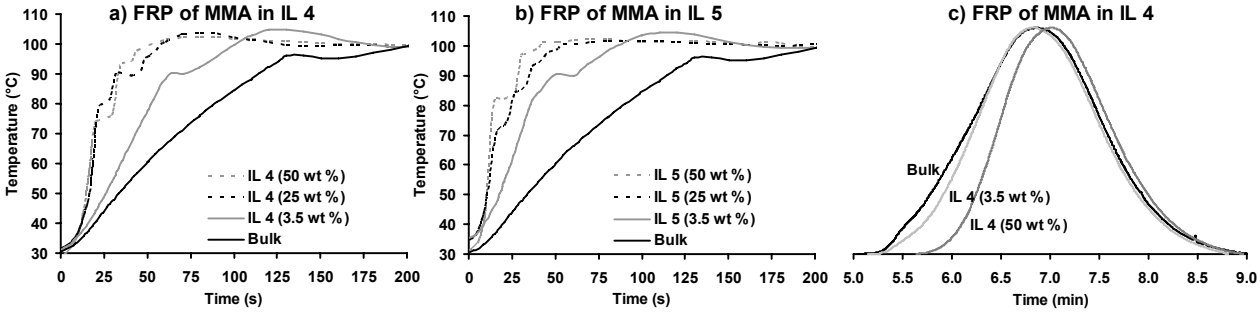

Figure 4-10: *(a) and (b): Heating profiles for the microwave-assisted free radical polymerizations (FRP) of methyl methacrylate (MMA) in bulk and in two water-soluble ionic liquids (1-butyl-3-methyimidazolium trifluoromethanesulfonate (**4**) and 1-butyl-3-methyimidazolium tetrafluoroborate (**5**) (Table 4-1, Figure 4-1)) as reaction media at different concentrations. (c) Normalized GPC traces of selected polymers of this set of experiments (Exps. **1**-**7**, Table 4-3).*

Regarding the FRP of MMA, it was found that MMA is a monomer fully soluble in IL **4** and shows partial solubility in IL **5**. Poly(methyl methacrylate) (PMMA) shows a similar behavior to its monomer, this means, fully soluble in IL **4** and insoluble in IL **5**. Therefore, the FRP of MMA in IL **4** proceeds in a homogenous way whereas in IL **5** it proceeds in a kind of precipitation polymerization. Figure 4-10 displays the heating profiles for the onset of the polymerization experiments performed under microwave-assisted conditions for the FRP of MMA performed at 100 °C for 20 min (using 1 wt % of AIBN referred to amount of monomer in all cases) using IL **4** and IL **5** as reaction media at different concentrations as well as for the respective bulk case (Exps. **1**-**7**, Table 4-3). In addition, Figure 4-10 shows the obtained GPC traces of selected cases of this set of experiments. The heating profiles of Figure 4-10 reveal considerable differences in the heating rates (starting at room temperature and aiming at the desired reaction temperature) between the investigated reaction mixtures under microwave irradiation as the concentration of the two utilized ILs in the polymerization reactions changes. According to these differences, it is clear that incorporation of ILs into the polymerization reactions provides a more efficient absorption of microwaves (which means more efficient energy transfer and therefore higher heating rates at fixed irradiation conditions are obtained) allowing the desired reaction temperatures to be reached in shorter times than in the case of the absence of ILs (bulk polymerization). Moreover, the heating profiles of Figure 4-10 also show that the incorporation of even small amounts of IL (3.5 wt %) increases considerably the heating rates of the polymerization mixtures, whereby this increase is even more remarkable in the case of IL **5**; similar observations for different reaction systems have been reported in the literature.[11a,b] In addition, it can be observed that at higher concentrations of the ILs in the reaction systems, the heating rates become much less dependent on this variable (*e.g.*, for the cases of 25 and 50 wt % contents of ILs the heating profiles are quite similar especially in the case of IL **4**).

With regard to the properties of the obtained PMMAs in this set of experiments (Exps. **1**-**7**, Table 4-3), the polymers revealed molecular weight and PDI values for a typical FRP mechanism (Mn around 23 kDa

and PDI values greater than 3 for all the investigated cases as shown in Table 4-3). In addition, it was found that the yield of the polymerizations is influenced by the kind and/or concentration of IL. For instance, the bulk polymerization case (which is expected to have the highest polymerization rates owing to the higher concentration of monomer in the reaction system) yielded 94% (as determined by ^{1}H-NMR) at the investigated reaction conditions. Nevertheless, yields similar to the bulk case were obtained in the cases where IL **5** was used as a reaction media at different concentrations as shown in Table 4-3. These results suggest that the FRP of MMA in IL **5** proceeds as fast as in the bulk case (at least under the investigated reaction conditions). For these cases, it is thought that due to the partial solubility of MMA in IL **5** the polymerization may occur in a phase dispersed of pure MMA resulting in similar reaction rates as the bulk case. Increased polymerization rates, in particular, for the case of FRP of MMA conducted in ILs have also been observed previously.[6c] However, when the same polymerization reactions were carried out in IL **4**, the yields of the polymerizations (shown in Table 4-3) revealed an inverse dependence on the concentration of the IL (higher polymerization yields were observed at lower concentrations of IL **4**) as expected due to the lower concentration of monomer in the reaction system.

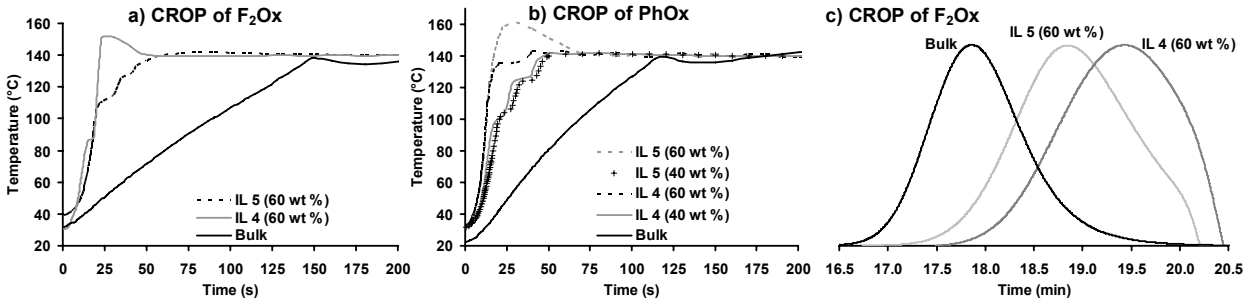

Figure 4-11: *(a) and (b): Heating profiles for the microwave-assisted cationic ring opening polymerizations (CROP) of 2-(m-difluorophenyl)-2-oxazoline (F_2Ox) and 2-phenyl-2-oxazoline (PhOx) in bulk and in two water-soluble ionic liquids (1-butyl-3-methyimidazolium trifluoromethanesulfonate (**4**) and 1-butyl-3-methyimidazolium tetrafluoroborate (**5**) (Table 4-1, Figure 4-1)) as reaction media at different concentrations. (c) Normalized GPC traces of selected polymers of this set of experiments (Exps. **8**-**15**, Table 4-3).*

F_2Ox and PhOx are monomers which can be polymerized by a CROP mechanism and the derived polymers are hydrophobic. However, it was observed that both polymers are fully soluble in ILs **4** and **5**. Regarding the solubility of these monomers, it was found that PhOx is fully soluble in both ILs whereas F_2Ox (which is a white powder at room temperature) is soluble in both ILs above 80 °C. Therefore, the CROP of these monomers in ILs **4** and **5** proceeds in a homogenous way at high temperatures and remarkably the resulting polymers do not precipitate in the ILs even at room temperature, which yields a highly viscous mixture. In Figure 4-11 the heating profiles at the onset of the performed polymerization experiments under microwave-assisted conditions for the CROP of F_2Ox and PhOx performed at 140 °C for 30 and 10 min, respectively (using 3 wt % of MeTos referred to the amount of monomer in the case of F_2Ox and, 2 wt % in the case of PhOx), using IL **4** and IL **5** as reaction media at different concentrations as well as for the coresponding bulk cases (Exps. **8**-**15**, Table 4-3) are displayed. In addition, Figure 4-11 shows the obtained GPC traces of selected examples of this set of experiments. The heating profiles of Figure 4-11 reveal similar effects to those observed in the cases of FRP of MMA (Figure 4-10), namely the incorporation of ILs into the reaction mixtures enhance their heating rates when exposed to microwave irradiation. Figure 4-11 also shows that at intermediate concentrations (40 wt %) of ILs in the polymerization mixtures, the kind of IL has practically no influence on the heating profiles under the investigated reaction conditions. However, at high concentrations (60 wt %) of ILs the polymerization mixtures can be heated extremely rapidly under microwave irradiation leading, in some cases (as shown

in Figure 4-11), to an overshoot on the desired reaction temperatures (140 °C in these cases) and, perhaps, in more exothermic systems to uncontrolled polymerizations.

With regard to the properties of the obtained polymers in this set of experiments, for the case of the CROP of F_2Ox, the obtained polymers revealed low PDI values (as shown in Table 4-3, GPC traces of these experiments are also shown in Figure 4-11) but their molecular weights were about twice as high compared to the expected theoretical values (Mn of 5.2 kDa at 100% of monomer conversion). This deviation can be attributed to the used analytical technique (*e.g.*, a polystyrene calibration was used to estimate the molecular weights of these fluorinated polymers). The observed polymer yields for the CROP of F_2Ox were lower in the cases of polymerizations containing ILs than in the bulk cases due to the lower concentration of monomer in the reaction systems. Regarding the CROP of PhOx, the molecular weight of the polymer obtained in the bulk case was in good agreement with the expected theoretical value (Mn of 8.7 kDa at 100% of monomer conversion). The characteristics of the obtained polymers of these experiments are summarized in Table 4-3. For the investigated cases of CROP of PhOx, the obtained polymers showed broad molecular weight distributions and therefore their PDI values were considerable higher than in the bulk case and important deviations of the expected theoretical values of molecular weight were observed. Nevertheless, it should be noted that the objective of this study was to investigate the CROP of hydrophobic polymers in WSILs under microwave irradiation and not the livingness of the polymerizations. With regard to the yields obtained during the CROP of PhOx, the polymerization reactions performed in ILs revealed lower yields than the bulk case, and the yields were higher in the case of IL **4** with respect to the case of IL **5** at fixed reaction conditions as summarized in Table 4-3. This observation can be attributed to concentration effects since the polymerizations performed in ILs have a lower monomer concentration than bulk polymerizations. However, as discussed in section 4.2.1 and reported in literature,[6c,n] the yields of polymerizations performed in ILs can be comparable or even higher than the observed in common VOCs where similar reactions conditions (monomer concentration, temperature and reaction time) are used. For instance, for a CROP of PhOx in IL **4** performed in this investigation (Exp. **13**, Table 4-3) a polymer yield of 70% was observed under the reaction conditions investigated (140 °C, 10 min of reaction time, and 60 wt % IL **4**), whereas in the literature a polymer yield of 60% has been reported for the same polymerization carried out in acetonitrile using similar reaction conditions (140 °C, 10 min of reaction time, 55 wt% of acetonitrile, and same microwave platform).[12a]

The isolation of the polymers obtained and the recovery of the ILs used for the polymerization reactions investigated was performed by the addition of purified water (five-fold excess) into the homogeneous reaction mixtures under vigorous stirring, and preferably, at high temperature in the cases of low concentrations of IL (highly viscous systems due to the higher concentrations of the polymers). During this procedure, the obtained hydrophobic polymers agglomerate and/or precipitate, and simultaneously, the used ILs form a homogeneous solution with water. Opposite to the analyzed case in section 4.2.1 for the synthesis of hydrophilic polymers performed in hydrophobic ILs, for the investigated cases in this section (homogeneous synthesis of hydrophobic polymers in ILs) the use of water-soluble ILs is particularly convenient since it facilitates the polymer isolation and the IL recovery for additional reaction cycles and keeps a suitable “green” scope for this synthetic method. For instance, the polymerizations investigated in this section were also performed homogenously in the hydrophobic IL 1-butyl-3-methylimidazolium hexafluorophosphate (IL **2**) (Table 4-1, Figure 4-1) and the obtained polymers showed comparable properties and yields to those discussed above for the cases of IL **4**. However, the isolation of the products and the recovery of the IL could not be successfully performed by precipitation with water owing to the fact that the entire reaction mixture is highly hydrophobic, which makes the use of hydrophobic ILs less attractive for the here discussed reaction systems.

Hence, the recovery of IL **5** from the resulting aqueous solution during the described polymerization process for its use in further reaction cycles was investigated by performing additional FRP of MMA (three reaction cycles in recovered IL) under the same reaction conditions. In these experiments, larger

reaction volumes were utilized in order to facilitate the recycling process. The distillation of water from the resulting IL **5** aqueous solutions after each reaction cycle was performed under microwave-assisted conditions taking advantage of the aforementioned high efficiency of ILs to absorb microwaves as observed in Figure 4-12a. Figure 4-12a compares the heating profiles of the two different ILs aqueous solutions of this study and pure water (for illustration purposes, IL aqueous solutions (50 wt% of IL) are programmed to be heated in the microwave setup for 1 s after reaching the desired temperature (140 °C), thereafter the system starts to cool the samples). According to Figure 4-12a the samples containing ILs are heated considerable faster than pure water and thus more efficient energy transfer is observed under microwave irradiation, which allowed for an efficient removal of water from the solutions even at atmospheric pressure conditions. ^{1}H-NMR investigations showed that the recovered IL by this procedure remains unmodified after three reaction cycles (as depicted in Figure 4-12b) and it is suitable to perform additional polymerizations.

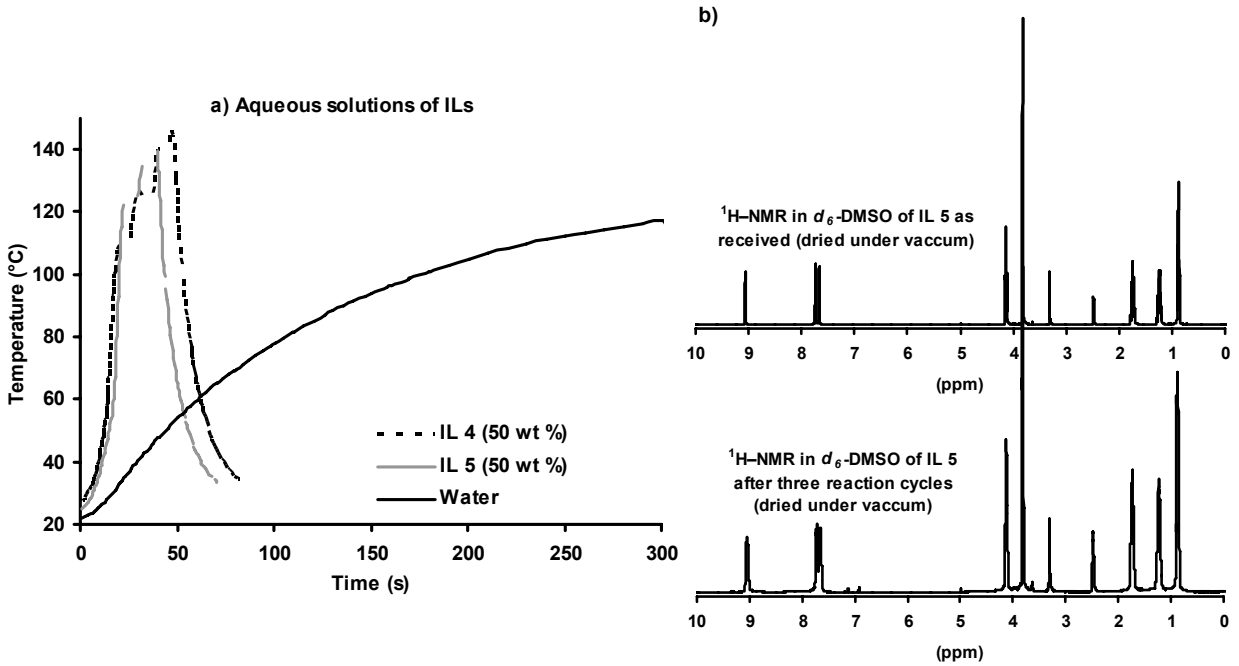

Figure 4-12: *(a) Heating profiles for ionic liquids aqueous solutions and water under microwave irradiation (1-butyl-3-methylimidazolium trifluoromethanesulfonate (**4**) and 1-butyl-3-methylimidazolium tetrafluoroborate (**5**) (Table 4-1, Figure 4-1)). b) ^{1}H-NMR spectra of IL **5** as received from the supplier and after its use as a reaction medium in three polymerization cycles of methyl methacrylate (Exps. **16**-**18**, Table 4-3).*

The obtained yields and molar masses in these additional polymerizations were comparable to each other as observed in Table 4-3 for Exps. **16**-**18**. The efficiency of the IL recovery during these experiments could not be accurately estimated due to the relatively small reaction volumes used in the polymerizations, which makes a full recycling of the IL difficult in the post-reaction steps (*e.g.,* in the filtration step of the polymer (see experimental part for details), a considerable amount of the IL aqueous solution remained in the used paper filter which clearly lowered the yield of the IL recycling). Thus, the obtained efficiency of the IL recovery using the described procedure in the experimental part (including the filtration and microwave-assisted distillation steps) was around 80%. However, it might be feasible to obtain higher yields (close to 100%) by optimizing and/or improving the involved separation steps. Figure 4-13 shows a conceptual scheme and images of the discussed microwave-assisted polymerization reactions.

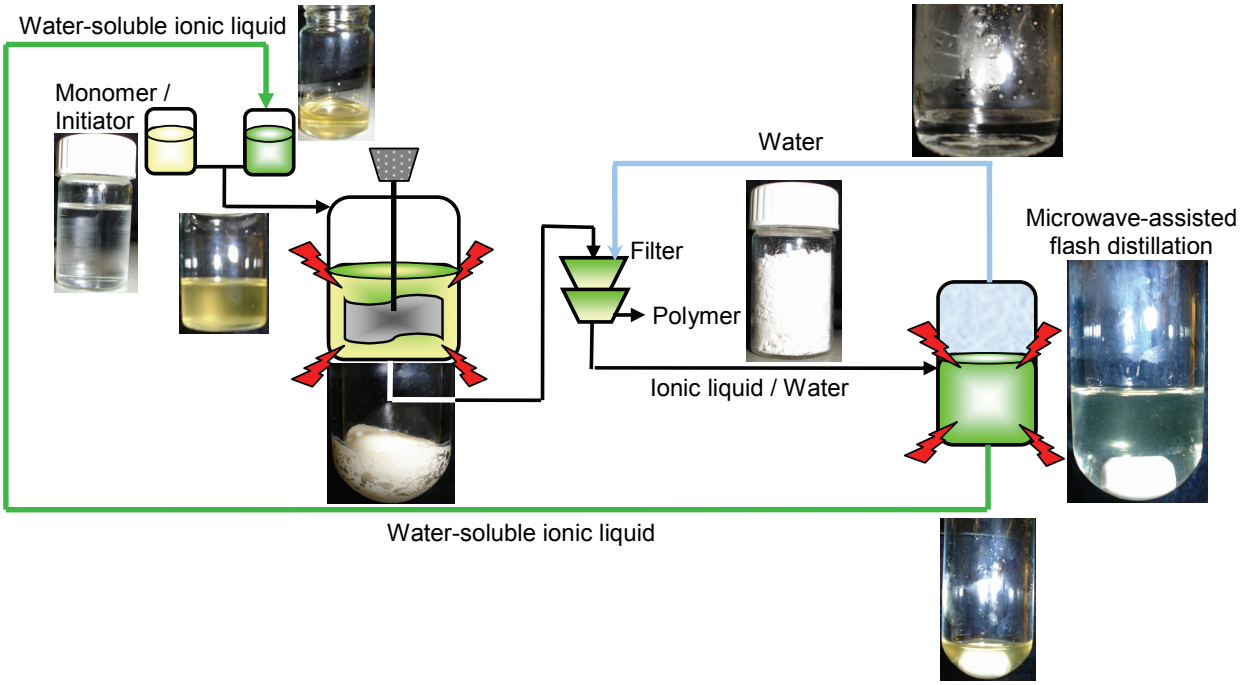

Figure 4-13: *Schematic representation of a "green" process for the continuous microwave-assisted synthesis of hydrophobic polymers in water-soluble ionic liquids which allows for the depletion of emissions of volatile organic compounds into the environment and may allow for energy savings.*

In Table 4-3 it can also be observed that in some of the investigated cases the yields of the polymerizations in ILs and the molar masses of their polymers are lower than the corresponding bulk cases. However, it is well-known that in bulk polymerization processes considerable amounts of energy must be spent (on heating to reach reaction temperatures up to 220 °C and on power supply for specialized pumps for high viscosity reaction media) to overcome the problems related to the high viscosity (*e.g.*, heat and mass transfers) of the polymer melts. Nevertheless, problems related to high temperatures, such as side-reactions and degradation of the products, often arise in many polymerization processes.[3] For these reasons, solution polymerizations in VOCs (or in ILs as suggested in this investigation) are preferred over bulk processes. On the one hand, it is clear that solution polymerizations can be performed at lower temperatures than bulk polymerizations without having the problems of highly viscous systems, but on the other hand longer reaction times are needed in solution processes to reach similar yields and molar masses to the bulk cases. It is obvious that bulk polymerizations, in general, will show higher polymerization rates than polymerization in ILs or in conventional VOCs due to monomer concentration effects. However, if a comparison is made between ILs and VOCs in solution polymerizations, it has been demonstrated, in this section as well as in the literature,[6c,n] that polymerizations in ILs show higher polymerization rates. In addition, solution polymerizations are more suitable processes to perform the synthesis of well-defined block copolymers via a sequential addition of monomer, which would be very difficult to perform in bulk processes due to the limited diffusion of the reagents as direct consequence of the high viscosity generated. Thus, the synthetic approaches described in these investigations arise "green" alternatives to bulk and/or conventional solution polymerization processes involving VOCs. However, it is clear that for specific polymerization systems several parameters must be optimized and evaluated in order to make a direct comparison between processes performed in ILs and in conventional VOCs or bulk conditions.

4.3 Heterogeneous polymerization reactions performed in ionic liquids and in their aqueous solutions: Engineering polymer beads

In section 4.2, the feasibility of performing efficient homogeneous polymerizations in ILs was demonstrated for two different reaction mechanisms (free radical and cationic ring opening polymerizations). In addition, it was shown that the utilized ILs liquids can be recovered and re-used for further polymerization cycles. However, there might be many polymers that are not soluble in ILs for which the proposed approach in section 4.2 can not be applied. For such cases, heterogeneous processes in ILs can be considered. Hence, the feasibility of performing heterogeneous polymerizations in ILs or in their aqueous solutions is addressed in this section.

4.3.1 Introduction to heterogeneous polymerization systems

The heterogenization of polymerization processes is desirable in some cases for an easy separation of the product. Heterogeneous polymerization processes, such as water-based emulsions and suspensions, have found good acceptance for the production of many commodity materials[14] as well as specialized polymers for advanced applications.[15] Materials synthesized via heterogeneous polymerization processes are regular beads with sizes between 50 nm and 3000 μm, depending on the characteristics of the used procedure (*e.g.*, emulsion, mini-emulsion, precipitation, dispersion, soap-free emulsion, seeded, or suspension polymerizations). Heterogeneous polymerization can be defined as a reactive liquid-liquid dispersion in which the nature of the suspended drops changes as the polymerization reaction proceeds. Common suspension polymerizations are carried out in stirred tank reactors, adding a stabilizing agent (protective colloid) to the aqueous phase in order to keep the suspended organic drops from coalescing as they change from the liquid to the solid state via a sticky phase. The size of the drops is determined by the balance between the rates of drop breakup and coalescence, which are influenced by several parameters, such as densities and viscosities of the continuous and dispersed phases, interfacial tension, type and concentration of suspending agent, type of impeller, stirring speed, and temperature. In addition to the aforementioned parameters, the continuous change in the properties of the dispersed phase, as a result of the ongoing polymerization reaction, contribute to the size of the drops and to their distribution.[16] Of major importance for the stability of suspensions is the type and amount of suspending agent utilized, due to the fact that it induces electrostatic charges on the surface of the suspended monomer-polymer particles, which retard their coalescence. Examples of stabilizing agents used in suspension polymerization are: polyvinylalcohol, polyvinylpyrrolidone, hydrophobic modified celluloses, phosphates,[14] steric stabilizers such as hydrophilic and hydrophobic copolymers, soap solutions, water–agarose gels,[15a] and perfluoropolyethers for suspension polymerizations carried out in supercritical CO_2.[17] The selection of the suspending agent will depend, mainly, on the desired particle size which is determined by the market requirements and/or applications (*e.g.*, bone cement, packing for chromatographic columns, expandable polystyrene, etc.).[14,15] However, nowadays the prediction of the particle size under specific polymerization conditions is still an aspect not fully understood.

4.3.2 Heterogeneous polymerization reactions of cross-linked systems using water-soluble ionic liquids as stabilizing agents and/or reaction media

As described in section 4.2, the use of ILs as a reaction media to synthesize diverse polymers and composites has opened a “new environmentally-friendly” and novel synthetic approach (in some cases

even with kinetic advantages over conventional solvents).[6] Despite the obtained progress in performing polymerizations in ILs, clear understanding of how to optimize the use of these novel reaction media in specific polymer systems is still lacking, since many factors must be optimized including, IL selection, polymer isolation, IL recycling, IL toxicity, etc. Recently, the heterogeneous synthesis of polymers using ILs as reaction media has been described, which resulted in a sort of gel systems containing dispersed chalky solids (polymer).[7] However, a full explanation of this observed phenomenon has not been properly described. Because ILs can also be defined as organic molten salts below 100 °C, it is thought that their use in suspension polymerizations may be equivalent to the use of common stabilizing agents. In other words, ILs may induce electrostatic charges on the surface of the monomer-polymer particles to keep them from coalescence as depicted in Figure 4-14. In addition, it is thought that the non-polar part of ILs may also act as a surfactant helping to stabilize the suspended organic phase (Figure 4-14). Based on these assumptions, the use of water-soluble ionic liquids (WSILs) as stabilizing agents in suspension polymerizations as well as their influence on the size and surface area of synthesized polymer beads is discussed in this section. To carry out this research, three WSILs (1-alkyl-3-methylimidazolium chlorides (**10**, **11** and **12**; Table 4-1, Figure 4-1)) were investigated as depicted in Figure 4-14. In addition, the effect on the stability of the suspension polymerizations due to the variation of the aliphatic side-chain length in the investigated ILs is also addressed.

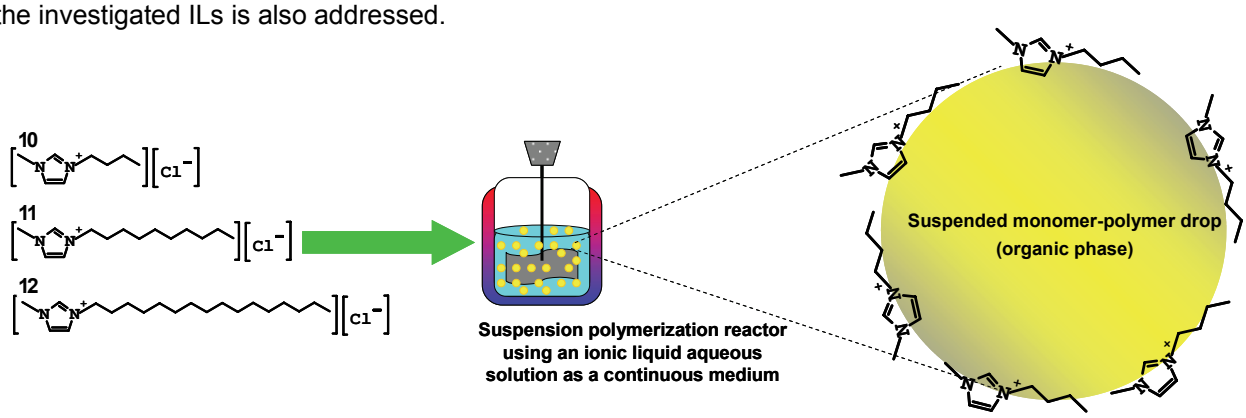

Figure 4-14: *Schematic representation of water-soluble ionic liquids acting as stabilizing agents and reaction media in a suspension polymerization reaction. The molecular structures of the investigated ionic liquids (Table 4-1, Figure 4-1) are also displayed (1-butyl-3-methyimidazolium chloride (**10**), 1-decyl-3-methyimidazolium chloride (**11**), and 1-hexadecyl-3-methyimidazolium chloride (**12**)).*

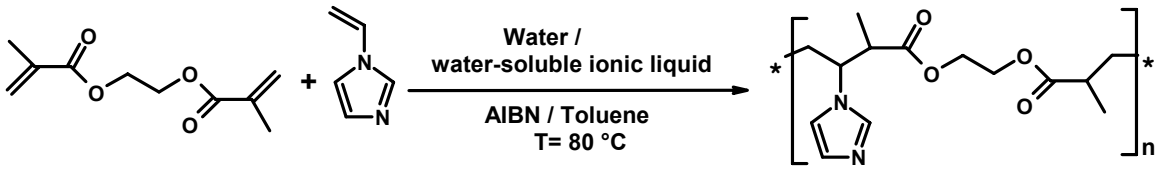

Figure 4-15: *Schematic representation of the synthesis of poly(ethylene glycol dimethacrylate-N-vinylimidazole) cross-linked polymer beads by free radical suspension polymerization using water-soluble ionic liquids as stabilizing agents (Figure 4-14) and 2,2´-azobisisobutyronitrile (AIBN) as initiator.*

Hence, the research in this section is dedicated to elucidate the influence of ILs used as a reaction media and/or stabilizing agents in suspension polymerization reactions in order to address the phenomena observed previously in similar heterogeneous polymerizations in ILs (gel systems containing dispersed chalky solids (polymer)).[7] This study mainly focuses on obtaining a deeper insight into heterogeneous polymerizations performed in ILs, which will allow a better understanding of these systems in order to develop more efficient and environmentally-friendly polymerization processes based on ILs. For the purposes of this investigation, the synthesis of poly(ethylene glycol dimethacrylate-*N*-

vinylimidazole) cross-linked beads was selected as a main suspension polymerization system according to the reaction scheme shown in Figure 4-15.[18]

Based on the assumption that ILs may provide electrical charges on the surface of the suspended monomer-polymer particles in order to keep them from coalescing in a suspension polymerization reaction, in the first experiments of this research the concentration and the kind of IL (different aliphatic side-chain lengths, Figure 4-14) in the aqueous phase of these heterogeneous systems were varied. As such, the effects of these parameters on the stability of the suspensions and on the average particle size of the resulting polymer beads could be evaluated. Hence, these suspension polymerization experiments were performed in the experimental setup displayed on Figure 4-16a (see experimental part for details about the experimental setups utilized for heterogeneous polymerization experiments). The results derived from these experiments are summarized in Table 4-4.

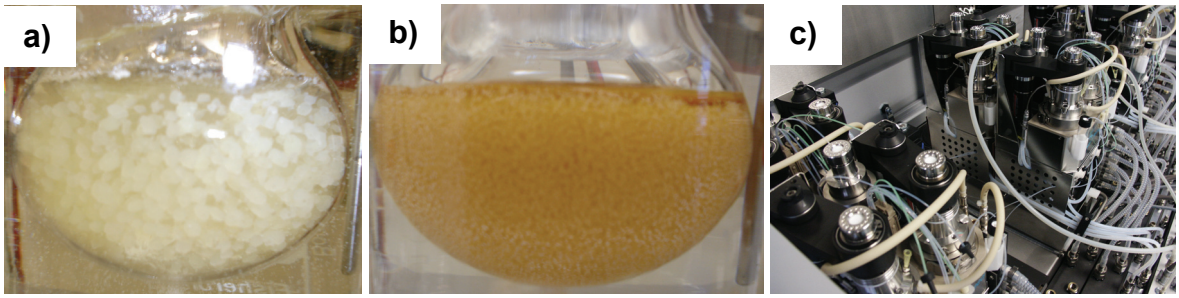

Figure 4-16: *Overview of the reaction setups utilized to perform suspension polymerization experiments (Figure 4-15) using water-soluble ionic liquids as stabilizing agents (Figure 4-14). (a) Laboratory-scale glass reactor (experiments summarized in Table 4-4). (b) An image of a gel-like reaction mixture obtained during suspension polymerization experiments performed in the glass reactor where a high content of ionic liquid is used in the continuous aqueous phase (Exps.* ***3****,* ***5****, and* ***7****; Table 4-4). (c) Automated parallel synthesizer A-100 minipilot plant from Chemspeed (experiments summarized in Table 4-5).*

Table 4-4: *Results of the average particle size for experiments performed in a glass reactor (Figure 4-16a) to evaluate three different water-soluble ionic liquids as stabilizing agents (Figure 4-14) in suspension polymerization reactions (Figure 15) (see Table 4-1 and Figure 4-1 for the properties and chemical structures of the ionic liquids, respectively).*

Exp.	Ionic liquid	Concentration of ionic liquid in the aqueous phase (wt %)	Average particle size
1	1-Butyl-3-methyimidazolium chloride (**10**)	10	2.7 mm
2	1-Butyl-3-methyimidazolium chloride (**10**)	70	1.6 mm
3	1-Butyl-3-methyimidazolium chloride (**10**)	100	0.5 mm
4	1-Decyl-3-methyimidazolium chloride (**11**)	20	1.7 mm
5	1-Decyl-3-methyimidazolium chloride (**11**)	40	600 nm
6	1-Hexadecyl-3-methyimidazolium chloride (**12**)	1	1.9 mm
7	1-Hexadecyl-3-methyimidazolium chloride (**12**)	5	500 nm

The results shown in Table 4-4 reveal that the concentration of WSILs has a large effect on the as-obtained particle size averages of the synthesized polymer beads (see experimental part for details about the used characterization technique). In short, for the three investigated WSILs, it was found that a low content of IL in the aqueous continuous medium of the suspension allows the synthesis of large polymer beads (with average sizes in the millimeter range), whereas for a high IL content the particle sizes decrease remarkably, down to the nanometer range in some cases.

Simultaneously, it can also be seen in Table 4-4 that the average bead size is not only affected by the IL/water ratio but the aliphatic-side chain length of the WSILs (Figure 4-14) also has an influence. By combining these effects (concentration and aliphatic-side chain length), it can be concluded that in order to obtain a specific average particle size the concentration of the investigated ILs in the aqueous phase of the suspension has to decrease as the aliphatic side-chain length becomes longer.

For example, the average particle size remained between 1.6 mm and 1.7 mm where the concentration of WSIL was 70 wt %, 20 wt %, and even 1 wt % for IL **10**, IL **11**, and IL **12**, respectively (Exps. **2**, **4**, and **6**; Table 4-4). Where the same WSIL is used to "tune" the average size of the particle, its concentration has to be increased in order to reduce the bead size (*e.g.*, Exps. **1**-**3**; Table 4-4). Nevertheless, the most remarkable reduction in the particle size (down to the nanometer scale) is mainly influenced by the aliphatic side-chain length of the WSIL. For instance, as shown in Table 4-4, nanometer-scale particles could not be synthesized in the cases where IL **10** was used, even at the highest possible concentration (pure IL) in the aqueous continuous medium of the suspension polymerization (Exp. **3**, Table 4-4). On the other hand, where ILs **11** and **12** (Exps. **5** and **7**, Table 4-4) were used as stabilizing agents, at a specific concentration, beads with sizes in the nanometer range were obtained as revealed by dynamic light scattering measurements (DLS).

To end up with gel-like reaction mixtures, suspended waxy solids, and/or chalky solids similar to those reported in the literature[7] and as shown in Figure 4-16b, a critical concentration of a specific IL in the aqueous phase of the suspension has to be reached. For instance, for the investigated WSILs these concentration were estimated to be around 100 wt % for IL **10**, 40 wt % for IL **11**, and 5 wt % for IL **12** under the reaction conditions of experiments of Table 4-4 (see experimental part for a full description of the reaction conditions). According to this finding, it is thought that this critical concentration may establish the limit of the smallest average particle size that is possible to obtain using a specific WSIL as stabilizing agent under certain experimental conditions (in this case under the experimental conditions used in the glass suspension polymerization reactor of Figure 4-16a). When the beads are small enough, they can be analyzed by DLS as well as by atomic force microscopy (AFM). DLS provides information on the average diameter of the cross-linked polymer beads in aqueous solution, when they are supposed to be in a swollen state due to the presence of the solvent (water) as reported in literature for this kind of materials.[18] AFM provides the diameter of the beads in dry conditions (non-swollen state) in a similar way as discussed in section 3.2.3 for the characterization of diblock copolymer micelles. For instance, Figure 4-17 shows an AFM image utilized for determining the average size of a sample of synthesized polymer beads (see below Exp. **4**, Table 4-5) in dry conditions; a value of 100 nm was obtained whereas in a swollen state (DLS measurements) the average size was 250 nm.

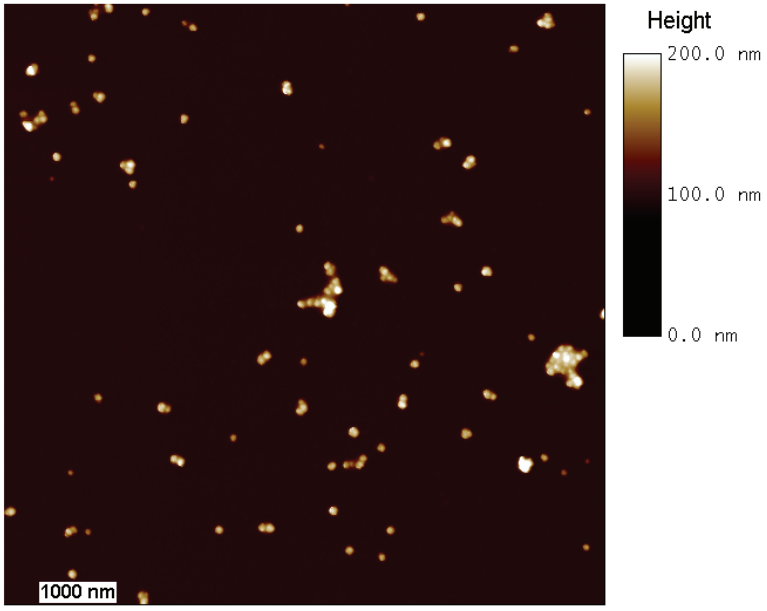

Figure 4-17: *Atomic force microscopy image recorded using dry conditions of polymer beads formed in Exp.* ***4*** *of Table 4-5. The image was used to determine the average size of the beads.*

The simultaneous effects of other reaction parameters on the stability of the suspensions and on the average size of the polymer beads were briefly investigated by performing additional polymerization reactions in the automated parallel synthesizer[21] shown Figure 4-16c (see experimental part for a detailed description of this experimental platform). The reaction conditions and the results of these experiments are summarized in Table 4-5. According to these results, qualitatively, it was found that the content of IL in the aqueous phase of the suspension ($\mathbf{x_1}$), acting as a stabilizing agent, is inversely proportional to the average particle size as already discussed above. The reaction temperature ($\mathbf{x_2}$) has an effect similar to $\mathbf{x_1}$; higher reaction temperatures lead to particles with smaller average size. The composition of *N*-vinylimidazole in the polymer beads ($\mathbf{x_3}$) showed also effects similar to $\mathbf{x_1}$ and $\mathbf{x_2}$; the higher the content of *N*-vinylimidazole, the smaller the average particle size. Finally, the content of toluene ($\mathbf{x_4}$) in the formulations is thought to have almost no influence on the stability of the suspensions and/or on the size of the particles but mainly on the formation of pores in the beads. For example, when toluene was not included in the formulation, the particles obtanied were translucent. On the other hand, when toluene was used, the particles obtained were white and opaque (the presence of pores may disperse the light through the beads turning them opaque). Similar effects of some of the reaction parameters investigated in the experiments reported in Table 4-5 (concentration of stabilizing agent and reaction temperature) on the average particle size of polymer beads synthesized by suspension polymerization have been reported in literature.[16]

Table 4-5: *Experimental design performed in the automated parallel synthesizer shown in Figure 4-16c for the synthesis of cross-linked beads (Figure 4-15) by suspension polymerization using a water-soluble ionic liquid as stabilizing agent (IL **10**, Figure 4-14) and a mechanical stirring speed of 400 rpm. Four reaction parameters were analyzed as follows: $\boldsymbol{x_1}$ = content of ionic liquid 1-butyl-3-methyimidazolium chloride (IL **10**) in the aqueous phase (– = 20 wt %, + = 70 wt %), $\boldsymbol{x_2}$ = reaction temperature (– = 75 °C, + = 90 °C), $\boldsymbol{x_3}$ = content of N-vinylimidazole in the polymer beads (– = 50% mol, + = 87.5% mol), and $\boldsymbol{x_4}$ = content of porogenic agent (toluene) in the organic phase (– = 0 vol %, + = 30 vol %). * Not determined due to the gel-like properties of the material obtained (no polymer beads).*

Exp.	x_1	x_2	x_3	x_4	Remarks	Average particle size
1	–	–	–	–	Collapsed translucent beads	Large (3 mm)
2	+	–	–	–	Collapsed translucent beads	Medium (1.5 mm)
3	–	+	–	–	Stable suspension, translucent beads	Medium (1.4 mm)
4	–	–	+	–	White stable suspension	Nanometer scale (250 nm)
5	–	–	–	+	Collapsed white beads	Large (2.8 mm)
6	+	+	–	–	Stable suspension, translucent beads	Small (0.65 mm)
7	–	–	+	+	Stable suspension, white beads	Small (0.8 mm)
8	+	–	–	+	Cloudy stable suspension	Nanometer scale (600 nm)
9	–	+	+	–	White stable suspension	Nanometer scale (525 nm)
10	–	+	–	+	Stable suspension, white beads	Small (0.7 mm)
11	+	–	+	–	Yellow stable suspension	Nanometer scale (405 nm)
12	+	+	+	–	Yellow swollen gel-like	*
13	+	+	–	+	White stable suspension	Nanometer scale (650 nm)
14	+	–	+	+	White stable suspension	Nanometer scale (400 nm)
15	–	+	+	+	Stable suspension, white beads	Small (0.75 mm)
16	+	+	+	+	White stable suspension	Small (0.35 mm)

It is known that the agitation speed has an important influence on the particle size in suspension polymerizations.[16] From the experiments performed in this work using the two experimental setups shown in Figure 4-16a and 4-16c, it was also found that the type of agitation influences the particle size and stability of the suspensions. For instance, in the experiments reported in Table 4-4 (magnetic agitation was applied to the glass polymerization reactor shown in Figure 4-16a), larger average particle sizes were obtained in comparison to those achieved in the experiments reported in Table 4-5 (note that the experiments of reported in Table 4-4 were aimed to investigate the WSILs of Figure 4-14 as stabilizing agents in suspension polymerizations under fixed reaction conditions). On the other hand, in the experiments reported in Table 4-5 (mechanical agitation was used in the experimental setup shown in

Figure 4-16c), polymer beads with sizes in the nanometer range could be obtained by using a low concentration of stabilizing agent (IL **10**). This was the case for Exp. **4** of Table 4-5, which showed an average particle size of 250 nm in solution, as revealed by DLS, and around 100 nm, as determined by AFM in dry conditions (Figure 4-17).

To investigate whether the phenomenon of "tuning" the size of the beads by utilizing WSILs as stabilizing agents in suspension polymerizations is just feasible with specific monomers (*e.g.*, *N*-vinylimidazole, which has a similar chemical structure to the utilized WSILs and, therefore, may be more compatible with the phase containing ILs in the suspension), additional polymerization experiments were performed using other monomers. These experiments were carried out under the same reaction conditions of Exps. **1**-**3** of Table 4-4, but by using styrene instead of *N*-vinylimidazole and divinylbenzene instead of ethylene glycol dimethacrylate as co-monomers. In these cases, findings similar to those discussed above for the cases of *N*-vinylimidazole containing polymer beads were observed. More specifically, a gel-like suspension was obtained when pure IL **10** was used as the continuous medium of the suspension, an average particle size of 1.5 mm when a 70 wt % aqueous solution of IL **10** was utilized in the system, and polymer beads with an average size of 2.5 mm in the case of a 10 wt % aqueous solution of of IL **10**.

Note that even though that the polymer beads synthesized in a high content IL aqueous continuous medium were of a small size, the reaction systems studied in this research differ from precipitation polymerization reactions. In precipitation polymerization reactions, monomers form a continuous phase with the reaction medium (solvent) but the polymers do not and precipitate as small nanoparticles. In the polymerizations investigated in this research, the organic phase (co-monomers and pore former mixture), in all cases, is separated from the IL aqueous phase and therefore they can be classified as suspension polymerizations.[15c]

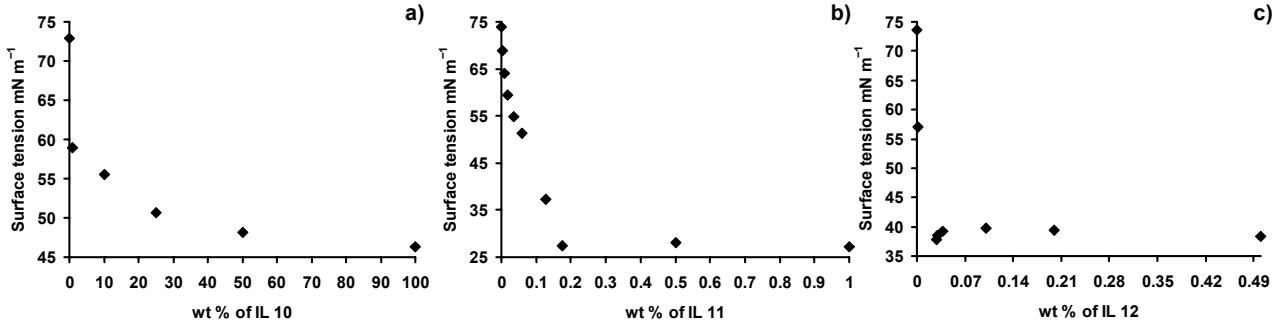

Figure 4-18: *Surface tension measurements of the aqueous solutions of the ionic liquids investigated as stabilizing agents for suspension polymerization reactions (Figure 4-14). (a) 1-Butyl-3-methyimidazolium chloride (**10**), (b) 1-decyl-3-methyimidazolium chloride (**11**), and (c) 1-hexadecyl-3-methyimidazolium chloride (**12**) (see Table 4-1 and Figure 4-1 for the properties and chemical structures of the ionic liquids, respectively).*

In addition to the fact that the investigated WSILs may provide electrical charges on the surface of the suspended monomer-polymer particles in order to stabilize them, the surface active properties of ILs, which have been recently discussed in literature,[19] may also contribute to the stabilization of the systems. These studies mainly report on the surface tension properties of some ILs and their aqueous solutions, as well as their dependence on temperature.[19a-f] Moreover, as an application of the surface active properties of ILs, WSILs have been utilized as novel templates for the preparation of highly ordered monolithic super-micro-porous lamellar silica materials via nano-casting technique.[19g] From those studies, one can conclude that some ILs show surface active properties and aggregation behavior in aqueous solutions. For this reason, surface tension measurements of the aqueous solutions of ILs **10**-**12** (Table 4-1, Figure 4-1) were performed and the results are shown in Figure 4-18. It was found that the critical concentration of aggregation was 0.17 and 0.03 wt % for ILs **11** and **12**, respectively. In the case

of IL **10** it was difficult to establish a value for the critical concentration of aggregation since the surface tension of the aqueous solutions decreases continuously as the concentration of IL increases; this means that a well-defined plateau was not reached. The value of critical concentration of aggregation for IL **12** was the lowest of the three WSILs; this was expected since it has the longer aliphatic side-chain. However, the lowest surface tension value obtained, once the critical concentration of aggregation was reached, was 27 mN m^{-1} for IL **11** in comparison to 38 mN m^{-1} for IL **12**. In the case of IL **10** the lowest possible surface tension was 46 mN m^{-1} (pure IL).

An important aspect that may help to understand the role of the WSILs in "tuning" the size of the synthesized polymer beads is the interfacial tension between the organic (co-monomers) and the IL aqueous phases. In polymerizations in which spontaneous emulsification occurs (*e.g.*, micro-emulsion),[7a] the interfacial tension between the monomer and the aqueous continuous medium phase approaches to zero due to the presence of surfactants that allow the synthesis of polymers beads in the nanometer range. In this context, interfacial tensions for some of the experiments of Table 4-4 were qualitatively estimated using the Du Nouy ring method (by considering the value of interfacial tension recorded by the tensiometer at the maximum value of the forced exerted on the ring as it passes through the interface of the organic mixture and the IL aqueous solution). For instance, the interfacial tension between the organic phase used for the polymerization reactions and pure water had a value of 4.5 mN m^{-1}, whereas the interface of the organic mixture and pure IL **10** (Exp. **3**, Table 4-4) had a valued of 1.8 mN m^{-1} and for the interface of Exp. **1** of Table 4-4 the value was 3.9 mN m^{-1}. These results show that the interfacial tension indeed decreases as the content of IL in the aqueous phase increases, suggesting the possibility of a spontaneous emulsification process in the system allowing for the synthesis of small-sized polymer beads.

After considering the measurements obtained for both surface tension (Figure 4-18) and particle sizes (Table 4-4), it is clear that the aliphatic side-chain length and not only the concentration of the WSILs plays an influential role in the stabilization of the monomer-polymer particles in suspension polymerization reactions. According to Figure 4-18 the experiments of Table 4-4 were performed above the critical concentration of aggregation of ILs (at least in the cases of ILs **11** and **12**) and therefore in a low surface tension aqueous phase. Similar to the case of emulsion polymerization, the availability of hydrophobic aliphatic chains in the system promotes the creation of more interfacial area between the organic phase (monomer-polymer particles) and the aqueous IL solutions. Therefore, the synthesis of polymer beads with smaller average particle size is possible.

This effect may be similar to the cases of current suspension polymerizations, in which poly(vinyl alcohol) (PVA) and other water-soluble polymers are used as a protective colloids. In these cases PVA supplies covalently linked carbon chains to the interface of the immiscible phases, avoiding coalescence of the monomer-polymer particles formed. However, one of the main disadvantages of using hydrophilic polymers (*e.g.*, PVA) as stabilizing agents in suspension polymerization reactions is the fact that it can take a long period of time to completely dissolve them in water at room temperature. Added to this is the limited understanding of how the average size of the polymer beads is affected by the use of conventional active surface modifiers. To investigate whether the use of conventional ionic surfactants in suspension polymerization reactions has the same effects as those obtained with the investigated WSILs, experiments were performed under the similar reaction conditions to those reported in Table 4-4. The main difference in these experiments is the use of sodium dodecyl sulfate (SDS) (a well-known ionic surfactant) as the stabilizing agent instead of the WSILs. Four different concentrations of SDS (0.1, 0.33, 1, and 5 wt %), one below and three above the critical micelle concentration value (0.23 wt %),[20] were used for these cases. The average sizes of the polymer beads obtained from these experiments were around 0.8 mm for all the cases. Therefore, the use of SDS does not allow the average size of the polymer beads to be "tuned" as the WSILs of Figure 4-14 do (at least for the reaction systems investigated).

Furthermore, in the cases where polymer beads with sizes in the millimeter scale were synthesized, the polymer can be easily isolated from the reaction medium by simple decanting and/or filtration and therefore the IL aqueous solutions can be reused to carry out new polymerizations reactions. This approach was investigated by reusing the IL aqueous solution of Exp. **6** of Table 4-4 to perform more polymerization cycles under the same reaction conditions. In this case, after three polymerization cycles the average size of the polymer beads (2 mm) was comparable to that of the first reaction cycle (1.9 mm). These results suggest that the IL aqueous solutions can be recovered and reused several times to synthesize new materials of comparable properties.

It has been reported that polymers containing imidazole groups are able to bind different transition metals on their surface, finding applications in the removal of transition metal ions from waste streams.[18,22] For this application, an important property of these polymeric materials is their surface area, since this factor determines to a large extent the amount of chemical species that can be loaded. Other polymer architectures with a large surface area and an intrinsic porosity have also found applications for replacing inorganic materials such as zeolites and/or activated carbon used as heterogeneous catalytic supports[23] and, more recently, in hydrogen storage.[24] Even though the incorporation of a pore former (toluene in this work) is essential to promote the synthesis of polymer beads with a large surface area,[18] it has been found in this investigation that the incorporation of a WSIL (IL **10**, Figure 4-14) into the aqueous continuous medium of the suspension also has an important influence on the creation of surface area in the particles, as shown in Table 4-6. The results given Table 4-6 show the surface area values (as determined by nitrogen gas adsorption) for different polymers beads synthesized in the experimental setup displayed in Figure 4-16a and under reactions conditions similar to those used in the experiments reported in Table 4-4. The pores have been classified according to the shape of the adsorption isotherms[25] obtained for each sample and according to the IUPAC classification. Figure 4-19 shows nitrogen adsorption/desorption isotherms for some of the experiments reported in Table 4-6. According to the shape of the isotherms, the materials can be classified with regard to the pore shape.[25]

Table 4-6: *Surface area properties, as determined by the nitrogen gas adsorption technique, of cross-linked polymer beads (Figure 4-15). The cross-linked beads were synthesized by suspension polymerization using a water-soluble ionic liquid as stabilizing agent (IL **10**, Figure 4-14) under similar reaction conditions to those used in the experiments reported in Table 4-4 (using the laboratory-scale glass reactor shown in Figure 4-16a).*

Exp.	Content of IL 10 in the aq. phase (wt %)	Average particle size (mm)	Langmuir surface area ($m^2\ g^{-1}$)	Porosity	Pore shape	BET average pore diameter (nm)
1	100	0.5	57.6	Nonporous	-	-
2	70	1.6	191.9	Mesopores	Ink bottle	3.8
3	50	1.9	208.8	Mesopores	Ink bottle	3.7
4	30	2.4	268.8	Mesopores	Slit	4.4
5	10	2.7	303.8	Mesopores	Slit	4.6
6	0 (90 °C)	2.7	158.8	Mesopores	Cylindrical	7.7
7	0 (90 °C, no toluene)	1.3	1.7	Nonporous	-	-

The results in Table 4-6 reveal that beads with “large” average particle size (> 1.5 mm) can be classified as good porous materials. More important, the results in Table 4-6 also reveal a strong influence of the content of IL **10** on the formation of surface area. First, when both IL **10** and pore former (toluene) are included in the synthetic formulation of the beads (Exps. **1**-**5**, Table 4-6) and the amount of toluene remains constant, the creation of surface area is strongly related to the content of IL in the aqueous continuous medium of the suspension and therefore to the size of the polymer beads obtained, as explained before. These results reveal that a low content of WSIL in the reaction medium yields particles with large sizes and surface areas whilst a high content of WSIL promotes the synthesis of beads with small sizes and surface areas. Second, the inclusion of a pore former has been found to be

essential to create surface area in the polymer beads, as revealed by additional experiments where toluene was not used, and even in presence of WSILs, nonporous materials were obtained. In general, the absence of WSILs or stabilizing agents in the reaction system leads to unstable systems or coalescence of the beads in suspension polymerization reactions. However, to investigate the pure effect of toluene as a pore former and in the absence of any stabilizers, Exps. **6** and **7** (Table 4-6) were performed. These suspension polymerization reactions were carried out at 90 °C owing to the fact that at lower reaction temperatures the suspension may be unstable and show coalescence. From these results, it is again confirmed that the absence of toluene yields nonporous materials with a small surface area (Exp. **7**, Table 4-6). In the case of Exp. **6**, polymer beads with a relatively large surface area were formed as expected with the inclusion of toluene. However, when comparing results of Exps. **5** and **6** (Table 4-6), it is clear that the combination of pore former and a relatively small amount of WSILs (10 wt %) in the reaction mixture promotes a more efficient formation of surface area (around twice as large) for polymer beads with similar average particle sizes (2.7 mm).

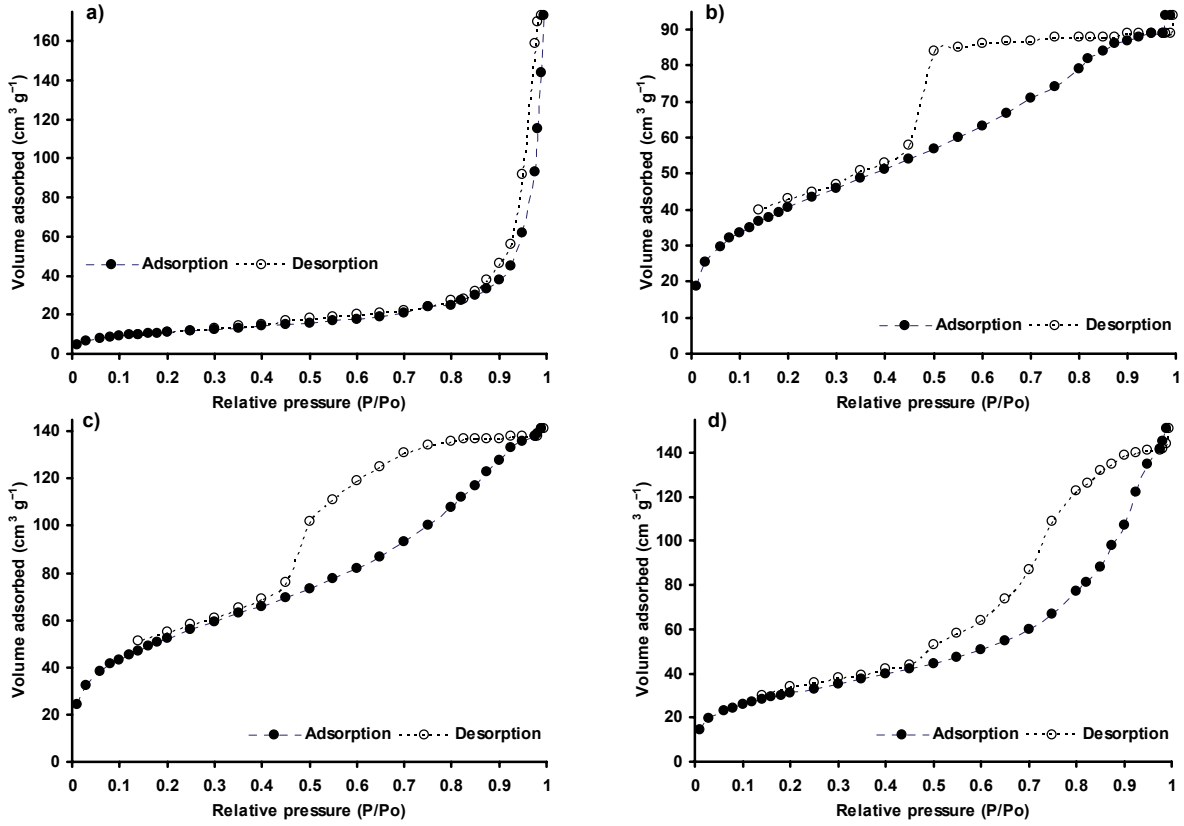

Figure 4-19: *Shape of the nitrogen adsorption/desorption isotherms at 77 K of some the experiments reported in Table 4-6. The materials can be classified according to the shape of the adsorption isotherms. (a) Experiment **1** (Table 4-6), nonporous polymer beads. (b) Experiment **3** (Table 4-6), mesoporous polymer beads with ink-bottle-like pores. (c) Experiment **4** (Table 4-6), mesoporous polymer beads with slit-shape pores. (d) Experiment **6** (Table 4-6), mesoporous polymer beads with cylindrical pores.*

The morphology of some of synthesized polymer beads was also investigated by scanning electron microscopy (SEM) to gain an insight into the formation of pores. Images of the obtained morphologies are shown in Figure 4-20, which shows the presence of pores in the polymer beads. Moreover, from the results of Table 4-6 and the shape of the adsorption/desorption isotherms of Figure 4-19 it can also be observed that the shape of the pores formed in the polymer beads can be modified by varying the concentration of the WSIL during the synthesis. From these findings one can conclude that, at least for the investigated reaction systems, the combination of a pore former and the use of a WSIL as stabilizing

agent in suspension polymerization reactions may allow the surface area of polymer beads to be “tuned” during their synthesis.

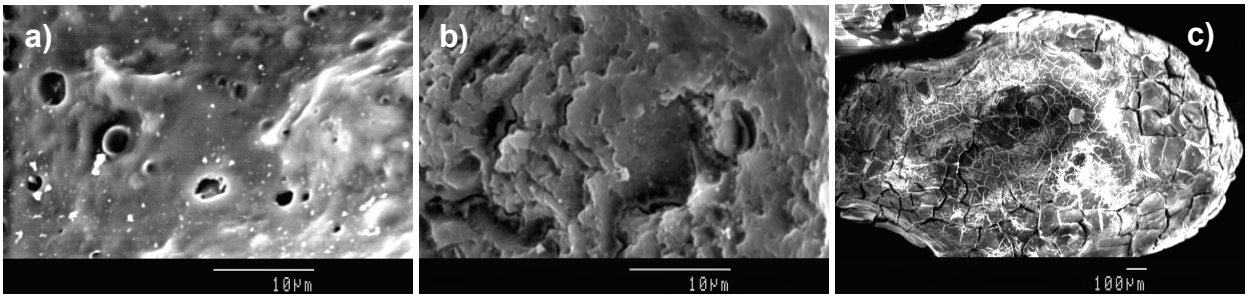

Figure 4-20: *Morphology of some of the synthesized cross-linked polymer beads (Figure 4-15). The cross-linked beads were synthesized by suspension polymerization using a water-soluble ionic liquid as stabilizing agent (IL* ***10****, Figure 4-14) under similar reaction conditions to those used in the experiments reported in Table 4-4 (using the laboratory-scale glass reactor shown in Figure 4-16a). (a) and (b) images obtained from Exp.* ***5*** *(Table 4-6). (c) Image obtained from Exp.* ***2*** *(Table 4-6).*

4.3.3 Heterogeneous polymerization reactions of non-cross-linked systems using water-soluble ionic liquids as reaction media

So far the discussion about heterogeneous polymerization reactions performed in WSILs and in their aqueous solutions has been focused on cross-linked systems. However, the synthetic heterogeneous method described above can also be extended to the preparation of non-cross-linked systems (linear homopolymers). This case is similar to the case described in section 4.2.2 for the homogenous preparation of hydrophobic polymers in hydrophilic ILs, but in the cases discussed next the synthesis of hydrophobic polymers in WSILs proceeds in a heterogeneous way since the monomers are not soluble in the ILs utilized. The linear homopolymers obtained by this method can be isolated by a similar process as described above (by washing with water followed by a filtration step). Moreover, the IL can also be recovered from the resulting aqueous solutions using a similar approach as reported in section 4.2.2.

This last polymerization procedure to be addressed is important due to the fact that many commodity homopolymers and copolymers are prepared industrially in continuous solution polymerization processes using large amounts of VOCs. As mentioned above, bulk polymerization methods are advantageous to prepare commodity polymers, but comprise problems as the components involved in the reactions are hard to mix uniformly and the control of the temperature becomes more difficult during the course of the reactions, concomitant with increases in viscosity. For this reason, solution polymerization processes are often preferred over bulk processes to obtain less viscous reaction media and, consequently, to gain a better control of the processes. Many important commodity polymers, such as poly(methyl methacrylate), poly(acrylonitrile), styrene-acrylonitrile copolymers and polyolefins are prepared by solution polymerization reactions.[3,26] Hence, VOCs such as ethylbenzene or toluene are industrially utilized in large amounts in solution polymerization processes to overcome the aforementioned problems. However, by using VOCs other problems arise such as the decrease of the productivity (due to the slower polymerization rates and larger reaction volumes) and the emission of VOCs into the environment.

Despite of the fact that in some cases the use of ILs as reaction media to perform polymerizations yields faster polymerization rates (as reported in section 4.2.1 and in the literature[6c,n]), the main interest to use these substances is due to their potential as “green solvents” compared to the well-established and previously unrivaled VOCs. To develop more efficient and environmentally-friendly processes for the preparation of commodity polymers, the use of WSILs as reaction media is a promising approach as

described above. Hence, the main objective of this last discussion in this chapter is to address briefly kinetic aspects of the heterogeneous synthesis of some commodity homopolymers performed in WSILs.

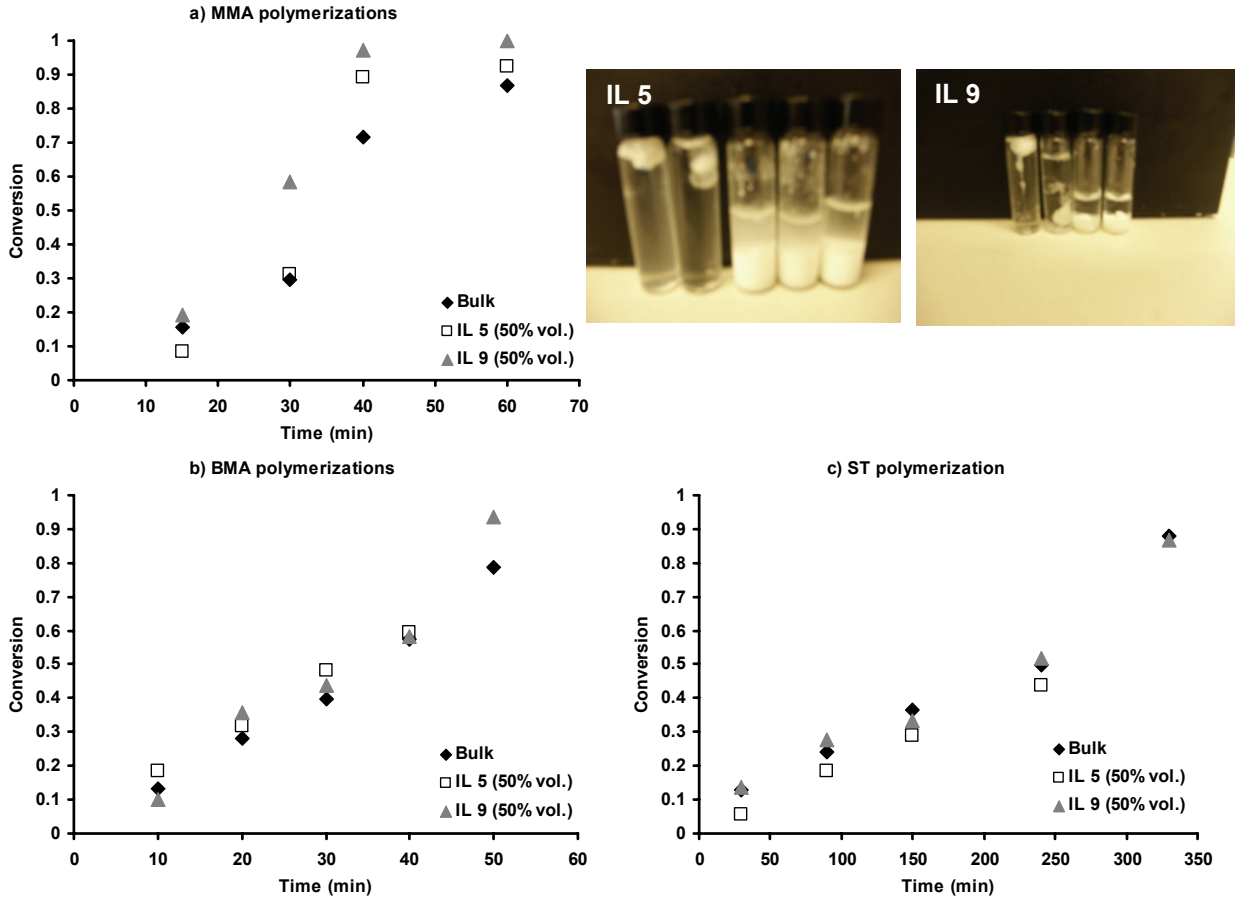

Figure 4-21: *Plots of monomer conversion against time for free radical polymerization reactions performed in bulk and in two water soluble ionic liquids (1-butyl-3-methyimidazolium tetrafluoroborate (IL **5**) and 1-ethyl-3-methyimidazolium tosylate (IL **9**); Table 4-1, Figure 4-1)) at 70 °C, and initiated by 2,2'-azobisisobutyronitrile (AIBN). (a) Polymerization reactions of methyl methacrylate (MMA) (images of the reaction vials within the kinetic measurements were performed and after the precipitation of the polymers with water, are also shown). (b) Polymerization reactions of butyl methacrylate (BMA). (c) Polymerization reactions of styrene (ST).*

Kinetic studies are important to determine the feasibility of performing polymerization reactions in the specific ILs and they may also provide useful information to scale-up the polymerization reaction to continuous processes. Thus, the free radical bulk and heterogeneous polymerizations of methyl methacrylate (MMA), butyl methacrylate (BMA) and styrene (ST) were performed in two WSILs (1-butyl-3-methyimidazolium tetrafluoroborate (IL **5**) and 1-ethyl-3-methyimidazolium tosylate (IL **9**); Table 4-1, Figure 4-1)) using a conventional heating system based on a heat transfer fluid (oil bath) (see the experimental part for a full description of the reaction systems). The kinetic measurements obtained for these polymerization reactions are shown in Figure 4-21. In Figures 4-21a and 4-21b, it can be observed that the polymerization rates for MMA and BMA in the WSILs are faster than in the case of bulk polymerization, being this effect more remarkable in the case of MMA. Reaction rates larger than those observed in conventional VOCs have been previously reported in the literature for the polymerization reaction of MMA performed in the hydrophobic IL 1-butyl-3-methylimidazolium hexafluorophosphate (**6**; Table 4-1, Figure 4-1).[6c,n] However, a faster reaction rate for a polymerization performed in ILs in comparison to the bulk case has not been reported previously as observed in Figure 4-21a for the free radical polymerization of MMA. Figure 4-21a also reveals that the “gel effect” characteristic of the bulk

polymerization of MMA[27] is stronger in the cases where ILs **5** and **9** are used as reaction media. Regarding the free radical polymerization of ST (Figure 4-21c), the acceleration of the reaction rate observed in the case of MMA due to the use of WSILs is not observed clearly. The observation that the use of ILs as reaction media for heterogeneous free radical polymerization reactions has almost no effect (or even positive effect) on the polymerization rates (compared to bulk reactions) is an important finding because conventional homogeneous (solution) polymerization reactions performed in VOCs, normally show lower polymerization rates when compared to bulk cases. According to the previous observation, the use of ILs as reaction media for heterogeneous free radical polymerization reactions does not decrease the polymerization rates as VOCs do in conventional solution polymerization reactions, which turn ILs even more attractive candidates for the replacement of VOCs in this kind of processes. Even though the use of ILs requires an increase of the volume of the reactors (compared to bulk polymerization reactions), the facts that the polymerization rate is not depleted and that an improved control over the reaction is enabled, perfectly counter-balance the change in the volume of the reactors (or the decrease in amounts produced).

The use of WSILs allows a satisfying precipitation of PMMA with water in the investigated cases as shown in the images of Figure 4-21a. After precipitation, the polymer can be separated from the aqueous media by filtration, and the ILs can be recovered by distillation and reused in further reactions similar to the case displayed in Figure 4-13. In the polymerization reactions of BMA and ST, the precipitation process of the polymers with only water was less effective (but still efficient), especially for the low conversion reaction vials. For this reason, a mixture of methanol/water (20/80% vol.) was used to improve the precipitation process and to obtain more reliable kinetic measurements. Note that, even though the monomers and polymers investigated are not soluble in the WSILs used, stable suspension reactions, with similar characteristics to those displayed in Figure 4-16b (suspended waxy solids, and/or chalky solids similar to those reported in the literature[7]), were observed by stirring slightly the mixtures. Therefore, the polymerization reactions investigated take place in suspension, which facilitates the isolation of the polymers with water and avoids the use of VOCs.

The findings in this research related to the polymerization of MMA are of especial interest in terms of scaling-up the process to a pilot plant and/or industrial scales. Because the continuous bulk polymerization of MMA is difficult to perform in an industrial scale, solution processes are often utilized.[3a,b,26] Normally, a solution polymerization process, in ethylbenzene and/or other VOCs, is used in the industrial production of PMMA to ensure manageable levels of viscosity in continuous processes. At the end of the polymerization reactions, the VOCs utilized must be removed from the product by using a devolatilization step. This latter procedure is usually carried out by heating the reaction mixture (up to 200 °C for a sufficient devolatilization),[3a] followed by a strong pressure drop (flash). Furthermore, this devolatilization step limits significantly the overall yield of the process due to the relatively poor thermal stability of PMMA, which provokes the partial degradation of the polymer backbone into monomeric units.[3a] For these reasons the use of WSILs as reaction media for this specific continuous polymerization processes may become an alternative approach for polymer industry (using a similar continuous process as conceptualized in Figure 4-13). Among the advantages of the synthetic method proposed are: (1) Minimum or even no emissions of VOCs into the environment, (2) polymerization rates similar (or even faster) to those observed in bulk polymerization reactions (at least under the explored reaction conditions), (3) energy savings (the reactions can be performed at lower temperatures), and (4) a convenient recycling method of the reaction media (WSILs) for further polymerizations.

Other industrial polymerization processes that may be considered to investigate the approach presented in this work are: (1) The production of poly(vinyl chloride) (usually produced by suspension polymerization; the polymer is soluble in 1-butyl-3-methylimidazolium chloride (IL **10**; Table 4-1, Figure 4-1) and can be precipitated with water),[6s] (2) the production of poly(acrylonitrile) (very exothermic polymerization reaction when it is performed in bulk conditions; the polymer is also soluble in IL **10**

(Table 4-1, Figure 4-1) and can be precipitated with water),[6s] and (3) the production of styrene-acrylonitrile copolymers. Even though the feasibility of performing the "green" synthesis of linear polymers in WSILs has been demonstrated, the advantages of the methods proposed in this work when compared to other green polymerization approaches (emulsion and suspension polymerization processes) still have to be determined. As addressed in section 4.3.2, the main advantage of using WSILs in cross-linked systems is the control of the properties (average size and surface area) of the polymer beads synthesized, which can not be easily achieved in conventional suspension systems. However, the size of the beads is not a critical issue for the non-cross-linked systems (linear polymers) analyzed in this section, since commodity polymers produced by these methods will still have to be reprocessed before the final applications of the materials. Therefore, the advantages of using heterogeneous processes based on ILs over the conventional emulsion and suspension methods based on water for the cases analyzed in this section must be still evaluated by mean of a detailed analysis and comparison of the parameter space of both approaches.

4.4 Conclusions

In this chapter the feasibility to carry out polymerizations by different reaction mechanisms (cationic ring opening and free radical) and methods (homogeneous and heterogeneous), utilizing ILs as reaction media has been analyzed. In addition, a combination of microwave irradiation, as an efficient and alternative heating source, with the highly ionic reaction medium supplied by ILs has been also investigated. The results revealed that polymerization reactions performed under microwave irradiation and in the presence of ILs show higher heating rates than their corresponding bulk and solution (in conventional VOCs) polymerization cases. In some of the investigated reactions the use of ILs as reaction media have also revealed that polymerizations performed under these conditions can show increased polymerization rates in comparison to the reactions performed in conventional VOCs (case of the cationic ring opening polymerization (CROP) of 2-ethyl-2-oxazoline (EtOx) and, in some cases, even in bulk conditions (case of the free radical polymerization of methyl methacrylate). Moreover, the CROP of EtOx in one of the ILs investigated keeps its living character opening the possibility of constructing well-defined block copolymers with an environmentally-friendly approach.

This chapter also addressed the use of water-soluble ionic liquids (WSILs) as stabilizing agents for the synthesis of polymers by suspension polymerization reactions. Due to the surface active properties shown by the described WSILs, the method investigated allowed tuning of the average particle size (from the macro- to the nanoscale) and of the surface area of the polymer beads synthesized by adjusting the concentration and the aliphatic side-chain length of the WSILs in the aqueous phase of the suspension polymerization reactions.

Thus, it has been demonstrated that the homogeneous and heterogeneous synthesis of hydrophilic and hydrophobic polymers can be performed efficiently using a "green" approach. The selection of a suitable IL for a specific polymerization reaction is the key factor for the development of efficient and clean polymerization processes, which may allow for the depletion of emissions of VOCs into the environment and for energy savings. In addition, the combination of ILs as reaction media with microwave irradiation may allow more efficient heating of polymerization reactions and, therefore, for energy savings. The right selection of an IL in combination with water facilitates the isolation of the polymers and the recycling of the IL utilized for further polymerization reactions. In this regard three possible scenarios were identified: (1) The homogeneous synthesis of hydrophilic polymers (*e.g.*, CROP of EtOx) can be carried out efficiently in hydrophobic ILs (where both monomer and polymer are soluble). This approach facilitates the isolation of the hydrophilic polymer by a simple extraction with water and the IL can also be recovered easily and reused in further polymerization cycles. (2) The homogeneous synthesis of

hydrophobic polymers can be carried out in hydrophilic ILs (where both monomer and polymer are soluble). In this case, the isolation of the hydrophobic polymer can be performed by precipitating the polymer with water and followed by a filtration step. In addition, the IL can be recovered from the resulting aqueous solutions by a distillation process, which can be carried out efficiently utilizing a microwave-assisted distillation. (3) The heterogeneous synthesis of hydrophobic polymers can also be carried out in a hydrophilic IL (where both monomer and polymer are insoluble) by suspension polymerization reactions. Similar to the previous case, the isolation of the hydrophobic polymer in this case can be improved by a precipitation step with water and followed by a filtration procedure. Like in the previous case, the IL can be recovered from the resulting aqueous solutions by a distillation process (*e.g.*, under microwave irradiation).

In addition to the efficient polymer isolation and the IL recycling in the investigated polymerization systems by utilizing water as a co-solvent, it has been demonstrated that the IL recovered can be reused to perform additional polymerization reactions, which have yielded polymers with comparable properties to those obtained in previous cycles. This completes the “green” approach of the polymerization methods proposed in this chapter and opens opportunities for the development of more efficient and cleaner processes in polymer synthesis.

Even though the feasibility of performing polymerizations using ILs as reaction media has been demonstrated, a detailed knowledge of all the reaction parameters involved in the polymerizations discussed here is necessary before developments may be implemented in the polymer industry. It is clear that future research in this direction might be focused on optimization procedures of the synthetic approaches proposed in this chapter in order to determine its potential for a real implementation in industrial scales. These optimization procedures must take into account the influence and inter-relationship of numerous variables on specific polymerization systems (such as the concentration of IL necessary in the polymerization mixture to keep manageable viscosity levels under certain reaction conditions, the cost and toxicity of the ILs utilized, the yield of the polymerization reactions, the energy spent during the recycling operation of the IL, etc.).

As described in this chapter, there are many polymers that are soluble in different ILs whereas other polymers not. By combining different polymeric chains into block copolymers, it is expected that they self-assemble into micellar aggregates in the presence of an IL that is a thermodynamically good solvent for one of the blocks and a bad solvent for the other block. These new and interesting micellar systems are the topic for the discussion presented in the next chapter.

4.5 Experimental part

4.5.1 Experimental part for homogeneous polymerization reactions in ionic liquids and under microwave irradiation

Reagents and solvents. 2-Ethyl-2-oxazoline (EtOx), 2-phenyl-2-oxazoline (PhOx), and methyl methacrylate (MMA) monomers were distilled under vacuum and stored under argon (EtOx and PhOx at room temperature, and MMA at –25 °C) prior to use. 2-(*m*-Difluorophenyl)-2-oxazoline (F_2Ox) was synthesized and purified as reported elsewhere.[28] 2,2'-Azo*bis*isobutyronitrile (AIBN) was re-crystallized from methanol and stored under argon at –25 °C prior to use. Methyl tosylate (MeTos) was distilled under vacuum and stored under argon at room temperature prior to use. Acetonitrile was died over molecular sieves (3 Å). Ionic liquids (ILs) (see Table 4-1 and Figure 4-1): 1-Butyl-3-methylimidazolium hexafluorophosphate (**2**), 1-butyl-3-methylimidazolium trifluoromethanesulfonate (**4**), 1-butyl-3-methylimidazolium tetrafluoroborate (**5**), trihexyltetradecylphosphonium chloride (**8**), and 1-ethyl-3-methylimidazolium tosylate (**9**) were synthesis grade and obtained from Merck KGaA (**4** and **8**) and Solvent Innovation GmbH (**2**, **5** and **9**) as kind gifts. ILs were dried in a vacuum oven at 40 °C for at least 3 days prior to use.

Microwave-assisted polymerizations and ionic liquid recycling procedures. Microwave-assisted polymerizations (in bulk or in ILs as reaction media) were performed in a single-mode microwave system Emrys Liberator (Biotage) (see, for example, ref.[9b] for a detailed description of the microwave platform) using a power of 150 watts, conical glass reaction vials (1.5 mL) and magnetic stirring. All polymerizations experiments were carried out under an argon atmosphere and the total amount of the reaction mixture in the different reaction vials was kept constant in order to allow a direct comparison of the obtained results and heating profiles between the polymerization systems.

For the cationic ring opening polymerizations (CROP) of EtOx, reaction vials were filled under an argon atmosphere with 350 mg of distilled monomer (EtOx), 11 mg of distilled initiator (MeTos), and 540 mg of the respective reaction medium (IL or an acetonitrile/IL mixture (50/50 wt %)), exposed to the desired reaction conditions under microwave irradiation (temperatures and times), and quenched by cooling the reaction vials with nitrogen gas followed by adding 50 µL of de-mineralized water into the reaction mixture. Due to the relatively small reaction volumes used for the kinetic studies of this investigation, the recycling procedure of IL **2** is demonstrated qualitatively as depicted in Figure 4-9. Thus, the recycling procedure was performed as follows. For the CROP experiments performed in pure IL **2** in different polymerization vials (different reaction temperatures and times), all remaining reaction mixtures (after molecular weight and conversion determinations) were combined and mixed with a 3-fold excess of purified water in order to extract the polymer and un-reacted monomer (which are better soluble in water than in IL **2**) into the aqueous phase. This mixture (15 reaction vials) was magnetically stirred for 0.5 h at room temperature. The resulting heterogeneous mixture was placed into an extraction funnel until a clear phase separation occurred (Figure 4-9). Subsequently, IL **2** was recovered from the funnel, dried under vacuum at 40 °C, and analyzed by ^{1}H–NMR (which confirmed the absence of polymer and monomer). Thereafter, the recovered IL **2** was utilized in a second series of polymerization experiments yielding similar results to the ones obtained in the first cycle. In addition to the IL recovery, the polymer can be isolated by evaporation of the water as depicted in Figure 4-9.

CROP of PhOX and F_2Ox were performed in a similar way as in the case of EtOx. For these cases, CROP of PhOx and F_2Ox were initiated by 2 and 3 wt % of MeTos (referred to the amount of monomer), respectively. The polymerizations were carried out at 140 °C for 10 min in the case of PhOx and for 30 min in the case of F_2Ox. In these polymerizations the IL recycling and the polymer isolation were performed in a similar way as described below for the free radical polymerizations of MMA.

The microwave-assisted free radical polymerizations (FRP) of MMA were initiated by AIBN (1 wt % referred to amount of monomer). The polymerization vials were filled under an argon atmosphere with the corresponding amount of reagents. The polymerizations were performed at 100 °C for 20 min and quenched by cooling the reaction vials with nitrogen gas. Additional experiments of microwave-assisted FRP of MMA (Exps. **16**-**18**, Table 4-3) using a larger reaction volume (15 mL at a concentration of 25 wt %of MMA in IL **5**) were performed in a single-mode microwave system Discover (CEM) (see, for example, ref.[9b] for a detailed description of the microwave platform) in order to illustrate better the IL recycling concept. For these experiments the IL recycling and polymer isolation were performed as follows. A five-fold excess of water was added into the reaction mixtures at the end of the polymerizations in order to precipitate the polymer and to obtain the corresponding IL aqueous solutions. Subsequently, the polymers were isolated by filtration and the aqueous solutions recovered. Thereafter, microwave-assisted distillations of water from the resulting IL aqueous solutions were performed in the Discover microwave platform utilizing a temperature of 140 °C for 20 min at atmospheric pressure in order to recover the IL for further polymerization cycles. For this purpose, the microwave apparatus was utilized with an open system configuration and the obtained distillated (water) was recovered and condensed through a flexible tubing.

Characterization techniques. Gel permeation chromatography (GPC) measurements of the obtained polymers were performed on a Shimadzu system with a RID-6A refractive index detector and a Plgel 5 µm Mixed-D column. A solution of 4% triethylamine and 2% isopropanol in chloroform was used as an eluent at a flow rate of 1 mL min^{-1} and a column temperature of 50 °C for the materials derived from the polymerizations of EtOx, PhOx and MMA samples. In a similar GPC platform, a solution of 49.5 mmol L^{-1} of lithium choloride in *N,N*-dimethylacetamide was used as an eluent at a flow rate of 1 mL min^{-1} and a column temperature of 60 °C for the analysis of the materials derived form the polymerizations of F_2OX. Molecular weights were calculated against poly(methyl metacrylate) or polystyrene (in the cases of PhOx and F_2Ox) standards. The conversion of the polymerizations were estimated by proton nuclear magnetic resonance spectroscopy (^{1}H-NMR) on a Varian Gemini 400 spectrometer at 25 °C by dissolving small amounts of the reaction mixtures after the polymerizations in a proper deuterated solvent (chloroform

($CDCl_3$) for EtOx and MMA, acetonitrile for F_2Ox and dichloromethane for PhOx). The purity of the utilized ILs was also investigated by ^{1}H-NMR using deuterated dimethyl sulfoxide (d_6-DMSO) at 25 °C.

4.5.2 Experimental part for heterogeneous polymerization reactions in ionic liquids and in their aqueous solutions.

Reagents and solvents. 1-Methylimidazole and *N*-vinylimidazole (Aldrich) were distilled under reduced pressure and stored at room temperature prior to use. Ethylene glycol dimethacrylate (Aldrich) was purified by passing through active alumina (Merck) and stored at 4 °C prior to use. Methyl methacrylate (MMA), butyl methacrylate (BMA), and styrene (ST) were dried under calcium hydride, distilled under vacuum and stored under argon at –18 °C prior to use. 2,2'-Azo*bis*isobutyronitrile (AIBN) was re-crystallized from methanol and stored under argon at –25 °C prior to use. Ionic liquids (ILs) (see Table 4-1 and Figure 4-1): 1-butyl-3-methylimidazolium tetrafluoroborate (**5**), and 1-ethyl-3-methylimidazolium tosylate (**9**) were synthesis grade and obtained from Solvent Innovation GmbH. These ILs were dried in a vacuum oven at 40 °C for at least 3 days prior use. 1-Butyl-3-methylimidazolium chloride (**10**), 1-decyl-3-methylimidazolium chloride (**11**), and 1-hexadecyl-3-methylimidazolium chloride (**12**) water-soluble ionic liquids (WSILs) (see Table 4-1 and Figure 4-1) were obtained by microwave-assisted synthesis as described below. All other materials were used as received.

Water-soluble ionic liquids by microwave-assisted synthesis. WSILs were synthesized by microwave heating in a similar way to those methods reported in literature,[11b] by reacting 1-methylimidazole with a molar excess (1.1 mol) of the corresponding chloroalkane (1-chlorobutane, 1-chlorodecane, or 1-chlorohexadecane; Aldrich). The reactions were performed in sealed reaction vials (10 mL) specially designed for the single-mode microwave system Emrys Liberator (Biotage). These vials were filled with the reagents, sealed and degassed with argon for 2 min. The reaction volume for every batch was 5 mL (per vial). The reagents were mixed during the microwave-assisted reaction by using a magnetic stirring system included in the microwave apparatus. Optimal reactions conditions for the synthesis of these WSILs in the aforementioned microwave platform were found to be 170 °C and a reaction time of 6-7 min under a high absorption reaction mode (150 Watts). At the end of the reaction time the vials were decapped and any un-reacted material (upper organic phase) were decanted. Note that under the reaction conditions described, the lower organic phases in the reaction vials (WSILs) were almost colorless liquids in the case of 1-butyl-3-methylimidazolium chloride (IL **10**) and 1-decyl-3-methylimidazolium chloride (IL **11**), and a white solid in the case of 1-hexadecyl-3-methylimidazolium chloride (IL **12**). The synthesized WSILs (**10**, **11**, and **12**; Table 4-1, Figure 4-1) were further purified to remove traces of un-reacted starting materials as follows: IL **12** was re-crystallized from acetone and dried under vacuum at 40 °C, IL **11** was washed several times with ethyl acetate before drying under vacuum at 40 °C, and IL **11** was just dried under vacuum at 40 °C since the yield of this reaction was close to 100%. ^{1}H-NMR spectra of the synthesized WSILs confirmed their chemical structure (Figure 4-1) and the purity of the materials. The long aliphatic chain WSIL, **12** (Table 4-1, Figure 4-1), was obtained as a white powder at room temperature. Even though its melting point was found to be 41 °C as revealed by differential scanning calorimetry (DSC) measurements, it can still be classified as an IL (melting points below 100 °C).[1g] The melting point of IL **11** (Table 4-1, Figure 4-1), found by DSC, was around 4 °C. Although IL **10** (Table 4-1, Figure 4-1) was obtained as a liquid substance at room temperature from the microwave-assisted synthesis, after some days it started to crystallize; its melting point was determined to be around 55 °C. The rest of the experiments in this work involving IL **10** (Table 4-1, Figure 4-1) were performed using the liquid substance before crystallization (as obtained from the synthesis and purification procedures).

Synthesis of cross-linked polymer beads by free radical suspension polymerization reactions in ionic liquids aqueous solutions. Typical suspension polymerization experiments were performed using a similar formulation reported in literature for the synthesis of poly(ethylene glycol dimethacrylate-*N*-vinyl imidazole) cross-linked beads.[18] The main difference between this latter synthetic approach and the one used here lies in the preparation of the aqueous phase. In order to study the stability of the suspensions using WSILs as stabilizing agents, the aqueous phases were prepared by dissolving predetermined amounts of the corresponding WSILs (instead of poly(vinyl alcohol))[18] in purified water (de-mineralized). The organic phase was formulated (on the basis of 50 g of aqueous phase) with ethylene glycol dimethacrylate (6 mL; 32 mmol), toluene (4 mL; 38 mmol) (pore

former), *N*-vinylimidazole (3 mL; 33 mmol), and AIBN (100 mg; 0.6 mmol). The aqueous phase was placed in the corresponding experimental setup (as described below) at the desired reaction temperature. Subsequently, the organic phase was dispersed into the aqueous medium by vigorous stirring. This moment was considered to be the beginning of the polymerization reaction, which was conducted for 0.5 h to obtain almost 100% yield of polymer beads based on the initial amount of monomers (as determined by gravimetry). The polymer beads obtained were separated from the aqueous phase by filtration, washed with water and ethanol to remove un-reacted monomer and pore former (toluene), dried, and stored at room temperature.

To determine the stability of the suspension polymerization reactions in the presence of WSILs, two different experimental setups were employed. A typical laboratory-scale glass reactor (Figure 4-16a) consisting of a round-bottomed flask (50 mL) placed in an oil-bath (80 °C) and stirred (400 rpm) by a cylindrical PTFE-coated magnetic stirring bar. The experimental scale for this laboratory setup was 25 mL based on the aqueous phase. This setup was utilized to evaluate the potential of WSILs as stabilizing agents in the suspension polymerization reactions described and therefore the rest of the reaction conditions remained unmodified (under the previously mentioned conditions). The reaction conditions utilized in the suspension polymerization experiments performed with the experimental setup shown in Figure 4-16a are summarized in Table 4-4.

A second experimental setup consisting of an automated parallel synthesizer[21] (A-100 auto-plant, Chemspeed Technologies) (Figure 4-16c) was used to perform a qualitative study involving the variation of more reaction conditions simultaneously. In this way, the influence of the reaction temperature and the content of one of the utilized WSILs (IL **10**; Table 4-1, Figure 4-1), co-monomers, and pore former on the stability of the suspension polymerization reactions could be qualitative investigated. The advantage of performing experiments in parallel (using the same type of reactors, the same stock solutions of reagents, etc.) is that the reaction conditions can be varied systematically and that the results are, therefore, easily comparable. The main characteristic of this experimental setup is the mechanical agitation that can be applied to the reaction systems, which is, next to the stabilizing agent, one of the most important variables influencing the stability of monomer-polymer drops in suspension polymerization reactions. An anchor-type impeller and an agitation speed of 400 rpm were found to be suitable for performing the required suspension polymerization experiments. The experimental scale for this setup was 50 mL based on the aqueous phase. The reaction conditions of the suspension polymerization experiments carried out in the synthesizer shown in Figure 4-16c are summarized in Table 4-5.

Kinetic investigations of free radical bulk and heterogeneous polymerization reactions in water-soluble ionic liquids as reaction media. Kinetic measurements of the free radical polymerization reactions of methyl methacrylate (MMA), butyl methacrylate (BMA) and styrene were performed in 8 mL vials with magnetic stirring. 0.5 mL of a 1 wt % solution of AIBN in the respective monomer and 0.5 mL of the corresponding WSIL were transferred to each reaction vial. Subsequently, the vials were sealed with rubber septa and degassed with argon for 5 min. The vials were placed in a constant temperature oil bath (70 °C). After the desired reaction times, the vials were cooled in an ice bath and 0.1 mL of a 1 wt % solution of hydroquinone in tetrahydrofuran was added into the vials. Thereafter, 5 mL of deionized water were added into the vials containing the suspensions formed to achieve the complete precipitation of the polymer synthesized. The polymers precipitated were filtered from aqueous solution and dried in a vacuum oven at 50 °C overnight. Conversions were determined by gravimetry. The WSILs utilized can be recovered from the respective aqueous solution by distillation.

Characterization techniques.

^{1}H-NMR spectra of the synthesized WSILs were recorded at 25 °C on a Varian Gemini 300 spectrometer using deuterated dimethyl sulfoxide (d_6–DMSO) (Cambridge Isotopes Laboratories).

The melting points of the synthesized WSILs were determined by differential scanning calorimetry (DSC) on a Netzsch DSC 204 F1 instrument calibrated with indium. Multiple heating and cooling scans (20, 40 and 10 °C min^{-1} scan rates) were generated over a temperature range of –100 to 250 °C using nitrogen as the purge gas. The melting point temperatures were noted at the maximum points of the heat capacity peaks during the heating scans.

Surface and interfacial tension parameters were measured using a Krüss K10T tensiometer with a Wilhemy plate and by the Du Nouy ring method, respectively. From the surface tension measurements the critical micellar concentrations were determined.

Particle sizes and particle-size distributions were determined using digital image analysis techniques.[29] Images of large- and medium-sized particles (> 1 mm) (for the particle sizes see Tables 4-4 and 4-5) were obtained with a conventional digital camera. Images of small-sized particles (< 1 mm) (for the particle sizes see Table 4-5) were obtained with an optical microscope (Optem, zoom 125) equipped with a digital camera (Sony Exwave HAD). In both cases, the images obtained were analyzed using the image processing toolbox incorporated into the MATLAB software to obtain the average particle size and particle-size distribution (see the results given in Tables 4-4 and 4-5). Figure 4-22 shows an overview of this characterization technique for two selected experiments reported in Tables 4-4 and 4-5. Some of the experiments reported in Tables 4-4 (Exps. **5** and **7**) and 4-5 (Exps. **4**, **8**, **9**, **11**, **13**, and **14**) yielded particles with average sizes in the nanometer range. In these cases, the materials obtained had a similar appearance to those synthesized in other pure ILs (gel, waxy solid, and/or chalky solid compounds).[7] In all the experiments described, the composites were dispersed in water (~0.1 g L^{-1}) under vigorous stirring until stable emulsion-like dispersions were obtained. The resulting dispersions were analyzed by dynamic light scattering (DLS); the average particle sizes are reported in Tables 4-4 and 4-5. The DLS measurements were performed at 25 °C at 90° on a Malvern 4700 DLS Particle Size Analyzer apparatus equipped with a 488 nm laser. The values of the refractive index and viscosity of water used were 1.331 and 0.89 cPoise (1 cPoise ≈ 0.001 Kg m^{-1} s^{-1}), respectively. Imaging of one selected sample (Exp. **4**, Table 4-5) in dry conditions was performed by atomic force microscopy (AFM) (in a similar way as described in section 3.2.3 for block copolymer micelles) as shown in Figure 4-17. For this measurement, a sample from Exp. **4** (Table 4-5) used during the DLS measurements was additionally diluted with water (100-fold) and spin-cast (to obtain near monolayer coverage) onto a clean silicon wafer substrate. Imaging was performed in intermittent contact mode on a Multimode SPM (Digital Instruments, Santa Barbara, CA) using NSC36-type tips (~1 N m^{-1}, Mikromasch, Spain). The height of the beads was determined from histograms after zeroth-order leveling of the images (in a similar way as described in section 3.2.3 for block copolymer micelles).

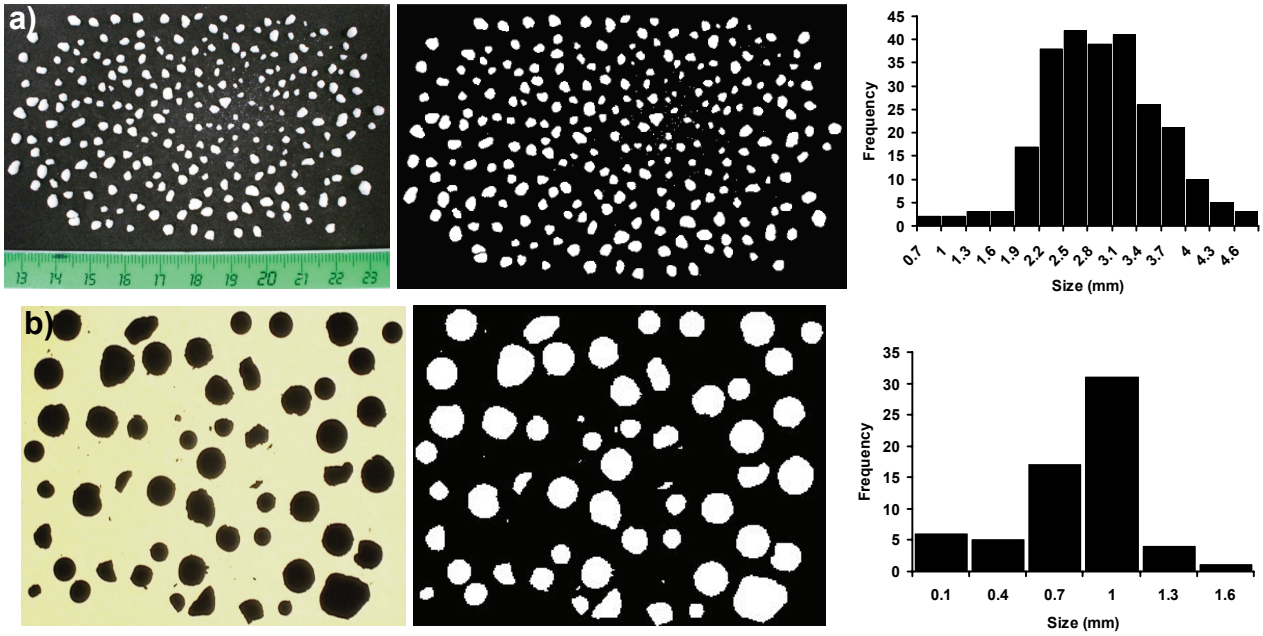

Figure 4-22: *Overview of the determination of the average particle size and particle-size distribution of some of the synthesized cross-linked polymer beads (Figure 4-15) by digital image analysis techniques. (a) Digital images of large-sized particles (Exp.* ***1****, Table 4-4) and their respective particle-size distribution, as obtained after the corresponding statistical analysis. (b) Digital images of small-sized particles (Exp.* ***15****, Table 4-5) and their respective particle-size distribution, as obtained after the corresponding statistical analysis.*

Surface area, pore size and pore-size distribution of the synthesized polymer beads were determined using nitrogen adsorption (TriStar 3000 apparatus of Micromeritics) at 77 K. Samples were dried under vacuum at 40 °C for three days just prior to the measurement.

The surface morphology and porosity of the polymer beads were examined using scanning electron microscopy (SEM) (JEOL JSM-840A). The samples were initially dried under vacuum at 40 °C for three days before being

analyzed. Dried polymer beads were mounted on a SEM sample holder, sputter coated with gold for 2 min, and scanned at the desired magnification.

4.6 References

[1] (a) A. Matlack, *Green Chem.* **2003**, *5*, G7. (b) T. Welton, *Chem. Rev.* **1999**, *99*, 2071. (c) J. D. Holbrey, K. R. Seddon, *Clean Prod. Proc.* **1999**, *1*, 223. (d) D. Zhao, M. Wu, Y. Kuo, E. Min, *Catal. Today* **2002**, *74*, 157; (e) R. D. Rogers, K. R. Seddon, *Ionic Liquids: Industrial Applications for Green Chemistry*, *ACS Symp. Ser., 818*, Oxford University Press: Oxford, **2002**. (f) P. Wasserchеid, T. Welton, *Ionic Liquids in Synthesis*, Wiley-VCH Verlag: Weinheim, **2003**. (g) M. Deetlefs, K. R. Seddon, *Chim. Oggi* **2006**, *24(2)*, 16. (h) S. Kumar, W. Ruth, B. Sprenger, U. Kragl, *Chim. Oggi* **2006**, *24(2)*, 24. (i) M. J. Earle, J. M. S. S. Esperanca, M. A. Gilea, J. N. Canongia-Lopes, L. P. N. Rebelo, J. W. Magee, K. R. Seddon, J. A. Widegren, *Nature* **2006**, *439*, 831. (j) M. Smiglak, W. M. Reichert, J. D. Holbrey, J. S. Wilkes, L. Sun, J. S. Thrasher, K. Kirichenko, S. Singh, A. R. Katritzky, R. D. Rogers, *Chem. Commun.* **2006**, 2554.

[2] C. Guerrero-Sanchez, E. Saldivar, M. Hernandez, A. Jimenez, *Polym. React. Eng.* **2003**, *11*, 457.

[3] (a) P. Nising, T. Zeilmann, T. Meyer, *Chem. Eng. Techol.* **2003**, *26*, 599. (b) H. S. Lee and Y. C. Jang, *US Patent 6488898,* **2002**. (c) J. Stepek, H. Daoust, *Additives for Plastics*, Springer Verlag: New York, **1983**. (d) T. Kashiwagi, T. Hirata, J. E. Brown, *Macromolecules* **1986**, *19*, 2160.

[4] (a) M. Szwarc, *Nature* **1956**, *78*, 1168. (b) D. A. Tomalia, D. P. Sheetz, *J. Polym. Sci.* **1966**, *4*, 2253. (c) R. R. Schrock, *"Ring Opening Polymerization"*, Hansa Verlag: München, **1993**. (d) M. Morton, L. J. Fetters, *Rubber Chem. Technol.* **1975**, *48*, 359. (e) N. Hadjichristidis, H. Iatrou, S. Pispas, M. Pitsikalis, *J. Polym. Sci. Part A: Polym. Chem.* **2000**, *38*, 3211. (f) S. Ndoni, C. M. Papadakis, F. S. Bates, K. Almdal, *Rev. Sci. Instrum.* **1995**, *66*, 1090.

[5] (a) J. L. Kendall, D. A. Canelas, J. L. Young, J. M. DeSimone, *Chem. Rev.* **1999**, *99*, 543. (b) A. I. Cooper, *J. Mater. Chem.* **2000**, *10*, 207.

[6] (a) P. Kubisa, *Prog. Polym. Sci.* **2004**, *29*, 3. (b) J. Ryan, F. Aldabbagh, P. B. Zetterlund, B. Yamada, *Macromol. Rapid Commun.* **2004**, *25*, 930. (c) S. Harrison, S. R. Mackenzie, D. M. Haddleton, *Macromolecules* **2003**, *36*, 5072. (d) H. Zhang, K. Hong, J. W. Mays, *Macromolecules* **2002**, *35*, 5738. (e) T. Biedron, P. Kubisa, *J. Polym. Sci., Part A: Polym. Chem.* **2002**, *40*, 2799. (f) Y. L. Zhao, J. M. Zhang, J. Jiang, C. F. Chen, F. Xi, *J. Polym. Sci., Part A: Polym. Chem.* **2002**, *40*, 3360. (g) H. Zhang, K. Hong, M. Jablonsky, J. W. Mays, *Chem. Commun.* **2003**, 1356. (h) A. J. Carmichael, D. M. Haddleton, S. A. F. Bon, K. R. Seddon, *Chem. Commun.* **2002**, 1237. (i) S. Perrier, T. P. Davis, A. J. Carmichael, D. M. Haddleton, *Eur. Polym. J.* **2003**, *39*, 417. (j) R. Vijayaraghavan, D. R. MacFarlane, *Chem. Commun.* **2004**, 700. (k) T. Biedron, P. Kubisa, *J. Polym. Sci., Part A: Polym. Chem.* **2004**, *42*, 3230; (l) T. Biedron, M. Bednarek, P. Kubisa, *Macromol. Rapid Commun.* **2004**, *25*, 878. (m) R. Vijayaraghavan, D. R. MacFarlane, *Chem. Commun.* **2005**, 1149. (n) S. Perrier, T. P. Davis, A. J. Carmichael, D. M. Haddleton, *Chem. Commun.* **2002**, 2226. (o) H. Ma, X. Wan, X. Chen, Q. F. Zhou, *Polymer* **2003**, *44*, 5311. (p) S. Csihony, C. Fischmeister, C. Bruneau, I. T. Horvah. P. H. Dixneuf, *New J. Chem.* **2002**, *26*, 1667. (q) M. Basko, T. Biedron, P. Kubisa, *Macromol. Symp.* **2006**, *240*, 107. (r) M. A. B. H. Susan, T. Kaneko, A. Noda, M. Watanabe, *J. Am. Chem. Soc.* **2005**, *127*, 4976. (s) C. S. Brazel, R. D. Rogers (Eds.), *Ionic liquids in polymer systems: solvents, additives, and novel applications. ACS Symp. Ser., 913*, American Chemical Society: Washington D. C., **2005**.

[7] (a) F. Yan, J. Texter, *Chem. Commun.* **2006**, 2696. (b) P. Snedden, A. I. Cooper, K. Scott, N. Winterton, *Macromolecules* **2003**, *36*, 4549. (c) P. Snedden, A. I. Cooper, Y. Z. Khimyak, K. Scott, N. Winterton, *ACS Symp. Ser.* **2005**, *913*, 133.

[8] (a) C. O. Kappe, *Angew. Chem. Int. Ed.* **2004**, *43*, 6250. (b) M. Nüchter, B. Ondruschka, D. Weiß, R. Beckert, W. Bonrath, A. Gum, *Chem. Eng. Technol.* **2005**, *28*, 871.

[9] (a) D. Bogdal, P. Penczek, J. Pielichowski, A. Prociak, *Adv. Polym. Sci.* **2003**, *163*, 193. (b) R. Hoogenboom, R. M. Paulus, A. Pilotti, U. S. Schubert, *Macromol. Rapid Commun.* **2006**, *27*, 1556. (c) C. Koopmans, M. Iannelli, P. Kerep, M. Klink, S. Schmitz, S. Sinnwell, H. Ritter, *Tetrahedron* **2006**, *62*, 4709.

[10] (a) C. Struppe, M. Nüchter, B. Ondruschka, *Chem. Technik* **1999**, *51*, 127. (b) O. Muñoz, D. Velez, M. L. Cervera, R. Montoro, *J. Anal. Atom. Spectrom.* **1999**, *14*, 1607. (c) P. Bermejo-Barrera, M. Aboal-Somoza, A. Bermejo-Barrera, M. L. Cervera, M. De la Guardia, *J. Anal. Atom. Spectrom.* **2001**, *16*, 382.

[11] (a) K. S. A. Vallin, P. Emilsson, M. Larhed, A. Hallberg, *J. Org. Chem.* **2002**, *67*, 6243. (b) M. Deetlefs, K. R. Seddon, *Green Chem.* **2003**, *5*, 181. (c) J. Habermann, S. Ponzi, S. V. Ley, *Mini-Rev. Org. Chem.* **2005**, *2*, 125. (d) R. S. Varma, V. V. Namboodiri, *Tetrahedron Lett.* **2002**, *43*, 5381.

[12] (a) F. Wiesbrock, R. Hoogenboom, M. A. M. Leenen, M. A. R. Meier, U. S. Schubert, *Macromolecules* **2005**, *38*, 5025. (b) F. Wiesbrock, R. Hoogenboom, C. H. Abeln, U. S. Schubert, *Macromol. Rapid Commun.* ***2004***, *25*, 1895.

[13] J. Hofmans, L. Maeseele, G. Wang, K. Janssens, M. van Beylen, *Polymer* **2003**, *44*, 4109.

[14] (a) J. Scheirs, D. Priddy, *Modern styrenic polymers*, Wiley: West Sussex, **2003**. (b) T. Bilgic, M. Karali, O. T. Savasci, *Angew. Makromol. Chem.* **1993**, *213*, 33.
[15] (a) P. Giusti, L Lazzeri, G. Pizzirani, G. Polacco, C. Rizzo, *J. Mater. Sci. Mater. M.* **1994**, *5*, 858. (b) Y. Hatate, Y. Uemura, K. Ijichi, Y. Kato, T. Hano, Y. Baba, Y. Kawano, *J. Chem. Eng. Jpn.* **1995**, *28*, 656. (c) H. Kawaguchi, *Prog. Polym. Sci.* **2000**, *25*, 1171. (d) D. Hoffmann, K. Landfester, M. Antonietti, *Magnetohydrodynamics* **2001**, *37*, 217. (e) J. H. Yeum, Q. Sun, Y. Deng, *Macromol. Mater. Eng.* **2005**, *290*, 78.
[16] F. Jahanzad, S. Sajjadi, B. W. Brooks, *Ind. Eng. Chem. Res.* **2005**, *44*, 4112.
[17] H. M. Woods, C. Nouvel, P. Licence, D. J. Irvine, S. M. Howdle, *Macromolecules* **2005**, *38*, 3271.
[18] A. Kara, L. Uzun, N. Besirli, A. Denizli, *J. Hazard. Mater.* **2004**, *106B*, 93.
[19] (a) J. Bowers, C. P. Butts, P. J. Martin, M. C. Vergara-Gutierrez, *Langmuir* **2004**, *20*, 2191. (b) G. Law, P. R. Watson, *Langmuir* **2001**, *17*, 6138. (c) J. Sung, Y. Jeon, D. Kim, T. Iwahashi, T. Iimori, K. Seki, Y. Ouchi, *Chem. Phys. Lett.* **2005**, *406*, 495. (d) M. Gonzalez-Melchor, F. Bresme, J. Alejandre, *J. Chem. Phys.* **2005**, *122*, 104710/1. (e) A. Bagno, C. Butts, C. Chiappe, F. D'Amico, J. C. D. Lord, D. Pieraccini, F. Rastrelli, *Org. Biomol. Chem.* **2005**, *3*, 1624. (f) S. L. Zang, Q. G. Zhang, M. Huang, B. Wang, J. Z. Yang, *Fluid Phase Equilibr.* **2005**, *230*, 192. (g) Y. Zhou, M. Antonietti, *Chem. Mater.* **2004**, *16*, 544.
[20] F. H. Quina, P. M. Nassar, J. B. S. Bonilha, B. L. Bales, *J. Chem. Phys.* **1995**, *99*, 17028.
[21] C. Guerrero-Sanchez, R. M. Paulus, M. W. M. Fijten, M. J. de la Mar, R. Hoogenboom, U. S. Schubert, *Appl. Surf. Sci.* **2006**, *252*, 2555.
[22] N. Pekel, O. Güven, *Polym. Bull.* **2004**, *51*, 307.
[23] (a) A. Corma, *Chem. Rev.* **1997**, *97*, 2373. (b) I. F. J. Vankelecom, *Chem. Rev.* **2002**, *102*, 3779.
[24] (a) P. M. Budd, B. S. Ghanem, S. Makhseed, N. B. McKeown, K. J. Msayib, C. E. Tattershall, *Chem. Commun.* **2004**, 230. (b) N. B. McKeown, B. Ghanem, K. J. Msayib, P. M. Budd, C. E. Tattershall, K. Mahmood, S. Tan, D. Book, H. W. Langmi, A. Walton, *Angew. Chem. Int. Ed.* **2006**, *45*, 1804.
[25] S. J. Gregg, K. S. W. Sing, *Adsorption, surface area and porosity*, 2nd ed., Academic press: London, **1982**.
[26] (a) Y. Higuchi, S. Kuwahara, S. Hieda, M. Kurokawa, *US Patent 5719242,* **1998**. (b) M. Uchida, M. Iwamoto, A. Nakajima, M. Takaku, H. Morita, K. Kawano, *US Patent 6060564,* **2000**. (c) X. Gao, Q. Wang, R. E. von Haken Spence, S. J. Brown, P. Zoricak, *US Patent 6221985,* **2001**. (d) N. Takami, K. Uchimura, K. Yoshioka, K. Nakazawa, *US Patent 6403761,* **2002**. (e) L. M. Tau, R. O. Swindoll, C. Kao, P. Jain, *US Patent 6420516,* **2002**.
[27] P. Nising, T. Meyer, *Ind. Eng. Chem. Res.* **2004**, *43*, 7220.
[28] M. Lobert, R. Hoogenboom, U. S. Schubert, in preparation.
[29] T. Allen, *Particle size measurement. Vol. 1: Powder sampling and particle size measurement,* 5th ed., Chapman & Hall: Padstow, **1997**.

CHAPTER 5

Block copolymer micelles in ionic liquids

Abstract

A detailed overview about the state of the art (preparation, characterization and applications) of block copolymer micellar systems in ionic liquids (ILs) is presented. The self-assembly of several (poly(styrene-block-methyl methacrylate), poly(2-nonyl-2-oxazoline-block-2-ethyl-2-oxazoline), poly(styrene-block-ethylene glycol) supramolecular diblock copolymer, and poly(2-nonyl-2-oxazoline-block-2-ethyl-2-oxazoline-block-2-methyl-2-oxazoline)) block copolymers into micellar aggregates was investigated in the presence of hydrophobic and hydrophilic ionic liquids. Furthermore, alternative methods for the characterization of these systems are proposed and compared with previously used approaches. Experimental results revealed that the nature of the ionic liquids could exert an influence on the structure of the formed micellar aggregates for the same block copolymer. In addition, the thermo-reversible micellar phase transfer process between an ionic liquid phase and an aqueous phase was investigated and results showed that the transfer process is a completely reversible phenomenon which can be controlled. Moreover, encapsulation of guest molecules into the micellar cores as well as their phase transfer process between the two abovementioned phases were successfully achieved and it was found that the thermo-reversible phase transfer of encapsulated dye molecules is also feasible. Other observations demonstrated the one-way transfer and release of guest molecules, the recovery and reload of previously used micelles with new guest molecules, and the use of block copolymer micelles as confined nano-environments. These findings may be applied, for example, for the development of advanced heterogeneous micellar catalytic systems with novel features such as the recovery of expensive or toxic catalysts from the final products, more efficient separation processes, the delivery of highly accurate amounts of chemical substances in multiphase systems, or the recovery of micellar aggregates for further use.

Parts of this chapter have been and will be published: (1) C. Guerrero-Sanchez, J. F. Gohy, D. Wouters, S. Hoeppener, H. Thijs, C. Ott, R. Hoogenboom, U. S. Schubert, *Polym. Mat. Sci. Eng.* **2007**, *96*, 936. (2) C. Guerrero-Sanchez, J. F. Gohy, C. D'Haese, D. Wouters, S. Hoeppener, H. Thijs, C. Ott, R. Hoogenboom, U. S. Schubert, in preparation.

5.1 Introduction to block copolymer micelles in ionic liquids

As mentioned in chapter 4, ionic liquids (ILs)[1a] are substances composed entirely of ions, which are in a liquid state below 100 °C. Unlike conventional solvents, the properties of ILs (such as viscosity, solubility, electric conductivity, melting point, etc.) can be easily tuned by varying the composition of their ions. Nowadays, around 300 ILs are commercially available (and a considerable number of new ILs could be synthesized) covering a wide range of properties. Due to their negligible vapor pressure (see ref.[1b] for a detailed description of this property of ILs) and flammability (see ref.[1c] for a detailed description of this property of ILs), ILs are considered to be "environmentally friendly" compounds. Moreover, ILs are characterized by their outstanding chemical and physical stabilities in a broad range of temperature. Due to these unique properties, ILs have been intensively investigated in recent years to perform different chemical reactions and are already utilized in different industrial processes (for a recent overview about ILs see ref.[1a]). Even though the toxicity of ILs remains relatively unknown the first studies in this regard have been recently reported,[2] which will certainly contribute to a better understanding for their reasonable use in specific applications.

In materials research ILs have been combined with polymers to obtain diverse composites with novel properties (for a recent overview about this topic see ref.[3]). For instance, ILs have been utilized as plasticizers for polymers[4] and for the preparation of polymer electrolytes,[5] polymers with reduced flammability,[6] and polymer-cellulose composites.[7] In addition, as discussed in detail in chapter 4 of this work, ILs have also been used as reaction media for polymer synthesis[8] in both heterogeneous[9] and homogeneous[10] processes. The existence of heterogeneous and homogeneous polymerization processes in ILs implies that ILs behave as thermodynamically bad and good solvents, respectively, for specific polymers. This fact allows also the preparation of self-assembled block copolymers micelles in ILs.[11] Thus, when a block copolymer is dissolved in an IL that is a thermodynamically good solvent for one of the blocks and a bad solvent for the other block the copolymer chains associate to form micelles.[11a] Block copolymer micelles[12] have received increasing attention because of their possible applications as carriers of small molecules in diverse environments[13] and as chemical nano-reactors.[14] Thus, block copolymer micelles have been proposed for, *e.g.*, drug delivery applications[15] and phase transfer vehicles.[16] The micellization behavior of poly(1,2-butadiene-*block*-ethylene glycol) and poly(styrene-*block*-methyl methacrylate) block copolymers with different chain lengths and block compositions has been recently investigated in the IL 1-butyl-3-methylimidazolium hexafluorophosphate (IL **2**) (see Table 4-1 and Figure 4-1 for some properties and the chemical structure of IL **2**, respectively).[11] IL **2** acts as a thermodynamically good solvent for the poly(ethylene oxide) and poly(methyl methacrylate) blocks, and as bad solvent for the poly(butadiene) and poly(styrene) blocks. Spherical and wormlike micelles, as well as vesicles have been detected for these systems.[11a,c] Moreover, the thermo-reversible transfer of the micelles between different phases (IL and an aqueous phases) has been achieved without perturbing the micellar structures.[11b] Unlike most of the studied micellar systems which only demonstrate one direction delivery capability, micellar systems in ILs may expand the applications of micellar reactions or micellar catalysis since encapsulated guest molecules may be reversibly transferred from one phase to another.

Hence, in this chapter various amphiphilic block copolymers have been utilized for the preparation of micellar systems in two different ILs. The investigated block copolymer systems were found to self-assemble into micellar aggregates in the presence of the hydrophobic IL 1-butyl-3-methylimidazolium hexafluorophosphate (IL **2**) as well as in the presence of the hydrophilic IL 1-butyl-3-methylimidazolium trifluromethanesulfonate (IL **4**) (see Table 4-1 and Figure 4-1). The micellar systems investigated have been characterized in detail by several techniques, including transmission electron microscopy (TEM) and dynamic light scattering (DLS). In addition, the thermo-reversible transfer mechanism of the micellar aggregates from an IL phase (in the case of IL **2**) to an aqueous phase has been investigated. Moreover,

it is demonstrated that the encapsulation of small organic molecules (dyes) in this type of micellar systems, as well as their thermo-reversible and non-reversible transfer between the two abovementioned phases are possible.

5.2 Block copolymer micellar systems in ionic liquids

Table 5-1: *Molecular characteristics and measured properties of block copolymer (poly(styrene-block-methyl methacrylate) (PS-b-PMMA), poly(2-nonyl-2-oxazoline-block-2-ethyl-2-oxazoline) (PNonOx-b-PEtOx), poly(styrene-block-ethylene glycol) metallo-supramolecular diblock copolymer (PS-[Ru]-PEG), and a poly(2-nonyl-2-oxazoline-block-2-ethyl-2-oxazoline-block-2-methyl-2-oxazoline) triblock copolymer (PNonOx-b-PEtOx-b-PMeOx)) micellar systems in ionic liquids (hydrophobic ionic liquid 1-butyl-3-methyimidazolium hexfluorophosphate (**2**) and hydrophilic ionic liquid 1-butyl-3-methyimidazolium trifluoromethanesulfonate (**4**)) investigated in this work. Mn stands for the average number molecular weight of the block copolymers as measured by gel permeation chromatography. Rh and PDI stand for the hydrodynamic radius and polydispersity indices of the micellar systems, respectively, as measured by dynamic light scattering (* values not determined).*

Sample	Block copolymer	Mn (kDa)	Ionic liquid	Rh (nm)	PDI
M1	PS_{73}–*b*–$PMMA_{66}$	14.2	**2**	85	0.65
M2	PS_{73}–*b*–$PMMA_{66}$	14.2	**4**	92	0.71
M3	PS_{110}–*b*–$PMMA_{3060}$	317.8	**2**	142	0.38
M4	PS_{90}–*b*–$PMMA_{2980}$	307.7	**2**	137	0.39
M5	PS_{60}–*b*–$PMMA_{640}$	70.3	**2**	40	0.24
M6	$PNonOx_{20}$–*b*–$PEtOx_{80}$	11.9	**2**	96	0.42
M7	$PNonOx_{40}$–*b*–$PEtOx_{60}$	13.8	**2**	92	0.48
M8	$PNonOx_{50}$–*b*–$PEtOx_{50}$	14.8	**2**	90	0.32
M9	$PNonOx_{60}$–*b*–$PEtOx_{40}$	15.8	**2**	152	0.39
M10	$PNonOx_{80}$–*b*–$PEtOx_{20}$	17.8	**2**	518	2.18
M11	$PNonOx_{20}$–*b*–$PEtOx_{80}$	11.9	**4**	54	0.48
M12	$PNonOx_{40}$–*b*–$PEtOx_{60}$	13.8	**4**	50	0.47
M13	$PNonOx_{50}$–*b*–$PEtOx_{50}$	14.8	**4**	43	0.39
M14	$PNonOx_{60}$–*b*–$PEtOx_{40}$	15.8	**4**	72	0.44
M15	$PNonOx_{80}$–*b*–$PEtOx_{20}$	17.8	**4**	484	0.31
M16	PS_{72}–[Ru]–PEG_{70}	10.6	**2**	*	*
M17	$PNonOx_{33}$–*b*–$PEtOx_{33}$–*b*–$PMeOx_{33}$	12.6	**2**	118	0.29
M18	$PNonOx_{33}$–*b*–$PEtOx_{33}$–*b*–$PMeOx_{33}$	12.6	**4**	84	0.54

Due to the fact that ILs can act as thermodynamically bad or good solvents for several polymers,[3,8-11] various amphiphilic block copolymers with different chemical compositions and block lengths are investigated in this chapter for the preparation of self-assembled micelles in either a “hydrophobic” IL **2** or a “hydrophilic” IL **4**. The amphiphilic block copolymers utilized include: Poly(styrene-*block*-methyl methacrylate)s (PS-*b*-PMMA), poly(2-nonyl-2-oxazoline-*block*-2-ethyl-2-oxazoline)s (PNonOx-*b*-PEtOx), a poly(styrene-*block*-ethylene glycol) metallo-supramolecular diblock copolymer (PS-[Ru]-PEG), and a poly(2-nonyl-2-oxazoline-*block*-2-ethyl-2-oxazoline-*block*-2-methyl-2-oxazoline) triblock copolymer (PNonOx-*b*-PEtOx-*b*-PMeOx). The PS-*b*-PMMA diblock copolymers have been synthesized by sequential anionic polymerization as described in section 2.4.2,[17a] whereas the PS-[Ru]-PEG diblock copolymer has been prepared using terpyridine-functionalized polymer precursors as addressed in section 3.3.3.[17b] The PNonOx-*b*-PEtOx and the PNonOx-*b*-PEtOx-*b*-PMeOx block copolymers have been synthesized by sequential “living” cationic ring opening polymerizations in a similar way as addressed in section 4.2.1, but using acetonitrile as reaction medium (a conventional volatile organic solvent); a detailed description of these synthetic methods can be found elsewhere.[18] The molecular characteristic features of the copolymers investigated are summarized in Table 5-1 (sub-indices in the tags of the materials indicate the average number of monomer units incorporated into the block copolymers which were estimated by gel permeation chromatographic (GPC) measurements in combination with proton nuclear magnetic resonance (^{1}H-NMR) spectroscopy; thus the average molecular weights and composition of the block

copolymers can be obtained). Both investigated ILs act as thermodynamically good solvents for PMMA,[10,11c] PEG,[11a,b] PEtOx (as observed in section 4.2.1) and PMeOx blocks, whereas they are bad solvents for the PS[11c] and PNonOx blocks as reported elsewhere or observed in this work. The micelles obtained after dissolving the investigated copolymers in both ILs have been characterized by (cryogenic) transmission electron microscopy ((cryo-)TEM) and dynamic light scattering (DLS). In addition, the thermo-reversible transfer of these micelles from the IL phase to an aqueous phase has been studied by turbidity and ultra-violet visible (UV-Vis) spectroscopic measurements. Finally, the encapsulation of guest molecules in these micelles as well as their thermo-reversible transfer from an IL phase to an aqueous phase have also been investigated by UV-Vis measurements. The results of all the investigations performed on these micellar systems are discussed in the following sections.

5.2.1 Characterization of block copolymer micelles in ionic liquids by (cryogenic) transmission electron microscopy

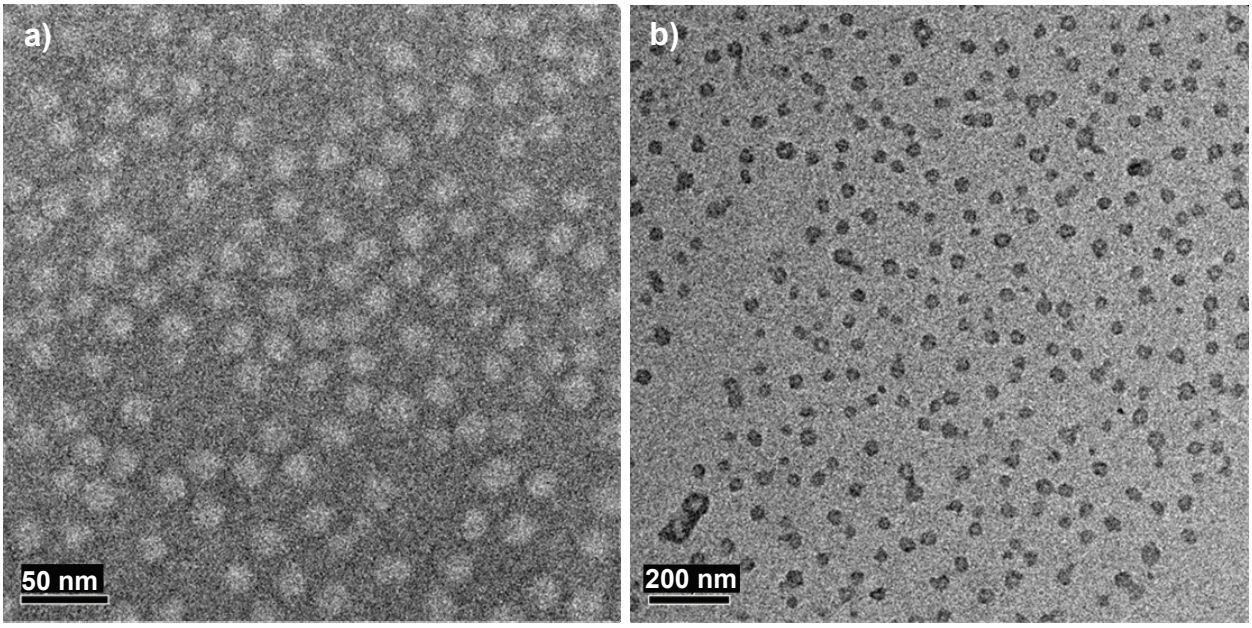

Figure 5-1: *Transmission electron micrographs of self-assembled block copolymer micelles in ionic liquids (PS-b-PMMA block copolymer micelles in the hydrophobic ionic liquid 1-butyl-3-methyimidazolium hexafluorophosphate (IL **2**)). (a) Sample **M1** of Table 5-1 recorded under cryogenic conditions. (b) Sample **M1** of Table 5-1 after the removal of IL **2** with acetornitrile (co-solvent) recorded at room temperature conditions.*

In a very recent publication,[11c] it has been reported that PS-*b*-PMMA diblock copolymers self-assemble into micellar structures in the presence of IL **2** and that a morphological transition from spherical to cylindrical micelles occurs upon reduction of the PMMA content. In that report the co-existence of 10 nm spherical and cylindrical (wormlike) micelles was observed for a block copolymer containing a fraction volume of PS of 0.47 using cryogenic transmission electron microscopy (cryo-TEM). Unlike those results, spherical micelles with a diameter of 20 nm have been observed by cryo-TEM in the present study for sample **M1** (Figure 5-1a), although the molecular characteristic features of **M1** (see Table 5-1) are very similar to those of the sample investigated in the previous report.[11c] This apparent discrepancy could be accounted for a different preparation method for the block copolymer micelles investigated in this study. In this work, the block copolymer chains have been first molecularly dissolved in a non-selective solvent, and subsequently a selective solvent for one of the blocks (*e.g.*, IL **2** or **4**) has been gradually added in order to trigger micellization (see experimental part). In previous reports[11c] the

block copolymers were directly dissolved in a selective solvent for one of the blocks (*e.g.*, IL **2**) by stirring and heating the samples above the glass transition temperature (*Tg*) of the polymeric materials (without using non-selective solvents). The selection of the non-selective solvent as well as the speed at which the selective solvent is added can affect the morphology and size of the accordingly obtained micelles.[19] In this regard, in the case of block copolymer micelles in ILs, it has been reported that the morphology of the micelles is strongly dependent on the preparation method and that an excessive heating of the micellar dispersions can lead to the formation of much larger aggregates (up to 70 nm).[11c]

The fact that ILs show negligible vapor pressure and require extreme conditions to be evaporated[1a,b] complicates considerably the characterization of micellar dispersions in ILs. In conventional volatile organic solvents, the size of the core of block copolymer micelles can be determined by well-established microscopic techniques, such as transmission electron microscopy (TEM) or atomic force microscopy (AFM) at dry conditions (in the absence of the carrier solvent for the micelles, in a similar way as addressed in section 3.2.3).[12] However, for micellar systems in ILs such dry conditions would be very difficult to obtain, since the removal of the ILs might be almost impossible to achieve without affecting the morphology of the micelles. Hence, cryo-TEM techniques have been proposed to analyze these systems.[11] Nevertheless, the relatively high viscosity of ILs (*e.g.*, 200 and 110 mPa s for IL **2** and for IL **4**, respectively at 25 °C (see Table 4-1)) complicates the preparation of films with suitable thicknesses required for their analysis by cryo-TEM. For this reason, an alternative TEM method at room temperature and at dry conditions is proposed in this work to characterize such systems. In this approach, a micellar dispersion in IL is placed on a TEM grid and washed with a proper conventional volatile solvent in order to remove the IL. The characteristics of this conventional solvent must fulfill the following requirements: It must solubilize the utilized IL, and it must be a thermodynamically compatible solvent for the coronal polymer chains but an incompatible one for the core-forming polymer chains. With these characteristics, it is expected that the conventional solvent washes off the IL and, at the same time, keeps the structure of the micelles intact. Thereafter, the conventional solvent can be removed under vacuum and the dried micelles can be analyzed at normal conditions by the aforementioned microscopic techniques. In the case of PS-*b*-PMMA block copolymer micelles, both IL **2** and IL **4** can be washed off with acetonitrile since they are fully miscible with this solvent (as found in section 4.2.1). Moreover, acetonitrile is a thermodynamically good solvent for the PMMA block but a bad one for the PS block and therefore the structure of the micelles may remain unaltered. Figure 5-1b displays a TEM micrograph of dried micelles obtained from **M1** with this new preparation method. The comparison between the micrographs of micelles of sample **M1** shown in Figures 5-1a and 5-1b yields interesting conclusions. It is known that contrast in TEM images arises due to the differences in electron density between the different components in a sample. Hence, regions of a sample with high electron density will allow fewer electrons to pass through, and thus appear darker than regions with lower electron density. The electron density of IL **2** is considerable higher than that of the block copolymer chains forming the micelles therefore the cores appear lighter than the background composed of an IL matrix as has been also reported elsewhere[11c] and as observed in Figure 5-1a. For the sample displayed in Figure 5-1b, the IL matrix does not exist anymore to create a dark background since the IL has been washed off. Therefore the micelles are seen as dark spheres probably due to the differences in thickness between the micelles and the TEM grid (no contrasting agent was added). A more detailed analysis of the micellar structures of Figure 5-1b reveals that the micelles are larger in size (the micellar structures in Figure 5-1b have an average size around 35 nm) than those of Figure 5-1a (average size around 20 nm) and their shapes also became slightly less regular. These differences can be explained by factors related to the sample preparation method of the micelles. In a closer look to Figure 5-1b, it can be seen that in the center of several of the dark shapes lighter regions arise. These lighter regions are, obviously, smaller in size than the whole dark shapes but, more surprisingly, are approximately about the same size as the micelles of Figure 5-1a (around 20 nm). Based on these observations, it is proposed that lighter regions in the dark structures of

Figure 5-1b correspond to the cores of the micelles investigated surrounded by a thin layer of IL that may be trapped in the corona of the micelles, which could not be totally removed during the washing procedure with acetonitrile. As a consequence of this, a good contrast in TEM micrographs is obtained allowing for a better visualization of the micelles investigated. Moreover, according to these findings it is thought that the morphology of the micellar structures (sphere in this investigated case) is kept in both, cryo-TEM and TEM, experimental procedures. This observation may also allow, for instance, for an approximate estimation of the actual overall size of block copolymer micelles with coronas of a relatively short length, and hence of the corona thickness. Furthermore, if the assumption that the IL goes deep into the corona of the micelles is correct (as shown in Figure 5-1b), this means that the corona can not be observed in cryo-TEM experiments and that nanostructures displayed in Figure 5-1a most likely corresponds to the core of the micelles (compare, for example, the micellar sizes of sample **M1** obtained by DLS (85 nm) (Table 5-1) with the sizes obtained by cryo-TEM (20 nm) (Figure 5-1a)). It is worth noting that for the method of analysis proposed in this work, an excess of washing co-solvent, during the removal of the IL on the TEM grid, can lead to the complete removal of the micelles. However, the experimental approach proposed to wash the IL off the micellar systems with an appropriate solvent may be a reliable preparation technique, and an alternative to the previously proposed cryo-TEM conditions in the literature,[11a,c] where the sample preparation procedure is more complicated and may not always lead to a good visualization of the micellar structures.

For the cases of block copolymer micellar systems with hydrophilic coronas and hydrophobic cores (samples **M6**-**M18** in Table 5-1), the preparation of the micelles in a hydrophilic IL is a more suitable approach in combination with the TEM technique proposed at dry conditions. This facilitates the removal of the IL on the TEM grid by using water as a co-solvent. The use of water in these specific cases, apart from washing off the hydrophilic IL, may preserve the structure of the micelles since the co-solvent will neither precipitate the coronas nor dissolve the cores. This approach was tested by analyzing sample **M18** (Table 5-1) and the resulting TEM micrograph is displayed in Figure 5-2. Figure 5-2 reveals the presence of spherical micelles of about 90 nm in size and, like in the case of Figure 5-1b, the absence of a dark background is also here observed due to the removal of the IL medium. Unlike the micelles shown in Figure 5-1b, the micelles displayed in Figure 5-2 do not show a lighter region at the center showing the micellar cores and, in addition, their shapes are also more regular (well-defined spheres). The relatively large size of the spheres observed in Figure 5-2 also suggests that these structures may correspond to the overall size of the micelles (core and corona) and that, in this specific case, the IL may be trapped inside the whole corona of the micelles and not only next to the cores like in the case of Figure 5-1b (compare, for instance, the micellar sizes of sample **M18** obtained by DLS (84 nm) (Table 5-1) with the sizes obtained by TEM (90 nm) (Figure 5-2)). In fact, the formation of highly viscous gel-like composites (*e.g.*, solid-like compounds) have been observed when polymeric materials (*e.g.*, PEtOx or PEG) are dissolved in suitable ILs, as addressed in chapter 4 and described in the literature[11d] for concentration values of polymers in IL as low as 4 wt %. The formation of stable gel-like composites between the polymeric chains of the micellar corona and the surrounding IL it might turn difficult to remove the IL trapped inside the corona due to the highly viscous characteristics of the formed micellar corona-IL composites. It is thought that upon washing these specific micellar dispersions with a co-solvent which dissolve the IL (water in this particular case) it is sufficient to remove the matrix of IL, but not enough to break apart the highly viscous micellar corona-IL composite formed and therefore a considerable amount of IL remains trapped in the corona of the micelles. This potential scenario may be a suitable explanation for the good contrast observed in the TEM micrograph displayed in Figure 5-2 (high electron density due to the presence of IL **4** trapped in the entire corona of the micelles) and for supporting the hypothesis that the structures observed correspond to the overall size of the micelles. Nevertheless, the relatively large structures observed in Figure 5-2 may also suggest the presence of micellar aggregates, which could be formed by the use of the co-solvent (water) during the sample preparation method described above for

the TEM measurements. In this case the existence of relatively large micellar aggregates could also contribute to the creation of the good contrast observed in the TEM micrograph displayed in Figure 5-2 due to the differences in thickness between the TEM grid and the micelles. Future work in this direction might be focused on a detailed investigation of the TEM preparation method proposed in this study in order to elucidate whether micellar structures corresponding to entire single micelles (overall size) or micellar aggregates can be obtained by the proposed approach.

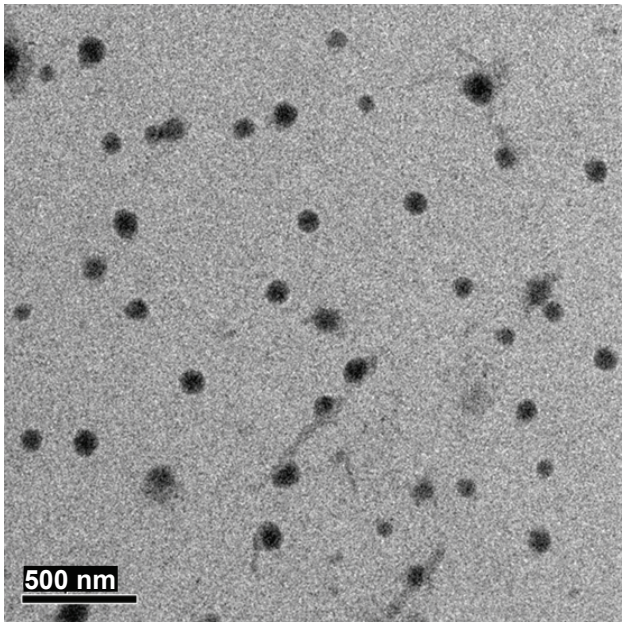

Figure 5-2: *Transmission electron micrograph of self-assembled block copolymer micelles in ionic liquids (PNonOx-b-PEtOx-b-PMeOx block copolymer micelles in the hydrophilic ionic liquid 1-butyl-3-methyimidazolium trifluoromethanesulfonate (IL **4**)). Sample **M18** of Table 5-1 after the removal of IL **4** with water (co-solvent) recorded at room temperature conditions.*

5.2.2 Characterization of block copolymer micelles in ionic liquids by dynamic light scattering

Whereas experimental techniques, such as TEM or AFM, can provide information about the characteristics of the cores of self-assembled block copolymer micelles in the dried state, the hydrodynamic radius (R_h) of the micelles in solution can be studied by dynamic light scattering (DLS)[11,12] (see section 3.2.3). Therefore, DLS measurements of the micellar systems in ILs investigated in this work were performed and the values of R_h obtained are summarized in Table 5-1. Unlike block copolymer micelles prepared in conventional solvents, which typically diffuse at the millisecond timescale, the diffusion timescale for these systems in ILs has been observed to be in the range of 0.1–1 s.[11] This increase in diffusion timescale is obviously related to the increase in viscosity of the media (ILs) where the micelles diffuse. According to the results of Table 5-1, micelles with relatively large R_h are observed for all the investigated samples. The polydispersity index (PDI) of these micelles was always large, in agreement with the formation of aggregated species. Nevertheless, the CONTIN analysis of these results never succeeded in resolving a population of large aggregates beside the micelles. Because CONTIN results should be carefully considered, these results do not totally exclude the formation of aggregates of micelles.[20] Dilutions of the initial micellar solutions with the respective ILs did not result in significant changes in R_h, which is in agreement with the formation of kinetically frozen micelles (the results given in Table 5-1 are thus those obtained for the starting micellar solutions at a concentration of 5 g L^{-1}). Therefore, dilutions were not successful to dissociate the hypothetical aggregates into isolated micelles.

The observation of kinetically frozen micelles in ILs is in agreement with previous results,[11c] and indicates that micellar systems out of the thermodynamic equilibrium are obtained in ILs. This also explains why the micellar characteristic features are strongly dependent on the used preparation protocol. Besides this limitation, interesting conclusions can still be drawn from the DLS results given in Table 5-1.

In a first step, the influence of the block copolymer composition on the micellar characteristic features in ILs was studied. Micelles formed by a PS core and a PMMA corona have been obtained in the case of PS-*b*-PMMA copolymers in IL **2** (samples **M3**-**M5** in Table 5-1). The correlation functions of these micelles are shown in Figure 5-3 and reveal long diffusion time scales. These characteristic timescales are larger than the values obtained in a previous study[11c] and indicate the formation of larger micelles. Indeed, the R_h of these micelles increases from 40 nm for sample **M5** up to 142 nm for sample **M3**. Although these R_h values are probably too large to fit to isolated micelles, there is, however, a correlation between the degree of polymerization (DP) of the PS blocks and the R_h of the micelles, in agreement with the scaling laws observed for block copolymer micelles.[12,21] In addition to this, a series of PNonOx-*b*-PEtOx diblock copolymers in IL **2** (samples **M6**-**M10**) has also been examined. These diblock copolymers are characterized by a constant total DP and a varying composition (Table 5-1). According to solubility tests realized on the constituent homopolymers in the investigated ILs, these micelles should consist of a PNonOx core surrounded by a PEtOx corona. The influence of the DP of the PNonOx block on the R_h is however less clear than for the previously discussed PS-*b*-PMMA diblock copolymer cases. In this respect, micelles with an almost constant R_h value around 93 nm were observed for samples **M6**, **M7** and **M8** while the R_h increases sharply for the high PNonOx content in samples **M9** and **M10**. Once again these R_h values are too large to fit to single micelles and the presence of aggregated species could be the reason why no clear trend between the DP of the core-forming block and the R_h of the micelles could be observed. As observed in Table 5-1, very large aggregates were detected for sample **M10** in agreement with the large PNonOx content in this diblock copolymer that impedes the formation of stable micelles.

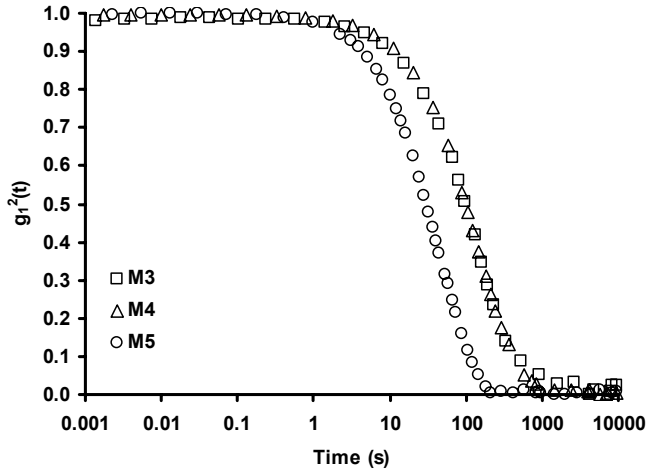

Figure 5-3: *Normalized correlation functions obtained by dynamic light scattering measurements of self-assembled block copolymer micelles in ionic liquids. Samples **M3**-**M5** of Table 5-1 (PS-b-PMMA block copolymer micelles in the hydrophobic ionic liquid 1-butyl-3-methyimidazolium hexfluorophosphate (IL **2**)).*

In a second step, the influence of the type of IL on the micellar characteristic features has been evaluated. No influence has been noted in case of the PS-*b*-PMMA system since nearly identical R_h and comparable PDI value were observed in both ILs (compare samples **M1** and **M2** in Table 5-1). This probably indicates that the interaction parameters between the constituent blocks of the copolymer and the ILs are very similar whatever the IL. This conclusion does not hold for the oxazoline-based copolymers where micelles with a smaller R_h are systematically observed in the more hydrophilic IL (IL **4**) (compare samples **M6**-**M10** to samples **M11**-**M15** and sample **M17** to sample **M18** in Table 5-1).

In addition to the reported R_h, the scattered light intensity of the micelles was systematically larger in IL **2** than in IL **4**, supporting that smaller micelles are formed in IL **4**. The correlation functions of the diblock copolymer micelles based on poly(oxazoline)s in ILs **2** and **4** are shown in Figures 5-4a and 5-4b, respectively. In general, it is observed that the correlation curves of diblock copolymer micelles based on poly(oxazoline)s become zero in a shorter time in the cases of IL **4** (Figure 5-4b) than in the cases of IL **2** (Figure 5-4a). The observed differences between the same materials prepared in IL **2** and in IL **4** suggest that the type of IL plays an important role in the assembly mechanism of block copolymer micelles. From these preliminary experiments, it could be anticipated that the more hydrophobic IL (IL **2**) has a better affinity for the PNonOx blocks than IL **4** (a water-soluble IL) and would therefore swell slightly more the PNonOx cores resulting in larger micelles.

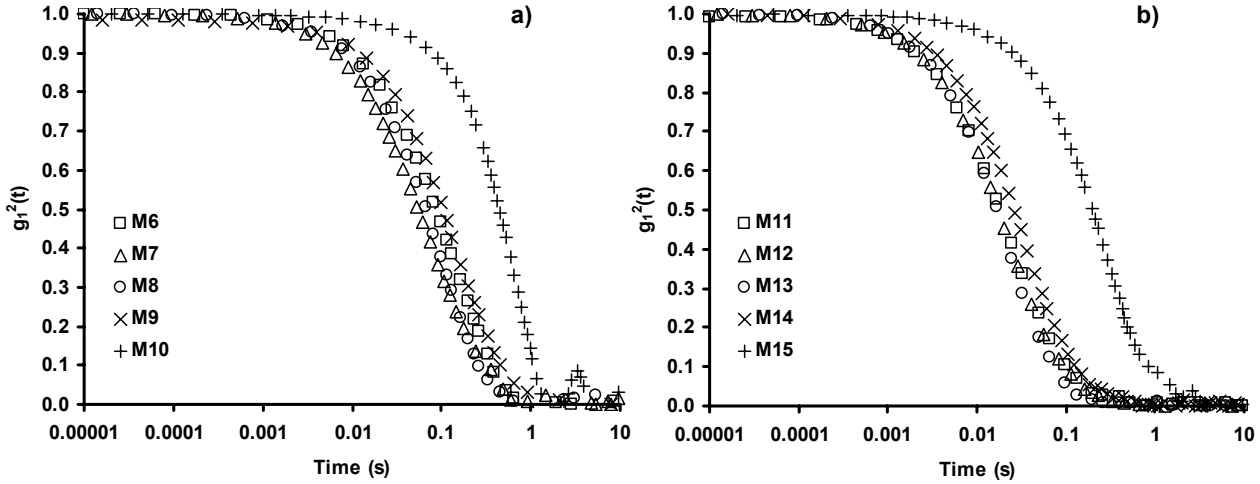

Figure 5-4: *Normalized correlation functions obtained by dynamic light scattering measurements of self-assembled block copolymer micelles in ionic liquids. (a) Samples **M6-M10** of Table 5-1 (PNonOx-b-PEtOx block copolymer micelles in the hydrophobic ionic liquid 1-butyl-3-methyimidazolium hexfluorophosphate (IL **2**)). (b) Samples **M11-M15** of Table 5-1 (PNonOx-b-PEtOx block copolymer micelles in the hydrophilic ionic liquid 1-butyl-3-methyimidazolium trifluoromethanesulfonate (IL **4**)).*

5.2.3 Thermo-reversible transfer of block copolymer micelles between a hydrophobic ionic liquid phase and an aqueous phase

The thermo-reversible transport of block copolymer micelles between an IL phase, formed by the hydrophobic ionic liquid 1-butyl-3-methylimidazolium hexafluorophosphate (IL **2**) (see Table 4-1 and Figure 4-1), and water has been recently addressed in the literature.[11b] Micelles formed by poly(1,2-butadiene-*block*-ethylene glycol) PB-*b*-PEG block copolymers were investigated in that work. On the one hand, the block copolymer micelles originally prepared in IL **2** migrate to an aqueous phase at room temperature conditions (water and IL **2** are relatively immiscible and form a two phase system) since the PEG chains show more preference for the aqueous phase than for the IL phase. On the other hand, when these two-phase systems are heated at temperatures higher than 70 °C, the micelles return to the IL phase as a consequence of the well-known lower critical solution temperature (LCST) phenomenon observed for PEG chains. This results in the rupture of the hydrogen bonds formed between the EG units and water molecules, followed by the coalescence of the micelles due to the fact that they are not stabilized by the corona (PEG block) any longer. At this stage, the micelles are precipitated in the aqueous phase and start to migrate into the IL phase. In addition, it was also demonstrated that the size of the micelles and their structure are preserved during this reversible transfer process.[11b] The authors of that contribution also make emphasis on the peculiarity of this transfer process which relies on a polymer

(PEG) that is nearly equally soluble in two immiscible solvents of a completely different nature. However, the results obtained in section 4.2.1 related to the homogeneous synthesis of EtOx homo-polymers in IL **2** and their isolation by an extraction process with water (see Figure 4-9) suggest that amphiphilic block copolymers containing a PEtOx block could show a similar behavior to that described above for amphiphilic block copolymers with PEG blocks.[11b] Based on this approach, experimental results in this work demonstrate that micelles formed of amphiphilic block copolymers containing an PEtOx block (*e.g.*, samples **M6**-**M10** and **M17** in Table 5-1) also show the aforementioned thermo-reversible transfer phenomenon between an IL phase (IL **2**) and an aqueous phase. Figure 5-5 displays an illustration of these systems.

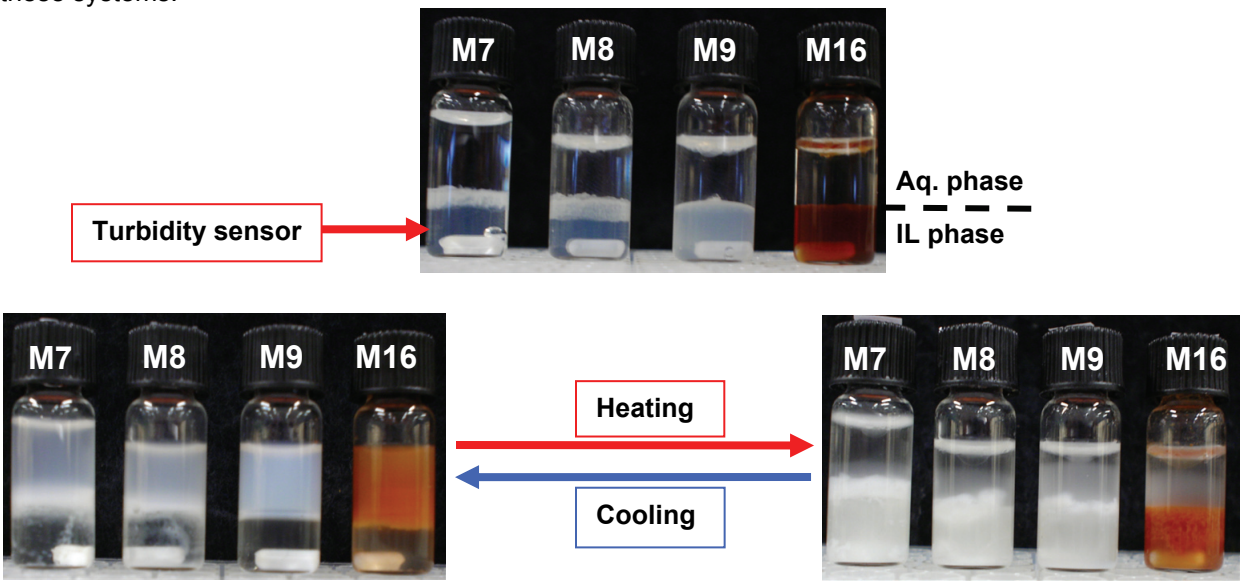

Figure 5-5: *Graphical overview of thermo-reversible micellar transfer experiments between an aqueous phase and a hydrophobic ionic liquid phase formed by 1-butyl-3-methyimidazolium hexfluorophosphate (IL **2**). The transfer of the micelles between the two phases has been followed by turbidity measurements. Samples **M7**-**M9** (Table 5-1) correspond to micelles formed by PNonOx-b-PEtOx diblock copolymers, whereas the micelles in sample **M16** (Table 5-1) are formed by the metallo-supramolecular diblock copolymer PS-[Ru]-PEG (see section 3.3.3).*

In Figure 5-6 the results of turbidity measurements (transmission) correlated with temperature for a two-phase system formed by sample **M9** (Table 5-1) (1 g of micellar solution in IL **2**) and an aqueous phase (0.75 g of water) are shown. At the onset of the measurements at 25 °C, the transmitted light intensities in the IL phase are close to 100% indicating the absence of micelles (the turbidity sensor is located at the IL phase (bottom phase) in the micellar systems investigated (see Figure 5-5)). This means that, after a considerable period of time at room temperature (at least 3 days period before the turbidity measurements shown in Figure 5-6), the two-phase micellar system is in a thermodynamic equilibrium, and the block copolymer micelles are only present in the aqueous phase. In this state, the aqueous phase is cloudy due to the presence of the micelles and, on the other hand, the IL phase is almost transparent due to the absence of micelles (see Figure 5-5). As soon as the temperature is increased up to 95 °C (at a heating rate of 5 °C min^{-1}), the transmitted light intensity values rapidly decrease down to 0%. This corresponds to the situation where the micelles have migrated to the IL phase due to the aforementioned LCST behavior of the block copolymer system investigated. For this reason, the IL phase becomes cloudy while the aqueous solution, now free of micelles, becomes almost transparent (see Figure 5-5). According to the abovementioned transfer mechanism, the micelles must eventually return to the aqueous phase upon cooling and keeping the system at room temperature. However, this process is rather slow and can take a considerable period of time to reach the new equilibrium state. This situation is observed in Figure 5-6a, where after the first heating/cooling cycle the system is kept at 25 °C for 30 min

and no significant increase in the transmission measurements is revealed, confirming that the micelles are still present in the IL phase. It has been observed that when the system is kept at those conditions long enough, from 3 to 5 days, the equilibrium state is eventually reached and the micelles are transferred back to the aqueous phase. Nevertheless, it was found that the transfer of the micelles from the IL phase to the aqueous phase can be immediately achieved and triggered by supplying energy to the system. For instance in Figure 5-6a, it can be observed that after the 30 min period at 25 °C, the system is again heated up to 95 °C (at a heating rate of 5 °C min^{-1}) causing a sudden increase in the transmission values up to a maximum of 85% followed by a decrease down to 0% whereas the system is kept at high temperature conditions. This observation is confirmed in further heating/cooling cycles as can be seen in Figures 5-6b and 5-6c, a continuation of Figure 5-6a and an overview of the whole experiment, respectively.

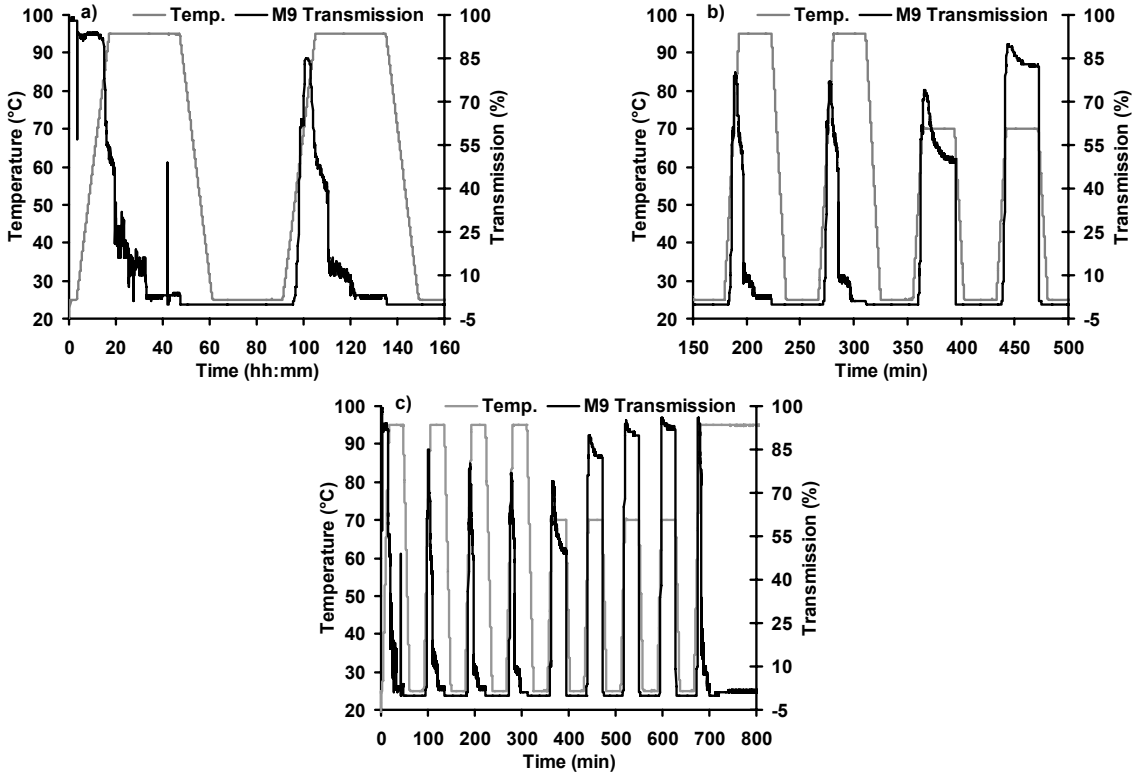

Figure 5-6: *Thermo-reversible micellar transfer experiments between an aqueous phase and a hydrophobic ionic liquid phase formed by 1-butyl-3-methyimidazolium hexfluorophosphate (IL* ***2****). Turbidity measurements (as determined by light transmission) are plotted as a function of temperature and time for the ionic liquid phase (lower phase in the systems shown in Figure 5-5) of sample* ***M9*** *of Table 5-1 (micelles formed by PNonOx-b-PEtOx diblock copolymers). (a) and (b) are close-ups of c), whereas (b) is the continuation of (a) in time.*

In Figure 5-6b it can also be observed that when the micellar system is exposed to heating/cooling cycles only between 70 and 25 °C, the transfer process of the micelles between the phases is different to the previous analyzed case (heating/cooling cycles between 95 and 25 °C) according to the turbidity measurements obtained. It can be observed that when the system is heated only up to 70 °C and kept at those conditions for 30 min, the transmission values only slightly decrease and do not drop down to 0%. This observation suggests that the transfer process of the micelles from the aqueous phase to the IL phase at these conditions (70 °C) considerably slows down (or does not occur at the investigated experimental conditions) in comparison to the observations at higher temperature (90 °C). Remarkably, after this period of time at 70 °C, when the system is subjected to a cooling process (at a cooling rate of 5 °C min^{-1}) the transmission values drop immediately down to 0% indicating that the micelles have been transferred from the aqueous phase to the IL phase. This means that the transfer process of the micelles

from the aqueous phase to the IL phase at these experimental conditions (70 °C) can also be achieved and triggered by removing energy from the system (in a similar way to the aforementioned opposite process where the micelles are transferred from the IL phase to the aqueous phase at lower temperatures). It is thought that this effect may be related to the fact that when the temperature of the system is close to the LCST value of the hydrophilic corona the investigated micelles have almost no preference for one of the two phases. Finally, the confirmation of all these findings can be fully seen in Figure 5-6c, where repetitions of the investigated heating/cooling cycles in the system produce always similar light transmission curves. In addition, further experiments demonstrated that the variation of the heating/cooling rates from 5 °C min^{-1} to 1 °C min^{-1} during the experiments had almost no influence on the results described above. The stirring speed during the experiments was found to be a very important factor for the phase transfer process of the micelles. For instance, higher stirring speeds cause a faster phase transfer of the micelles; this finding is more distinct in the case where the micelles are transferred from the aqueous phase to the IL phase at high temperatures. Even though the obtained results provide a good insight into the observed phenomena, it is clear that this thermodynamic process is very complex and a considerable amount of variables have to be further investigated in order to reach a full understanding of the transfer mechanism. For instance, the diffusion processes of the micelles in the two phases and in the interface, as well as the kinetic processes of formation and rupture of the hydrogen bonds related to the LCST behavior of the investigated polymers, might be the key processes and the starting points of future investigations on theses systems. It is clear that these processes will also be strongly affected by many other variables such as the viscosity of the phases, interfacial tension between the phases, temperature, characteristics of the block copolymers used for the preparation of the micelles (composition of the blocks and molecular weight), etc.

It is known that most supramolecular block copolymers linked by a transition metal ion, as well as their corresponding nanostructures, are colorful compounds and absorb in the visible region of the light spectrum depending mainly on the transition metal ion utilized for their synthesis (see, for example, section 3-3). Based on this approach, the poly(styrene-*block*-ethylene glycol) supramolecular diblock copolymer linked by ruthenium(II) ions (PS-[Ru]-PEG) discussed in section 3.3.3[17b] was used to prepare supramolecular block copolymer micelles in IL **2**. These supramolecular micellar structures show a characteristic UV-Vis absorption band at 485 nm (see section 3.3.3) and therefore, their presence or absence either in the IL or in the aqueous phases could be investigated by UV-Vis spectroscopic measurements. Similar to the abovementioned micellar phase transfer experiments, the supramolecular micelles investigated have been reversibly transferred between an aqueous and an IL phase as depicted in Figure 5-5 (sample **M16**, Table 5-1). In the UV-Vis spectra of Figure 5-7, it can be observed that the presence or the absence of the supramolecular micelles in one or another phase depends mainly on the temperature of the system. On the one hand, in Figure 5-7 it can be seen that IL **2** and water do not show any absorption band in the region of interest of the spectrum. On the other hand, a strong absorption band at 485 nm arises for supramolecular micelles originally prepared in IL **2** (curve "**M16** in IL (original)" in Figure 5-7). Upon adding an aqueous phase into this original micellar solution in IL **2** and reaching the equilibrium state of the system at 20 °C, it is observed that the absorption band at 485 nm appears in the aqueous phase (curve "**M16** in aq. phase 20 °C" in Figure 5-7), and vanishes in the IL phase (curve "IL phase 20 °C" in Figure 5-7), indicating that the transfer of the micelles between the two phases has occurred. In addition, upon heating the system up to 95 °C the absorption band at 485 nm returns to the IL phase (curve "**M16** in IL phase 95 °C" in Figure 5-7) and disappears in the aqueous phase (curve "Aq. phase 95 °C" in Figure 5-7) (the less intense absorption values shown by the curve "**M16** in IL phase 95 °C" in Figure 5-7 in comparison to the curve "**M16** in IL (original)" might be related to concentration effects and/or to the turbidity shown by the system after the phase transfer experiments (see Figure 5-5)). This indicates once more that the micelles have been transferred between the two phases and that the reversible transfer cycle is complete.

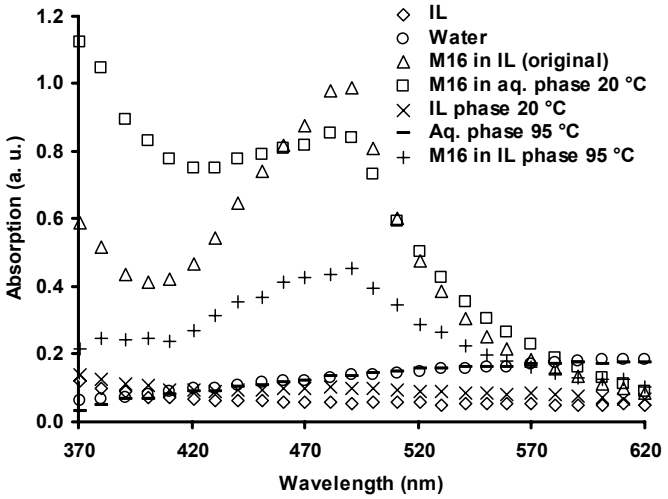

Figure 5-7: *Thermo-reversible micellar transfer experiments between an aqueous phase and a hydrophobic ionic liquid phase formed by 1-butyl-3-methyimidazolium hexfluorophosphate (IL **2**). UV-Vis spectra of the aqueous and ionic liquid phases for investigating the location of metallo-supramolecular block copolymer micelles (PS-[Ru]-PEG) (sample **M16** of Table 5-1) at different temperature conditions.*

5.2.4 Encapsulation as well as reversible and non-reversible transfers of guest molecules between a hydrophobic ionic liquid phase and an aqueous phase utilizing block copolymer micellar systems

Block copolymer micelles and dendritic core-shell architectures have been reported as delivery or phase-transfer vehicles of molecules and nano-objects.[22] Thus, micellar systems have been utilized, for instance, for the encapsulation of moieties with catalytic activity,[22c,e] and of drugs showing a steady release process.[22f] In addition, the encapsulation and delivery of organic molecules in a pH-responsive two-phase system have been also described.[22d] Nevertheless, most of the previously reported micellar systems have shown the delivery of encapsulated moieties in only one direction. On the one hand, the reversible transfer of catalytic moieties from one phase to another would be desirable in dedicated applications, such as heterogeneous micellar catalytic systems.[14] This approach would allow for an easier recovery of expensive or toxic catalysts from the final products and for the development of more efficient catalytic reactions and separation processes. On the other hand, it would be of interest to develop heterogeneous systems where the recovery of the micellar aggregates themselves is also possible after the delivery of their freights (encapsulated species) in one of the phases. This approach would allow the delivery of highly accurate amounts of chemical substances in different systems, as well as for the recovery of expensive (or perhaps toxic) micellar aggregates for their reloading with new guest molecules and reuse in further delivery cycles.

Based on the thermo-reversible micellar transfer phenomena between an aqueous phase and a hydrophobic IL phase discussed in the previous section, in this section the transfer (or release) between the two phases of guest molecules encapsulated into the micellar cores is discussed. Remarkably, both aforementioned approaches (full reversible transfer and/or one direction delivery capability of the guest molecules between the two phases) were experimentally found in this work. This is illustrated by the preparation of PNonOx-*b*-PEtOx-*b*-PMeOx triblock copolymer micelles in IL **2** (similar system to **M17** in Table 5-1) with encapsulated molecules in their hydrophobic cores (see the experimental part for details) followed by phase transfer experiments of the loaded micelles between the hydrophobic IL phase and an aqueous phase. These transfer experiments were performed in a similar way as discussed above.

For this purpose, UV-Vis measurements of the two phases during the different stages of the experiments were recorded in order to localize the encapsulated molecules within the two-phase systems investigated.

The starting point for this discussion is to determine the UV-Vis absorption properties of the micellar systems investigated before the addition of any dye. In this regard, Figure 5-8 demonstrates that neither the pure solvents (IL **2** and water) nor the pure micellar solutions show strong absorption bands in the range of 350 to 900 nm, which will allow for a better analysis of the presence of dye molecules in the two phases of the system.

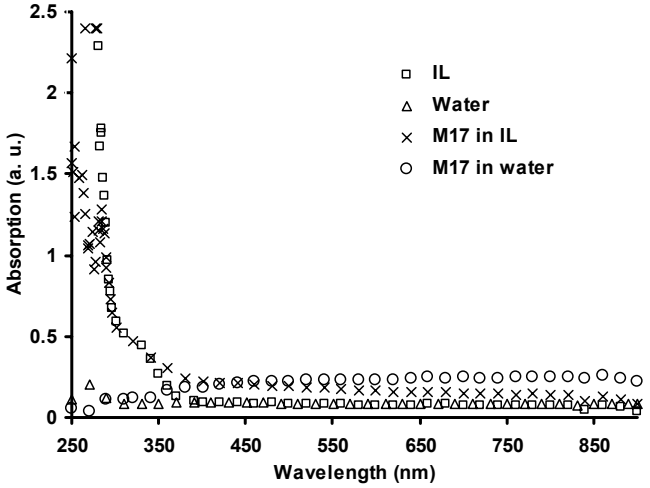

Figure 5-8: *UV-Vis spectra of the hydrophobic ionic liquid 1-butyl-3-methyimidazolium hexfluorophosphate (IL* ***2****) and water in the absence and in the presence of micellar aggregates formed by PNonOx-b-PEtOx-b-PMeOx triblock copolymers (sample* ***M17*** *of Table 5-1).*

Figure 5-9 displays the results of the phase transfer experiments of a system composed of encapsulated molecules of disperse red 1 dye (**D1**) (see experimental part for a schematic representation of the chemical structure of **D1**) in the cores of micelles formed by PNonOx-*b*-PEtOx-*b*-PMeOx triblock copolymer chains, a hydrophobic IL phase (IL **2**), and an aqueous phase. First of all, in the absence of micelles, **D1** (which is fully soluble in IL **2**) shows a strong absorption band in the region of the UV-Vis spectrum around 500 nm (Figure 5-9a, curve "**D1** in IL"). On the other hand, the same dye in the absence of micelles shows a remarkable shift of the absorption band to 420 nm when water is used as a solvent (Figure 5-9a, curve "**D1** in water"). **D1** is however poorly soluble in water. After the micellar encapsulation process of **D1** was performed in IL **2** (see experimental part for details), the micellar dispersion obtained reveals the same absorption band at 500 nm (Figure 5-9a, curve "D1 + **M17** in IL") as in the case of **D1** in IL **2** in the absence of micelles (Figure 5-9a, curve "**D1** in IL"). Note that at this point it can not be concluded whether **D1** is encapsulated or not in the micellar cores since in both cases the absorption band observed is due to the presence of **D1** molecules. However, when an aqueous phase is added into the system and the thermodynamic equilibrium in the two-phase system is reached at 20 °C, the micelles originally present in the IL phase not only have migrated into the aqueous phase, but in addition have also transported the dye molecules encapsulated in their cores into the aqueous phase. A proof that this situation has occurred can be observed in the UV-Vis spectrum displayed by curve "Aq. phase 20 °C" in Figure 5-9a. This spectrum shows a strong absorption band at 500 nm which can not be observed for the case of **D1** in water in the absence of micelles (Figure 5-9a, curve "**D1** in water"). This finding demonstrates that the dye molecules have been effectively encapsulated into the core of the micelles and transferred into the aqueous phase. Nevertheless, at the equilibrium conditions of 20 °C the spectrum corresponding to the IL phase (Figure 5-9a, curve "IL phase 20 °C") shows also that dye molecules are still present in this phase demonstrating that not all the utilized amount of dye was encapsulated into the micelles. According to this observation, it is thought that the number of present micelles is insufficient to

encapsulate all the dye molecules under the experimental conditions investigated (note that it is possible to estimate the amount of dye left in the IL phase (by a quantitative UV-Vis analysis) and thus to estimate the number of encapsulated dye molecules; however these investigations will be performed in future work). When this micellar system, in equilibrium at 20 °C, is subjected to a heating process up to 95 °C, the micelles containing the encapsulated dye molecules migrate from the aqueous phase to the IL phase through a similar transfer process as discussed before. This phenomenon will leave the aqueous phase of the system again free of micelles and therefore free of dye molecules. This can be observed in the spectrum corresponding to the curve "Aq. phase 95 °C" in Figure 5-9a, which does not show the absorption band at 500 nm related to **D1** found in the curve "Aq. phase 20 °C" in the same figure. The spectrum of the IL phase at these conditions of high temperature (curve "IL phase 95 °C" in Figure 5-9a) obviously shows a signal at 500 nm due to the presence of the dye molecules either encapsulated in the micelles or dissolved in IL **2**. Three more cycles of this thermo-reversible transfer process of micelles bearing dye molecules between an aqueous phase and a hydrophobic IL phase (IL **2**) were additionally carried out, and the results obtained showed identical characteristics as discussed above for Figure 5-9a. The process described of encapsulation of dye molecules into the cores of micelles and their thermo-reversible phase transfer is graphically summarized in Figure 5-9b. In addition, another organic dye (of characteristics similar to **D1**) was also utilized in the described experimental micellar system in order to investigate whether or not the findings addressed above were applicable to other guest molecules. Hence, the use of disperse orange 3 (**D2**) (see experimental part for a schematic representation of the chemical structure of **D2**) in the micellar system has shown a very similar behavior to the one found for the case of **D1** (Figure 5-9).

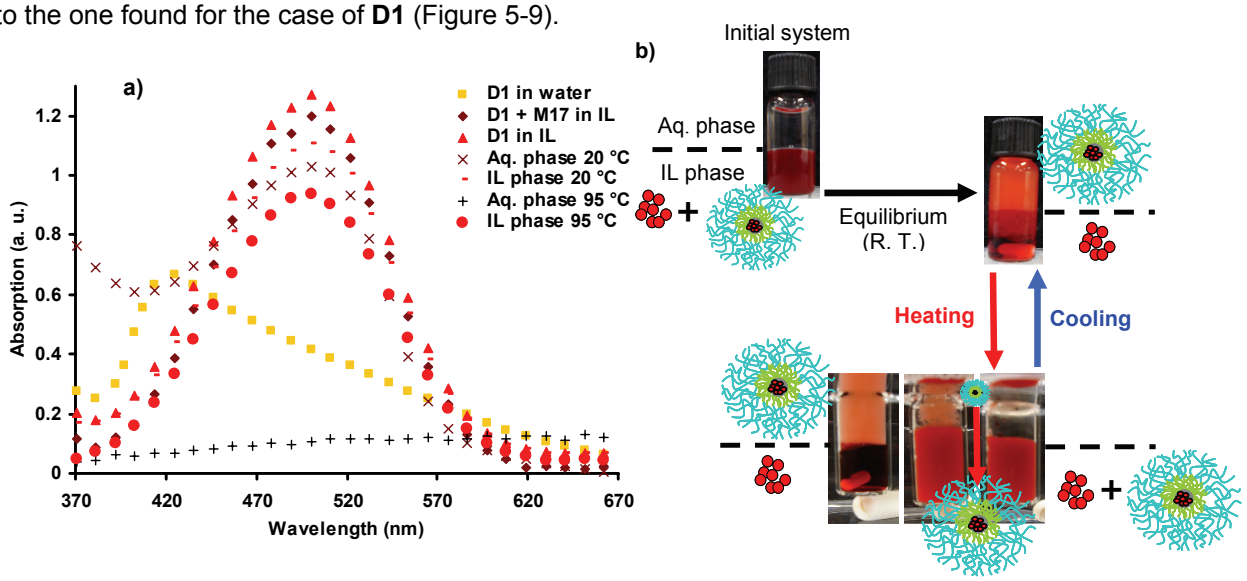

Figure 5-9: *Thermo-reversible transfer experiments between an aqueous phase and a hydrophobic ionic liquid (1-butyl-3-methyimidazolium hexfluorophosphate (IL **2**)) phase of organic dye molecules (disperse red 1 (**D1**)) encapsulated into the cores of micelles formed by PNonOx-b-PEtOx-b-PMeOx triblock copolymers (sample **M17** of Table 5-1). (a) UV-Vis spectra of the aqueous and ionic liquid phases recorded for investigating the location of the encapsulated molecules at different temperature conditions. (b) Graphical overview of the experiment.*

To investigate in more detail the reversibility of the phase transfer process of encapsulated molecules into the micellar cores, the experiment displayed in Figure 5-10 was carried out using **D2** as guest molecules of the micelles. This experiment starts with a micellar system similar to the one shown in Figure 5-9b in equilibrium at room temperature. This initial stage consist of encapsulated molecules of **D2** into the cores of PNonOx-*b*-PEtOx-*b*-PMeOx triblock copolymer micelles, which have migrated from an IL **2** phase (bottom phase containing dissolved dye in excess) to an aqueous phase (upper phase containing micelles with encapsulated dye) at room temperature. In the next step of the experiment, the

aqueous phase of the initial system is transferred into a vial containing a new IL **2** phase (same amount of IL **2** as in the initial system was used for this purpose). Thereafter, this new two-phase system is heated (5 °C min^{-1}) up to 95 °C, resulting in the transfer of the dye-loaded micelles into the new IL **2** phase in a similar way as described before. When this latter system is placed at room temperature and the thermodynamic equilibrium is reached after some time, the micelles have migrated again into the aqueous phase, but this time without the dye molecules. This means that the release of the dye molecules into the new IL **2** phase has occurred as can be observed in Figure 5-10 (compare the change of color in both phases in relation to the previous stages of the system before the phase transfer process at high temperatures). In addition, these observations were confirmed by UV-Vis measurements of the two phases of the system at its final stage; the aqueous phase containing the micelles did not show any absorption band related to **D2** dye molecules, whereas the new IL **2** phase did, confirming the presence of **D2**.

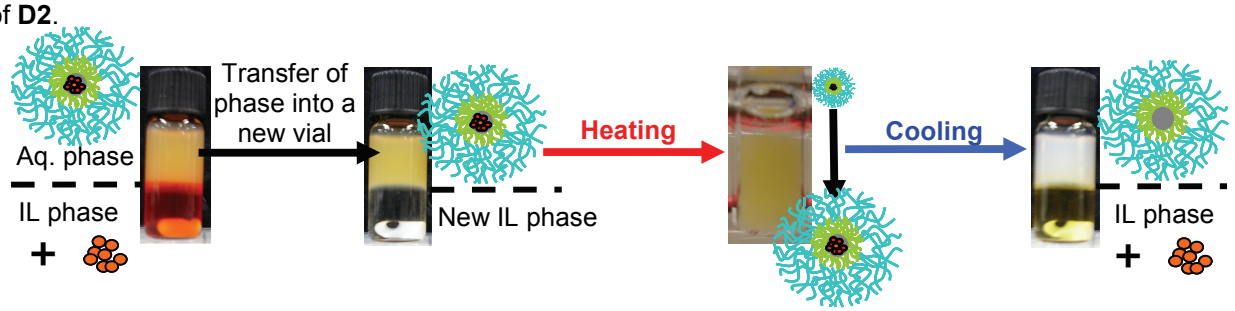

Figure 5-10: *Graphical overview of a transfer experiment between an aqueous phase and a hydrophobic ionic liquid (1-butyl-3-methyimidazolium hexfluorophosphate (IL **2**)) phase of organic dye molecules (disperse orange 3 (**D2**)) encapsulated into the cores of micelles formed by PNonOx-b-PEtOx-b-PMeOx triblock copolymers (sample **M17** of Table 5-1). The experiment shows the phase transfer and release of encapsulated guest molecules **D2** into the hydrophobic ionic liquid phase (IL **2**) allowing the recovery of the utilized micelles.*

From the results of this previous experiment (Figure 5-10) the possibility arises to recover from the aqueous phase the unloaded micelles in order to reuse them in a new encapsulation process. Thus, an additional encapsulation experiment with recovered micelles was performed and its results are summarized in Figure 5-11. This experiment starts with a micellar system similar to that one shown at the end of Figure 5-10 (unloaded micelles in an aqueous phase in equilibrium at room temperature with a hydrophobic IL (IL **2**) phase containing released dye molecules from the micelles). In a next step the aqueous phase of this initial system is transferred into a new vial containing a solution of a dye in IL **2** (**D1** in the case of the experiment in Figure 5-11, same amount of IL phase as used in the previous experiments). Thereafter, this new two-phase system is heated up to 95 °C, which provokes the transfer of the empty micelles into the IL phase containing the dissolved dye. Figure 5-11a shows that when this latter system is placed at room temperature for some time until a new thermodynamic equilibrium state is reached, the originally empty micelles have migrated again into the aqueous phase but this time bearing a new load of dye molecules. These observations were additionally confirmed by UV-Vis measurements of the phases at the different stages of the experiment and the results are displayed in Figure 5-11b. For instance, the initial micellar aqueous phase at 20 °C (recovered from an experiment similar to that one shown in Figure 5-10) shows a weak absorption band in the region of the spectrum around 500 nm (Figure 5-11b, curve “Aq. phase 20 °C”), whereas the IL phase reveals a much stronger signal in the same region (Figure 5-11b, curve “IL phase 20 °C”) indicating the presence of dye molecules as expected. After the micellar process transfer is completed at high temperature, the absorption band at 500 nm completely vanishes for the aqueous phase (Figure 5-11b, curve “Aq. phase 95 °C”) due to the absence of any dye molecules, and obviously it remains for the IL phase (Figure 5-11b, curve “IL phase 95 °C”). Finally, when the system is placed at room temperature and reaches the thermodynamic equilibrium, the micelles reloaded with new dye molecules have migrated into the aqueous phase as confirmed in the UV-Vis spectrum corresponding to the curve “M17 reloaded (aq. phase 20 °C)” in

Figure 5-11b. Similar to the experiment described in Figure 5-9, three more cycles of thermo-reversible phase transfers of the micelles bearing the reloaded dye molecules between the aqueous and the IL phases were additionally performed for the experiment shown in Figures 5-11. The obtained results were similar to those ones discussed above for Figure 5-9 (the micelles bearing the dye molecules were thermo-reversible transferred between the phases in every cycle).

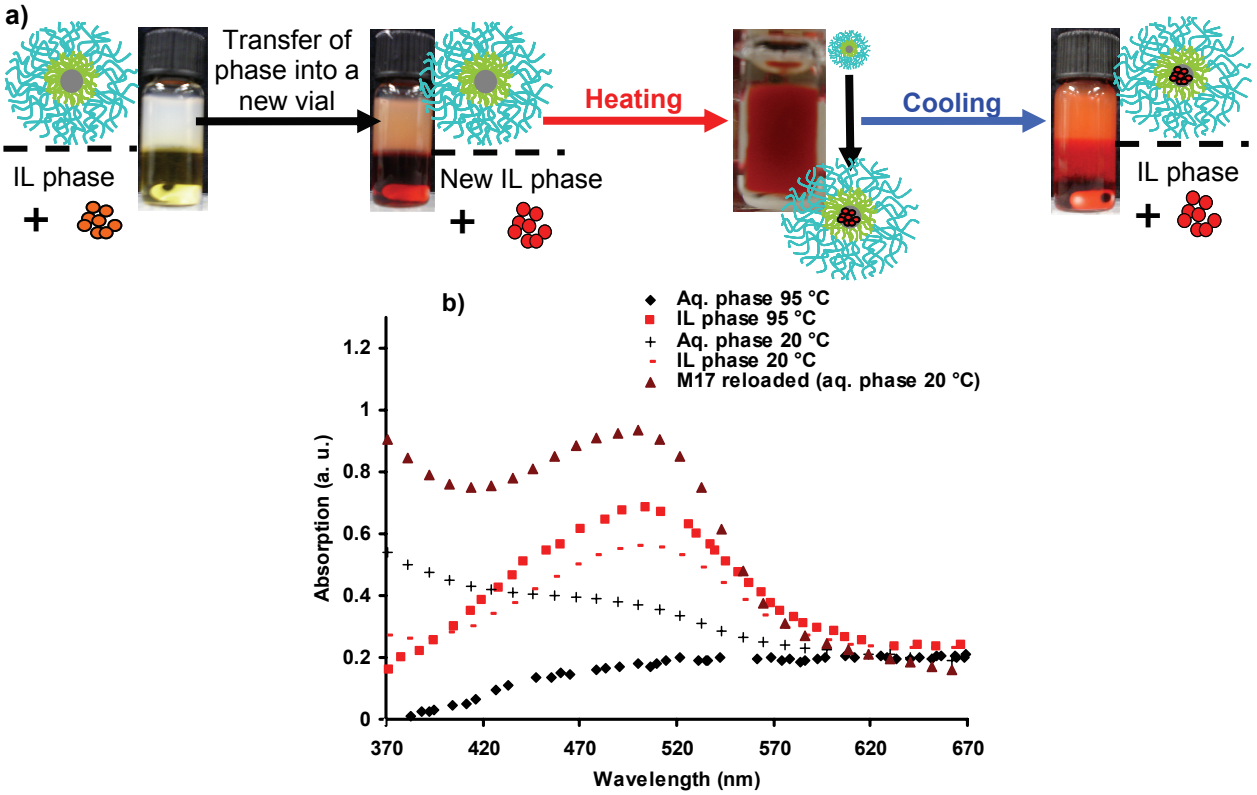

Figure 5-11: *Reloading experiment of previously utilized micelles formed by PNonOx-b-PEtOx-b-PMeOx triblock copolymers (sample **M17** of Table 5-1) with additional organic dye molecules (disperse red 1 (**D1**)) and their thermo-reversible transfer between an aqueous phase and a hydrophobic ionic liquid (1-butyl-3-methyimidazolium hexfluorophosphate (IL **2**)) phase. (a) Graphical overview of the experiment. (b) UV-Vis spectra of the aqueous and ionic liquid phases at different stages of the experiment in order to investigate the re-encapsulation process of **D1** molecules into the cores of previously used micelles.*

Based on the results given in Figures 5-9 to 5-11, three main conclusions can be drawn for the systems investigated: (1) The thermo-reversible phase transfer of encapsulated dye molecules can occur when the amount of dye in the system exceeds considerably the amount of dye that can be encapsulated in the core of the micelles. (2) One direction phase transfer (from the aqueous phase to the IL phase) and release of previously encapsulated dye molecules into the hydrophobic IL phase can occur where the system has originally an IL phase free of dye molecules. This means that the concentration of the dye molecules in the system has an important influence on the reversibility of the transport of previously encapsulated species. (3) The recovery of previously utilized micelles (for example, in case (2)) and their reloading with new dye molecules is feasible. The resulting system behaves similar to the one described in situation (1). Note that the obtained results are qualitative at this stage. However, a detailed quantitative study, in terms of the amounts of dye present in the core of the micelles and/or in the entire systems, is necessary for a better understanding of the transfer process. These experiments will be a topic for future research.

The last experiments related to the encapsulation of guest molecules into the micellar cores as well as their phase transfer in the system described correspond, unlike the previous cases, to the use of a

water soluble but IL insoluble dye molecule. For these experiments the water blue organic dye (**D3**) (see experimental part for a schematic representation of the chemical structure of **D3**) was selected due to the fact that it fulfills the mentioned characteristics of solubility. Additionally, water blue is a pH indicator which is colorless in the range of pH from 9.4 to 14. The starting point for these experiments is the investigation related to the behavior of the dye in the two-phase system in the absence of block copolymer micelles. As mentioned, the water blue dye is well soluble in water but it shows a poor solubility in IL **2** even at high temperatures. Therefore, the investigation of **D3** in the two-phase system, starts with the solubility of the dye in an aqueous phase, which is placed in contact with an IL **2** phase as displayed in Figure 5-12a. At this starting point the aqueous and IL phases have a pH of 7.5 and 5.8, respectively, and therefore the aqueous phase shows an intense blue color due to the fact that the pH of the water is lower than 9.4. However, after a while at room temperature conditions, the blue color of the aqueous phase surprisingly vanishes yielding a colorless solution, which indicates that the pH of the system has changed when the two phases are in contact. This phenomenon is depicted in Figure 5-12a. Final pH measurements of the system showed that the aqueous and IL **2** phases reached pH values of 11.9 and 8.8, respectively. This effect may be related to changes in the two phase system of IL **2** and water as discussed elsewhere[1a] (*e.g.*, formation of small amounts of secondary chemical species due to the presence of water and/or other impurities in ILs might change the pH of the system investigated; for instance, it has been reported that some ILs hydrolyze under certain conditions).[1a] It was also found that this final equilibrium state can be reached more rapidly with the supply of a slight stirring to the two phase system. The second experimental stage regarding the use of **D3** in the two-phase system includes the utilization of self-assembled block copolymer micelles (from sample **M17**; Table 5-1) aiming at the encapsulation of the dye molecules into the micellar cores. There are two possible ways to investigate this encapsulation process as depicted in Figure 5-12b: either in the aqueous phase or in the hydrophobic IL phase (where the dye is not soluble). The experimental procedure to achieve the encapsulation of the dye molecules was the same for both cases (see experimental section). In the first approach, an aqueous phase containing encapsulated molecules in the micellar cores together with dissolved dye molecules in water is obtained. This aqueous phase was then added into a vial containing IL **2** phase to obtain a system similar to the one shown in the bottom left in Figure 5-12b. In the second approach the encapsulation procedure is originally performed in the IL **2** phase. Note that **D3** is not soluble in IL **2** (even at high temperatures) and therefore the IL **2** phase remains colorless in the absence of block copolymer micelles. Nevertheless, in the presence of PNonOx-*b*-PEtOx-*b*-PMeOx triblock copolymer micelles (sample **M17**, Table 5-1), a system containing **D3** and IL **2** show an intense blue color. Upon adding water into this latter IL **2** phase, a similar two-phase system is obtained as displayed in the upper left in Figure 5-12b. Moreover, when this latter system reaches the thermodynamic equilibrium at room temperature conditions, the micelles loaded with **D3** are transferred from the IL **2** phase to the aqueous phase (upper right in Figure 5-12b) by a similar transfer mechanism as addressed before. In contrast to the experiments in the absence of micelles (Figure 5-12a), in both cases (either where the encapsulation of **D3** was performed originally in the aqueous phase or in the IL **2** phase) shown in Figure 5-12b, the blue color shown by **D3** remains stable in time where block copolymer micelles are present in the two-phase system. This is an additional proof that molecules of **D3** have been successfully encapsulated into the micellar cores in both preparation methods described. In addition, this finding also demonstrates the ability of self-assembled block copolymer micelles to act as nano-confined environments since the persistence of the blue color in the systems investigated is an indication that, most likely, the found changes of pH in the overall system do not affect the pH inside the micellar cores allowing the encapsulated dye molecules to remain blue (pH in the micellar cores below 9.4). Moreover, in the right hand side of Figure 5-12b it can be observed that the systems obtained by these two preparation methods also show a thermo-reversible micellar phase transfer process upon heating or cooling (for both, micelles and encapsulated dye molecules).

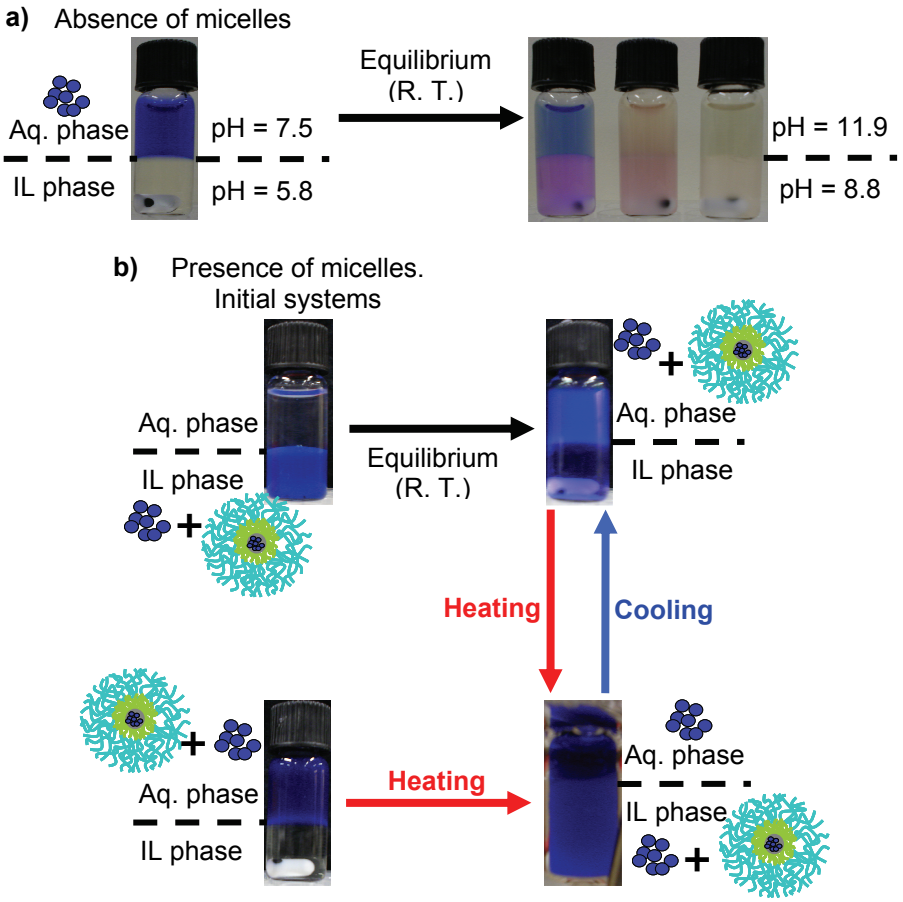

Figure 5-12: *Experiments showing the use of micelles formed by PNonOx-b-PEtOx-b-PMeOx triblock copolymers (sample **M17** of Table 5-1) as confined environment for encapsulated water blue dye molecules (**D3**). (a) In the absence of micelles a change in the pH occurs, which turns the system almost colorless. (b) In the presence of micelles the changes of pH in the system do not affect the color of **D3** molecules, which indicates that the encapsulation of the dye molecules into the micellar core was successful and that block copolymer micelles can act as confined environments.*

5.3 Conclusions

In this chapter, a detailed overview about the state of the art of the recently proposed block copolymer micellar systems in ILs[11] was addressed. During the course of these studies, it was found that several amphiphilic block copolymer systems self-assemble into micellar aggregates in the presence of a hydrophobic and a hydrophilic ILs. In addition, an alternative method for the TEM characterization of these systems was proposed, which has shown to be in agreement with characterization approaches previously utilized. DLS results revealed that the nature of the ILs has generally an influence on the sizes of the formed micellar aggregates for the same amphiphilic block copolymer system. Moreover, the thermo-reversible micellar phase transfer process between a hydrophobic IL phase and an aqueous phase was investigated by turbidity measurements for specific cases. The results have confirmed that the micellar phase transfer between the two phases is a fully reversible phenomenon and have shown that this phase transfer can be triggered by suitable heating or cooling processes. Furthermore, investigations on the encapsulation of guest molecules into the micellar cores as well as their phase transfer process between the aforementioned phases have been carried out. From these investigations, it was found that the thermo-reversible phase transfer of encapsulated dye molecules between an aqueous phase and a hydrophobic IL phase is also feasible. Other observations derived from these investigations reveal the

possibilities of the transfer and release of guest molecules only in one direction (from the aqueous to the hydrophobic IL phase), the recovery and reload of previously used micelles with new guest molecules for further use in additional phase transfer cycles, and the use of block copolymer micelles as confined environments for the protection of molecules from changes in the conditions of the surroundings.

The findings of this investigation may allow, for example, the development of advanced heterogeneous micellar catalytic systems with novel features such as the recovery of expensive or toxic catalysts from the final products, more efficient separation processes, the delivery of highly accurate amounts of chemical substances in multiphase systems, or the recovery of expensive micellar aggregates for further use. Future work on this topic may be focused, for instance, on the detailed elucidation of the thermo-reversible micellar phase transfer mechanism, quantitative investigations on the micellar encapsulation process of guest molecules as well as the development of a two-phase micellar catalytic system.

In the previous chapter as well as in this chapter, it has been shown that the emerging field of ionic liquids can be efficiently applied in the development of cleaner synthetic processes of polymeric materials as well as in the preparation of new block copolymer micellar systems. Thus, ILs were used as novel solvents for both homogeneous and heterogeneous polymeric systems. In the next chapter, ILs are not only used as novel solvents any longer, but they are also combined with other substances aiming at the preparation of advanced composite materials. More specifically, the incorporation of magnetic properties into these novel ionic systems is discussed.

5.4 Experimental part

Reagents and solvents. Ionic liquids (ILs) (see Table 4-1 and Figure 4-1): 1-Butyl-3-methylimidazolium hexafluorophosphate (**2**) and 1-butyl-3-methylimidazolium trifluoromathenesulfonate (**4**) were synthesis grade and obtained from Solvent Innovation GmbH as a kind gift. All other materials were used as received from the suppliers.

Synthesis of the block copolymer systems. All the block copolymers investigated in this chapter were synthesized using similar procedures as described in previous chapters or reported elsewhere. The poly(styrene-*block*-methyl methacrylate)s (PS-*b*-PMMA) diblock copolymers have been synthesized by sequential anionic polymerization as described in section 2.4.2, whereas the poly(styrene-*block*-ethylene glycol) metallo-supramolecular diblock copolymer (PS-[Ru]-PEG) has been prepared using terpyridine-functionalized polymer precursors as addressed in section 3.3.3. The poly(2-nonyl-2-oxazoline-*block*-2-ethyl-2-oxazoline)s (PNonOx-*b*-PEtOx) diblock copolymers and the poly(2-nonyl-2-oxazoline-*block*-2-ethyl-2-oxazoline-*block*-2-methyl-2-oxazoline) triblock copolymer (PNonOx-*b*-PEtOx-*b*-PMeOx) have been synthesized by sequential cationic ring opening polymerizations in a similar way as addressed in section 4.2.1, but using acetonitrile as reaction media (a conventional volatile organic solvent); a detailed description of these synthetic methods can be found elsewhere.[17,18] All polymers showed narrow mono-modal molecular weight distributions as revealed by gel permeation chromatography (GPC). Proton nuclear magnetic resonance (^{1}H-NMR) spectroscopy in combination with GPC measurements were utilized for calculating the chain lengths composition of the different block copolymers.

Preparation of block copolymer micelles in ionic liquids. Self-assembled micelles of the investigated block copolymers were prepared utilizing the co-solvent method as reported elsewhere[12] and in a similar way as described in section 3.2.3. The block copolymers were dissolved in a thermodynamically good solvent for both blocks (in acetone at 50 °C for block copolymers derived from oxazoline monomers and in tetrahydrofuran at room temperature for the rest of the block copolymers investigated in this chapter) at a concentration of 10 wt %. Subsequently, ILs **2** or **4** were gradually added into the polymeric solutions as selective precipitants for the blocks composed of styrene and 2-nonyl-2-oxazoline under vigorous stirring in order to reach a concentration of 0.5 wt % of the polymeric materials. The removal of the co-solvents from the micellar dispersions was achieved by a controlled heating of the solutions up to 150 °C under vigorous stirring in open vials for 10 min. Upon cooling, the vials were placed in a vacuum oven at 40 °C for at least one day.

Encapsulation of guest molecules into the cores of block copolymer micelles in ionic liquids. The encapsulation of three different organic dyes in the micellar system composed of PNonOx-*b*-PEtOx-*b*-PMeOx triblock copolymer in IL **2** was achieved by placing predetermined amounts of the corresponding dye and block copolymer (10 wt % of dye in respect to the total amount of block copolymer) in a vial before the addition of the non-selective solvent (acetone in this case); the rest of the encapsulation procedure was identical to the micelle preparation method explained above. The investigated organic dyes were disperse red 1 (*N*-ethyl-*N*-(2-hydroxyethyl)-4-(4-nitrophenylazo)aniline) (**D1**), disperse orange 3 (4-(4-nitrophenylazo)aniline) (**D2**), and water blue (pH indicator) (**D3**). **D1** and **D2** show a poor solubility in water but they were found to be well-soluble in IL **2**. **D3** is well-soluble in water but completely insoluble in IL **2**. In addition, **D3** acts as a pH indicator becoming colorless in the range of pH from 9.4 to 14. Figure 5-13 depicts schematic representations of the chemical structures of the organic dyes utilized in this work.

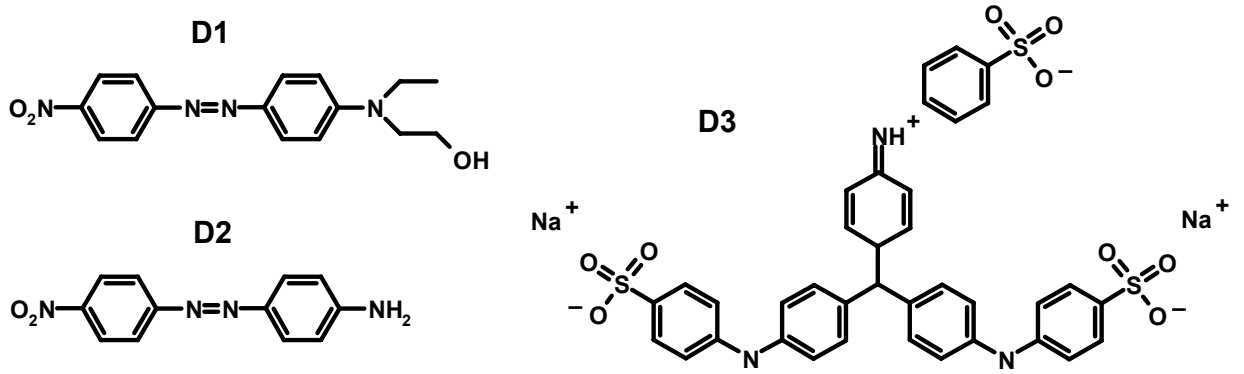

Figure 5-13: *Schematic representation of the chemical structures of the organic dyes utilized in the investigations of the encapsulation of guest molecules into the cores of block copolymer micelles (section 5.2.4).* ***D1****: N*-ethyl-*N*-(2-hydroxyethyl)-4-(4-nitrophenylazo)aniline *(disperse red 1).* ***D2****:* 4-(4-nitrophenylazo)aniline *(disperse orange 3).* ***D3****: Water blue (pH indicator).*

Characterization techniques.

Dynamic light scattering (DLS) measurements were performed at 25 °C at 90° on a Malvern CGS-3 apparatus equipped with a 633 nm laser. The values of refractive index for IL **2** and IL **4**, used during the analysis, were 1.41 and 1.44, respectively; whereas the used values of viscosity for IL **2** and IL **4** were 196 and 113 mPa s, respectively. The hydrodynamic radius and polydispersity indices of the micelles were calculated form a cumulant analysis. The distribution of the hydrodynamic radius was obtained by a deconvolution of the data with the CONTIN algorithm.

Turbidity measurements were performed in an Avantium Crystal 16 platform which is composed of 16 wells designed to hold 1.5 mL vials, each with its on-line turbidity (light transmission intensity) sensor. The wells can be magnetically stirred at a fixed speed and are grouped into four zones that can be independently heated and cooled. Block copolymer micellar systems were heated and cooled at 1 °C min^{-1} or at 5 °C min^{-1} in a range temperature from 20 °C to 95 °C using a stirring speed of 700 rpm. To verify the reproducibility of the measurements related to the thermo-reversible transfer process of the micelles between a hydrophobic IL phase (IL **2**) and an aqueous phase, the heating/cooling cycle was repeated several times. The turbidity sensor of the equipment was located at the lower phase (IL phase) of the micellar systems. Additionally, the transfer of the micelles between the two mentioned phases (change in turbidity upon heating/cooling) was verified by visual inspection in a conventional oil bath setup.

Ultraviolet-visible (UV-Vis) spectroscopy measurements were recorded on a FlashScan 520 (AnalyticJena, Germany) in 96-well microtiter plates (poly(propylene), flat bottom) from Greiner (Greiner Bio-One, Germany) in a range from 250 to 800 nm. All spectra were referenced to an empty microtiter plate and measurements were performed utilizing four flashes.

(Cryogenic) transmission electron microscopy (cryo-TEM) images of selected micellar systems were recorded on a Technai G^2 Sphera (FEI) electron microscope using an acceleration voltage of 200 kV. Samples for cryo-TEM were prepared using a similar approach as reported elsewhere[11a,c] in a Vitroblot preparation chamber.

pH measurements of micellar dispersions as well as of pure substances were performed in poly(propylene) containers using a HI 8417 Hanna Instruments bench-top pH meter supplied with a HI 1131B glass-body combination pH electrode.

GPC measurements of the PS-*b*-PMMA diblock copolymers were performed on a Shimadzu system with a RID-6A refractive index detector and a 3 x Mixed-B (Polymer Labs) column utilizing tetrahydrofuran as an eluent at a flow rate of 1 mL min^{-1} and a column temperature of 20 °C. Molecular weights were calculated against poly(methymethacrylate) standards. GPC measurements of the rest of the copolymers were performed on a Waters GPC system consisting of an isocratic, a 2414 refractive index detector, a 2996 photo diode array detector, and a Waters Stryragel HT4 column. A *N,N*-dimethylformamide solution containing 5 mM of NH_4PF_6 was used as an eluent at a flow rate of 0.5 mL min^{-1} and a column temperature of 50 °C. Molecular weights were calculated against poly(methyl methacrylate) standards in the case of copolymers derived from oxazoline monomers and poly(styrene) standards in the case of the PS-[Ru]-PEG supramolecular diblock copolymer.

^{1}H-NMR spectra were recorded on a Varian Gemini 400 MHz spectrometer at room temperature using deuterated chloroform ($CDCl_3$).

5.5 References

[1] (a) M. Deetlefs, K. R. Seddon, *Chim. Oggi* **2006**, *24(2)*, 16. (b) M. J. Earle, J. M. S. S. Esperanca, M. A. Gilea, J. N. Canongia-Lopes, L. P. N. Rebelo, J. W. Magee, K. R. Seddon, J. A. Widegren, *Nature* **2006**, *439*, 831. (c) M. Smiglak, W. M. Reichert, J. D. Holbrey, J. S. Wilkes, L. Sun, J. S. Thrasher, K. Kirichenko, S. Singh, A. R. Katritzky, R. D. Rogers, *Chem. Commun.* **2006**, 2554.

[2] (a) B. Jastorff, R. Störmann, J. Ranke, K. Mölter, F. Stock, B. Oberheitmann, W. Hoffmann, J. Hoffmann, M. Nüchter, B. Ondruschka, J. Filser, *Green Chem.* **2003**, *5*, 136. (b) C. Pretti, C. Chiappe, D. Pieraccini, M. Gregori, F. Abramo, G. Monni, L. Intorre, *Green Chem.* **2006**, *8*, 238. (c) A. S. Wells, V. T. Coombe, *Org. Process Res. Dev.* **2006**, *10*, 794. (d) S. Kumar, W. Ruth, B. Sprenger, U. Kragl, *Chim. Oggi* **2006**, *24(2)*, 24. (e) M. Smiglak, W. M.Reichert, J. D. Holbrey, J. S. Wilkes, L. Sun, J. S. Thrasher, K. Kirichenko, S. Singh, A. R. Katritzky, R. D. Rogers, *Chem. Commun.* **2006**, 2554.

[3] N. Winterton, *J. Mater. Chem.* **2006**, *16*, 4281.

[4] M. Rahman, H. W. Shoff, C. S. Brazel, *ACS Symp. Ser.* **2005**, *913*, 103.

[5] H. Ohno, S. Washiro, M. Yoshizawa, *ACS Symp. Ser.* **2005**, *913*, 89.

[6] D. M. Fox, S. Bellayer, M. Murariu, J. W. Gilman, P. H. Maupin, H. C. De Long, P. C. Trulove, *ACS Symp. Ser.* **2005**, *913*, 175.

[7] J. D. Holbrey, J. Chen, M. B. Turner, R. P. Swatloski, S. K. Spear, R. D. Rogers, *ACS Symp. Ser.* **2005**, *913*, 71.

[8] P. Kubisa, *Prog. Polym. Sci.* **2004**, *29*, 3.

[9] (a) F. Yan, J. Texter, *Chem. Commun.* **2006**, 2696. (b) P. Snedden, A. I. Cooper, K. Scott, N. Winterton, *Macromolecules* **2003**, *36*, 4549. (c) P. Snedden, A. I. Cooper, Y. Z. Khimyak, K. Scott, N. Winterton, *ACS Symp. Ser.* **2005**, *913*, 133.

[10] S. Perrier, T. P. Davis, A. J. Carmichael, D. M. Haddleton, *Chem. Commun.* **2002**, 2226.

[11] (a) Y. He, Z. Li, P. Simone, T. P. Lodge, *J. Am. Chem. Soc.* **2006**, *128*, 2745. (b) Y. He, T. P. Lodge, *J. Am. Chem. Soc.* **2006**, *128*, 12666. (c) P. M. Simone, T. P. Lodge, *Macromol. Chem. Phys.* **2007**, *208*, 339. (d) Y. He, P. G. Boswell, P. Buhlmann, T. P. Lodge, *J. Phys. Chem. B* **2007**, *111*, 4645.

[12] G. Riess, *Prog. Polym. Sci.* **2003**, *28*, 1107.

[13] M. A. R. Meier, S. N. H. Aerts, B. B. P. Staal, M. Rasa, U. S. Schubert, *Macromol. Rapid Commun.* **2005**, *26*, 1918.

[14] T. Dwars, E. Paetzold, G. Oehme, *Angew. Chem. Int. Ed.* **2005**, *44*, 7174.

[15] S. Q. Liu, Y. W. Tong, Y. Y. Yang, *Biomater.* **2005**, *26*, 5064.

[16] H. M. Juang, K. E. Price, D.T McQuade, *J. Am. Chem. Soc.* **2003**, *125*, 5351.

[17] (a) J. M. Yu, P. Dubois, R. Jerome, *Macromolecules* **1997**, *30*, 4984. (b) J. F. Gohy, B. G. G. Lohmeijer, S. K. Varshney, U. S. Schubert, *Macromolecules* **2002**, *35*, 7427.

[18] (a) F. Wiesbrock, R. Hoogenboom, M. Leenen, S. F. G. M. van Nispen, M. van der Loop, C. H. Abeln, A. M. J. van den Berg, U. S. Schubert, *Macromolecules* **2005**, *38*, 7957. (b) R. Hoogenboom, F. Wiesbrock, H. Huang, M. A. M. Leenen, H. M. L. Thijs, S. F. G. M. van Nispen, M. van der Loop, C. A. Fustin, A. M. Jonas, J. F. Gohy, U. S. Schubert, *Macromolecules* **2006**, *39*, 4719.

[19] V. Vogel, G. Mayer, B. G. G. Lohmeijer, J. F. Gohy, J. A. van den Broek, W. Haase, U. S. Schubert, D. Schubert, *J. Polym. Sci. Part A: Polym. Chem.* **2004**, *42*, 4458.

[20] O. Regev, J. F. Gohy, B. G. G. Lohmeijer, S. K. Varshney, D. H. W. Hubert, U. S. Schubert, *Colloid Polym. Sci.* **2004**, *282*, 407.

[21] M. Daoud, J. P. Cotton, *J. Phys.* **1982**, *43*, 531.
[22] (a) V. Chechik, M. Zhao, R. M. Crooks, *J. Am. Chem. Soc.* **1999**, *121*, 4910. (b) T. P. Lodge, A. Rasdal, Z. Li, M. A. Hillmyer, *J. Am. Chem. Soc.* **2005**, *127*, 17608. (c) M. A. R. Meier, M. Filali, J. F. Gohy, U. S. Schubert, *J. Mater. Chem.* **2006**, *16*, 3001. (d) M. Kramer, J. F. Stumbe, H. Turk, S. Krause, A. Komp, L. Delineau, S. Prokhorova, H. Kautz, R. Haag, *Angew. Chem. Int. Ed.* **2002**, *41*, 4252. (e) M. E. Piotti, F. Rivera, R. Bond, C. J. Hawker, J. M. J. Frechet, *J. Am. Chem. Soc.* **1999**, *121*, 9471. (f) C. Allen, J. Han, Y. Yu, D. Maysinger, A. Eisenberg, *J. Control. Release* **2000**, *63*, 275.

CHAPTER 6

Advanced composite materials based on ionic liquids

Abstract

Ionic liquids (ILs) are combined with polymers and/or magnetic particles to prepare novel electro and magneto responsive composite materials. Thus, the preparation of magnetic particle dispersions in ILs has yielded a new class of magnetorheological fluids (MRFs). In contrast to previously reported work, MRFs based on ILs have shown a remarkably low sedimentation rate in the absence of stabilizing agents. Thus, the sedimentation rates of the dispersions investigated depend mainly on the type of IL, as well as the concentration and size of the dispersed magnetic particles. The control of the rheological characteristics of the investigated dispersions by applying a magnetic field in combination with the desirable properties of ionic liquids (e.g., negligible vapor pressure and flammability, and adjustable properties such as: solubility, viscosity, melting point, electric conductivity, etc.) have allowed the development of new and outstanding stable MRFs. These fluids can be applied in diverse areas including: Medical therapies (drug delivery and cancer therapeutic methods), engineering devices (dampers and breaks), and accurate transportation and delivery of substances in multi-phase biological and chemical systems. In addition, the developed dispersions of magnetic particles in ILs were used as precursor materials in the fabrication of novel polymer-ILs-magnetic composites, which have shown both electro conductive and magnetic properties. Moreover, the mechanical, electro conductive and magnetic properties of the composite materials proposed can be readily manipulated upon varying the parameters involved in the preparation procedure proposed. A potential application for the developed polymer-IL-magnetic composites might be the fabrication of micro-engineering devices such as sensors and/or actuators, which could be applied in many areas of science and technology (e.g., in micro fluidic technologies, electronic apparatuses, control systems, and medical therapies).

Parts of this chapter have been and will be published: (1) C. Guerrero-Sanchez, M. Rasa, U. S. Schubert, *PCT Application: PCT/EP2006/010654*, Dutch Polymer Institute. (2) C. Guerrero-Sanchez, T. Lara-Ceniceros, E. Jimenez-Regalado, M. Rasa, U. S. Schubert, *Adv. Mater.* **2007**, *19*, 1740 (front cover). (3) C. Guerrero-Sanchez, C. Fabrie, B. Koopmans, S. Hoeppener, U. S. Schubert, in preparation.

6.1 Polymeric composites based on ionic liquids and their application in stimuli-responsive materials

In the previous two chapters, ionic liquids (ILs)[1] were used as novel solvents to perform polymer synthesis and to prepare block copolymer micellar systems. In this chapter, ILs are combined with polymers and/or magnetic particles aiming at the preparation of novel stimuli-responsive materials. In a first stage, a brief introduction to the state of the art of polymeric composites based on ILs and their application in stimuli-responsive materials is given. Thereafter, dispersions of magnetic particles in ILs are investigated in detail and proposed as a new class of magnetic fluids and as precursor materials for the preparation of novel polymer-IL-magnetic composites, which is briefly addressed in the third part of the chapter. Potential applications of the proposed materials in this chapter as well as recommendations for future developments in this emerging field of stimuli-responsive polymer-ILs composites are also given.

Due to their interesting and intriguing properties (*e.g.*, negligible vapor pressure (see ref.[1c] for a detailed description of this property of ILs), negligible flammability (see ref.[1d] for a detailed description of this property of ILs), stability in a broad temperature range, and electric conductivity), ILs[1] have been combined with different substances and polymers to prepare novel composite materials.[2] For instance, ILs have been utilized as plasticizers for polymers[3] and for the preparation of polymers with reduce flammability,[4] polymer-cellulose composites,[5] and polymer electrolytes.[6]

The use of polymer electrolytes in the emerging field of stimuli-responsive micro and nanotechnologies has received increasing research interest in recent years. Current and potential applications of these technologies are diverse in the fields of electronics, biotechnology, medicine and micro-electromechanical systems (MEMS), to name a few. For instance, an important application area of these technologies is the handling of liquids in micro-systems.[7] Various actuation principles and structures have been employed in the fabrication of micro devices for these systems which include piezoelectric,[8] electrostatic,[9,10] thermopneumatic,[11] electrochemical,[12] bimetallic,[13] shape memory alloy[14] and electromagnetic[15] principles. Electro responsive materials are among the most frequently used approaches for the fabrication of stimuli-responsive actuators and membranes. Solid-state electrolytes with high ionic conductivities have been the subject of extensive research in recent years for their application in electro responsive systems and for other purposes such as power sources[16-18] as well as for electrochemical devices.[19,20] Solid-state electrolytes have shown obvious advantages over their liquid counter parts (*e.g.* leakage, flammability, toxicity, stability). Some of the most interesting solid-state electrolytes are composed of polymeric materials which can diminish the concerns related to the safety and stability problems while offering other attractive properties, such as thin-film forming ability, flexibility, transparency and printability. Printable electrical devices[21,22] are attractive for the development of MEMS including sensors, switches, and micro-machines. In particular, printable actuators that can infinitely operate in air at low voltages would provide a breakthrough in the design of miniaturized mechanical devices. On the one hand, polymer electrolytes can be defined as solid solutions of electrolyte salts in a polymeric matrix.[23-27] Ionic motion in these polymer electrolytes, and hence the ionic conductivity, is limited by the segmental mobility of the structuring polymers, especially those with high glass transition temperatures (*Tg*). Attention in the past has been focused on synthesizing polymers with lower *Tg* or minimizing their crystallinity to enhance the ionic conductivity, and new approaches have recently emerged which make use of the design of room temperature molten salts (ILs) for the preparation of polymer electrolytes.[28-31] On the other hand, conjugated polymers can be considered as other potential materials for the fabrication of electro responsive devices.[32-36] Although a few examples of conjugated polymer actuators that can work in air (dehydratation and the corresponding loss in performance is an important limitation of these materials) have been reported,[37,38] their complicated and relatively expensive configuration require multi-stage processing that involve, for example, sputter deposition of metallic layer electrodes and electrochemical deposition of polymer layers. To overcome the hydratation

problem, ILs have been proposed as the solvents in this kind of electro responsive devices,[39,40] since they have the prospect of being electrolyte salts. Due to the high ionic conductivity and the wide electrochemical window of ILs, polymer-IL composites show electro conductive properties.[41-43] These composites have been already used in the fabrication of electro responsive actuators,[44,45] as conducting membranes for fuel cells,[46] and for the fabrication of thin-film transistors[47] (see, for example, Figure 6-1).

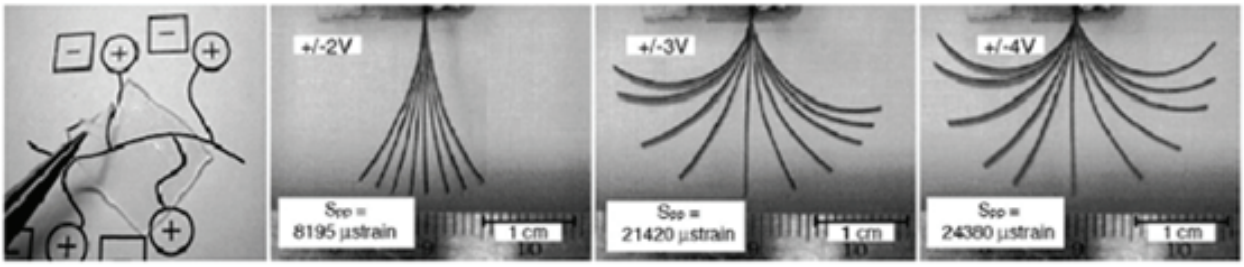

Figure 6-1. *Conductive films and electro responsive actuators prepared from polymerizable ionic liquids or polymer-ionic liquid composites (see, for example, references[42,44,45,47]).*

As described above, research on polymer electrolytes for the fabrication of electro responsive devices has been of great interest in recent years. However, a less explored area in these stimuli-responsive micro and nanotechnologies is the preparation of polymer-magnetic composites. Magnetic actuation has some unique advantages, such as achievable large forces and displacements. Furthermore, magnetic fields can be supplied externally without using wires for current or voltage, allowing the design of wireless devices. For instance, micro devices based on magnetic actuation have been reported in the past.[15,48-50] Magnetic thin films in the nano-meter range have great promise for electronic and electric devices, sensors, electromagnetic shielding, and high density storage.[51] Biomedical applications of such magnetic materials that are being explored include, for example, retinal detachment therapy,[52] cell separations methods,[53,54] tumor hyperthermia,[55] improved MRI diagnostic contrast agents,[56-58] and magnetic field-guided carriers for localizing drugs or radioactive therapies.[59-61] On the one hand, the preparation of polymer-magnetic composites has been achieved by encapsulating magnetic particles into micro and nano-sized polymer beads via heterogeneous polymerization processes.[62,63] On the other hand, the incorporation of magnetic materials (particles) into bulk polymers remains an almost unexplored research area, probably due to the considerable immiscibility shown by the most common magnetic materials with commodity polymers. Recently, ILs have also been used for the stabilization of different heterogeneous systems due to their surface active properties,[64] which allows the homogeneous dispersion of different materials (see, for example, section 4.3) in both ILs and polymer-IL composites.[65] Moreover, ILs have also been used for the preparation of novel magneto responsive materials[66] including polymer-carbon nanotubes composites with enhanced mechanical and electro conductive properties.[67]

So far, all the aforementioned approaches for the design of stimuli-responsive materials based on polymer composites have been proposed in separated paths. The development of material composites which could response to more than one stimuli (*e.g.*, electro and magneto responsive materials) would be of remarkable interest for industry and academia as well as from applications point of view. Such a breakthrough in the development of “smart” materials can be achieved by a combination of the established knowledge about polymers-IL composites used as polymer electrolytes in electro responsive materials,[41-47] on the one hand, with the emerging field of polymer-IL-magnetic composites, on the other hand. These proposed polymer-IL-magnetic composites would be of great interest for several areas of research and technology. For instance, these materials could be readily applied in micro fluidic technologies,[7] electronic devices,[51] control systems, and perhaps in medical therapies.[52-61]

Furthermore, it may be the first time that polymeric composite materials combining both electro and magneto responsive properties are developed and investigated (see, for example, Figure 6-2).

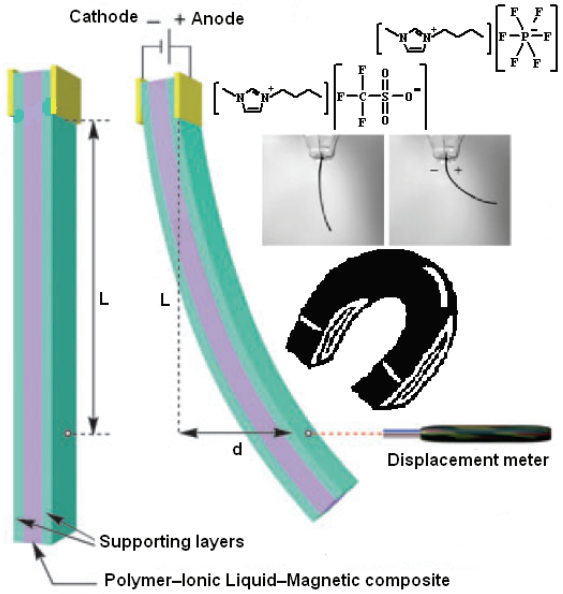

Figure 6-2. *Schematic representation of a micro device (actuator) fabricated with the polymer-ionic liquid-magnetic composites proposed in this work (adapted from reference[44]). These devices can show both electro and magneto responsive characteristics at the same time due to the nature of the proposed composites.*

An important prerequisite for the development of polymer-IL-magnetic composites, is the preparation of dispersions of magnetic particles in ILs as precursor materials for the proposed polymer composites, which is addressed in the next section. Surprisingly, the preparation of the magnetic dispersions in ILs have yielded other types of magnetic materials which, due to their relevance and enormous potential applications, are worth to be analyzed and discussed in detail. Thus, these dispersions of magnetic particles in ILs have allowed the development of a new class of the so-called magnetorheological fluids (MRFs), which have shown outstanding properties. In a subsequent step, these magnetic dispersions can be combined with suitable polymers or polymerized themselves in order to prepare the polymer-IL-magnetic composites proposed. This step is briefly discussed in the last part of the chapter.

6.2 Dispersions of magnetic particles in ionic liquids: A new class of magnetorheological fluids

The preparation of dispersions of magnetic particles in ionic liquids (ILs) is addressed in detail in this section from the point of view of magneto responsive liquids (*e.g.*, control of the viscosity of the fluids by mean of a magnetic field). In the next section, these dispersions are utilized for the preparation of polymer-ILs-magnetic composites, which are analyzed from the point of view of electro and magneto responsive solids (*e.g.*, actuators that can be controlled by means of an electric current or a magnetic field).

Magnetorheological fluids (MRFs) are dispersions of micrometer-sized (from 1 to 20 μm) magnetic particles in a carrier fluid, whose rheological behavior can be controlled by means of a magnetic field.[68-71] Thus, MRFs can change from a liquid to a solid-like state and vice versa almost instantaneously upon applying a magnetic field. MRFs have been used in various technological applications since their first preparation.[72,73] Applications of MRFs include semi-active shock absorbers in the automotive industry, dampers for seismic damage controls in civil engineering, seals, valves, robotics and microelectronic

devices.[74-77] In medicine, MRFs have been proposed for drug delivery and cancer therapeutic methods.[78-81] Current fundamental research on MRFs focuses, mainly, on the settling of dispersed magnetic particles (and re-dispersion phenomena), which may restrict their use in specific applications.[82] To overcome the problem of sedimentation, several strategies have been proposed (*e.g.*, addition of thixotropic agents, surfactants, and nanoparticles, as well as the use of viscoplastic media as carriers, and polymeric core-shell structured magnetic particles).[69,83,84] The sedimentation problem in MRFs is of such importance that it has even been investigated (together with other properties) under microgravity conditions in the outer space.[77,82] From a technological point of view, important aspects of MRFs include the so-called property of "In-Use-Thickening" (IUT) and durability. IUT can be observed when certain MRFs are subjected to high shear rates over prolonged periods of time; in such instances, an initially low viscosity MRF progressively shows a continuous increase in its viscosity until it becomes an unmanageable paste. In specific applications, the durability of MRFs is a more significant aspect than the sedimentation problem.[85] So far, most of the MRFs used in different fields of research and technology have been prepared in certain carriers (such as water, glycols and diverse oils) using a wide variety of additives to reduce settling.[86-89] However, the use of these carriers and additives may limit the potential applications of MRFs in specific areas and increase their cost.

As mentioned above, ILs are substances composed entirely of ions in a liquid state at temperatures below 100 °C.[1] Unlike conventional carriers of MRFs, the properties of ILs (*e.g.*, viscosity, solubility, electric conductivity, melting point, etc.) can be tuned by varying the composition of their ions. In addition, ILs are considered to be very stable and "environmentally friendly" compounds due to their negligible vapor pressure (see ref.[1c] for a detailed description of this property of ILs), negligible flammability (see ref.[1d] for a detailed description of this property of ILs), and liquid state in a broad temperature range.[1a] Nowadays, around 300 ILs are commercially available (and a considerable number of new ILs can be readily synthesized),[1a] covering a wide range of properties. Owing to these characteristics, it is thought that the use of ILs as carriers of MRFs may expand and/or improve their applications in several areas of science and engineering.

A recent study reports on the rheological behavior of suspensions of hematite nanoparticles in an IL.[90] On the one hand, it was found that concentrated suspensions of nanoparticles show non-Newtonian characteristics, including shear thinning and shear thickening, which are probably originated by particle-particle interactions and, on the other hand, it is addressed that suspensions with a low content of nanoparticles follow a Newtonian behavior similar to the one shown by pure IL. However, this study does not provide any information about the magnetorheological behavior of the suspensions and/or the influence of the structure of ILs on the stability of the suspensions against sedimentation. It has also been reported recently that ILs can be used as stabilizing agents in different heterogeneous systems[91,92] (see, for example, section 4.3 for a detailed description of heterogeneous polymerization reactions stabilized by water-soluble ILs). For these reasons, it is thought that the use of ILs as carriers of MRFs may lead to magnetic dispersions which are colloidally stable (against flocculation) and which offer an improved stability against sedimentation (in this report the term stability is used relative to sedimentation, unless otherwise indicated). Based on this hypothesis, MRFs using several ILs as carriers were prepared and characterized (see the experimental section for details). In Table 6-1, the characteristics of the prepared MRFs are summarized (see Table 4-1 and Figure 4-1 for a summary of the properties and chemical structures of the ILs utilized as carriers of MRFs in this investigation).

Figure 6-3a displays the results of the sedimentation measurements of the MRFs of Table 6-1; low sedimentation rates for MRFs containing 25 wt % of micrometer-sized dispersed magnetic particles can be observed. According to these results, MRF3 (carrier IL **2**) revealed an outstanding stability of the dispersed magnetic particles against sedimentation, with a sedimentation ratio of 0.95 over a period of 1680 h (10 weeks) (see experimental section for the definition of sedimentation ratio as used in this work). This finding may turn MRF3 into a highly attractive MRF for applications where the settling of the

dispersion for long periods of time is an important factor to be considered (*e.g.*, seismic dampers). The reasons why MRF3 has shown such an outstanding stability against sedimentation is still under investigation. However, it is thought that this observation might be related to the chemical characteristics of IL **2** and its affinity for the magnetic material, which were used in the preparation of MRF3. A high affinity of the IL for the dispersed magnetic particles might provide sufficient electrostatic repulsion on their surfaces to keep them in suspension for a considerable period of time. The influence of the concentration of the magnetic particles and their size on the colloidal and sedimentation stability of the dispersions was also briefly investigated and the obtained results are depicted in Figure 6-3b.

Table 6-1: *Composition and measured properties of the magnetorheological fluids (MRFs) based on ionic liquids investigated in this work (* values not determined).*

Sample	Ionic liquid	wt % magnetite / type	Density (g cm^{-3})	Saturation / remnant magnetizations (kA m^{-1})
MRF1	1-Ethyl-3-methyimidazolium diethylphosphate (**1**)	25 / micro	1.40	27.9 / 8.95
MRF2	1-Ethyl-3-methyimidazolium diethylphosphate (**1**)	25 / nano	*	* / *
MRF3	1-Butyl-3-methyimidazolium hexfluorophosphate (**2**)	25 / micro	1.67	34.4 / 9.4
MRF4	1-Hexyl-3-methyimidazolium chloride (**3**)	25 / micro	1.23	23.7 / 7.09
MRF5	1-Butyl-3-methyimidazolium trifluoromethanesulfonate (**4**)	25 / micro	1.58	33.7 / 9.60
MRF6	1-Butyl-3-methyimidazolium tetrafluoroborate (**5**)	25 / micro	1.48	30.3 / 8.84
MRF7	AMMOENG 100™ (**6**)	25 / micro	*	* / *
MRF8	1-Ethyl-3-methyimidazolium ethylsulfate (**7**)	25 / micro	1.51	32.3 /10.0
MRF9	Trihexyltetradecylphosphonium chloride (**8**)	25 / micro	1.12	24.1 / 7.93
MRF10	Trihexyltetradecylphosphonium chloride (**8**)	8.5 / micro	0.95	7.03 / 2.40
MRF11	Trihexyltetradecylphosphonium chloride (**8**)	2 / micro	0.91	* / *
MRF12	Trihexyltetradecylphosphonium chloride (**8**)	0.2 / micro	0.89	0.13 / 0.04

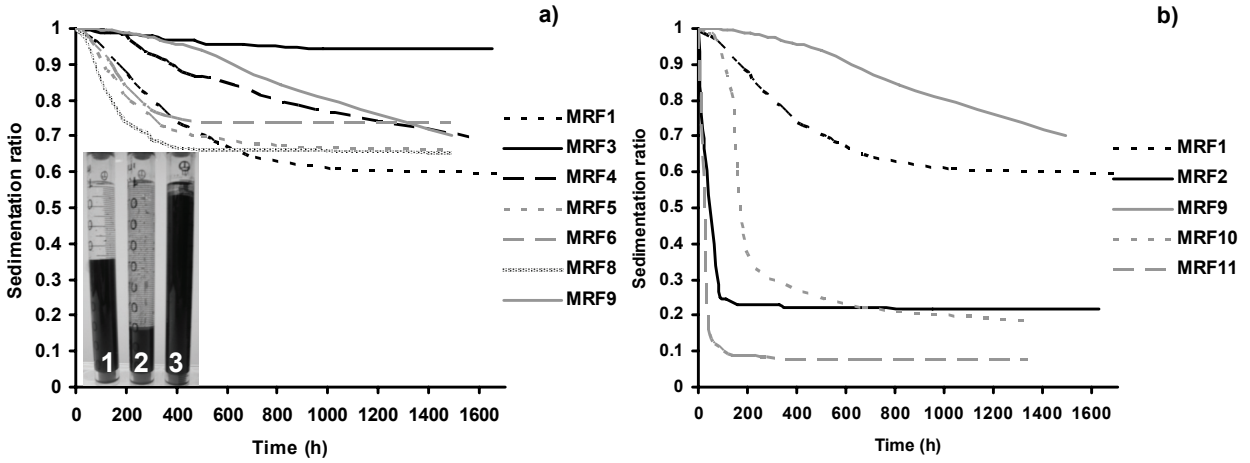

Figure 6-3: *Sedimentation measurements of the magnetorheological fluids (MFRs) based on ionic liquids (ILs) given in Table 6-1. (a) displays MRFs with slow sedimentation rates, whereas MRFs with fast sedimentation rates shown in (b). The inset in (a) displays an image of the measurements after 1680 h; the numbers 1, 2 and 3 correspond to MRF1, MRF2 and MRF3 (Table 6-1), respectively.*

Regarding the influence of the particle size, Figure 6-3b reveals that MRF2, which is composed of magnetic nanoparticles dispersed in IL **1**, showed a fast sedimentation rate. When particles in the micrometer range are used, at the same concentration and in the same carrier, the stability of the dispersions improved remarkably (*e.g.*, MRF1). The use of nanoparticles for magnetic dispersions leads to the so-called ferrofluids (*i.e.*, dispersions of magnetic nanoparticles in a liquid carrier),[93-95] which must be stabilized against aggregation, for example by using surfactants, as describe in the literature.[93-95] The goal of preparing MRF2 was to investigate whether the use of an IL (IL **1**) as carrier could itself provide sufficient colloidal stability to the dispersed nanoparticles; however, this could not be observed

under the experimental conditions used for investigation. A possible method that may lead to the preparation of colloidally stable ferrofluids in ILs would be to perform the synthesis of the magnetic nanoparticles *in-situ* (directly in ILs) in a similar way as reported for the preparation of conventional ferrofluids[96] and/or other inorganic nanoparticules in ILs.[92] Nevertheless, such investigations are beyond the scope of this work. The study of ILs containing magnetic ions has been reported in recent years.[97-103] Even though these materials have similar characteristics to other ILs (*e.g.*, negligible vapor pressure, negligible flammability, liquid state in a broad temperature range, etc.) and have shown a strong response to a magnetic field, their magnetorheological behavior have not been disclosed in detail.[103] ILs containing magnetic ions are described as single-component materials free from phase separation and therefore it is thought that they may have a behavior similar to the so-called magnetic fluids or ferrofluids,[103] in which the rheological changes under the influence of a magnetic field may not be so pronounced as in the case of MRFs limiting their application in certain areas.[82]

Regarding the concentration effect of the particles on the settling phenomenon of the dispersions, Figure 6-3b reveals an inverse relationship between the particle content and the sedimentation rate. This is due to the fact that interactions between the particles are stronger at higher concentrations and decrease the sedimentation velocity. For example, it is thought that for suspensions containing a high concentration of hematite nanoparticles in an IL, the particle-particle interactions are much stronger than in the low-concentration cases, which may be responsible for the non-Newtonian behavior observed in such systems.[90] For instance, MRF9 (25 wt % of dispersed micrometer-sized magnetic particles in IL **8**) revealed a considerable lower sedimentation rate than MRF11 (2 wt % of dispersed micrometer-sized magnetic particles in the same IL); an intermediate case, MRF10 (8.5 wt % of dispersed micrometer-sized magnetic particles in IL **8**), is also displayed in Figure 6-3b. Summarizing this point, Figure 6-3a shows that the use of ILs as carriers in dispersions of micrometer-sized magnetic particles allow the preparation of MRFs with improved stability against sedimentation in the absence of anti-settling additives (at least under the experimental conditions investigated).

MRF2 and MRF7 (Table 6-1) were not completely investigated due to their physical characteristics: MRF2 was colloidally unstable (as revealed in Figure 6-3b) and MRF7 showed a considerable IUT[82,85] during the preparation procedure. However, MRF7 recovered its original consistency after a prolonged period of time (30 days) at rest and, thus, its rheological characterization could be performed.

Table 6-1 summarizes the densities and magnetic properties of the MRFs investigated. The values of saturation magnetization (Ms) and remnant magnetization (Mr) of the MRFs reported in Table 6-1 were calculated by dividing the magnetic moments of the samples (as obtained from the magnetization measurements) by their corresponding volumes (which were estimated from mass and density measurements). The Ms values were estimated by measuring the maximum values of magnetization in the magnetic hysteresis loops (see Figure 6-4a). Similarly, the Mr values were estimated to be the intercept of the magnetization with the ordinate (see Figure 6-2a). The coercive field (Hc) values were estimated to be at the interception of the magnetization curve with the abscissa (see Figure 6-4a). Figure 6-4a shows the magnetic hysteresis loop for MRF3 (which is representative for the rest of MRFs of Table 6-1 containing 25 wt % of micrometer-sized magnetic particles dispersed in the investigated ILs). Magnetization measurements of the pure ILs were performed in order to investigate whether the utilized ILs as carriers have any influence on the magnetic properties of the prepared MRFs. Figure 6-4b displays the results of these measurements for IL **4**, IL **8**, and an empty sample holder which shows the diamagnetic character of the analyzed ILs. Thus, it is considered that they have practically no contribution to the magnetic properties of their corresponding MRFs. However, it has been reported that ILs containing magnetic ions will be magnetized in the presence of a magnetic field[103] and their use as carriers of MRFs certainly may show an influence on the magnetorheological response of the corresponding dispersions. These investigations are beyond the scope of this work and may be subject for future research in the field.

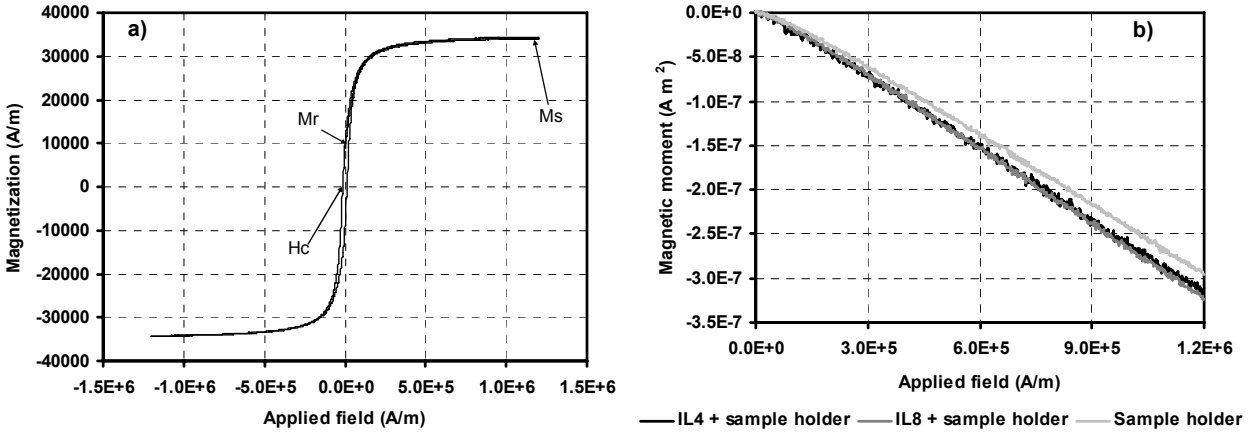

Figure 6-4: *(a) Magnetic hysteresis loop of magnetorheological fluid MRF3 (Table 6-1). (b) Magnetization measurements of a sample holder and ionic liquids* ***4*** *(1-butyl-3-methyimidazolium trifluoromethanesulfonate) and* ***8*** *(trihexyltetradecylphosphonium chloride) with their respective sample holders reveal the diamagnetic properties of these materials.*

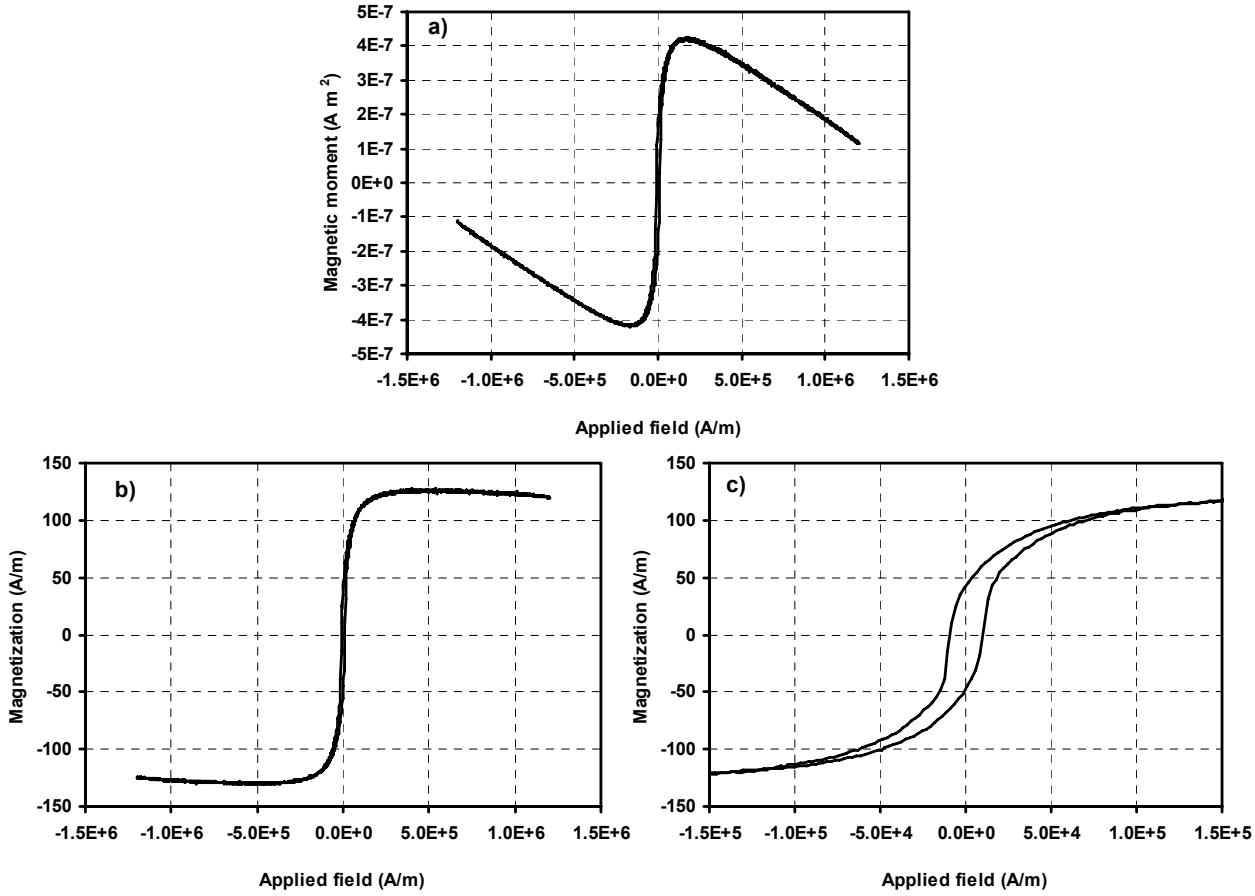

Figure 6-5: *(a) Magnetic hysteresis loop for magnetorheological fluid MRF12 (0.02 wt. % of magnetite dispersed in IL* ***8****; Table 6-1). (b) Corrected magnetic hysteresis loop for the sample magnetorheological fluid MRF12; plot (c) displays a zoom in of plot (b).*

When a magnetic field is applied to MRFs, the interactions between their magnetic particles become much stronger, so that complex structures in the form of thick chains of magnetic particles develop.[82,104] To study this phenomenon for the systems investigated here, a dilute dispersion of magnetic particles in IL **8** (MRF12; Table 6-1) was subjected to magnetization measurements and optical microscopy (a low concentration of particles in the fluids was used in these studies allowing a better observation of the

dispersions). In the case of magnetization measurements, the diamagnetism of the sample holder was observed due to the low concentration of magnetic particles in the sample, as shown in Figure 6-5a. For this reason a correction on the magnetic loop of Figure 6-5a was necessary in order to determine the magnetic properties of the sample. This correction was performed by subtracting the magnetic moments of the sample holder containing the carrier IL **8** (see Figure 6-4b) from the magnetic loop of Figure 6-5a and its result is shown in Figure 6-5b. Figure 6-5c shows in detail the corrected magnetic loop of MRF12. Finally, from Figures 6-5b and 6-5c the magnetic properties (Ms, Mr, and Hc) of MRF12 were determined and summarized in Table 6-1.

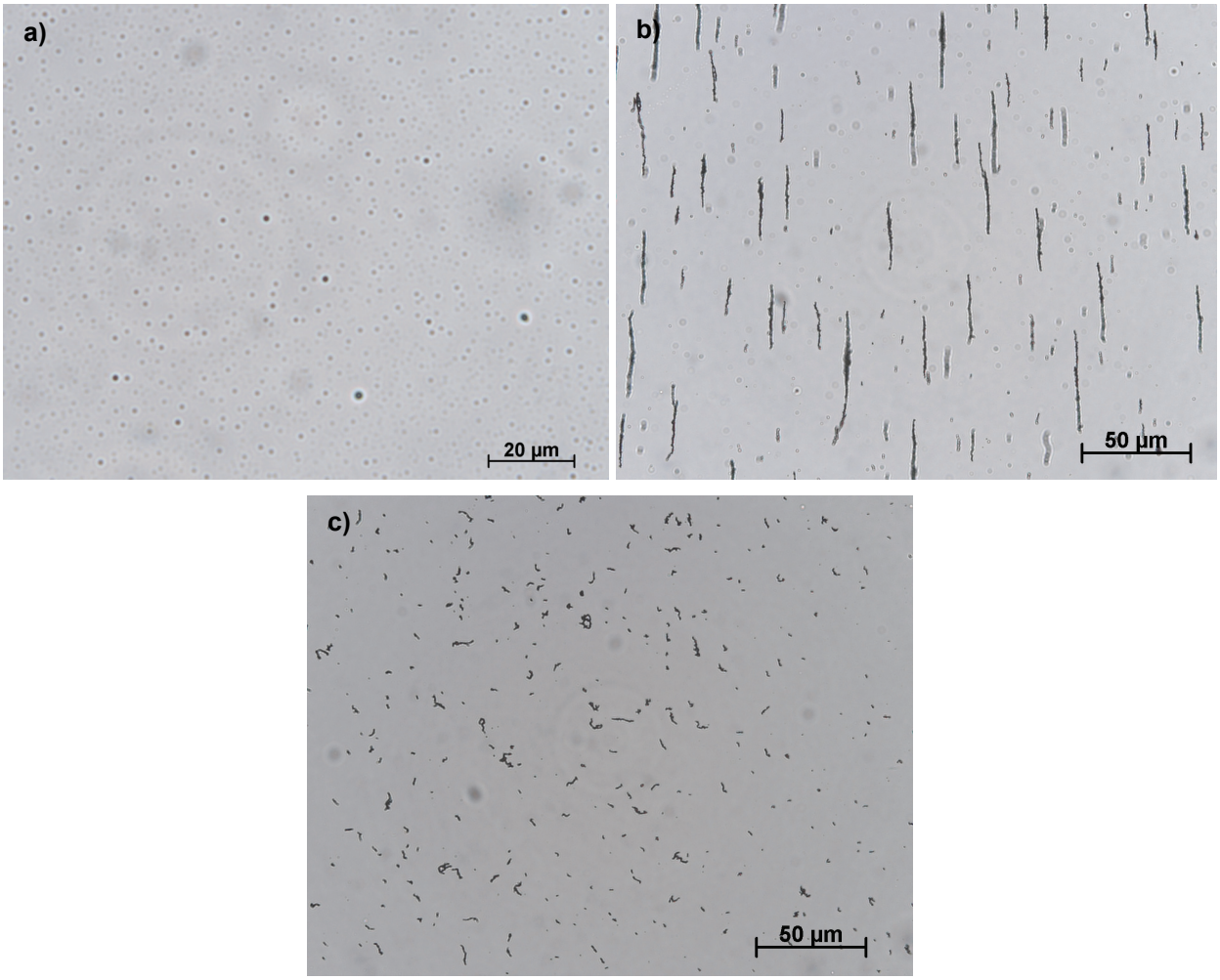

Figure 6-6: *Optical microscopic images of magnetorheological fluid MRF12 at room temperature are displayed: (a) Fluid in the absence of a magnetic field, (b) fluid in the presence of a magnetic field (note that the rod-like structures are aligned parallel to the direction of the applied magnetic field), and (c) fluid immediately after removing the magnetic field.*

It is thought that the hysteresis observed in the magnetic loops of the investigated MRFs (illustrated in Figures 6-4a and 6-5c) is related to the aggregation process of the magnetic particles and the slow reversibility in the presence and the absence of a magnetic field, respectively.[82] This phenomenon is illustrated in the images displayed in Figure 6-6. Figure 6-6a shows MRF12 in the absence of a magnetic field whereas Figure 6-6b shows it in the presence of a magnetic field. Figure 6-6c shows the remnant aggregation of magnetic particles. These small aggregates observed still had a magnetic moment but it was considerably smaller than the one in the presence of a magnetic field. The observed coercive field H_C (shown, for example, in the magnetic loop of Figure 6-4a), was around –13 kA m^{-1} for all investigated

MRFs, except for MRF12 (sample at diluted conditions) which revealed a value of –8.9 kA m^{-1}. These results confirm that the magnetic hysteresis is due the aggregation/redispersion process of magnetic particles, which, in turn, are influenced by their concentration in the fluid. Nevertheless, even though the use of MRFs with a low concentration of magnetic particles facilitates their study by optical methods, it is thought that the aggregation process of the magnetic particles may be different in concentrated MRFs than in diluted conditions.[82] In fact, it is reported that lateral attractions between the chains of particles increases with the concentration of the dispersion.[82] It was also observed that the time scale of the formation of the microstructures in MRFs is on the order of several hundred milliseconds, which increases with higher viscosities of the carrier liquid and with decreasing concentration of magnetic particles in the fluid.[82]

Owing to the strong aggregation of magnetic particles in the presence of a magnetic field, MRFs show considerable changes in their rheological behavior. With regard to this property, magnetorheological measurements of the MRFs investigated were performed at constant temperature (25 °C). For these measurements only MRFs with a content equal to or greater than 8.5 wt % of micrometer-sized magnetic particles were analyzed.

One of the most intuitive starting points in the study of the magnetorheological behavior of the investigated MRFs would be the measurement of their rheological properties in the absence of a magnetic field. Basically, there are two contributions to the rheological behavior of the MRFs investigated: The contribution of the carriers (ILs as pure substances) and the contribution of the magnetic particles dispersed in the fluid. On one hand, it is known that most of the ILs are typically more viscous than common organic solvents (see, for example, Table 4-1), that small amounts of impurities can have important effect on their viscosity, and that, in general, most ILs show Newtonian behavior (a few examples are known where ILs form a liquid crystalline phase, which show a thixotropic behavior).[90,105,106] On the other hand, it has been reported in literature that the viscosity of suspensions, in both, ILs[90] and conventional solvents,[94] will differ from that of the carrier liquid due to the presence of the suspended particles. Thus, the viscosity of the MFRs investigated in the absence of a magnetic field is determined by the viscosity of the carrier liquid (ILs) and the volume fraction of suspended magnetic material (ϕ) according to established theories of the viscosity of suspensions. These established models include: Einstein's equation of viscosity for highly diluted suspensions,[94] the modification performed by Batchelor to the Einstein's equation for more concentrated magnetic fluids ($0.1 < \phi < 0.27$),[94] the extension of Rosensweig to Batchelor's equation for relatively concentrated systems (ϕ of the order of 0.3),[94] and Pshenichnikov's approach for fluids with a high content of suspended particles (ϕ up to approximately 0.6).[94] Other rheological models for suspensions are also described in literature (see, for example, ref.[90]). Rheological measurements in the absence of a magnetic field at 25 °C revealed that the MRFs investigated in this work show "quasi-Newtonian" behavior. In other words, the dispersions show a slightly pseudo-plastic behavior (shear thinning) at low shear rates as revealed in Figure 6-7a. However, the dispersions become Newtonian-like (linear dependences in shear stress *vs.* shear rate plots) for shear rates greater than 16 s^{-1} as illustrated in Figure 6-7b. Figure 6-7c displays a logarithmic plot of the apparent viscosity *vs.* shear rate for the analyzed MRFs. The influence of the concentration of the dispersed magnetic particles on the measured rheological properties can also be seen in the plots shown in Figure 6-7 for the samples MRF9 and MRF10 (25 and 8.5 wt. % of particles, respectively, both in IL **8**; Table 6-1). As expected, Figure 6-7c reveals lower viscosity values for the less concentrated dispersion (MRF10) especially at low shear rates. Similar observations have been recently reported in literature for relatively high contents of hematite nanoparticles dispersed in an IL.[90] Those investigations were performed at 40 °C and varying the content of nanoparticles dispersed. It was concluded that in the high shear range the suspensions reveal Newtonian flow behavior and that the increase in the concentration of particles of the suspensions will lead to an increase in the shear stress and in the yield stress (similar to Figures 6-7a and 6-7b for samples MRF9 and MRF10). Thus, it is

thought that the development of the yield stress is determined by the content of particles, and therefore, by the median distances between them.[90] As the content of solids in the suspensions increases so does the interactions between the particles. Therefore these interactions have to be overcome until the yield stress is reached and as soon as they are diminished the rheological behavior of the suspensions becomes Newtonian. In the plots displayed in Figure 6-7 the influence of varying the structure of ILs in the suspensions can also be seen. For example, ILs containing more bulky cations (ILs **3**, **6** and **8**) are expected to show higher viscosities (see, for instance, Table 4-1 and Figure 4-1) and shear stresses, and therefore, their corresponding suspensions (MRFs 4, 7 and 9; Table 6-1) will also show higher viscosities and shear stresses than suspensions prepared in ILs containing less bulky ions (as shown in the plots displayed in Figure 6-7).

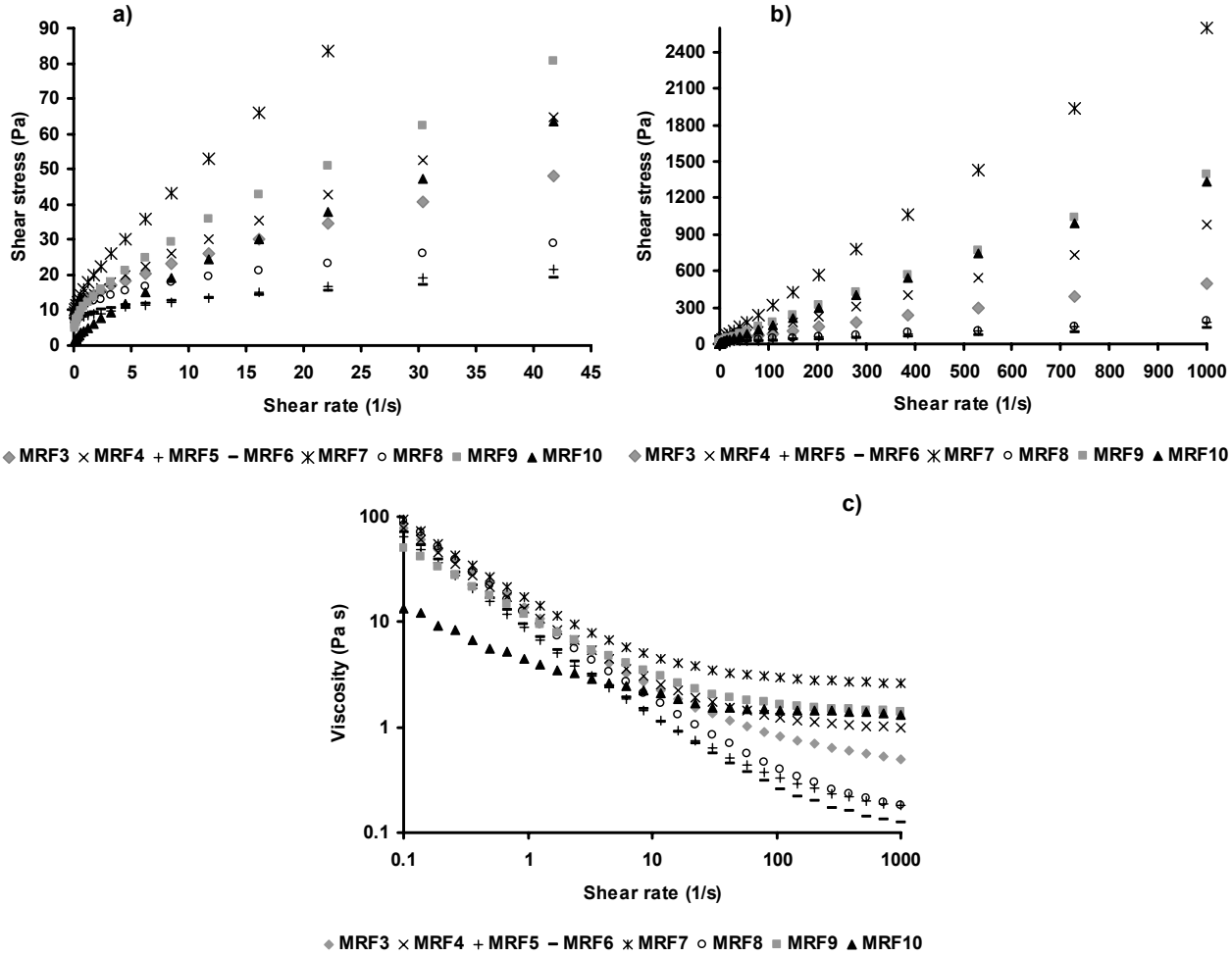

Figure 6-7: *Rheological measurements of magnetorheological fluids (MRFs) based on ionic liquids (ILs) (Table 6-1) in the absence of a magnetic field at 25 °C. (a) and (b) display shear stress vs. shear rate plots showing a slight pseudo-plastic behavior (shear thinning) at low shear rates and a Newtonian behavior (linear dependences) for shear rates greater than 16 s^{-1}, respectively. (c) shows a logarithmic plot of the apparent viscosity vs. shear rate.*

The plots displayed in Figure 6-8 illustrate the magnetorheological behavior of the MRFs investigated, which reveal that their shear stress and apparent viscosity values increase as the intensity of the applied magnetic field increases up to values where quasi-saturation of magnetization of the samples is approached (see, for instance, Figure 6-4a). The presence of a magnetic field considerably changes the interactions between the magnetic particles in the MRF, leading to the formation of complex microstructures in the form of thick chains (as shown in Figure 6-6b), which consequently lead to significant changes in the viscous behavior of the fluid.[82,104]

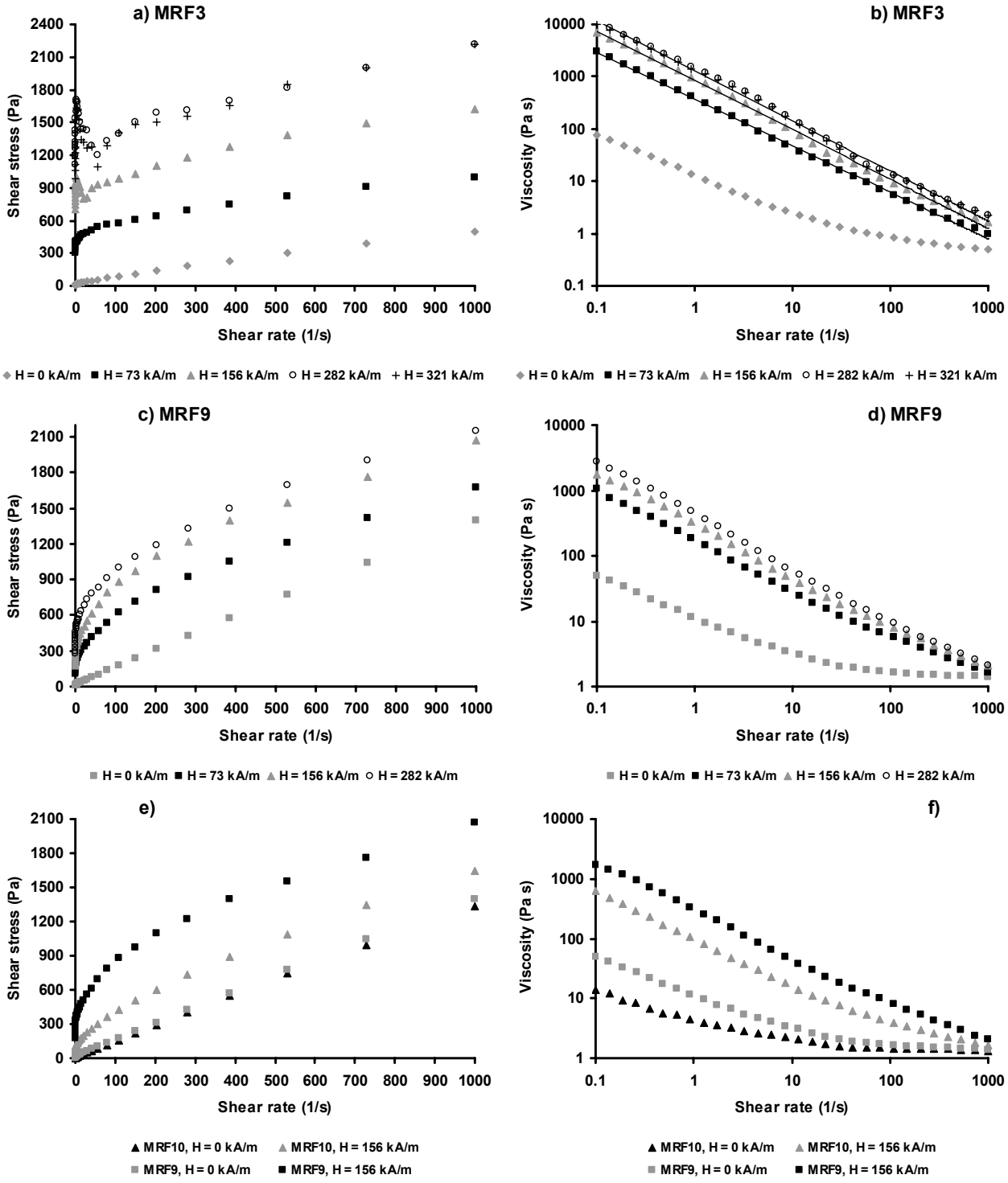

Figure 6-8: *Rheological measurements of magnetorheological fluids (MRFs) based on ionic liquids (ILs) (Table 6-1) in the presence of magnetic fields of different intensities at 25 °C. Solid lines in (b) fit the experimental data obtained of apparent viscosity to the power law model. (e) and (f) reveal the influence of the content of magnetic particles on the magnetorheological effect in MRFs containing the same carrier (MRF9 and MRF10, 25 and 8.5 wt % of magnetic particles dispersed in IL* ***8****, respectively).*

In Figures 6-8a and 6-8b it can be seen that the maximum shear stresses and viscosity values are reached with a magnetic field of 282 kA m^{-1}; as the saturation of the sample was already reached, the use of higher intensities (321 kA m^{-1}) does not have a significant effect on the rheological properties.

Note that the MRFs investigated show a plastic or Bingham-type behavior in the presence of a magnetic field (plots displayed in Figure 6-8) and the observed yield stress (minimum shear stress below which no shear flow takes place) depends on the strength of the applied magnetic field as reported in the literature.[82] Figures 6-8a and 6-8c also show that, depending on the IL used during the preparation of the magnetic dispersions, the corresponding MRF can show highly non-linear behavior in the shear stress *vs.* shear rate plots (Figure 6-8a, MRF3 at low shear rates and relatively high intensities of magnetic field) in addition to the aforementioned Bingham-type behavior (Figure 6-8c). Note that the observed singular behavior in the flow curve of Figure 6-8a (MRF3) at low shear rates and relatively high intensities of a magnetic field has been previously reported and explained for some cases of the so-called electrorheological fluids (ERFs).[107-111] These situations show that the shear stress developed by the applied magnetic field (or electric field in the cases of ERFs) slightly decreases as the shear rate increases up to a certain transition value, and thereafter it starts to increase again. Similar to the cases reported for ERFs,[108] in the plot of the MRF displayed in Figure 6-8a, these transition points were observed at higher shear rates when the magnetic field strength was increased. The decrease in shear stress below a critical shear rate might be a consequence of the destruction rate of the particle chain structures exceeding the reformation rate of the particle chains, as the shear rates are increased.[111] This may be the first time that such situation has been observed for a MRF. The data for the apparent viscosities obtained from the measurements at different magnetic field intensities of the MRFs investigated obey the power law model (as shown by the solid lines in Figure 6-8b), which is one of the simplest and most frequently used models for describing non-Newtonian fluids.[112] The influence of the content of the dispersed magnetic particles in the MRFs investigated on their rheological properties in the absence and presence of a magnetic field is depicted in Figures 6-8e and 6-8f. As expected, the lower the magnetic material content in a same carrier (IL **8**) is, the lower the aggregation is between the magnetic particles and, as a result, lower values of apparent viscosity and shear stress (less pronounced magnetorheological effects) are observed for a fixed intensity of magnetic field.

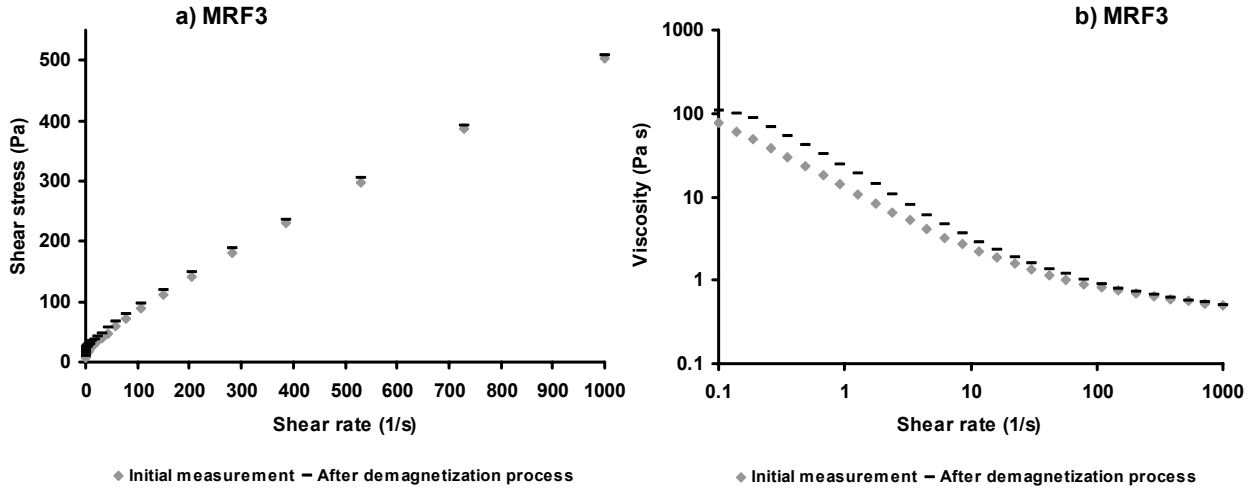

Figure 6-9: *Rheological measurements of a magnetorheological fluid MRF3 (Table 6-1) in the absence of a magnetic field at 25 °C. The plots show the quasi-reversibility of the magnetorheological phenomenon for MRF3 (an initial measurement before the application of any magnetic field and another one of the sample after being magnetized for the magnetorheological measurements followed by a demagnetization process were performed).*

Finally, the plots displayed in Figure 6-9 show rheological measurements of MRF3 (Table 6-1): An initial measurement performed before the application of any magnetic field and another measurement of the sample after being temporarily magnetized for the magnetorheological measurements followed by a demagnetization process. Both measurements in the plots shown in Figure 6-9 reveal only slight differences from each other, confirming that the observed magnetorheological effect is a quasi-reversible

process, which is not observed in the absence of a magnetic field. These slight differences can be attributed to the remnant magnetization (see, for example, the hysteresis observed in the magnetic loop displayed in Figure 6-4a) shown by the fluids, which is related to the presence of residual small aggregates of magnetic particles as discussed before and shown in Figure 6-6c. The contribution of these small aggregates to the rheological behavior of the fluid is considerably less significant in comparison to their contribution observed in the presence of a magnetic field. The disappearance of the remaining aggregates may occur when the time between measurements is sufficiently long and/or where the shear rates are strong enough to break them apart (as depicted in the plot displayed in Figure 6-9b for high shear rates).

6.3 Polymer-ionic liquid-magnetic composites based on dispersions of magnetic particles in ionic liquids

As mentioned in section 6.1, the preparation of dispersions of magnetic particles in ionic liquids to be used as precursor materials for the synthesis of novel polymer-IL-magnetic composites surprisingly yielded a new class of the magnetorheological fluids, which have been addressed in detail in the previous section due to their novelty and their importance from the application point of view. In this section, these magnetic dispersions in ILs are combined with a polymer in order to prepare the polymer-IL-magnetic composites proposed originally.

As addressed in the previous section, the content and type of magnetic particles dispersed in the respective carriers will mainly determine the magnetic properties of the corresponding composite materials. In general, the higher the content of magnetic material, the higher the response of the composite to a magnetic field (see, for example, Figures 6-8e and 6-8f). However, the effective and homogeneous dispersion of magnetic materials in polymer matrices (carriers) requires specialized heterogeneous preparation methods which have to use diverse emulsifiers.[62,63] Hence, an effective and homogeneous dispersion process is necessary for the preparation of polymeric composite materials with homogeneous magnetic properties. In addition to the use of ILs as surfactants to stabilize heterogeneous systems described in section 4.3 and for the preparation of remarkably stable magnetorheological fluids based on ILs described above, in section 4.2 and in chapter 5, it has been addressed that several polymers form homogeneous mixtures with certain ILs. Thus, it is thought that the combination of a suitable magnetorheological fluid based on ILs with a proper polymer might yield a homogeneous dispersion of magnetic particles in a polymer-IL matrix. The polymer-IL-magnetic composites derived from this process are expected to show both electro and magnetic responsive characteristics (see, for example, Figure 6-2).

Regarding the preparation of the polymer-IL-magnetic composites proposed in this work, three approaches can be investigated. (1) In the first preparation method, the direct blending of ILs with compatible polymeric materials in the presence of magnetic particles can be performed at temperatures well above the *Tg* of the utilized polymers. The main drawback of this approach is that due to the high viscosities of the systems the dispersion of the magnetic particles might be ineffective, which may result in non-homogeneous composites and affect mainly the magnetic properties of the composites. (2) The second preparation method is similar to the first approach; however, in this method the use of a co-solvent is required to achieve the blending between the involved components. This method has been previously described in literature for the preparation of polymer-IL composites as polymeric electrolyte materials.[43] Similar to the first approach, in this approach previously synthesized polymeric materials are mixed with compatible ILs (in the cases of block copolymers, ILs have to be miscible with at least one of the blocks of the copolymer) via dissolution in a thermodynamically good co-solvent for the involved components.[43] Thereafter, the co-solvent is removed by evaporation at ambient temperature followed by

treatment in a vacuum oven at higher temperatures. The main drawback of this technique is the use of volatile organic compounds which can also be a restriction for certain applications of the composites due to the potential toxicity of the organic solvents. Moreover, the use of diluted systems during the fabrication of the polymer-IL-magnetic composites can lead to a faster sedimentation of the dispersed magnetic particles before the complete removal of the co-solvent which can lead to non-homogeneous dispersions. (3) The third preparation method is based on performing *in-situ* homogeneous polymerization reactions in dispersions of magnetic particles in ILs previously prepared, using similar approaches to the described in section 4.2.

Due to the aforementioned drawbacks of the first two preparation methods of the polymer-IL-magnetic composites proposed, only the third preparation method is considered in this investigation. Nevertheless, the second technique may be worth investigating in future research due to the fact that it can facilitate the processability of these composites by techniques such as inkjet printing[22,113,114] and/or micro-pattering[115] aiming at the fabrication of well-defined devices in the micrometer range based on the materials proposed. Under the scope of the third approach, homogeneous polymerization reactions, such as “living” cationic ring opening and controlled/free radical polymerizations (see, for instance, section 4.2), in magnetic dispersions based on ILs can be performed for the preparation of polymer-IL-magnetic composites.

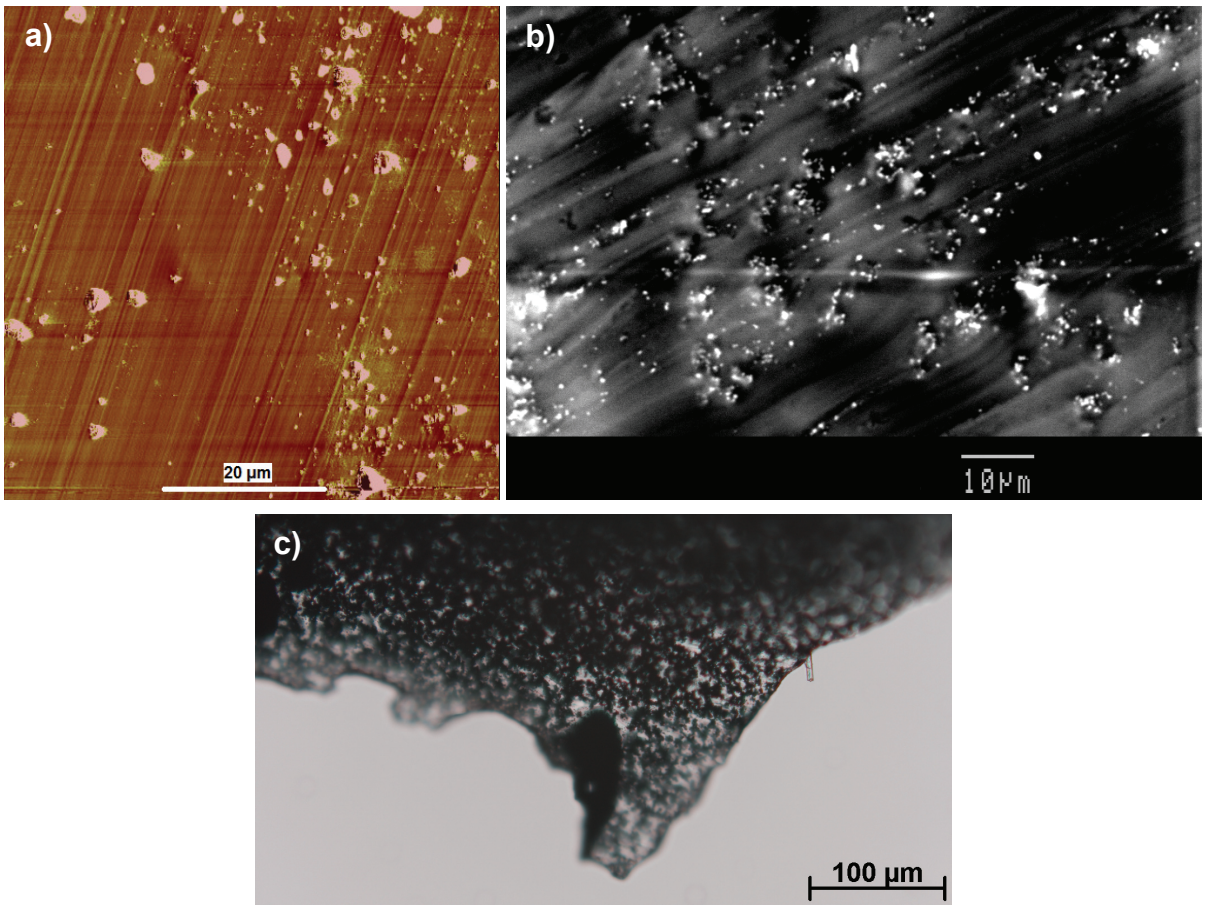

Figure 6-10: *Microscopic images showing micrometer-sized magnetic particles homogeneously dispersed in a poly(methyl methacrylate) / 1-butyl-3-methyimidazolium trifluoromethanesulfonate (PMMA / IL **4**) matrix. The PMMA-IL **4**-magnetic composite is formed by 32 wt % of PMMA, 45 wt % of IL **4**, and 23 wt % of micrometer-sized magnetic particles. (a), (b), and (c) micrographs were recorded using atomic force, scanning electron, and optical microscopes, respectively; white clusters in images (a) and (b) correspond to the magnetic particles.*

To investigate whether the third method described above would allow the preparation of homogeneous polymer-IL-magnetic composites, the free radical polymerization of methyl methacrylate (MMA) initiated by 2,2'-azo*bis*isobutyronitrile (AIBN) was performed in a dispersion of magnetic particles (micrometer-sized) in IL **4** (1-butyl-3-methylimidazolium trifluoromethanesulfonate) (see experimental part for details). As addressed in chapters 4 and 5, poly(methyl methacrylate) (PMMA) is soluble in IL **4**. Hence, the polymerization reaction of MMA performed in a magnetic dispersion based on IL **4** has yielded a homogeneous PMMA-IL **4**-magnetic composite. Figure 6-10 displays microscopic images of a PMMA-IL **4**-magnetic composite (32 wt % of PMMA, 45 wt % of IL **4**, and 23 wt % of micrometer-sized magnetic particles) prepared by the method described; in the micrographs it can be observed that the magnetic particles are homogeneously dispersed in the PMMA-IL **4** matrix. This demonstrates that homogeneous polymer-IL-magnetic composites can be easily prepared by the investigated method.

The plots displayed in Figure 6-11 show that the investigated PMMA-IL **4**-magnetic composite (32 wt % of PMMA, 45 wt % of IL **4**, and 23 wt % of micrometer-sized magnetic particles) responds to magnetic fields of different intensities (Figure 6-11a) and is an electric conductive material (Figure 6-11b). From the magnetic hyteresis loop displayed in Figure 6-11a it was found that the saturation and the remnant magnetizations, and the coercive field of the investigated PMMA-IL **4**-magnetic composite were 22.4, 4.5, and −12 kA m^{-1}, respectively.

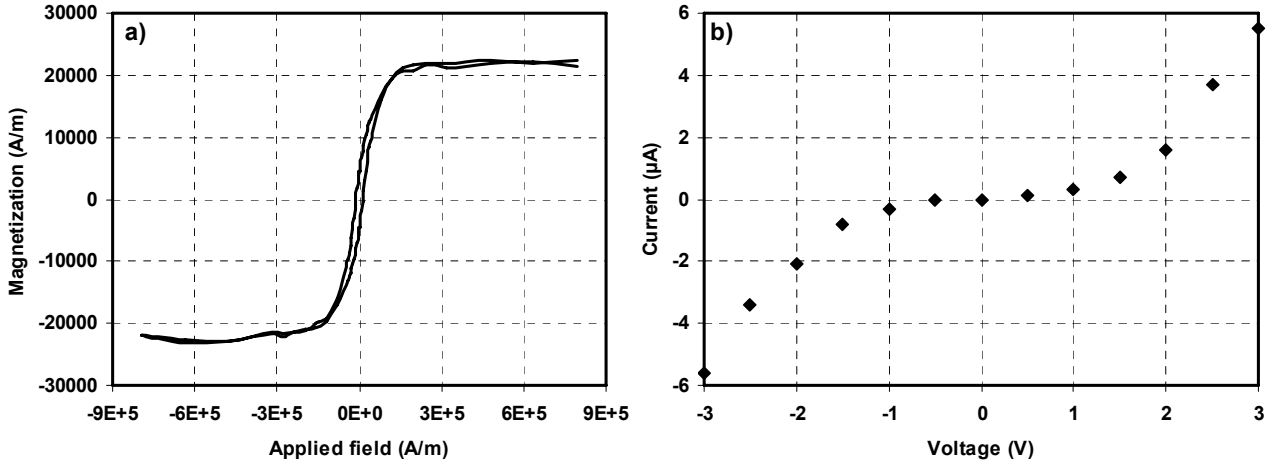

Figure 6-11: *(a) Magnetic hysteresis loop of a poly(methyl methacrylate) / 1-butyl-3-methyimidazolium trifluoromethanesulfonate / magnetic (PMMA-IL **4**-magnetic) composite. The PMMA-IL **4**-magnetic composite is formed by 32 wt % of PMMA, 45 wt % of IL **4**, and 23 wt % of micrometer-sized magnetic particles. (b) Electro conductive properties of this composite material.*

Note that the amount and the molecular characteristics of polymer synthesized in the magnetic dispersion based on IL will mainly determine the mechanical and electro conductive properties of the composite. Thus, large amounts of polymer will lead to harder composites, whereas small amounts can lead to rubber-like composites (plasticizing effect of ILs),[3] and even to gel-like composites.[43] Composite materials containing larger amounts of IL will show higher electro conductive properties up to values close to the electro conductivity values of pure IL. In addition to the fact that homogeneous polymer-IL-magnetic composites can be obtained by the preparation technique proposed, the properties of the composite materials, both mechanical and electro conductive, can be readily manipulated by varying the reaction conditions of the polymerizations, the amount and type of IL, the architecture of the polymer synthesized (*e.g.*, linear, graft, star-shaped, cross-linked polymers, etc.), type of polymer (*e.g.*, PMMA, poly(2-ethyl-2-oxazoline), poly(ethylene glycol), poly(acrylonitrile), etc) as well as the size and the amount of magnetic particles. For instance, polymerizable ILs can also be used to prepare the polymer-IL-magnetic composites proposed using similar approaches as reported in the literature[42,116,117]

and incorporating a suitable magnetic material. In this regard, the free radical polymerization of the dicationic salt 1,4-di(vinylimidazolium)-butane dichloride ($C_4(vim)_2$-Cl_2) initiated by AIBN was performed in the presence of dispersed magnetic particles (micrometer-sized) (see experimental part for details). The material obtained from this polymerization reaction is a cross-linked system. The plots displayed in Figure 6-12 show that the poly(1,4-di(vinylimidazolium)-butane dichloride)-magnetic ($PC_4(vim)_2$-Cl_2-magnetic) (77 wt % of $PC_4(vim)_2$-Cl_2 and 23 wt % of micrometer-sized magnetic particles) composite synthesized also responds to magnetic fields of different intensities (Figure 6-12a) and is also an electric conductive material (Figure 6-12b). From the magnetic hysteresis loop displayed in Figure 6-12a it was found that the saturation and the remnant magnetizations, and the coercive field of the $PC_4(vim)_2$-Cl_2-magnetic composite investigated had values of 17.9, 3.7, and −15.9 kA m^{-1}, respectively.

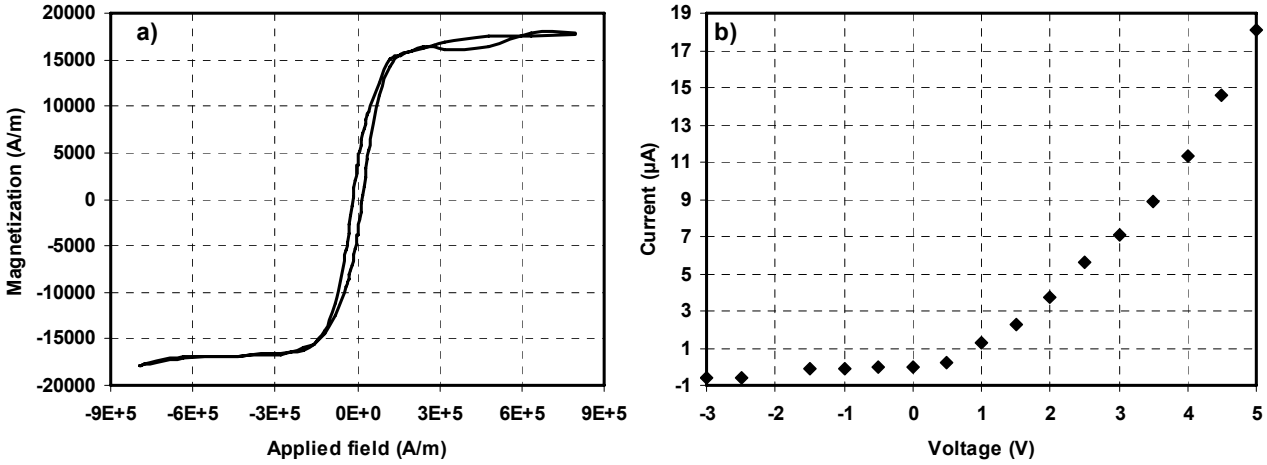

Figure 6-12: *(a) Magnetic hysteresis loop of a poly(1,4-di(vinylimidazolium)-butane dichloride)-magnetic ($PC_4(vim)_2$-Cl_2/magnetic) composite. The $PC_4(vim)_2$-Cl_2/magnetic composite is formed by 77 wt % of $PC_4(vim)_2$-Cl_2 and 23 wt % of micrometer-sized magnetic particles. (b) Electro conductive properties of this composite material.*

The magnetic properties of the polymer-IL-magnetic composites will be mainly ruled by the magnetic properties of the particles used during their preparation procedure. In the materials discussed above (Figures 6-11 and 6-12), micrometer-sized magnetic particles (magnetite) have been utilized for the preparation of the polymer-IL-magnetic composites. However, the use of nanometer-sized magnetic particles of the same material have yielded polymer-IL-magnetic composites with less pronounced hyteresis in their respective magnetic loops in comparison to the cases where micrometer-sized particles are utilized. This effect is illustrated in Figure 6-13 for the cases of PMMA-IL **4**-magnetic composites formed by 32 wt % of PMMA, 45 wt % of IL **4**, and 23 wt % of micrometer- or nanometer-sized magnetic particles. A similar effect has also been observed for the cases of $PC_4(vim)_2$-Cl_2-magnetic (77 wt % of $PC_4(vim)_2$-Cl_2 and 23 wt % of micrometer- or nanometer-sized magnetic particles) composites. From the magnetic hyteresis loops displayed in Figure 6-13 it was found that the saturation and the remnant magnetizations, and the coercive field of the PMMA-IL **4**-magnetic composite formed by nanometer-sized magnetic particles had values of 26, 1.8, and −4 kA m^{-1}, respectively. In a similar way, it was found that the saturation and the remnant magnetizations, and the coercive field of the $PC_4(vim)_2$-Cl_2-magnetic composite formed by nanometer-sized magnetic particles had values of 16.9, 1.6, and −4 kA m^{-1}, respectively. The decrease of hysteresis in these latter cases is thought to be related to the fact that the nanometer-sized magnetic particles resemble more to magnetic single domains than the micrometer-sized magnetic particles. Hence, the magnetic moments created in the composites during the magnetization measurements vanish more effectively in the absence of a magnetic field in the

cases of nanometer-sized magnetic particles, which is responsible for the hysteresis decrease observed and depicted in Figure 6-13.

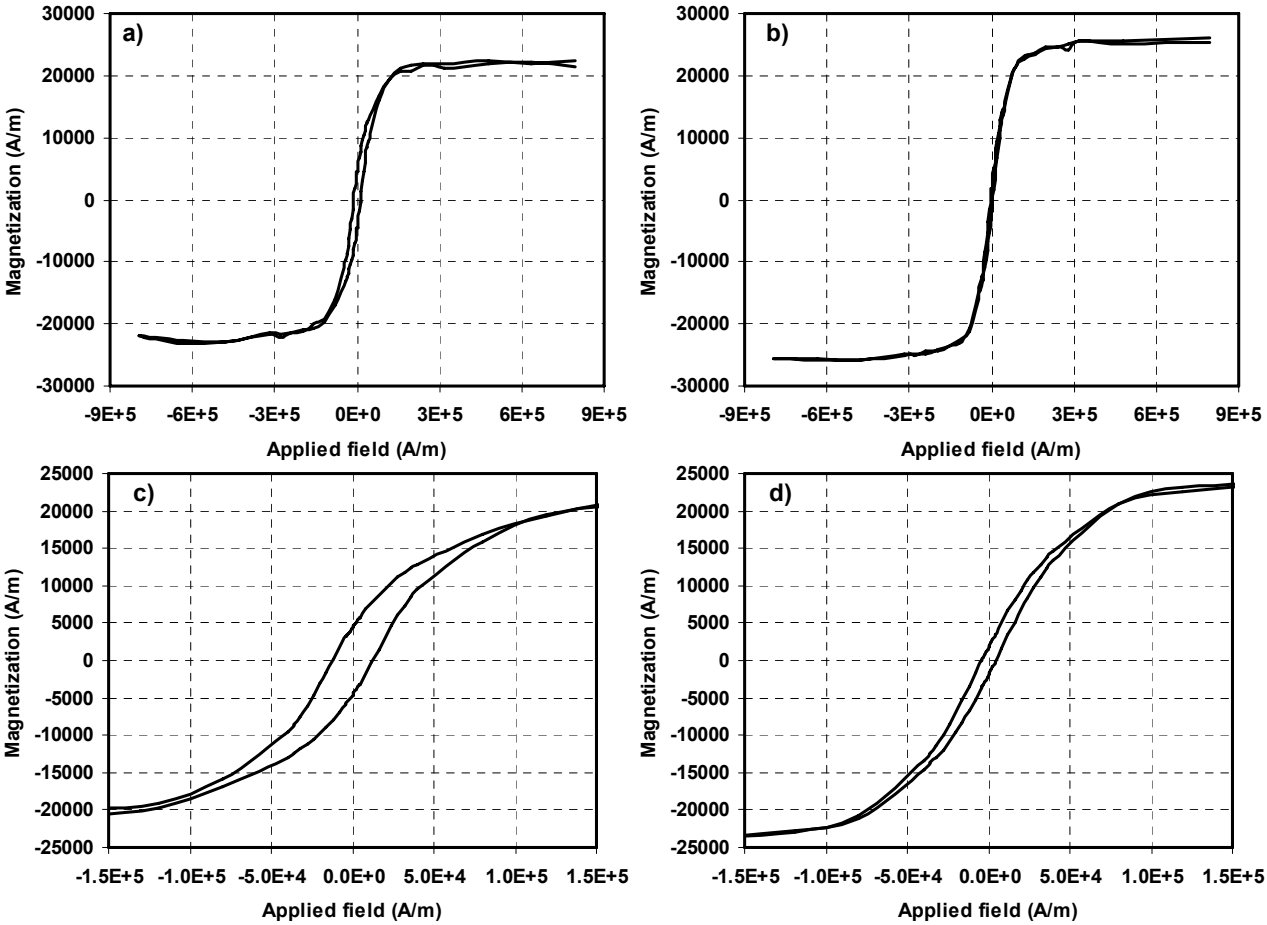

Figure 6-13: *Magnetic hysteresis loops of poly(methyl methacrylate) / 1-butyl-3-methyimidazolium trifluoromethanesulfonate / magnetic (PMMA-IL **4**-magnetic) composites. In (a) and (c) the PMMA-IL **4**-magnetic composite is formed by 32 wt % of PMMA, 45 wt % of IL **4**, and 23 wt % of micrometer-sized magnetic particles; plot (c) is a zoom in of plot (a). In (b) and (d) the PMMA-IL **4**-magnetic composite is formed by 32 wt % of PMMA, 45 wt % of IL **4**, and 23 wt % of nanometer-sized magnetic particles; plot (d) is a zoom in of plot (b). Note the hysteresis decrease in the case of nanometer-sized magnetic particles.*

Despite the achievements reported so far in the literature and in this work related to the properties of polymer-ILs(-magnetic) composites and their potential applications as stimuli-responsive materials, a clear and systematic understanding about the influence of the content of IL on the final properties (*e.g.*, ionic conductivity and mechanical properties) of these novel composites has yet to be identified. The content of IL is thought to be a key variable for determining the final properties of these composite materials. Future research in this field might be focused on the establishment of suitable formulation-property relationships which may allow the optimal design of the polymer-ILs-magnetic composites proposed for specific applications. By establishing suitable formulation-property relationships, the characteristics of these stimuli-responsive composite materials, such as *Tg*, flexibility, mechanical, thermal, magnetic and ionic conductivity properties, could be readily tuned for specific purposes. The electro and magneto responsive polymer-ILs-magnetic composites proposed in this section could be utilized, for instance, for the fabrication of novel sensors and/or actuators (see, for example, Figure 6-2).

6.4 Conclusions

In this chapter, ILs were combined with polymers and/or magnetic particles in order to prepare electro and magneto responsive composite materials. Surprisingly, the preparation of dispersions of magnetic particles in ILs to be used as precursor materials in the fabrication of polymer-ILs-magnetic composites proposed resulted in a new class of magnetorheological fluids (MRFs). Based on their relevance and enormous potential applications, these MRFs have been analyzed and discussed in detail. Hence, a series of MRFs based on ILs were successfully prepared, and their rheological and magnetorheological properties were evaluated. The use of ILs as carriers in dispersions of magnetic particles has yielded MRFs with low rates of sedimentation without the use of additional stabilizing additives. Thus, the rates of sedimentation of MRFs based on ILs depend on the kind of IL utilized and on the concentration of dispersed magnetic particles. Furthermore, the magnetorheological effect could also be observed in the investigated new MRFs which allows for the reversible manipulation of rheological properties of the fluid by means of a magnetic field. Thus the formation of large chains of magnetic particle aggregates, responsible for the instantaneous and quasi-reversible modification of the rheological properties in the fluids under the presence of a magnetic field, was also observed. The combination of the magnetorheological phenomenon with the remarkable properties of ILs has allowed for the preparation of outstanding stable fluids. The potential applications of MRFs based on ILs may be considerable, and may include the improvement of current technologies based on the magnetorheological phenomenon (*e.g.,* automotive industry, mechanical, electronic and civil engineering, as well as medical therapies) and, in addition, new applications may be developed. Owing to the variety of properties that ILs can provide, MRFs based on ILs could be used, for instance, in the magnetically-controlled transport and delivery of substances in different chemical and biological systems (heterogeneous and homogeneous),[118] and as reaction media with a magnetically-controlled diffusion process of reagents (even at extreme reaction conditions of temperature and pressure).

In addition to the development of a new class of MRFs, the dispersions of magnetic particles in ILs have been combined with suitable polymers, which have been synthesized *in-situ*, or polymerized themselves to prepare novel polymer-IL-magnetic composites. It was found that the use of IL allows the preparation of homogeneous polymer-IL-magnetic composites (well-dispersed magnetic particles in a polymer-IL matrix) due to the surface active properties shown by ILs. Indeed, the composites obtained by the preparation method proposed are electro and magneto responsive materials due to the presence of ILs and homogeneously dispersed magnetic particles, respectively. Moreover, it is thought that the mechanical, electro conductive and magnetic properties of the composite materials can be readily manipulated using the preparation method proposed upon varying the reaction conditions of the polymerization reactions, the amount and type of IL, the architecture and type of the polymer synthesized, and the amount and type of magnetic material. Among the possible applications for the polymer-IL-magnetic composites proposed in this chapter is the fabrication of micro-engineering devices such as sensors and/or actuators, which could be used in many areas of science and technology (*e.g.*, in micro fluidic technologies,[7] electronic apparatuses,[51] control systems, and medical therapies[52-61]).

6.5 Experimental part

6.5.1 Experimental part for dispersions of magnetic particles in ionic liquids

Materials. Iron(II, III) oxide (magnetite) powder (<5 μm, 98%, density 4.8-5.1 g cm^{-3} (25 °C), Aldrich) and magnetite nanopowder (spherical, 20-30 nm, >98%, density 0.84 g cm^{-3}, Aldrich) were selected as magnetic particles, and eight ionic liquids (ILs) were investigated as carriers for the preparation of the corresponding

magnetorheological fluids (MRFs). The utilized ILs were: 1-Ethyl-3-methylimidazolium diethylphosphate (**1**), 1-butyl-3-methyl-imidazolium hexafluorophosphate (**2**), 1-hexyl-3-methyl-imida-zolium chloride (**3**), 1-butyl-3-methylimidazolium trifluoromethanesulfonate (**4**), 1-butyl-3-methylimidazolium tetrafluoroborate (**5**), AMMOENG™ 100 (**6**), 1-ethyl-3-methylimidazolium ethylsulfate (**7**), and trihexyltetradecylphosphonium chloride (**8**). All the used ILs were synthesis grade and dried under vacuum at 40 °C at least 3 days before usage. ILs **1**, **2**, **5**, **6**, and **7** were obtained from Solvent-Innovation GmbH as a kind gift; ILs **3**, **4,** and **8** were obtained from Merck KGaA as a kind gift. In Table 4-1 some of the properties of the ILs investigated are listed, whereas in Figure 4-1 their chemical structures are displayed.

Preparation method of the magnetorheological fluids. The preparation of the MRFs using ILs as carriers was performed by mixing the corresponding IL with the magnetite particles. The compositions of the different MRFs prepared are summarized in Table 6-1. The mixing process was performed in cylindrical polyethylene containers using polyethylene stirring paddles. The mixing process was performed by mechanical stirring at a rate of 2400 rpm for 15 min at room temperature (21 °C).

Characterization techniques.

Sedimentation measurements were performed under the influence of gravity in a similar way as described in the literature.[69] The same volume amounts of the different prepared MRFs were poured into cylindrical polyethylene tubes of 4 mm diameter and 53 mm length and closed. The tubes were placed vertically on a heavy marble table to minimize vibrations. The experimental setup was placed in a room with a constant temperature of 21 °C. For these measurements, the lengths of the supernatant (clear layer formed at the top of the fluid due to the sedimentation of the dispersed magnetic particles in the corresponding ILs) were visually monitored over time. The lengths of the formed supernatant clear layers at different times were subtracted from the initial lengths of the corresponding MRFs (initially homogeneous), and the results were divided by the initial lengths of the corresponding MRFs in order to obtain the sedimentation ratios.

Magnetization measurements were carried out using an alternating gradient magnetometer (MicroMag 2900) at room temperature (21 °C). The sample holders were thin flat capillary glasses, placed in the magnetometer with the narrow section perpendicular to the magnetic field. In this case, the demagnetizing field is negligible.[112] The sample holders were filled with the MRF and weighted just before the measurements were performed. The volumes of the samples measured were obtained from the mass of the samples and the densities of the corresponding MRFs. The densities were measured with a picnometer at 21 °C (experimental values obtained are given in Table 6-1).

Magnetorheological measurements of the MRFs prepared were performed at 25 °C under steady shear at different shear rates (see Figures 6-7 to 6-9) using a Physica UDS200 rheometer (Anton Paar) coupled with a commercial magnetorheological device (MRD180-C, magnetorheological cell PP20/MR). The homogeneous magnetic field was oriented perpendicular to the shear flow direction. A parallel-plate measuring system with a diameter of 20 mm, which was made of non-magnetic metal to prevent the occurrence of radial component of magnetic forces on the shaft of the measuring system, was used.

Images of MRFs selected were recorded with an optical microscope using an Axioplan 2 imaging system (Zeiss). The samples were placed between glass microscope slides and the images were acquired with a CCD camera.

Before performing the characterization techniques described, the MRFs prepared were additionally homogenized by vigorous shaking. After shaking, the MRFs showed no inhomogeneities (*e.g.*, no supernatant clear layer formation) for at least two days as revealed by sedimentation measurements.

6.5.2 Experimental part for the preparation and characterization of polymer-ionic liquid-magnetic composites

Materials. Iron(II, III) oxide (magnetite) powder (<5 μm, 98%, density 4.8-5.1 g cm^{-3} (25 °C), Aldrich) and magnetite nanopowder (spherical, 20-30 nm, >98%, density 0.84 g cm^{-3}, Aldrich) were selected as magnetic particles. The hydrophilic ionic liquid (IL) 1-butyl-3-methylimidazolium trifluoromethanesulfonate (**4**), which is a thermodynamically good solvent for poly(methyl methacrylate), was synthesis grade and dried under vacuum at

40 °C at least 3 days before usage. Methyl methacrylate (MMA) and *N*-vinylimidazole (Aldrich) monomers were distilled under vacuum and stored under argon at –25 °C prior to use. 2,2'-Azo*bis*isobutyronitrile (AIBN) was re-crystallized from methanol and stored under argon at –25 °C prior to use. All other materials were used as received.

Preparation of the dicationic salt 1,4-di(vinylimidazolium)-butane dichloride ($C_4(vim)_2$-Cl_2) by microwave-assisted synthesis. $C_4(vim)_2$-Cl_2 cross-linker monomer was synthesized by microwave heating in a similar way to the method described in section 4.5.2 for the synthesis of water-soluble ILs. Hence, $C_4(vim)_2$-Cl_2 was obtained by reacting *N*-vinylimidazole with 1,4-dichlorobutane (Aldrich) (2:1 molar ratio, respectively). The reactions were performed in sealed reaction vials (10 mL) specially designed for the single-mode microwave system Emrys Liberator (Biotage). These vials were filled with the reagents, sealed and degassed with argon for 2 min. The reaction volume was 5 mL. The reagents were mixed during the microwave-assisted reaction by using a magnetic stirring system included in the microwave apparatus. Optimal reactions conditions for the synthesis of this cross-linker monomer in the microwave platform utilized were found to be 120 °C using a reaction time of 10 min with high absorption reaction mode (150 Watts). The product had a melting point around 160 °C.

Preparation of poly(methyl methacrylate) / 1-butyl-3-methyimidazolium trifluoromethanesulfonate / magnetic (PMMA-IL 4-magnetic) composites. Free radical polymerization reactions of MMA initiated by AIBN (1 wt % in respect to the amount of monomer) in dispersions of magnetic particles (micrometer or nanometer-sized) in IL **4** (previously prepared as describe in section 6.5.1) were performed in cylindrical glass vials (1 mL) using a reaction temperature of 70 °C and 3 h of reaction time. The polymer-IL-magnetic composites obtained by this method had a composition of 32 wt % of PMMA, 45 wt % of IL 4, and 23 wt % of micrometer- or nanometer-sized magnetic particles. The materials prepared by this method were solid and placed under vacuum at 40 °C at least 3 days in order to remove un-reacted monomer.

Preparation of poly(1,4-di(vinylimidazolium)-butane dichloride)-magnetic ($PC_4(vim)_2$-Cl_2 / magnetic) composites. Free radical polymerization reactions of $C_4(vim)_2$-Cl_2 cross-linker monomer initiated by AIBN (1 wt % in respect to the amount of monomer) were performed in the presence of magnetic particles (micrometer- or nanometer-sized) dispersed in ethanol. $C_4(vim)_2$-Cl_2 is soluble in ethanol, which was used as a solvent to perform the polymerization reaction in order to obtained a better homogeneous dispersion of the magnetic particles. The amount of ethanol utilized for the polymerization reactions was (33 wt % with respect to the amount of cross-linker monomer). The polymerization reactions were carried out in cylindrical glass vials (1 mL) using a reaction temperature of 70 °C and 3 h of reaction time. The polymer-IL-magnetic composites obtained by this method had a composition of 77 wt % of $PC_4(vim)_2$-Cl_2 and 23 wt % of micrometer- or nanometer-sized magnetic particles. The materials prepared by this method were solid and placed under vacuum at 40 °C at least 3 days in order to remove the solvent (ethanol).

Characterization techniques.

Magnetization measurements of the polymer-IL-magnetic composites prepared were measured a room temperature (21 °C) with a SQUID magnetometer. The direction of the applied magnetic field was parallel to the axis of cylindrical-shaped samples obtained. A linear background was subtracted from the data of the samples recorded in order to correct the substrate response using a proportionality constant obtained by fitting experimental data points at high magnetic fields. Finally, the magnetic moments of the samples were divided by the volume to obtain the magnetization values and the magnetic hysteresis loops of the composites.

Images of the polymer-IL-magnetic composites investigated were recorded by atomic force microscopy (AFM), scanning electron microscopy (SEM), and optical microscopy. For the AFM and SEM measurements, the solid composites investigated were frozen in liquid nitrogen and broken in order to obtained suitable flat surfaces for their imaging. For the case of optical microscopy a thin film of the solid composite investigated was obtained by cutting the sample with a blade and thereafter observed under the microscope.

AFM imaging was performed in intermittent contact mode on a Multimode SPM (Digital Instruments, Santa Barbara, CA) using NSC36-type tips (~1 N m^{-1}, Mikromasch, Spain).

SEM imaging was performed on a JEOL JSM-840A microscope. The sample was initially dried under vacuum at 40 °C for three days before being analyzed. The dried polymer-IL-magnetic composite was mounted on a SEM sample holder, sputter coated with gold for 2 min, and scanned at the desired magnification.

Optical microscopy imaging was carried out on an Axioplan 2 imaging system (Zeiss). The dried sample was placed directly under the microscope and the images were acquired with a CCD camera.

Electric conductivity measurements were performed on a home-made electric circuit composed by a power supply and two multi-meters to measure the voltage applied to the composites and the current passing through the samples.

6.6 References

[1] (a) M. Deetlefs, K. R. Seddon, *Chim. Oggi* **2006**, *24(2)*, 16. (b) S. Kumar, W. Ruth, B. Sprenger, U. Kragl, *Chim. Oggi* **2006**, *24(2)*, 24. (c) M. J. Earle, J. M. S. S. Esperanca, M. A. Gilea, J. N. Canongia-Lopes, L. P. N. Rebelo, J. W. Magee, K. R. Seddon, J. A. Widegren, *Nature* **2006**, *439*, 831. (d) M. Smiglak, W. M. Reichert, J. D. Holbrey, J. S. Wilkes, L. Sun, J. S. Thrasher, K. Kirichenko, S. Singh, A. R. Katritzky, R. D. Rogers, *Chem. Commun.* **2006**, 2554.

[2] N. Winterton, *J. Mater. Chem.* **2006**, *16*, 4281.

[3] M. Rahman, H. W. Shoff, C. S. Brazel, *ACS Symp. Ser.* **2005**, *913*, 103.

[4] D. M. Fox, S. Bellayer, M. Murariu, J. W. Gilman, P. H. Maupin, H. C. De Long, P. C. Trulove, *ACS Symp. Ser.* **2005**, *913*, 175.

[5] J. D. Holbrey, J. Chen, M. B. Turner, R. P. Swatloski, S. K. Spear, R. D. Rogers, *ACS Symp. Ser.* **2005**, *913*, 71.

[6] H. Ohno, S. Washiro, M. Yoshizawa, *ACS Symp. Ser.* **2005**, *913*, 89.

[7] M. Elwenspoek, T. S. J. Lammerink, R. Miyake, J. H. J. Fluitman, *J. Micromech. Microeng.* **1994**, *4*, 227.

[8] M. Koch, A. G. R. Evans, A. Brunnschweiler, *J. Micromech. Microeng.* **1998**, *8*, 119.

[9] J. Branebjerg, P. Gravesen, *Proc. of the IEEE Micro Electro Mechanical Systems, an Investigation of Micro Structures, Sensors, Actuators, Machines and Robots,* Travemunde, Germany, 4-7 February **1992**, 6.

[10] R. Zerlenge, A. Richter, H. Sandmaier, *Proc. of the IEEE Micro Electro Mechanical Systems, an Investigation of Micro Structures, Sensors, Actuators, Machines and Robots,* Travemunde, Germany, 4-7 February **1992**, 19.

[11] X. Yang, C. Grosjean, Y. C. Tai, C. M. Ho, *Proc. of the IEEE Micro Electro Mechanical Systems, an Investigation of Micro Structures, Sensors, Actuators, Machines and Robots,* Nagoya, Japan, 26-30 January **1997**, 114.

[12] C. R. Neagu, J. G. E. Gardeniers, M. Elwenspoek, J. J. Kelly, *J. Micro-electromech. Syst.* **1996**, *5*, 2.

[13] Y. Yang, X. Ye, Z. Zhou, W. Fang, Y. Li, *Proc. of the Transducers '95: Dig. Tech. Papers, Int. Conf. on Solid-State Sensors and Actuators,* Stockholm, Sweden, 25-29 June **1995**, *3*, 114.

[14] M. Kohl, K. D. Skrobanek, S. Miyazaki, *Sens. Actuators A* **1999**, *72*, 243.

[15] D. J. Sadler, T. M. Liakopoulos, J. Cropp, C. H. Ahn, H. T. Henderson, *Proc. of SPIE - the Int. Soc. for Optical Eng. Symp. on Micromachining and Microfabrication,* Santa Clara, CA, 21-22 September **1998**, *3515*, 46.

[16] J. R. Durrant, S. A. Haque, *Nat. Mater.* **2003**, *2*, 362.

[17] B. C. H. Steele, A. Heinzel, *Nature* **2001**, *414*, 345.

[18] J. M. Tarascon, M. Armand, *Nature* **2001**, *414*, 359.

[19] F. M. Gray, *Polymer Electrolytes*, Royal Society of Chemistry, Cambridge, England, **1997**.

[20] F. M. Gray, *Solid Polymer Electrolytes: Fundamentals and Technological Applications*, VCH, New York, **1991**.

[21] P. Calvert, *Chem. Mater.* **2001**, *13*, 3299.

[22] B. J. de Gans, P. C. Duineveld, U. S. Schubert, *Adv. Mater.* **2004**, *16*, 203.

[23] E. Staunton, Y. G. Andreev, P. G. Bruce, *J. Am. Chem. Soc.* **2005**, *127*, 12176.

[24] P. J. Alarco, Y. Abu–Lebdeh, A. Abouimrane, M. Armand, *Nat. Mater.* **2004**, *3*, 476.

[25] Z. Stoeva, I. Matin–Litas, E. Stauton, Y. G. Andreev, P. G. Bruce, *J. Am. Chem. Soc.* **2003**, *125*, 4619.

[26] Z. Gadjourova, Y. G. Andreev, D. P. Tunstall, P. G. Bruce, *Nature* **2001**, *412*, 520.

[27] D. R. Mac Farlane, J. H. Huang, M. Forsyth, *Nature* **1999**, *402*, 792.

[28] A. M. Christie, S. J. Lilley, E. Staunton, Y. G. Andreev, P. G. Bruce, *Nature* **2005**, *433*, 50.

[29] C. H. Zhang, E. Staunton, Y. G. Andreev, P. G. Bruce, *J. Am. Chem. Soc.* **2005**, *127*, 18305.

[30] C. Tiyapiboonchaiya, J. M. Pringle, J. Z. Sun, N. Byme, P. C. Howlett, D. R. MacFarlane, M. Forsyth, *Nat. Mater.* **2004**, *3*, 29.

[31] M. A. B. H. Susan, T. Kaneko, A. Noda, M. Watanabe, *J. Am. Chem. Soc.* **2005**, *127*, 4976.

[32] Y. Bar-Cohen, *Electroactive Polymer (EAP) Actuators as Artificial Muscles, Reality, Potential, and Challenges*, 2nd ed., SPIE Press, Washigton, DC, **2004**.

[33] Y. Osada, D. E. De Rossi, *Polymer Sensors and Actuators*, Springer, Berlin, **2000**.

[34] R. H. Baughman, *Synth. Met.* **1996**, *78*, 339.

[35] E. W. H. Jager, E. Smela, O. Inganas, *Science* **2000**, *290*, 1540.

[36] E. Smela, *Adv. Mater.* **2003**, *15*, 481.

[37] J. M. Sansinena, V. Olazabal, T. F. Otero, C. N. Polo da Fonseca, M. A. De Paoli, *Chem. Commum.* **1997**, 2217.

[38] D. Zhou, G. M. Spinks, G. G. Wallace, C. Tiyapiboonchaiya, D. R. MacFaarlane, M. Forsyth, J. Sun, *Electrochim. Acta* **2003**, *48*, 2355.
[39] M. D. Bennett, D. J. Leo, *Sens. Actuator A-Phys.* **2004**, *115*, 79.
[40] M. D. Bennett, D. J. Leo, *Proc. of the EAP Actuators and Devices SPIE* **2004**, 5385.
[41] C. Tiyapiboonchaiya, D. R. MacFarlane, J. Sun, M. Forsyth, *Macromol. Chem. Phys.* **2002**, *203*, 1906.
[42] S. Washiro, M. Yoshizawa, H. Nakajima, H. Ohno, *Polymer* **2004**, *45*, 1577.
[43] Y. He, P. G. Boswell, P. Buhlmann, T. P. Lodge, *J. Phys. Chem. B* **2007**, *111*, 4645.
[44] T. Fukushima, K. Asaka, A. Kosaka, T. Aida, *Angew. Chem. Int. Ed.* **2005**, *44*, 2410.
[45] B. J. Akle, M. D. Bennett, D. J. Leo, *Sens. Actuator A-Phys.* **2006**, *126*, 173.
[46] S. S. Sekhon, B. S. Lalia, J. S. Park, C. S. Kim, K. Yamada, *J. Mater. Chem.* **2006**, *16*, 2256.
[47] J. Lee, M. J. Panzer, Y. He, T. P. Lodge, C. D. Frisbie, *J. Am. Chem. Soc.* **2007**, *129*, 4532.
[48] C. Liu, *Mechatronics*, **1998**, *8*, 613.
[49] W. Zhang, C. H. Ahn, *Tech Dig.: 1996 Solid-State Sensor and Actuator Workshop,* Hilton Head Island, SC, 3-6 June **1996**, 94.
[50] M. Khoo, C. Liu, *Sens. Actuator A-Phys.* **2001**, *89*, 259.
[51] D. L. Leslie–Pelecky, R. D. Rieke, *Chem. Mater.* **1996**, *8*, 1770.
[52] J. P. Phillips, C. Li, J. P. Dailey, J. S. Riffle, *J. Magn. Magn. Mater.* **1999**, *194*, 140.
[53] R. S. Molday, D. MacKenzie, *J. Immunol. Methods* **1982**, *52*, 353.
[54] S. Roath, *J. Magn. Magn. Mater.* **1993**, *122*, 329.
[55] A. Jordan, R. Scholz, P. Wust, H. Schbirra, T. Schiestel, H. Schmidt, R. Felix, *J. Magn. Magn. Mater.* **1999**, *124*, 185.
[56] D. K. Kim,Y. Zhang, J. Kehr, T. Klason, B. Bjelke, M. Muhammed, *J. Magn. Magn. Mater.* **2001**, *225*, 256.
[57] L. Babes, B. Denizot, G. Tanguy, J. J. Le Jeune, P. Jallet, *J. Colloid Interface Sci.* **1999**, *212*, 474.
[58] M. I. Papisov, A. Bogdanov, B. Schaffer, N. Nossiff, T. Shen, R. Weissleder, T. J. Brady, *J. Magn. Magn. Mater.* **1993**, *122*, 383.
[59] K. Widder, G. Flouret, A. Senyei, *J. Pharm. Sci.* **1979**, *68*, 79.
[60] P. K. Gupta, C. T. Hung, F. C. Lam, D. G. Perrier, *Int. J. Pharm.* **1988**, *43*, 167.
[61] A. Ibrahim, P. Couvreur, M. Roland, P. Speiser, *J. Pharm. Phramacol.* **1982**, *35*, 59.
[62] R. Betancourt-Galindo, R. Saldivar-Guerrero, O. S. Rodríguez-Fernandez, L. A. Garcia-Cerda, J. Matutes-Aquino, *J. Alloy. Compd.* **2004**, *369*, 87.
[63] D. Hoffmann, K. Landfester, M. Antonietti, *Magnetohydrodynamics* **2001**, *37*, 217.
[64] Y. Zhou, M. Antonietti, *Chem. Mater.* **2004**, *14*, 544.
[65] J. D. Holbrey, J. Chen, M. B. Turner, R. P. Swatloski, S. K. Spear, R. D. Rogers, *ACS Symp. Ser.* **2005**, *913*, 71.
[66] R. P. Swatloski, J. D. Holbrey, J. L. Weston, R. D. Rogers, *Chim. Oggi* **2006**, *24(2)*, 31.
[67] T. Fukushima, A. Kosaka, Y. Yamamoto, T. Aimiya, S. Notazawa, T. Takigawa, T. Inabe, T. Aida, *Small* **2006**, *2*, 554.
[68] A. Chaudhuri, N. M. Wereley, S. Kotha, R. Radhakrishnan, T. S. Sudarshan, *J. Magn. Magn. Mater.* **2005**, *293*, 206.
[69] S. T. Lim, M. S. Cho, I. B. Jang, H. J. Choi, *J. Magn. Magn. Mater.* **2004**, *282*, 170.
[70] O. O.Park, J. H. Park, B. D. Chin, *US Patent 6 692 650*, **2004**.
[71] G. Bossis, S. Lacis, A. Meunier, O. Volkova, *J. Magn. Magn. Mater.* **2002**, *252*, 224.
[72] (a) J. Rabinow, *Proc. AIEE Trans.* **1948**, *67*, 1308. (b) J. Rabinow, *US Patent 2 575 360*, **1951**.
[73] W. M. Winslow, *J. Appl. Phys.* **1949**, *20*, 1137.
[74] I. Bica, *J. Magn. Magn. Mater.* **2002**, *241*, 196.
[75] M. R. Jolly, J. W. Bender, J. D. Carlson, *J. Intell. Mater. Syst. Struct.* **1999**, *10*, 5.
[76] J. D. Carlson, L. C. Yanyo, *US Patent Appl. Publ. US 2001 032967 A1*, **2001**.
[77] T. Phillips, P. L. Barry, *Robot blood?*, http://www.firstscience.com/home/articles/big-theories/robot-blood_1231.html (accessed: May 2, **2007**).
[78] U. O. Häfeli, G. J. Pauer, *J. Magn. Magn. Mater.* **1999**, *194*, 76.
[79] R. Sheng, G. A. Flores, J. Liu, *J. Magn. Magn. Mater.* **1999**, *194*, 167.
[80] J. Liu, G. A. Flores, R. Sheng, *J. Magn. Magn. Mater.* **2001**, *225*, 209.
[81] A. Meretei, *Eur. Patent Appl. EP 1676534 A1*, **2006**.
[82] S. Odenbach, in *Magnetoviscous effects in ferrofluids*, *Lecture notes in Physics: Monograph 71*, Springer-Verlag: Berlin, **2002**, Ch. 5.
[83] J. S. Choi, B. J. Park, M. S. Cho, H. J. Choi, *J. Magn. Magn. Mater.* **2006**, *304*, e374.
[84] M. T. López-López, A. Zugaldia, F. González-Caballero, J. D. G. Durán, *J. Rheol.* **2006**, *50*, 543.
[85] J. D. Carlson, *J. Intell. Mater. Syst. Struct.* **2002**, *13*, 431.
[86] V. R. Iyengar, T. J. Kacsandy, *US Patent 6 824 700*, **2004**.
[87] P. J. Rakin, A. T. Horvath, D. J. Klingenberg, *Rheol. Acta* **1999**, *38*, 471.
[88] J. D.Carlson, *US Patent 6 132 633*, **2000**.
[89] J. D. Carlson, *US Patent 6 475 404*, **2002**.

[90] E. Altin, J. Gradl, W. Peukert, *Chem. Eng. Technol.* **2006**, *29*, 1347.
[91] G. Clavel, J. Larionova, Y. Guari, C. Guérin, *Chem. Eur. J.* **2006**, *12*, 3798.
[92] M. Antonietti, D. Kuang, B. Smarsly, Y. Zhou, *Angew. Chem. Int. Ed.* **2004**, *43*, 4988.
[93] P. P. Phulé, J. M. Ginder, *MRS Bull.* **23**, 19-21 (1998).
[94] S. Odenbach, in *Magnetoviscous effects in ferrofluids*, *Lecture notes in Physics: Monograph 71*, Springer-Verlag: Berlin **2002**, Ch. 2.
[95] M. T. López-López, J. D. G. Durán, A. V. Delgado, F. González-Caballero, *J. Colloid Interface Sci.* **2005**, *291*, 144.
[96] P. Berger, N. B. Adelman, K. J. Beckman, D. J. Campbell, A. B. Ellis, G. C. Lisensky, *J. Chem. Edu.* **1999**, *76*, 943.
[97] M. H. Valkenberg, C. deCastro, W. F. Holderich, *Appl. Catalysis A: Gen.* **2001**, *215*, 185.
[98] Y. Katayama, I. Konishiike, T. Miura, T. Kishi, *J. Power Sources* **2002**, *109*, 327.
[99] W. Xu, E. I. Cooper, C. A. Angell, *J. Phys. Chem. B* **2003**, *107*, 6170.
[100] F. Shi, J. Peng, Y. Deng, *J. Catalysis* **2003**, *219*, 372.
[101] J. Z. Yang, W. G. Xu, Q. G. Zhang, Y. Jin, Z. H. Zhang, *J. Chem. Thermodyn.* **2003**, *35*, 1855.
[102] S. Hayashi, H. Hamaguchi, *Chem. Lett.* **2004**, *34*, 1590.
[103] S. Hayashi, S. Saha, H. Hamaguchi, *IEEE Trans. Magn.* **2006**, *42*, 12.
[104] R. Saldivar-Guerrero, R. Richter, I. Rehberg, N. Aksel, L. Heymann, O. S. Rodríguez-Fernandez, *Magnetohydrodynamics* **2005**, *41*, 385.
[105] K. R. Seddon, A. Stark, M. J. Torres, *Pure Appl. Chem.* **2000**, *72*, 2275.
[106] T. Schubert, *Viscosity of ionic liquids*, http://www.merck.de/servlet/PB/menu/1303700/index.html (accessed: May 2, **2007**).
[107] H. Block, J. P. Kelly, *J. Phys. D: Appl. Phys.* **1998**, *21*, 1661.
[108] M. S. Cho, H. J. Choi, I. J. Chin, W. S. Ahn, *Microporous Mesoporous Mater.* **1999**, *32*, 233.
[109] M. S. Cho, Y. H. Cho, H. J. Choi, M. S. Jhon, *Langmuir* **2003**, *19*, 5875.
[110] M. S. Cho, H. J. Choi, M. S. Jhon, *Polymer* **2005**, *46*, 11484.
[111] Y. H. Shih, H. Conrad, *Int. J. Mod. Phys. B* **1994**, *8*, 2835.
[112] M. Raşa, A. P. Philipse, D. Jamon, *Phys. Rew. E* **2003**, *68*, 031402.
[113] A. M. J. van den Berg, A. W. M. de Laat, P. J. Smith, J. Perelaer, U. S. Schubert, *J. Mater. Chem.* **2007**, *7*, 677.
[114] A. M. J. van den Berg, P. J. Smith, J. Perelaer, W. Schrof, S. Koltzenburg, U. S. Schubert, *Soft Matter* **2007**, *2*, 238.
[115] S. Palacin, P. C. Hidber, J. P. Bourgoin, C. Miramond, C. Fermon, G. M. Whitesides, *Chem. Mater.* **1996**, *8*, 1316.
[116] M. J. Muldoon, C. M. Gordon, *J. Polym. Sci. Part A: Polym. Chem.* **2004**, *42*, 3865.
[117] R. Marcilla, J. A. Blazquez, J. Rodriguez, J. A. Pomposo, D. Mecerreyes, *J. Polym. Sci. Part A: Polym. Chem.* **2004**, *42*, 208.
[118] M. Okuno, H. Hamaguchi, S. Hayashi, *Appl. Phys. Lett.* **2006**, *89*, 132506.

Ionic systems in materials research: New materials and processes based on ionic polymerizations and/or ionic liquids

Summary

Systems based on ionic interactions are usually related to reversible processes and/or transitory chemical states and, nowadays, they are believed to be key factors for the understanding and for the development of processes in several branches of chemistry and materials research. During the last decades, scientists have developed different approaches for the preparation of new materials and/or substances with outstanding properties based on ionic and other non-covalent interactions. In this thesis, different chemical systems, based on ionic interactions, have been employed for the preparation of different materials and for the development of more efficient synthetic methods in materials research. On the one hand "classical" and emerging applications of ionic interactions are utilized for the preparation of polymeric moieties and other materials, and on the other hand some of the results derived from these single approaches are combined to produce and investigate more complex systems. These systems may find applications in different fields of science and technology: From drug delivery and medical therapies to engineering devices and novel catalytic reactions systems. Thus, this dissertation is divided in three sections.

In the first section, the synthetic approach for the well-established anionic polymerization procedure is enhanced by incorporating this technique into a high-throughput work-flow. The development of this experimental approach has allowed and accelerated the systematic synthesis of new block copolymer libraries. Some of the obtained block copolymers were utilized to prepare self-assembled micelles, which were investigated and characterized in detail. Furthermore, the proposed experimental approach was also applied for the development of a new synthetic route to prepare well-defined end-functionalized polymeric architectures bearing supramolecular moieties (*e.g.*, terpyridine groups). In addition, this technique has shown to be a very useful tool for performing detailed kinetic investigations in a short time. Thus, the high-throughput approach was established for one of the most demanding experimental techniques in polymer synthesis. This new tool may help to speed-up research in this field, which will allow a better understanding of structure-property relationships in polymer science.

In the second part of the thesis, ionic liquids are investigated as reaction media to carry out polymerizations by different reaction mechanisms. Due to their outstanding chemical and physical stabilities, ionic liquids are proposed as new ionic systems that can offer multiple advantages in polymer synthesis. Thus, it is demonstrated that ionic liquids can be efficiently utilized to perform homogeneous and heterogeneous polymerization reactions. In the homogeneous case, another important ionic polymerization mechanism, cationic ring opening polymerization, was selected as an example for the development of efficient and environmentally-friendly polymerization processes based on ionic liquids as reaction media and microwave irradiation as a heating source. Polymerizations performed in ionic liquids have shown faster reaction rates when compared to other solution polymerization methods, and also

allow the synthesis of well-defined and chain extended polymers due to the fact that the investigated polymerization reactions reveal a “living” character. Furthermore, it is shown that the proposed synthetic method is not only limited to one reaction mechanism and can be readily extended to other types of polymerizations, such as free radical processes. Due to the fact that not all monomers and/or polymers are soluble in specific ionic liquids, it is also demonstrated that heterogeneous polymerization processes can be carried out in these substances. For these cases, ionic liquids do not only act as a reaction medium, but they also behave as surfactants to stabilize these heterogeneous systems. This has allowed the synthesis of polymer beads with controlled particle sizes and surface areas. For all the investigated polymerization reactions in ionic liquids, suitable and efficient approaches for the ionic liquid recycling and polymer isolation were developed by the use of water as secondary substance during the separation processes, which entirely avoids the use of volatile organic solvents. In addition, it is also demonstrated that, with the approaches proposed, cleaner and more efficient polymerization processes can be developed due to the known “green” characteristics of ionic liquids (*e.g.*, negligible vapor pressure, negligible flammability, and liquids in a broad range of temperatures) and to the high efficiency of microwave irradiation in the presence of ionic liquids. The proposed environmentally-friendly polymerization processes certainly arise as alternative methods for reducing emissions of harmful volatile organic compounds still widely used throughout the polymer industry and for energy savings.

In the last part of the thesis, the materials and/or concepts developed in the first two sections are combined in order to obtain more complex materials and systems. Specifically, amphiphilic block copolymers that were synthesized in the first part of this thesis, or obtained by other methods, are utilized for the preparation of self-assembled micelles in ionic liquids. This has revealed interesting properties due to the fact that these block copolymer micelles, with and without encapsulated guest molecules in their respective core, can be thermo-reversible transferred between two different phases (an aqueous phase and an ionic liquid phase). Furthermore, it is also demonstrated that the investigated block copolymer micelles provide confined environments that protect the encapsulated guest molecules from (sudden) external changes in the surroundings. Finally, the surfactant properties revealed by ionic liquids are utilized for the preparation of composite materials, which is illustrated by two examples: The utilization of ionic liquids has allowed for the efficient and homogeneous dispersion of inorganic materials (*e.g.* magnetite) into a polymeric matrix. Thus, polymer composites with both magnetic and conductive properties were prepared by an inexpensive method. In addition, this latter concept is also extended to the preparation of composite materials in a liquid state. As a result, novel magnetorheological fluids based on ionic liquids were prepared by dispersing magnetic particles in ionic liquids. The use of ionic liquids has allowed for the preparation of dispersions with low sedimentation rates and magnetorheological fluids with enhanced properties. A combination of the outstanding properties of ionic liquids with the magnetorheological technology led to the fabrication of new and “smart” fluids, which may find applications in several areas of research and technology, such as medical therapies (drug delivery and cancer therapeutic methods), engineering devices (dampers and breaks), as well as accurate transportation and delivery of substances in multiphase biological and chemical systems.

Samenvatting

Systemen gebaseerd op ionische interacties zijn gewoonlijk gebaseerd op reversibele processen en/of overgangstoestanden bij chemische reacties. Deze ionische interacties nemen een sleutelrol in bij het begrip van en bij het ontwikkelen van nieuwe processen in verschillende onderdelen van chemisch- en materiaalkundig onderzoek. Gedurende de laatste decennia zijn verscheidene nieuwe materialen ontwikkeld met buitengewone eigenschappen gebaseerd op ionische en andere niet covalente interacties. Binnen dit promotieonderzoek is gebruik gemaakt van ionische interacties voor de synthese van nieuwe materialen en voor het ontwikkelen van nieuwe, efficiëntere synthese routes ten behoeve van de materiaalkunde. In eerste instantie zijn 'klassieke' en opkomende toepassingen van ionische interacties gebruikt voor de synthese van polymeren en materialen. Tevens zijn sommige van de resulterende inzichten gecombineerd om nieuwe geavanceerde materialen te maken die mogelijk toegepast kunnen worden in medicijn afgifte systemen, medische behandelingen en nieuwe katalytische systemen. Om de verschillende onderdelen te beschrijven is dit proefschrift onderverdeeld in drie secties.

In het eerste deel van dit proefschrift wordt het onderzoek behandeld dat gewijd is aan het vergroten van de toepasbaarheid en mogelijkheden van anionische polymerisatie procedures door deze te integreren in een combinatorisch werkschema. De resulterende combinatorische procedureheeft de snelle synthese van een systematische serie blokcopolymeren mogelijk gemaakt. Sommige van deze blokcopolymeren zijn gebruikt om zelf-assemblerende micellen te maken welke in detail gekarakteriseerd zijn. Tevens zijn de nieuwe experimentele procedures gebruikt om goed gedefinieerde polymeer ketens te verkrijgen met functionele supramoleculaire eindgroepen zoals terpyridines. Daarnaast is gedemonstreerd dat de combinatorische aanpak zeer geschikt is om de kinetiek van polymerisatie reacties te bestuderen. Geconcludeerd kan worden dat een combinatorische procedure ontwikkeld is voor een van de meest veeleisende polymerisatie methodes. Deze procedure zal het huidige polymeeronderzoek in deze richting versnellen, waardoor wellicht een beter inzicht in de relaties tussen de structuur en de eigenschappen van de polymeren kan worden verkregen.

Het tweede deel van dit proefschrift beschrijft de toepassing van ionische vloeistoffen als reactiemedia voor diverse polymerisatiereacties. Vanwege de uitstekende chemische en fysische eigenschappen zijn ionische vloeistoffen potentiële kandidaten voor het ontwikkelen van nieuwe en betere polymerisatie systemen. Zo wordt gedemonstreerd dat ionische vloeistoffen bij zowel homogene als heterogene reacties als reactiemedia gebruikt kunnen worden. Voor het eerste geval is aan de hand van een kationische ring-opening polymerisatie gedemonstreerd dat ionische vloeistoffen een efficiënt en milieuvriendelijk oplosmiddel zijn waarbij gebruik gemaakt werd van microgolf straling als verhittingsbron. De polymerisaties uitgevoerd in ionische vloeistoffen vertoonden een hogere reactiesnelheid dan met niet ionische oplosmiddelen. Tevens behielden de polymerisaties het levende karakter in de ionische vloeistof wat de synthese van goed gedefinieerde en keten-verlengde polymeren mogelijk maakte. Bovendien is nog gedemonstreerd dat de voorgestelde synthetische methoden niet alleen toepasbaar zijn voor kationische polymerisaties maar dat ze ook eenvoudig gebruikt kunnen worden bij andere reactiemechanismen zoals vrije radicaal polymerisaties. Vanwege het feit dat niet alle monomeren en/of

polymeren oplosbaar zijn in alle ionische vloeistoffen kon de toepassing daarvan in heterogene polymerisaties eveneens gedemonstreerd worden. In deze gevallen fungeert de ionische vloeistof niet alleen als reactiemedium maar tevens als surfactant om deze reactiemengsels te stabiliseren. Hierbij konden polymeerkorrels met controleerbare korrel grootte en porositeit gemaakt worden. Voor alle genoemde reacties is de recyclering van de ionische vloeistof gedemonstreerd waarbij water als scheidingsmiddel gebuikt werd zodat het gebruik van vluchtige organische oplosmiddelen volledig is uitgesloten. Dit in combinatie met de 'groene' eigenschappen van de ionische vloeistoffen, verwaarloosbare dampspanning, onbrandbaarheid en het vloeibare karakter in een breed temperatuurbereik, evenals de efficiënte verwarming door microgolf straling in aanwezigheid van ionische vloeistoffen betekent dat schonere en efficiëntere polymerisatie processen ontwikkeld konden worden. Deze voorgestelde, milieuvriendelijke reactie procedures kunnen ingezet worden als alternatieven voor tegenwoordige productieprocessen waarbij immer nog schadelijke vluchtige organische oplosmiddelen vrijkomen.

In het laatste deel van dit proefschrift worden materialen en concepten resulterend uit de eerste twee delen, gecombineerd om te komen tot complexere materialen en systemen. Zo worden de amfifiele blokcopolymeren uit de eerste twee delen ingezet om micellaire aggregaten te verkrijgen in ionische vloeistoffen. Deze micellen hebben in twee fase-systemen interessante eigenschappen aangezien er, zowel met als zonder insluiting van gastmoleculen in de kern van de micellen, de mogelijkheid bestaat temperatuur gestuurde reversibele faseovergangen te bewerkstelligen. Daarnaast is aangetoond dat de verkregen blokcopolymere micellen een beschermende omgeving vormen voor ingesloten gastmoleculen hetgeen ze kan beschutten tegen plotselinge veranderende omgevingsfactoren. Tenslotte zijn de ionische vloeistoffen nog gebruikt in een tweetal composiet materialen. In het eerste geval zijn ionische vloeistoffen gebruikt om magnetische magnetiet deeltjes homogeen te dispergeren in een polymere matrix. Zo kunnen op goedkope wijze polymeren verkregen worden met zowel magnetische als geleidende eigenschappen. In het tweede voorbeeld zijn magnetische deeltjes gesuspendeerd in ionische vloeistoffen. De aldus verkregen magneto-rheologische vloeistoffen worden gekenmerkt door goede eigenschappen en zeer lage sedimentatie snelheden. Deze combinatie van bijzondere 'slimme' eigenschappen betekent dat deze materialen toegepast kunnen worden in zowel de medische wereld (bij gecontroleerde medicijn afgifte, bijvoorbeeld bij behandelingen tegen kanker) alsook in technologische toepassingen (schokdempers en als remvloeistof) en bij accurate gespecialiseerde transport toepassingen in meerfasen systemen binnen de biologie en chemie.

Curriculum vitae

Carlos Guerrero Sanchez was born on the 4th of April of 1976 in Mexico City where he grew up and earned a bachelor degree in chemical engineering in 1999 from the National Autonomous University of Mexico (UNAM). He also obtained a masters degree in chemical engineering in 2001 from the Celaya Institute of Technology in Guanajuato, Mexico. Both bachelor and masters graduation projects were related to the modelling and simulation of polymerization reactors under the supervision of professor Enrique Saldivar Guerra. After these studies he worked for two years at the research and development centre of the chemical sector of DESC (a major Mexican company). His work at DESC was connected to the start-up of a combinatorial materials research laboratory. In July 2003, he moved to the Netherlands to start a Ph. D. program in combinatorial materials research and polymer science under the supervision of professor Ulrich Schubert at the Eindhoven University of Technology. The most relevant results of his Ph. D. studies can be found in thesis.

List of publications

A. Refereed publications:

1. C. Guerrero-Sanchez, T. Lara-Ceniceros, E. Jimenez-Regalado, M. Rasa, U. S. Schubert; "Magnetorheological Fluids Based on Ionic Liquids", *Adv. Mater.* **2007**, *19*, 1740-1747 (front cover).
2. C. Guerrero-Sanchez, M. Lobert, R. Hoogenboom, U. S. Schubert; "Microwave-Assisted Homogeneous Polymerizations in Water-Soluble Ionic Liquids: An Alternative and Green Approach for Polymer Synthesis", *Macromol. Rapid Commun.* **2007**, *28,* 456-464.
3. C. Guerrero-Sanchez, T. Erdmenger, P. Šereda, D. Wouters, U. S. Schubert; "Water-Soluble Ionic Liquids as Novel Stabilizers in Suspension Polymerization Reactions: Engineering Polymer Beads", *Chem. Eur. J.* **2006**, *12*, 9036-9045.
4. C. Guerrero-Sanchez, R. Hoogenboom, U. S. Schubert; "Fast and Green Living Cationic Ring Opening Polymerization of 2-Ethyl-2-Oxazoline in Ionic Liquids under Microwave Irradiation", *Chem. Commun.* **2006**, 3797-3799.
5. C. Guerrero-Sanchez, R. M. Paulus, M. W. M. Fijten, M. J. de la Mar, R. Hoogemboom, U. S. Schubert; "High-Throughput Experimentation in Synthetic Polymer Chemistry: From RAFT and Anionic Polymerizations to Process Development", *Appl. Surf. Sci.* **2006**, *252*, 2555-2561.
6. C. Guerrero-Sanchez, U. S. Schubert; "Experimental Techniques in (Parallel) Anionic Polymerizations. An Overview", *Chim. Oggi* **2005**, *23(6)*, 24-27.
7. V. Sciannamea, C. Guerrero-Sanchez, U. S. Schubert, J. M. Catala, R. Jerome, C. Detrembleur; "Ability of Nitrones of Various Structures to Control the Radical Polymerization of Styrene Mediated by in situ Formed Nitroxides", *Polymer* **2005**, *46*, 9632-9641.
8. C. Guerrero-Sanchez, B. G. G. Lohmeijer, M. A. R. Meier, U. S. Schubert; "Synthesis of Terpyridine-Terminated Polymers by Anionic Polymerization", *Macromolecules* **2005**, *38*, 10388-10396.
9. C. Guerrero-Sanchez, D. Wouters, C. A. Fustin, J. F. Gohy, B. G. G. Lohmeijer, U. S. Schubert; "Structure-Property Study of Diblock Copolymer Micelles: Core and Corona Radius with Varying Composition and Degree of Polymerization", *Macromolecules* **2005**, *38*, 10185-10191.
10. C. Guerrero-Sanchez, C. Abeln, U. S. Schubert; "Automated Parallel Anionic Polymerization: Enhancing the Possibilities of a Widely Used Technique in Polymer Synthesis", *J. Polym. Sci. Part A: Polym. Chem.* **2005**, *43*, 4151-4160.
11. C. Guerrero-Sanchez, F. Wiesbrock, U. S. Schubert; "Polymer Synthesis in Ionic Liquids: Radical Polymerizations in Water-Soluble Systems", *ACS Symp. Ser.* **2005**, *913*, 37-49.

B. Non-refereed publications:

1. C. Guerrero-Sanchez, C. Ott, U. S. Schubert; "Synthesis of Terpyridene-Functionalized (Metallo-)Star Polymers", *Polym. Mat. Sci. Eng.* **2007**, *96*, 248-249.
2. C. Guerrero-Sanchez, J. F. Gohy, D. Wouters, S. Hoeppener, H. Thijs, C. Ott, R. Hoogenboom, U. S. Schubert; "Block Copolymer Micelles in Ionic Liquids" *Polym. Mat. Sci. Eng.* **2007**, *96*, 936-937.
3. C. Guerrero-Sanchez, M. W. M. Fijten, U. S. Schubert; "Automated Parallel Heterogeneous Polymerizations", *Polym. Prepr.* **2007**, *48(1)*, 147-148.
4. C. Guerrero-Sanchez, U. S. Schubert; "Synthesis of Terpyridene-Functionalized Polyisoprene by Anionic Polymerization", *Polym. Mat. Sci. Eng.* **2006**, *94*, 226-227.
5. C. Guerrero-Sanchez, U. S. Schubert; "Towards Automated Parallel Anionic Polymerizations", *Polym. Mat. Sci. Eng.* **2004**, *90*, 647-648.
6. C. Guerrero-Sanchez, U. S. Schubert; "Polymer Synthesis in Ionic Liquids: Towards a Green Industry", *Polym. Prepr.* **2004**, *45(1)*, 321-322.

C. Patents:

1. C. Guerrero-Sanchez, M. Rasa, U. S. Schubert. "Magnetic Fluids and their Use", Dutch Polymer Institute. *PCT Application: PCT/EP2006/010654.*

D. Refereed publications prior to the Ph D thesis:

1. C. Guerrero-Sanchez, E. Saldivar, M. Hernandez-Hernandez, A. Jimenez; "A Practical and Systematic Approach for the Modeling of Industrial Copolymerization Reactors", *Polym. React. Eng.* **2003**, *11*, 457-506.
2. E. Saldivar, O. Araujo, R Giudici, C. Guerrero-Sanchez; "Modeling and Experimental Studies of Emulsion Copolymerization. III. Acrylics", *J. Appl. Polym. Sci.* **2002**, *84*, 1320-1338.

Acknowledgements

Definitevely, this work would not be possible without the help (and no help) of many people. This work is, indeed, also theirs. For all of you, who contributed somehow to this research, please accept my most sincere thanks for your help and support during this period.

Firstly, I want to thank my promoter, Prof. Dr. Ulrich S. Schubert, for his support, advice and open discussions during these four years. Dear Uli, I do remember well that time when we met in the ACS in New Orleans for the first interview to apply for the Ph D position in Eindhoven. Definitevely, that trip would change completely my professional horizon. Thus, I also want to thank you for beliving in me since then, for letting me be part of your group, and specially for that fruitful discussion we had once when I was not able to go forward and I wanted to give up.

Secondly, I want to thank the members of the core-committee, Prof. Dr. U. S. Schubert, Dr. R. Hoogenboom, Prof. Dr. J. F. Gohy, Prof. Dr. N. Hadjichristidis, and Prof. Dr. C. E. Koning for accepting to be part of this evaluation procedure as well as for the hard job of reading and commenting this thesis. The participation of other members of the committee, Prof. Dr. R. D. Rogers and Dr. H. Haeger, is also greatly appreciated.

I am in debt with all those colleagues and friends form the Laboratory of Macromolecular Chemistry and Nanoscience (SMN) who make this thesis and an enjoyable life in the Netherlands possible with their collaboration and encouragement:

Emma, I have no words to thank you for all your help with the paper work and for your friendship during this four years, I hope when I have my “five-star beach resort” finished you can visit (together with Nathalie, Rick, and Stephanie) me in my country.

Thanks a lot to Martin, Renzo, Hannekke, Antje and Caroline for all their kind help and support regarding the synthesis or characterization of my materials, for teaching me how to deal with the different equipments in the lab, as well as for keeping them always in good shape. You guys do a great job and are (or were) the main backbone of the group.

Special thanks to Daan, who is always willing to help others, Daan thanks for all the measeurements related to the AFM and TEM (chapters 3 and 4, and of course the “painful” micelles in ionic liquids), for checking most of my papers as well as part of this thesis, for the rides to Belgium, and for being an excellent person (I’ll buy you beer and cook real Mexican food for you whenever you like).

I also thank Harald, Bas and Mike for their help and fruitful discussions mainly with the terpyridine-functionalized polymers (chapter 3). Harald, I still remember the nice beer from the Trafalgar pub as well as the trips to Maastricht and Six Flags (I wish you a lot of success with your carrer, you are a great scientist). Mike, the combination of baseball and yoga on Thursdays and ice skating nights were fantastic (it was a pity that we could not continue with that); all the best for you and Jutta.

Richard and Matthias, thanks a lot for your collaboration, discussions and the supply of monomers and polymers based on oxazolines (chapters 4 and 5). Richard, additional thanks for reading and commenting some of my papers, posters, abstracts and, of course, this thesis. The tennis nights, together with Stephanie, Frank, Hans and Emma, were very nice (specially, after De Fort it was a bit difficult for me to distinguish between the ball and my nose). Hans, I still remember when we could not come back to Eindhoven after the RPK course because of the snow; it was a great adventure trying to find a place where to stay.

I am also in debt with Stephanie for her help with the conductivity, AFM and TEM measurements. I also thank all the german community (Tina, Nicole, Claudia, Christoph, Rebecca, Sabine, Steve, Andreas, Kristian, Christina, Frank, Stephanie, and… Daan???) for the nice beer, sussagges, barbeques, sushi sessions, Glühwein, the summer trip to Germany, and other nice moments and food they shared with me. Additional thanks to Tina who contributed with the synthesis of some ionic liquids used (chapter

3), to Christoph for some GC-MS measurements, and to Christina for the supramolecular block copolymer (chapter 5).

I thank Dr. Mircea Rasa (el “cabronazo”) for bringing the fascinating field of magnetic fluids to my scope; I wish you a lot of success at Oce and an enjoyable life in the Netherlands. Furthermore, the analysis of the magnetic materials of chapter 6 would not have been possible without the support and help of Prof. Albert Philipse (Debye Research Institue, University of Utrecht), Dr. Corine Fabrie from the group of Prof. Koopmans (Physics Department at TU/e) Tania Lara and Prof. Enrique Jimenez (CIQA, Mexico) (Tania, les deseo lo mejor de la vida a ti, a Jose y a su bebe en esta nueva etapa que empiezan juntos), and Chris Hendriks (Chris, I wish you, Pauline and your son all the best).

The collaboration, joint publications, and help of Prof. Jean-François Gohy and his research group (especially Dr. Fustin and Dr. D’Haese) regarding DLS measurements is greatly appreciated.

Other persons from TU/e who contribute to this Ph. D. formation are: Hans Kanenburg (Raman measurements), Monique Kirkels and Peter Lipman (surface area measurements), Dr. Marshall Ming and Tamara Dikic (surface tension measurements), Nick Lousberg, Dr. Kodentsov, and Dr. Srdjan Kisin (SEM images).

I thank the rest of the colleagues (and former colleagues) for their contribution to a nice and relaxing working atmosphere at the SMN group (I hope not to forget anyone): Philip, Huiqi, Berend-Jan, Alexander, Dmitry, Andriy, Dennis, Nico, Stefan, Elisabeth, Gabrielle, Veronica, Emine, Tamara D., Tamara E., Laszlo, Bernard, Tina (from China), Mark, Sanne, Mariska, Bas, Hannes, Thijs, David, Andrew, Daniel, Andreas Winter, Oana, Georgy, Jurgen, Patrick, Frank (thanks for the collaboration with the ionic liquids part (chapter 4)), Meta, Seda, Bart (paracetamol de la placenta), Remzi (thanks for that wonderful Turkish diner; lots of success for you and Ayse in Germany), Joe (thanks for the mole and correcting my paper of magnetic fluids), Manuela (thanks for the nice trip to Dublin and the nice drinks in the Irish Pub), Jolke (thanks as well for the trip to Dublin), Issam and Hector (not just colleagues but my two very good friends, I wish you both the best), Marcela (muchas gracias por hablar un poco de español conmigo todos los dias, le deseo lo mejor).

I thank the Dutch Polymer Institue for financial support during my Ph D as well as the Eindhoven University of Technology for the research facilities to perform this work.

Among other external collaborations are: Dr. V. Sciannamea and Dr. C. Detrembleur (University of Liege, Belgium), M. Sc. J. Bonilla and Prof. E. Saldivar (CIQA, Mexico), Dr. I. Garcia (DKI, Germany), Dr. J. Bozovic and Dr. D. J. Voorn (SPC, TU/e). Thanks a lot to Solvent-Innovation GmbH (Dr. M. Wagner) and Merck KGaA (Dr. W. Pitner) for the collaboration and kind gifts of most of the ionic liquids which were utilized in this work.

Outside the working environment there were a lot of people who make a marvelous life in the Neteherlands possible. To all of them, from the deepest of my heart, my most sincere thanks for your friendship, for food and drinks we have shared, for the trips, and wonderful and unforgettable moments we have spent together (Chingao… (words do not come easy) I feel/felt so alive when I am/was with all of you guys!!!):

Dr. Petr Sereda (pinche Pedrito) thanks a lot for your help with the digital image analysis of the mexican balls (polymer beads, chapter 4). I also thank Tamara, Petr, Issam, Anabel, Olavio, Ana, Srdjan, Yohan, Francisco, Anka, Hugo, Amandine, Marie Claire, Maurice, Francesca, Przemek, Erik-Jan, Martin, Natalia, Alberto, Elodie, Carmen, Laurene, Fabiola, Severine, Vincent, Ton, and many more people for the very good times at “our” home in Eindhoven. I have enjoyed very much traveling with some of you guys, and making many unnumerable activitivities (climbing, drinking, eating, stratum, parties, cooking, cleaning, playing, dancing, swimming, etc.…). Pinche Pedro the trip to Mexico was the best; I have discovered some many beautiful places of my own country that I was not aware they were there, of course Czech Republic is also nice. Tamara, I wish you the best in life and I thank you for the time we spent together.

To all my buddies from the (~~drinking and domino sessions on Fridays~~) sport club: Hector, Carlos (and Ana of course), Ivo, the Ukranian guy (Yvgen?), Niels, Marie Claire, Christina, Patricia, Olavio, Yohan, Hugo, Julio, Armando, Gil, Paty, Lolis, Edward, Daan, Tina, Baptiste, and many more, I want to say thank you for the nice Hoogarden (Grand Cru), Leffe, Palm, “Jupiter” (Belgium beer number one) and broodje rookworst.

I thank Kiki, Dylan and Shawn (and their family), Emma, Nathalie, Rick (and snoopy of course), Miriam and all the people who open the doors of their house for me when I was a newcomer in this country and culture.

A toda la bandera latinoamericana (Hector, Ruy, Armando, Ana, Gil, los dos Julios, Edward, los mil y un Alex, Cristian, Antonio, Irsa, Lolis, Paty, David, Angela, Oscar, espero no olvidar a nadie) gracias por su amistad, por las canciones, por el tequila, el mole, los tacos, los chiles en nogada, la cerveza, fiestas de independencia y de navidad, asi como demas tiempo que compartimos. Pero sobre todo por traer muy arraigado un pedazo de nuestra muy querida tierra dentro de ustedes. La verdad no se como hubiese podido sobrevivir por estos rumbos sin su compañía y su alegria. Les deseo lo mejor de la vida a todos y VIVA MEXICO CABRONES!!! (y toda nuestra amada latinoamerica; somos candela).

A escala muy personal, quiero dedicar todo el esfuerzo y sacrificio que hay detrás de este libro: A ese ser supremo (sin importar la mascara donde se esconda) que lo hizo todo. A mi querido Mexico y a su insufrible y valeroso pueblo que pudo darme una educacion (a pesar de todos los problemas) (ojala algun dia podamos organizarnos juntos y vencer esos flagelos de corrupcion, desigualdad, injusticia, marginacion y fraude electoral que tanto nos han perjudicado y no tengamos la necesidad de salir de nuestra patria a buscar las oportunidades). A mi segunda patria, Holanda, y a su gente, que me calurosamente me albergo en su pais durante este tiempo y que de alguna forma hizo posible estos estudios con sus impuestos; espero algun dia poder regresarles algo de lo mucho que me aportaron (to my second home country Holland and its people, which allow me to be here during these yeras and in a certain way they made these studies with their taxes possible; I hope one day I can pay them something back from all the things they have provided to me). A los que se quedaron en Mexico (mi querida familia y amigos, imposible nombrarlos a todos pero ellos saben quienes son) y no puediron acompañarme en esta gran aventura pero que contibuyeron de igual manera con mi formacion y educacion (gracias por criarme, enseñarme a vivir y estar ahí en el telefono o en internet y conversar un poco con este loco a 10000 km de distancia; todos uds. me ayudaron y me alegraron mucho cuando me senti solo y lejos de casa. En especial dedico este esfuerzo a mis hermanos (David (recuperate pronto de tu accidente pinche carnal) y Temo), a mi tia Marga, a esa mujer increible y mi heroina personal (mi abuela), a mi tia Pompeya, a Marina y a Monique (siento que el destino, las circunstancias y la distancia nos hayan alejado, con todo mi coranzon les deseo lo mejor de la vida). Tambien agradezco aquellos amigos mexicanos que alguna vez llegaron a visitarme en Eindhoven (mi primo hermano Daniel, Grecia, Lupita, Mariamne, Rene (la rana), Alfonso Gonzalez, Jose Bonilla, y Enrique Saldivar (Prof. suerte con esa lucha tan cruenta que estas librando en estos tiempos).

At the end, but most important, I thank Christina for her comprehension, for being an excellent person, for accepting me as I am, for sharing her time, space, life and many things more with me. I hope destiny will keep us together for a long time. We are a unique team.

Finally, after four years time has come to deliver this book. Note that it does not necessary mean that I deserve a Ph D title. However, a title is just a piece of paper to satisfy our ego. I think the real value of this effort is in how much you can improve as a person, learn, deal with others, and achieve with the available resources during this period. The title may help me to get a better job but does not change me as a person at all; I am the same as before (just a bit older) (el pinche mexicano, Carlito, Neos, Aeos, el pareja, mi chavo, el Carlos, el pinche roto, chilango, desalineado, the pinche pig, etc. or whatever you have called me once).

Good luck to everybody!!! Your friend Carlos.